The Chemistry of Aloga Bay Ascidians

A thesis submitted in fulfilment of the

requirements for the degree of

Doctor of Philosophy

of

Rhodes University

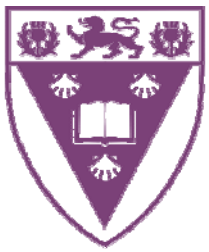

by

Candice Leigh Bromley

May 2015

Abstract

This thesis investigates the chemistry of 25 ascidian species collected from Algoa Bay, South Africa with a concerted focus on metal accumulation by these ascidians and the possible interaction of these metals with ascidian metabolites. Chapter 2 details the screening techniques employed to establish the presence of nitrogenous metabolites (^{1}H- ^{15}N HMBC), hyper-accumulated metal ions (ICP-MS) and potential metal ion/ ascidian metabolite complexes (LC-ICP-MS/ESI-MS). Unfortunately, exhaustive attempts to detect intact metal ion/ascidian metabolite complexes through the use of liquid chromatography with parallel inductively coupled plasma mass spectrometry/electrospray mass spectrometry (LC-ICP-MS/ESI-MS) were unsuccessful. However, the LC-ICP-MS/ESI-MS data obtained for the crude organic extracts of six of the Algoa Bay ascidian species, *Distaplia skoogi*, *Aplidium monile*, *Aplidium* sp., *Didemnum* sp., *Leptoclindines* sp. and *Polycitor* sp. enabled identification of a number of ten halogenated metabolites, namely the indoles **2.28**-**2.30**, and the tyramine and tyrosine derivatives (**2.31**-**2.33**, **2.41**, **2.43**, **2.44** and **2.46**), within the ascidian extracts. This study confirmed that LC-ICP-MS/ESI-MS is a powerful tool for the dereplication of halogenated metabolites in complex mixtures especially where these compounds are present in very small amounts. This study is also the first report of these compounds (eight of which are known) in African ascidians. Compounds **2.32** and **2.46** have not been reported before from a marine source. Compounds **2.28**-**2.30** and **2.33** were present in sufficient amounts in the respective ascidian extracts to allow their isolation and structure elucidation using standard spectroscopic techniques

Chapter 3 explores the ability of ascidians to accumulate a wide range of metal ions at concentrations which are often orders of magnitude higher than those of the surrounding sea water. Inductively coupled plasma mass spectrometry (ICP-MS) was used to determine the total ion concentrations of 24 metals in 25 Algoa Bay ascidian species. To the best of our knowledge this is the largest and most extensive investigation of metal concentrations in a group of different ascidians occurring in the same area. Hypotheisizing that the metal ion concentrations for each ascidian specimen screened may represent a unique fingerprint for each specimen principal component analysis (PCA) was used in an attempt to establish whether there were spatial, temporal or phylogenetic relationships associated with the metal concentration fingerprints of the ascidians that formed part of this study. The PCA results showed that there were no statistically significant relationships between ascidian metal ion concentrations and either the collection year or the collection site of the ascidians. However, species from the family Didemnidae provided the clearest statistical evidence supporting a phylogenetic relationship between these ascidians and their hyperaccumulated metal ion profiles. Furthermore, these results suggested that ascidian species are indeed actively concentrating metal ions from the surrounding sea water and are not simply sinks for passively accumulated metal ions. Interestingly, the concentration of vanadium in the set of

ascidians studied did not appear to correlate with any of the other metals accumulated by these ascidians suggesting that there is possibly a unique method employed for the accumulation of vanadium by ascidians. Chapter 4 investigated this possibility further after the nucleosides **4.10**, **4.11**, **4.13**, **4.15**, **4.17** and **4.40** were isolated from the vanadium accumulating ascidian *Aplidium monile*.

Studies into the interactions between nucleosides and vanadyl are unfortunately rare and usually qualitative in nature with limited information provided about the stability or structures of the complexes formed. The vanadyl accumulating aplousobranch ascidians *e.g. Aplidium monile* dominated our study of Algoa Bay ascidians therefore providing us with the rationale to investigate the relatively little studied binding ability and stability of vandyl-nucleoside complexes. Potentiometric studies were conducted to determine the stability constants of complexes formed between the oxovanadium ion vanadyl (VO^{2+}) and the commercially available nucleosides **4.10**-**4.14**. The data afforded by this analysis clearly confirmed the complexity of the vanadyl/nucleoside complexation and suggested that guanosine (**4.12**) formed the most stable complex with oxovanadium ions. We were also able to establish a third protonation constant for the hydroxyl moiety in **4.12** with a log*K* 8.87 which has not been previously reported.

Finally, Chapter 5 revisited the cytoxicity two Algoa Bay ascidians, *Clavelina* sp. and *Atriolum marinense* the extracts from which produced promising bioactivity results in previous studies against oesophageal cancer cells. The HP-20 fractionated extracts of *Clavelina* sp. and *Atriolum marinense* proved to be similalrly cytotoxic to breast cancer cells. With the exception for the 100% $acetone_{(aq)}$fractions the NMR data for both species suggested that most active non polar fractions were dominated by what appeared to be structurally unremarkable fatty acid glycerides and as such were not pursued further. Purification of the 100% $acetone_{(aq)}$fraction of *A. marinense* resulted in the isolation of a styrene trimer, **5.1,** common to both ascidian extracts. The NMR simulation software WIN-DAISY was employed to confirm the structure of **5.1**. Attempts to establish if **5.1** was an isolation artefact or a product of marine pollution were inconclusive.

Table of Contents

List of Figures

List of Schemes

List of Tables

List of Abbreviations

1D	one dimensional
2D	two dimensional
Ac	acetyl
ADC	antibody drug conjugate
amu	atomic mass units
aq	aqueous
Boc	*tert*-butylcarboxycarbonyl
br	broad
calcd	calculated
CNST	constant
conc.	concentrated
d	doublet
DCM	dichloromethane
ddd	doublet of double doublets
DEPT	distortionless enhancement of polarisation transfer
DMEM	Dulbecco's Modified Eagle Medium
DMSO	dimethyl sulfoxide
DNA	deoxyribonucleic acid
EIC	extracted ion chromatogram
EIMS	electron-impact mass spectrometry
E^o	standard elctrode potential
ESI	electrospray ionisation
ESR	electron spin resonance
EtOAc	ethyl acetate
EtOH	ethanol
FDA	Food and Drug Administration
Fn	fraction
GC	gas chromatography
gCOSY	gradient ^{1}H-^{1}H homonuclear correlation spectroscopy
gHMBC	gradient heteronuclear multiple bond correlation
gHSQC	gradient heteronuclear single quantum coherence
h	hour(s)
HPLC	high-performance liquid chromatography
HREIMS	high-resolution electron-impact mass spectrometry
HRESIMS	high-resolution electrospray ionisation mass spectrometry
IC_{50}	median inhibitory concentration
ICP	inductively coupled plasma
int.	integration

IR	infrared
LC	liquid chromatography
lit.	literature
m	multiplet
MeCN	acetonitrile
MeOH	methanol
mins	minutes
MMAE	monomethylauristatin
mmol	millimoles
mmu	millimass units
MNP	marine natural products
mol	moles
mp	melting point
MS	mass spectrometry
MTT	3-(4,5-dimethylthiazol-2-yl)-2,5-diphenyltetrazolium
mult.	multiplicity
NADH	Nicotinamide adenine dinucleotide
NADPH	Nicotinamide adenine dinucleotide phosphate
NCI	National Cancer Institute
NMR	nuclear magnetic resonance
NOE	nuclear Overhauser enhancement
NOESY	nuclear Overhauser enhancement spectroscopy
NP	normal phase
ocet.	octet
PC	principal component
PCA	principal component analysis
ppb	parts per billion
ppm	parts per million
PSDVB	poly(styrene-divinylbezene)
q	quartet
R	alkyl group
rel. int	relative intensity
RNA	ribonucleic acid
ROS	reactive oxygen species
RP	reversed-phase
RT	room temperature
s	singlet
SAIAB	South African Institute for Aquatic Biodiversity
SAM	*S*-adenosyl methionine
sat.	saturated

SCUBA	self-contained underwater breathing apparatus
SEC	size exclusion chromatography
sext	sextuplet
SIM-GC-MS	selective ion monitoring gas chromatography-mass spectrometry
sp.	species
t	triplet
TBDMS	*tert*-butyldimethylsilyl
TLC	thin-layer chromatography
tRNA	transfer ribonucleic acid
UV	ultra violet
v/v	volume per volume
XAS	X-ray absorption spectroscopy

Declaration

The following thesis has not been submitted to a university other than Rhodes University, Grahamstown, South Africa. The work presented here is that of the author unless otherwise stated.

Acknowledgements

It is with great gratitude that I thank the following people for their assistance and contributions throughout the course of this degree.

This research brought me numerous opportunities and positive experiences which would not have been possible if it wasn't for my supervisor Professor Mike Davies-Coleman. Prof, I will forever be thankful of the power you have to motivate and encourage me. The fascination and passion for your science is infectious and I only hope that you continue to inspire young chemists in your new role as Dean. Thank you for your perseverance as well as your mentorship, both scientific and paternal.

To my co-supervisors, Professor Denzil Beukes and Mrs Joyce Sewry, thank you for your guidance and support. It is not easy to take on a student part way through their degree; thank you both for stepping in and reminding me that I was not alone.

Thank you to Rhodes University, Henderson, the National Research Foundation and Professor Davies-Coleman for funding me during my PhD degree.

Thank you to Professor Bill Fenical and the National Cooperative Drug Discovery Groups (NCDDG) program for the generous donation of funding which enabled the first large scale SCUBA collection of marine ascidians in Algoa Bay which provided majority of the specimens investigated in this research. Special thanks go to Dr Shirley Parker-Nance for her valuable work into the collection and identification of the ascidians used in this research, as well as her continual advice on the complicated subject of ascidian phylogeny.

I am extremely grateful to have been able to attend a course in advanced ascidian biology hosted by the Smithsonian Tropical Research Institute in Bocas del Toro, Panama. I would like to thank the National Science Foundation (NSF) and the Panamerican Advanced Studies Institute (PASI) for funding my course and travel. Special thanks go to the instructors, Rachel Collins, Rosana Rocha, Xavier Turon, Billie Swalla, Euichi Hirose and Federico Brown, as well as my fellow students for introducing me to the fascinating world of ascidian biology.

I am also very thankful for the opportunity to work with Professor Marcel Jaspars and Dr Rainer Ebel at the Marine Biodiscovery Center (MBC) at Aberdeen University (AU), Scotland. Thank you to the Royal Society for funding this research. My time in Aberdeen was very positive and I am very grateful to the members of the MBC, especially Dr Jioji Tabudravu, Fredryk Mandey, Danug Sulistyo Putro and Morag Douglas who made me feel so welcome. Special thanks go to Dr Andrea Raab for her support and guidance throughout the LC-ICP-MS/ESI-MS work.

I am very grateful for the advice given by Graham Horgan (AU) and Sarah Radcliffe (RU) into the interpretation of the statistical analyses presented in Chapter 3. The potentiometric work presented in Chapter 4 would not have been possible without the help of Professor Zeni Tshentu. Thank you for giving your valuable time and experience and guiding me through this complicated work. I am grateful to Prof Adrienne Edkins and Dr Joanne de la Mare for the bioassay work performed throughout this research. A very special thank you to Edith Antunes for obtaining mass spectroscopy data for some very stubborn compounds. A special thank you to Dr Rosa Klein for remaining interested in my research and for always being available to brainstorm. I am very grateful to Dr Kevin Lobb for allowing me the space to work in a familiar lab and more importantly for all the advice and help with NMR.

Thank you to the students and staff of Rhodes University Chemistry department for the friendship and camaraderie over the years. To the past members of Prof Davies-Coleman's marine natural products group – I have always felt very fortunate to be a part of a group with such talented chemists many of whom I am happy to call my dear friends. I am very grateful to Drs Wendy Popplewell, Ryan Young and Sunny Sunassee for their influences in the early stages of my training. I will always be indebted to Dr Clint Veale for his support and friendship throughout this research; how lucky I have been to work alongside him and to share equally in the successes as in the disappointments that shaped our degrees. I hope we will have the opportunity to work together on many more occasions in the future.

I am extremely grateful to have had a strong social support throughout this research. Thank you to all of my friends for keeping me sane and for making my time in Grahamstown such a happy one. Special thanks go to Elodie, Annalene and Charlene for putting up with the brunt of my moaning. Thank you to my parents, Mick and Shirley, as well as Kirsten and Dawn for always believing in me and having much more faith in my abilities than I ever did. Thank you also to the Morley family for their ongoing encouragement and especially to Sally for helping with the final printing and submission of this thesis.

Last but not least I am incredibly grateful to Michael Morley for being such a patient and supportive husband. Thank you for caring for me and remaining by my side – I look forward to our "post-thesis" life together.

Chapter One:
General Introduction

1.1 Marine Natural Products and Modern Drug Discovery

Secondary metabolites or natural products are metabolites which do not appear to be involved in the primary cellular functions of the organism in which they are produced. This production of 'non-essential' metabolites is often energetically expensive and may be specific to a particular organism. The production of secondary metabolites in the ocean is confined to a high proportion of marine invertebrates, plants, and microorganisms, and has not been reported from marine vertebrates.[1,2] Generally, the biosynthesis of specific secondary metabolites is restricted to a single species, or a few very closely related species, usually within the same genus.[1,2] The marine reef is a very competitive environment and the exact function of many marine natural products in the life of the marine organisms that produce them, is often unknown. Some of the roles for marine natural products may include chemical defence against predators (antifeedants); inter-species growth inhibition to reduce competition for space and nutrients; and intra-species chemical communication cues.[1,2]

Oceans cover over 70% of the earth's surface, and comprise 95% of the earth's biosphere (*i.e.* the total volume available to life on earth).[1] The number of marine macro-organism species exceeds two million while the total species diversity of marine micro-organisms is completely unknown.[3] The ocean possesses a significant variation in environmental conditions (*i.e.* light, temperature and pressure) along a vertical transect from the surface of the ocean to the ocean floor. Not unexpectedly, the diversity and even the size of marine life changes with this vertical environmental differentiation.[3] However, while the vertical transition in environmental conditions in the ocean is pronounced, the environmental conditions especially temperature, pressure and salinity at each defined depth have remained constant over a long period of time.[1] Sponges (Phylum: Porifera) are the oldest known multicellular life forms on the planet, diverging from metazoans over 600 million years ago.[4] Evolving in a stable marine, depth related, niche environment over hundreds of millions of years has enabled sponges and other marine invertebrates to divert metabolic energy from the day to day survival in a constantly changing environment, to the evolution of diverse enzyme mediated biosynthetic pathways for the production of a vast array of novel secondary metabolites.[1] The structures of marine natural products are therefore generally more chemically diverse than those produced by terrestrial plants and this is regularly reflected in reviews of marine natural products published annually in Natural Product Reports.[2]

Recently, Grabowski *et al.*[5] explored the concept of chemical space as it pertains to natural products and known drug compounds. They consequently showed that marine derived compounds have the broadest general coverage of this space, incorporating many drug relevant structural features.[5] Bon and Waldmann[6] went further to explore the link between natural products and protein space. Small molecule modulators of protein function are one of the driving forces in chemical biology research and drug discovery. Bon and Waldmann[6] draw attention to the fact that both protein folds and natural product scaffolds are highly

conserved in nature. However, while changes in amino acid sequences may lead to changes in ligand binding sites in proteins, these binding sites will still conform to highly similar fold types.[5] Conversely, differentially substituted natural products, even within the same general structural class, can exhibit diverse biological activities. Therefore Bon and Waldmann[6] concluded that many natural products have evolved to interact with multiple proteins in order to elicit their biological functions. For example, they suggest that natural products responsible for toxicity reflect an ability to bind with multiple protein receptors. Similarly, Li and Vederas[7] have identified natural products as having privileged structures for drug discovery, through their production by enzymes to interact with a broad range of functional proteins. They support their argument with evidence from the drug discovery process in which 7,000 polyketide natural products have yielded over 20 commercial drugs (0.3% hit rate) whereas the hit rate from high throughput screening of synthetic compound libraries is only <0.001%. The link between marine natural products and new drug discovery is well established globally and has also been the driving force behind natural products research in South Africa for the last two and a half decades.[8] Therefore, in order to set the scene for the South African marine ascidian chemistry research described in this thesis, it is deemed necessary in this introductory Chapter to provide firstly, an overview of contemporary marine derived pharmaceuticals either in, or about to enter, the market place and secondly, introduce the marine invertebrate Class Ascidiacea through a brief introduction to ascidian biology. Further expansion of specific aspects of marine ascidian biology and chemistry are provided in the relevant chapters and sections that follow this Chapter.

1.2 Current Marine Natural Products and Their Derivatives with Food and Drug Administration (FDA) Approval

Currently there are two FDA or EU approved compounds whose chemical structures are the actual, unaltered, marine natural products isolated from their source organism, whilst a further five FDA approved drugs are synthetic compounds inspired by marine natural products.[9] A summary of these approved chemotherapeutic agents as well as a further 13 marine natural product inspired drugs currently in various stages of clinical trials are shown in Table 1.1 along with details relating to the original organism from which the compounds were isolated, the compounds chemical class and the disease areas for which these compounds provide a novel chemotherapeutic intervention.[9] This section will briefly discuss the processes involved in bringing the seven approved drugs onto the market.

Table 1.1: Marine natural products and marine natural product inspired compounds that are FDA-approved agents or in clinical trials. Details relating to their collected source organism, chemical class and disease area treated are included.

Clinical status	Compound name	Trademark	Natural product or derivative	Collected organism	Chemical class	Disease area
FDA approved	Cytarabine, Ara-C	Cytosar-U®	Derivative	Sponge	Nucleoside	Cancer
	Vidarabine, Ara-A	Vira-A®	Derivative	Sponge	Nucleoside	Antiviral
	Ziconotide	Prialt®	Natural Product	Cone Snail	Peptide	Pain
	Omega-3-acid ethyl esters	Lovaza®	Derivative	Fish	Omega-3 fatty acid	Hypertriglyceridemia
	Eribulin Mesylate (E7389)	Halaven®	Derivative	Sponge	Macrolide	Cancer
	Brentuximab vedotin (SGN-35)	Adcetris®	Derivative	Mollusk	ADC(MMAE)[a]	Cancer
	Trabectedin (ET-743) (EU registered only)	Yondelis®	Natural Product	Ascidian	Alkaloid	Cancer
Phase III	Plitiepsin	Aplidine®	Natural Product	Ascidian	Cyclic Depsipeptide	Cancer
Phase II	DMXBA (GTS-21)	NA	Derivative	Worm	Alkaloid	Cognition; Schizophrenia
	Plinabulin (NPI 2358)	NA	Derivative	Fungus	Diketopiperazine	Cancer
	Elisidepsin	Irvalec®	Derivative	Mollusk	Cyclic Depsipeptide	Cancer
	PM00104	Zalypsis®	Derivative	Mollusk	Alkaloid	Cancer
	Glembatumumab vedotin (CDX-011)	NA	Derivative	Mollusk	ADC(MMAE)[a]	Cancer
Phase I	Marizomib (Salinosporamide A; NPI-0052)	NA	Natural Product	Bactrium	β-lactone and γ-lactam	Cancer
	PM01183 (Trabectedin analogue)	NA	Derivative	Ascidian	Alkaloid	Cancer
	SGN-75	NA	Derivative	Mollusk	ADC(MMAF)[a]	Cancer
	ASG-5ME	NA	Derivative	Mollusk	ADC(MMAE)[a]	Cancer
	E7974 (Hemiasterlin derivative)	NA	Derivative	Sponge	Modified linear tripeptide	Cancer
	Bryostatin 1	NA	Natural Product	Bryozoan	Polyketide	Cancer; Alzheimer's
	Pseudopterosins	NA	Natural Product	Soft Coral	Diterpene glycoside	Wound Healing

[a]ADC(MMAE/MMAF) = Antibody drug conjugate (monomethyl auristatin E/ monomethyl auristatin F)

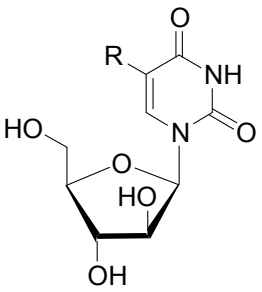

1.1 R= H
1.2 R = Me

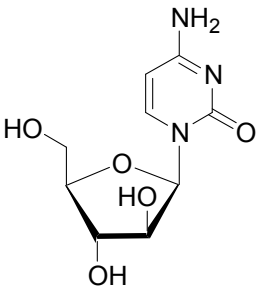

1.3

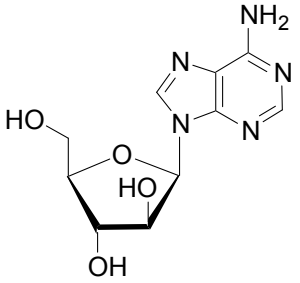

1.4

The first two natural product derived drugs currently on the market were inspired by the unusual nucleosides spongouridine (**1.1**) and spongothymidine (**1.2**) isolated from the Caribbean sponge *Tectitethya crypta* (previous synonym *Cryptotethya crypta*) in the early 1950's by Bergmann *et al.*.[9–11] The simple modification seen in **1.1** and **1.2**, where the normal 2-deoxyribose rings common to nucleosides are replaced by β-D-arabinofuranose rings, resulted in significant enhancement of biological activity. Further exploration of the bioactivity mechanism revealed that the cytosine arabinoside (aytarabine, Ara-C, **1.3**) was phosphoralyated in the cell and subsequently incorporated into the back bone of DNA where it served as a powerful inhibitor of DNA polymerase and DNA repair enzymes leading ultimately to cellular toxicity.[9] In 1969 **1.3** was granted FDA approval and entered the market under the trade name Cytosar-U® for the treatment of acute lymphocytic leukemia, acute myelocytic leukemia and blast crisis phase of chronic myelogenous leukemia and meningeal leukemia.[11] The arabinoside derivative of adenosine, vidrabine, Ara-A (**1.4**), was found to have significant antiviral activity.[9] Activation of **1.4** once again occurs with phosphorylation to give adenine arabinoside triphosphate which is a potent inhibitor of viral DNA polymerase and DNA synthesis in herpes, vaccinia and varicella zoster viruses.[11] FDA approval of **1.4** under the trade name Vira-A® was granted in 1976.[11] These early discoveries highlighted nucleoside biochemistry as an area for antiviral chemotherapy and more importantly provided the first clear examples of marine organisms' value as a potential source of new pharmaceuticals.[9]

The polypeptide, ω-conotoxin MVIIA (Ziconotide®, **1.5**), isolated from the marine cone snail *Conus magus*, was approved for clinical use in 2004, and was the first marine natural product to enter the market in over 25 years.[7,12] Compound **1.5** is used for the treatment of chronic pain caused by spinal cord injuries, and is injected directly into the spinal column as its peptide structure would be digested, and thus rendered ineffective, in the gastrointestinal tract if administered orally. The polypeptide structure of **1.5** may appear complex, however the total synthesis of this compound is achieved relatively simply through a series of synthetic peptide bond formations, allowing for the industrial production of virtually unlimited amounts of this drug.[13]

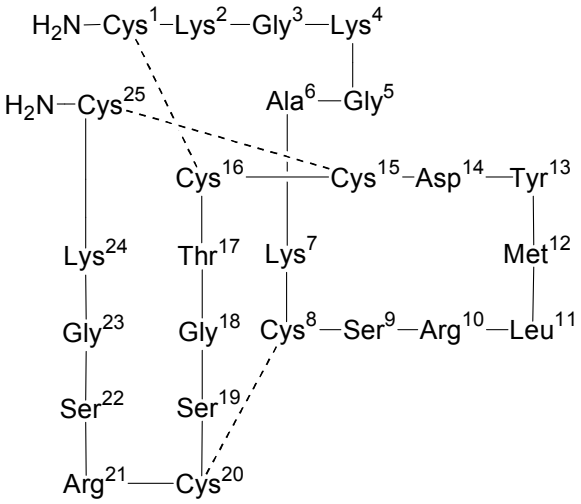

1.5

The hypertriglyceridemia reducing agent Lovaza® also received FDA approval in 2004.[14] Lovaza® contains synthetic esters (**1.6** and **1.7**) of ω-3 fatty acids originally obtained from oily fish species including anchovies, herring, mackerel and salmon.[9] Combined with an improved diet and regular exercise, Lovaza® has significantly lowered levels of triglyceride and VLDL-cholesteral in test patients.[9]

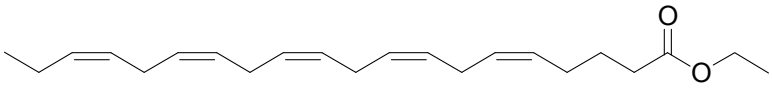

1.6

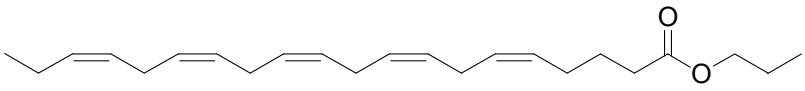

1.7

The synthetic production of compounds **1.3** – **1.7** is relatively easy which is fortunate as chemical synthesis is the ideal production method for natural product based pharmaceuticals as it eliminates the problem of supply and any possible adverse environmental impact. However, the remaining FDA approved marine natural products possess complex chemical structures, rich in chiral centers, requiring synthetic sequences involving numerous individual reaction steps which would often render total synthesis practically impossible and economically non feasible in an industrial context.[15]

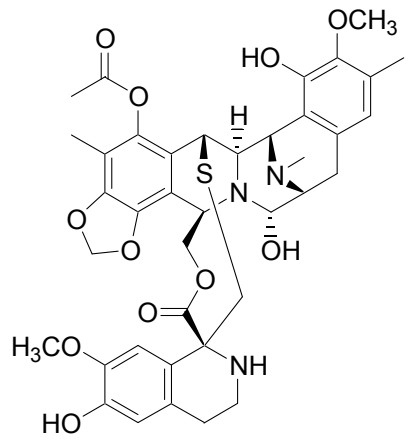

1.8

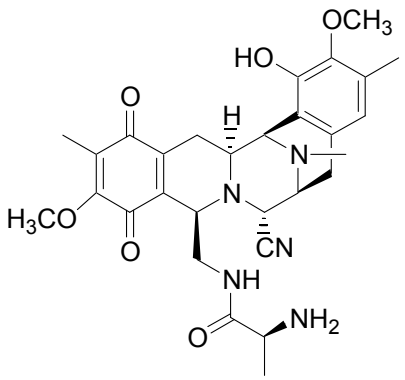

1.9

Yondelis® (**1.8**), the second underivatised marine natural product currently in clinical use, was introduced in 2007 for the treatment of soft tissue sarcoma.[9] Extracts from the ascidian *Ecteinascidia turbinata* were first found to have anti-tumor effects in 1969, but the active natural product, ecteinascidin-743 (ET-743, trabectedin, **1.8**) was only successfully isolated in low yields (1 g per metric tonne of ascidian) in 1990.[12] Mariculture of *E. turbinata* was used to obtain sufficient natural product for phase I and II clinical trials, however this method was not feasible for the production of larger quantities of **1.8** needed for phase III clinical trials, and eventual clinical use.[12] Although the natural product **1.8** has a complex chemical structure containing eight chiral centers, Corey *et al.*,[16] Endo *et al.*,[17] and Chen *et al.*[18] have all reported the total stereoselective synthesis of **1.8**. However, these syntheses all involved numerous synthetic steps and were thus deemed economically nonviable for the commercial production of sufficient quantities of **1.8**. Fortuitously, Cuevas *et al.*[19] noted that the structural features of **1.8** are very similar to cyanosafracin B (**1.9**) isolated from the bacterium *Pseudomonas fluorescens*, and suggested that the number of synthetic steps could be markedly reduced if **1.9** was used as a starting point in a semi-synthesis of **1.8**.[13] Compound **1.9** was accordingly produced through the fermentation of *P. fluorescens* and then used as a precursor in the semi-synthesis of **1.8**.[19] This semi-synthetic approach was a much more realistic method than total synthesis for the production of the large quantities of **1.8** needed for phase III clinical trials, and eventual introduction into the market.[9,12]

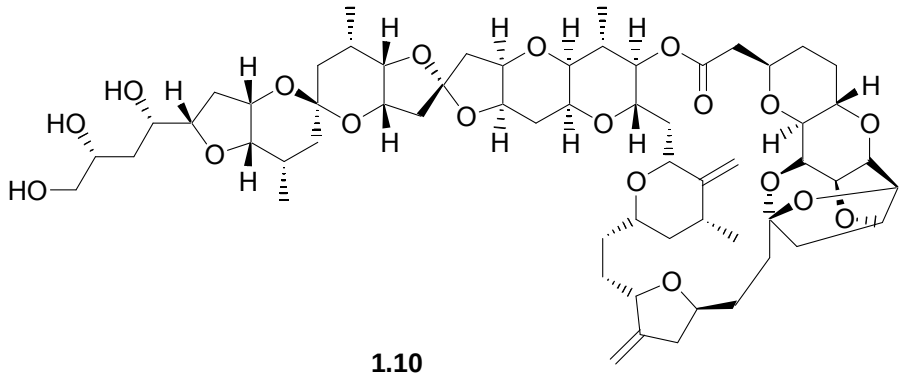

1.10

Halichondrin B (**1.10**), an extremely potent tubulin inhibitor, was originally isolated in small quantities from numerous widely dispersed sponge species including *Halichondria okadai* (Japan), *Axinella* sp. (Western Pacific), *Phakellia carteri* (Eastern Indian Ocean) and *Lissodendoryx* sp. (New Zealand).[10,15] In the case of the rare deep water (-80 to -100m) sponges *Lissodendoryx* sp. the yield of **1.10** was approximately 300 mg per metric tonne of sponge.[15,20] The National Cancer Institute (NCI) commissioned a survey of the naturally occurring *Lissodendoryx* sp. populations of New Zealand and established that the estimated total biomass of *Lissodendoryx* sponge is approximately 289 tonnes, clearly indicating that wild harvest would never result in enough **1.10** for commercial use.[20,21] Mariculture of the *Lissodendoryx* sp. was subsequently carried out in Beatrix Harbour, New Zealand by the New Zealand Institute of Water and Atmospheric Research (NIWA), in collaboration with the NCI.[20] *Lissodendoryx* sp. was successfully grown in mariculture, however, the overall yield of halichondrin B in the cultured sponge was not as high as that in the wild sponge.[20] Mariculture in general, requires a great deal of planning in terms of the positioning of the mariculture facility to ensure sustainability, as natural product production in marine organisms is very susceptible to environmental changes and even seasonal changes will affect the growth of the sponge and their production of secondary metabolites.[20] Synthesis was once again believed to be the best option for the production of **1.10** for pre-clinical and clinical trials. Compound **1.10** has a complex structure containing 32 stereocenters and the first total synthesis of **1.10** developed by Kishi and co-workers,[22] required over 100 synthetic steps with an overall yield of less than 1%. In general an economically feasible drug synthesis should not exceed 30 synthetic steps.[15]

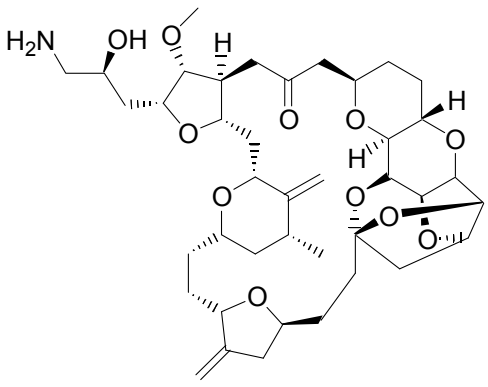

1.11

The Japanese pharmaceutical company Eisai explored the possibility that smaller simpler analogs of **1.10** might still elicit the desired anti-tumour effect.[15] This structure-activity relationship study involved the preparation of over 200 analogues of **1.10** and resulted in the discovery of eribulin (E7289, **1.11**), a simplified analogue with 19 stereocenters, which exhibited improved cytotoxicity when compared with **1.10**.[15,21,23] The synthetic analogue **1.11** was FDA approved in 2010 and is currently on the market under the trade name Halaven® for the treatment of metastatic breast cancer in phase III clinical trials for the treatment of

metastatic breast cancer.[24] However, the synthesis of **1.11** still requires more than 30 steps which makes its production for clinical use by synthesis possibly problematic and other options for natural product semi-synthesis, as in the example of **1.8** described earlier, will possibly also need to be explored.[15]

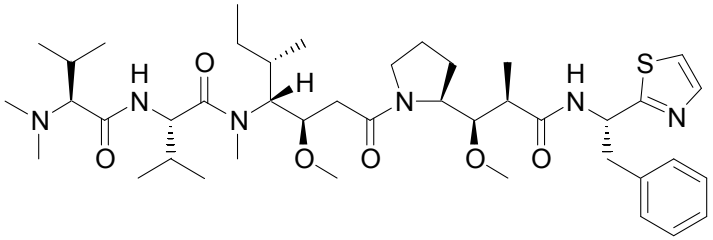

1.12

The most recent FDA approve natural product derived drug is a derivative of dolastatin 10 (**1.12**). The cytotoxic peptide **1.12** was first isolated by Pettit and co-workers in 1987 from a Mauritian sea hare, *Dolabella auricularia*.[9] In order to gain just 1 mg of **1.12** needed for structural elucidation an enormous number of sea hares, totalling approximately 2 tonnes, were required.[25] Dolastatin 10 was found to have a novel peptide structure with four unusual amino acids, namely *N*,*N*-dimethylvaline, dolaisoleucine, dolaproine and dolaphenine.[25] The absolute configuration of **1.12** was confirmed with the successful total sysnthesis of dolastatin 10 by Pettit and coworkers in 1989.[25] Later it was established the **1.12** was produced by the cyanobacteria (*Symploca* sp.) which form a major part of the sea hare's diet.[9] The powerful antimitotic properties of **1.12** saw it pass through phase I clinical trials. However, when **1.12** was entered into phase II clinical trials against a number of cancer cell lines it was not found to have significant clinical activity and was thus withdrawn from antitumor clinical trials.[25] Recently Katz *et al.*[26] linked a chimeric antibody to a derivative of **1.12** namely monomethylauristatin E (MMAE) to produce Brentuximab vendotin (SGN-35, **1.13**). The antibody drug conjugate **1.13** acts in such a way that the antibody will target CD30, an antigen present on the surface of Hodgkin's lymphoma cells, thus bringing the antimitotic agent, MMAE, into closer proximity to the cancer cells and vastly increasing its efficacy.[26] The success of **1.13** in phase I, II and III clinical trials against Hodgkin's lymphoma resulted in the accelerated FDA approval of the drug in 2011. Currently **1.13** is produced by Seattle Genetics and is on the market under the trade name Adcetris®.[9] Table 1.1 reveals that within the 13 marine natural product derived drugs in the clinical pipeline three are anticancer agents which a similar antibody conjugated structure as **1.13**.

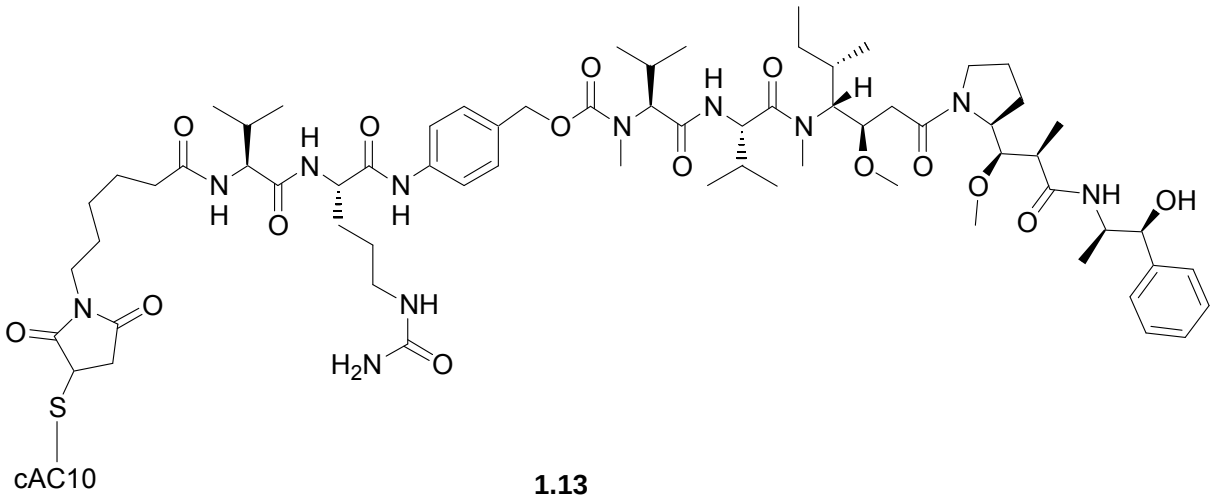

1.13

As Table 1.1 and the above discussion shows, marine invertebrates are a relatively rich source of medicinal compounds. Recently Schuhmann and co-workers[27] developed a model to evaluate how valuable marine biodiversity is to the pharmaceutical industry especially in terms of anti-cancer drug development. Schuhmann and co-workers[27] estimated that an outstanding 250,000-590,000 novel compounds were awaiting discovery from marine organisms. Their model predicted the pharmaceutical value of marine biodiversity to be as high as US$5.69 trillion and cautioned that a drop in biodiversity as small as 20% could equate to a market value loss of US$1.14 trillion.[27] These figures encourage biodiscovery and exploratory research into marine natural product chemistry whilst reinforcing the need for sustainable methods of production of drugs from the marine environment. In the context of this thesis which addresses our paucity of knowledge of the bioactive secondary metabolites produced by South African marine ascidians it is of interest to note that within their model, Schuhmann and co-workers predicted that secondary metabolites produced by marine chordates would be the more valuable from a pharmaceutical perspective over other organisms in the Kingdom Animalia.[27] Interestingly, very few organisms within the phylum Chordata are capable of producing secondary metabolites. One exception is the marine class of chordates, Ascidiacea, commonly known as ascidians, which have shown the potential to produce druggable compounds as indicated in Table 1.1 and from reports of other ascidian metabolites in preclinical trials.[23,28,29]

Didemnin B (**1.14**) first isolated from the ascidian *Tridemnum solidum* was one of the first non-derivatised marine natural products to enter anti-cancer clinical trials.[30] Promising *in vitro* testing results showed that **1.4** was active against lymphatic, colorectal and prostate cancers. Didemnin B performed well in phase I and II clinical trials against a range of tumours, however, trials were placed on hold due to undesirable side effects during treatment.[25,28] Aplidine (**1.15**) is closely related to **1.14** and was isolated form the ascidian *Aplidium albicans*.[28] As can be expected, **1.15** also possesses potent anti-cancer activity however,

contrary to **1.14** there appear thus far in clinical trials to be no harmful side effects associated with treatments using **1.15**.[11,28,31] In the EU **1.15** has been given "orphan drug" status for acute lymphoblastic leukemia and is synthetically produced by PharmaMar under the trade name Aplidin®.[10]

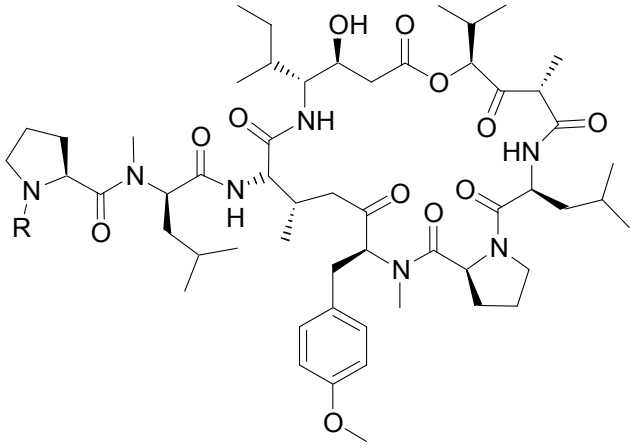

1.14 R =

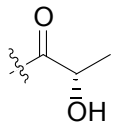

1.15 R =

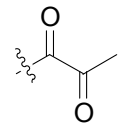

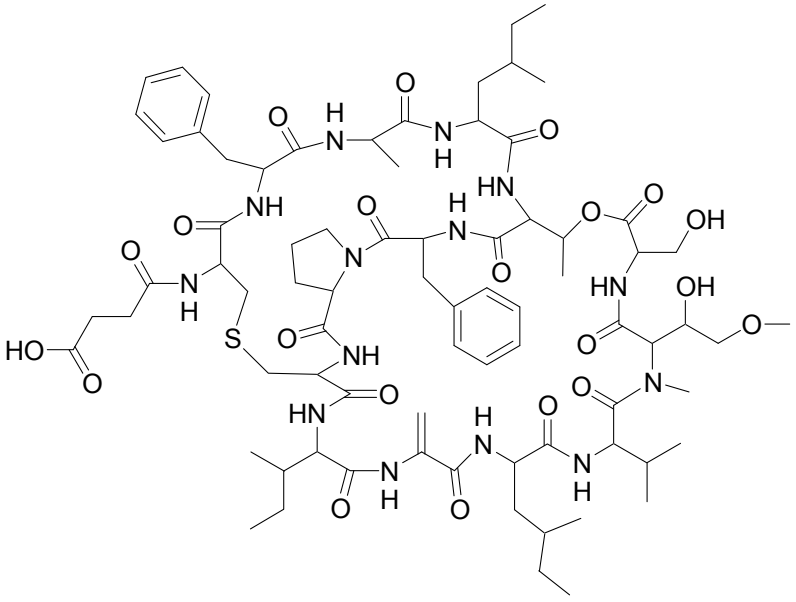

1.16

Two exciting tubulin targeting compounds currently in preclinical trials are the cyclic peptide vitilevuamide (**1.16**), isolated form the ascidians *Didemnum cuculiferum* and *Polysyncraton*

lithostrotum, and diazonamide A (**1.17**) isolated from *Diazona angulata* (initially misidentified as *Diazona chinensis*).[28,32] Although the exact mechanism of action for both **1.16** and **1.17** is still under investigations it appears that these two compounds not only interact with tubulin at different sites when compared to each other, but thus far seem to possess distinct bioactivity compared to any other tubulin targeting compounds in current studies.[28]

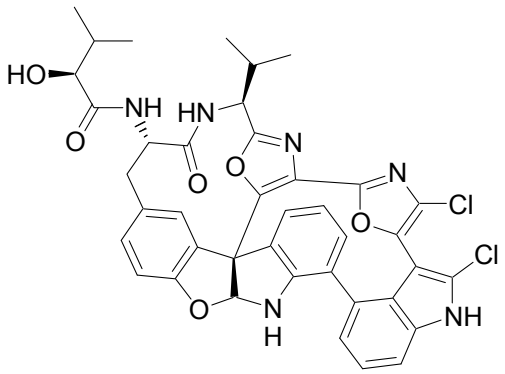

1.17

1.3 A brief introduction to ascidian biology

Ascidians are believed to be the simplest chordates. In the adult stage of life they are sedentary, soft bodied organisms which can either have solitary or colonial growth forms. Paradoxically, they produce swimming larvae which have a notochord, a quasi-equivalent of a vertebrate backbone hence their consideration by biologists as primitive chordates (Note: the notochord disappears in adult ascidians resulting in ascidians generally being referred to as invertebrates). In traditional metazoan phylogeny the phylum Chordata consisted of three subphyla namely Vertebrata, Cephalochordata and Urochordata (Tunicata).[33] Recent advances in phylogenetic research have however led Satoh *et al.* to recommend that Chordata be classified as a superphylum which is divided into three phyla due to distinctive characteristics of Vertebrata, Cephalochordata and Urochordata (Tunicata).[33] Within the class Ascidiacea (Phylum/Subphylum Urochordata) there are two orders namely Enterogona, consisting of the suborders Aplousobranchia and Phlebobranchia, and Pleurogona containing the suborder Stolidobranchia. Aplousobranch ascidians are all colonial and are believed to be the simplest ascidians in evolutionary terms. The suborders Phlebobranchia and Stolidobranchia are considered more advanced and are made up of both colonial and solitary ascidians. [34]

1.3.1 Tunic

The ascidian body is completely embedded in a thick covering known as the tunic, bringing about the common name tunicate. The tunic is akin to a flexible exoskeleton and maintains

the animals shape, provides protection and anchors the ascidian to the substrate.[33–36] The ascidian tunic is capable of rapid regeneration upon damage.[37] The consistency, colour and thickness of the tunic is a variable feature across as well as within ascidian species thus it is often not a reliable feature for taxonomic identifications, often causing SCUBA divers to mistake ascidians for sponges or algae.[34,35,38] The tunic is primarily made up of tunicin, a type of cellulose, which along with various proteins forms a matrix of fibres that give structure to the tunic.[33–36] The biosynthesis of cellulose is brought about by a large multimeric protein complex in the plasma membrane.[33] Cellulose synthase (CesA) and cellulase are two crucial enzymes involved in cellulose biosynthesis. Investigation into the genome of *Ciona* species revealed that a single copy of CesA (*Ci-CesA*) was present.[33] Through molecular phylogeny *Ci-CesA* was found to be within the same clade as *Streptomyces CesA* indicating that the bacterial *CesA* gene was likely transferred horizontally into the genome of a tunicate ancestor early in ascidian development.[33] This ability of urochordates to biosynthesise cellulose is the key feature that Satoh *et al.*[33] believe warrants the phylum-level classification of Urochordata.

1.3.2 The branchial sac and digestion

Ascidians are filter feeders and water enters though an oral siphon which is rimmed with oral tentacles (Figure 1.1) ensuring coarse filtration of larger particles.[33–36] The water is taken into the branchial sac also known as the pharangeal basket which has dual functionality of gaseous exchange with the water as well as the uptake of food. The branchial sac is a net like structure pierced with numerous stigmata each of which have a boarder of cilia which are responsible for the flow of water through the sac.[34,36] The number of rows of stigmata as well as their shape are often characteristic and can be used as tools for taxonomic identification of ascidian species. The overall shape of the walls of the branchial sac can also be a useful taxonomic identifier.[34]

Figure 1.1: Under water photograph of the solitary ascidian *Microcosmus exasperatus* clearly showing the ramified oral tentacle along the rim of the oral siphon. (Photo: Candice Bromley)

In the simplest forms of ascidians the surface of the branchial sac is flat with numerous stigmata whilst in more complex species the surface area of the branchial sac is further increase by the formation of pleats as seen in Figure 1.2.[34] The beating cilia in the walls of the branchial sac push water from the sac into the peribranchial cavity. The cilia are not, however, responsible for filtering the water and the uptake of planktonic food particles, this is achieved by a mucus net.[34–36] The endostyle (Figure 1.3a) on the ventral side of the branchial sac is homologous to the vertebrate thyroid and produces hormones as well the mucus net.[35] The mucus produced by the endostyle sweeps over the walls of the sac, driven by the beating cilia and traps food particles contained in the sea water. At the dorsal end of the branchial sac the mucus is rolled by the dorsal lamina to form a mucus chord (Figure 1.3 b) and moved towards the oesophagus for digestion.[35]

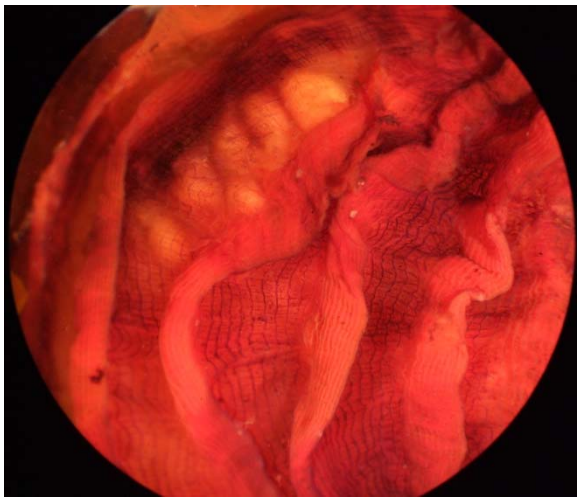

Figure 1.2: Microscope image of the pleated branchical sac of a Stolidobranch ascidian. (Photo: Candice Bromley)

The filtered water is then expelled from the ascidian peribranchial cavity, along with digestive waste, via the atrial siphon. Both the oral and the atrial siphons contain strong circular bands of muscle enabling the animal to close these openings.[34,35] The rapid closing of siphons often result in a jet of water to be propelled out of the ascidian hence the affectionate name of sea squirt given to this group of marine organisms. The filtration process is not selective and although the oral tentacles inhibit the entry of most of the larger particles, ascidians may have to periodically flush out the branchial sac by forcing the water back out the oral siphon in order to ensure that their respiratory and food filtration system does not become blocked by unwanted particles.[34]

a) 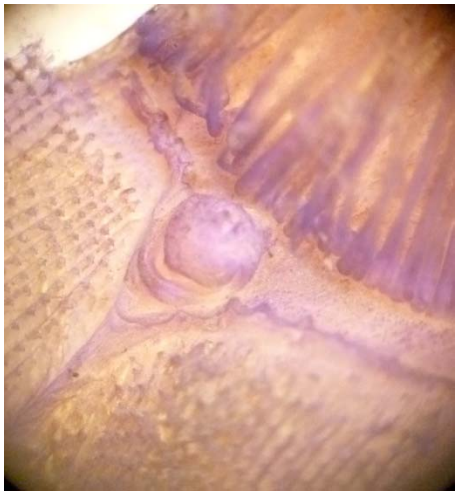 b) 

Figure 1.3: Microscope images of the U-shaped endostyle (a) and the mucus cord formed by the dorsal lamina (b) of *Phallusia nigra*. (Photo: Candice Bromley)

Mucus trapped food particles pass from the oesophagus to the stomach for digestion and the resultant faecal matter is expelled from the digestive tract through the anus into the peribranchial cavity.[34,35] Filtered water flowing out of the branchial sac is pushed through the atrial siphon sweeping the faecal matter out with it. In colonial ascidians the digestive tracts of zooids are found below the branchial sac whilst solitary ascidians have their digestive tracts situated alongside the branchial sac.[34,35]

1.3.3 The Circulatory System

Ascidians possess a complex network of channels, often loosely referred to as vessels, though which their blood flows transporting metabolites.[34,38] Ascidian hearts are fascinating in that they completely reverse the flow of blood every few minutes. The ascidian heart is a V-shaped muscular tube which rhythmically contracts pushing blood through in one direction before pausing for a few seconds and when it begins to contract again it drives the blood in the opposite direction.[34] Ascidian blood is isotonic to seawater and contains a number of circulatory cells.[34] Further detail of these circulatory cells as well as the controversial belief that the blood of ascidians plays a role in respiration is discussed in Chapter 4.

1.3.4 Reproduction

All ascidians are hermaphrodites and the arrangement and shape of the sexual organs is once again a taxonomic indicator.[34,35,39] Sperm is released into the peribranchial cavity where it is flushed out of the atrial siphon. Eggs on the other hand are released from the ovary but are retained in the peribranchial cavity of the zooid for fertilisation.[34] After fertilisation the

resultant ascidian larvae are brooded in the peribranchial cavity or in some species within a specialised brooding pouch.[34]

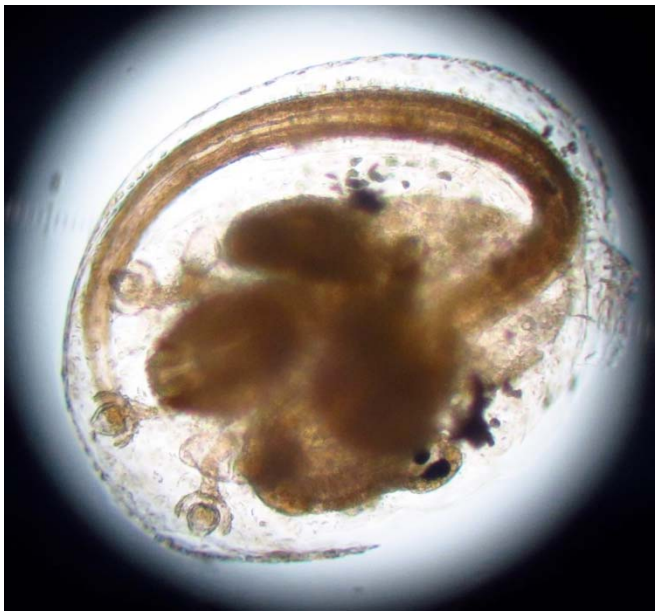

Figure 1.4: Microscope photograph of a brooding ascidian larva clearly showing the notochord-containing tail as well as three papillae at the front of the larval head which are characteristic of a didemnid species. (Photograph: Candice Bromley)

As seen in Figure 1.4 the larvae of ascidians have a tadpole structure with the body divided in to a head and a tail. The body is covered in a delicate tunic.[35] The tail of the larvae contains a notochord which is homologous to that found in vertebrates.[34] The muscle fibers in the tail propel the larvae and along with two sensory organs in the head namely the statocyst and ocellus, responsible for gravitropic and phototropic detection respectively, enable the larvae to swim.[34,40] Ascidian larvae are not capable of feeding and rely on energy stored in yolk cells. Adhesive papillae located at the front of the larval head detect suitable substrates to settle on. Once settled the larvae metamorphosise into the adult tunicate.[34] All ascidians reproduce sexually but colonial ascidians are also capable of asexual reproduction often meaning that all zooids in a colony, regardless of its size, are genetically identical.[34]

Aside from being a consistent source of novel bioactive compounds, ascidians have also attracted the interest of researchers because of their ability to accumulate metal ions in remarkably high concentrations and further explanations of both the mechanisms of metal ion accumulation and the proposed role of metal ions in ascidian biology are described in Chapters 2, 3, and 4.

1.4 Aims of this thesis

Exploring the interaction of hyper-accumulated metal ions and bioactive secondary metabolites in South African marine ascidians is the underlying theme that runs through this thesis. The marine natural products chemistry of South African marine ascidians has largely been neglected over the last two decades when compared with natural product studies of South African sponges, soft corals, nudibranchs and marine algae.[8,41–43] A focussed collection of specimens of 63 different ascidian species by SCUBA from Algoa Bay, South Africa in 2004, as part of the NCI's National Cooperative Drug Development Groups (NCDDG)[44] programme provided the initial unique source material for this thesis work (further collections of selected ascidians were made during this study from Algoa Bay). With the support of a Royal Society grant in 2010 Davies-Coleman (Rhodes University) and Jaspars (University of Aberdeen) anticipated exploiting this unique collection of ascidians to ascertain if examples of metal ion/ secondary chelation, as originally discovered by Jaspars and co-workers in the Australian ascidians *Lissoclinum patella*[45,46] and *Eudistoma gilboviride*[47] (described in detail in Chapter 2), were also evident in Algoa Bay ascidians containing similar nitrogenous metabolites. The hypothesis that such chelation was not limited to these two ascidian species and may be more widespread amongst ascidians needed ratification. The uniquely configured mass spectrometry infrastructure at the University of Aberdeen, designed to explore metal ion/secondary metabolite relationships, was unavailable in South Africa and the Royal Society grant provided the catalyst and the means to link state of the art chemical analysis infrastructure with a unique natural product resource. The results of this three year study are presented here.

Although the primary aim of the thesis was to explore the occurrence of possible metal ion/ secondary chelation in Algoa Bay ascidians, we also realised that the in-depth analysis of ascidian metal ion concentration required for such a study would provide a unique opportunity to explore the existence of possible relationships between metal ion accumulation and the phylogenetic, spatial and temporal distribution of Algoa Bay ascidians (Chapter 3). We also anticipated that the close scrutiny of the Algoa Bay ascidian extracts for nitrogenous and halogenated metabolites using contemporary nuclear magnetic resonance (NMR) techniques at Rhodes University and the mass spectrometry facilities at the University of Aberdeen respectively, would ultimately lead to the discovery of new and known natural products previously not encountered before in South African ascidians (Chapters 2 and 4) In addition, if these metabolites were present in sufficient quantities, opportunities would be provided to study in detail selected metabolites' potential chelation with ions regularly hyper-accumulated by ascidians *e.g.* vanadium (Chapter 4). Finally, the discovery of new bioactive metabolites with pharmaceutical potential remains the mainstay of the majority of marine natural products research programmes. Consequently, the source of the elusive potent cancer cell cytoxicity observed in extracts of two Algoa Bay ascidians *Atriolum marinense* Kott, 2001 and *Clavelina* sp. was pursued concurrently with the other research areas described above (Chapter 5).

Chapter Two:
Screening of South African Ascidians

2.1 Introduction to South African ascidians taxonomy, zoogeography and chemical diversity

2.1.1 Taxonomic diversity of South African ascidians

The first taxonomic descriptions of ascidian species collected along the southern African coast were conducted by the early taxonomists Herdman (1882, 1886), Sluiter (1898),[48] Michaelsen (1904) and Hartmeyer (1912). The five collections that provided ascidian specimens for taxonomy, formed part of larger expeditions, conducted from the vessels HMS Challenger, Siboga, and Valdivia Deutschen Tiefsee, which were used to explore the biodiversity of the world's oceans at the end of the 19th and early 20th centuries.[36,40,49] The primary method of collection on these expeditions was dredging which resulted in the majority of ascidians assimilated into these biodiversity investigations being those preferring to settle on softer substrates such as sand.[49] Some ascidian classifications made in these early studies are still considered ambiguous, or as in the case of *Clavelina enormis* Herdman 1882, incomplete as the initial short description was based on a single, immature specimen.[49]

Michaelsen's investigation of the ascidians of the Cape Province was the first concerted study of the ascidian population of South Africa.[50] After these early taxonomic studies there was a hiatus in activity until Millar took an interest in the taxonomic wealth of the ascidians of southern Africa. Millar's numerous publications on the subject made significant strides in our understanding of the diversity and distribution of ascidians in South Africa. [36,39,51,52]

More recently, a comprehensive collection of South African ascidians from Sodwana Bay on the east coast to Saldanha Bay on the west coast was made by Griffiths (University of Cape Town) and Schleyer (Oceanographic Research Institute, Durban). The ascidians collected by Schleyer and Griffiths were identified by the renowned French ascidian taxonomists, Claude and Francoise Monniot.[49] Their seminal treatise documents the collection and description of 82 South African ascidian species, 20 of which were new to science. In addition Monniot and Monniot reviewed an additional 63 species previously recorded from South Africa, that were not part of the Schleyer/Griffiths collection.[49]

Following shortly after the study by Monniot *et.al.* the South African ascidian taxonomist, Shirley Parker-Nance published her PhD thesis entitled 'Aplousobranch ascidians (Tunicata: Ascidiacea) of southern Africa' which included the description of 11 species of tunicates from Algoa Bay, South Africa, 5 of which were new to science.[40] This work was the last of the taxonomic reports on ascidians of South Africa to appear in the taxonomy literature, apart from a few cursory ascidian descriptions, some of which were new species, recently published in the chemistry literature in support of marine natural product studies of these organisms.[53–55] Details of the ascidian natural product chemical diversity emerging from these studies are reviewed in section 2.1.3 of this chapter.

The most recent estimation of the number of identified species of ascidian present in the waters off southern Africa is 168 species, and includes those reported from along the coastlines of South Africa, Namibia and Mozambique, in addition to the West Wind Drift Islands of Tristan de Cunha, Vema Seamount and Amsterdam Saint Paul, but excludes those reported by Parker-Nance.[56,57] Most taxonomists agree that even with a long history of ascidian taxonomic investigations along the South African coast, the sporadic nature of the sampling in terms of depths and locations, has created a fairly random inventory of species which grossly underestimates the ascidian diversity in South African coastal waters.[40,49,58]

2.1.2 Biogeography of the South African coast

The rich diversity of the marine flora and fauna in South African waters is noteworthy and has piqued the interest of many marine researchers for over a century.[58,59] The reason for such biodiversity is due, in part, to the long contiguous coast line of South Africa, stretching approximately 3,000 km from the Mozambican border in the east to the Namibian border in the west.[41,60] South Africa straddles the Indian and Atlantic oceans and the South African coastline is exposed to the two major oceanic currents that influence the biogeography of southern Africa.[60] These two large ocean current systems, namely the Agulhas and the Benguela currents, are predominantly responsible for creating three distinct bio-geographical zones along the South African coastline (Figure 2.1).[59,60]

The subtropical bio-geographical zone dominates the east coast of South Africa and is characterised by the presence of numerous circumtropical marine species. The environmental features of this zone are dictated by the influence of the Agulhas current which sweeps down from the tropics delivering warm tropical water to the east coast (Figure 2.1).[41,59,60] The core of the powerful Agulhas current flows southward, following the edge of the continental shelf. As the continental shelf widens off the southern Cape coast the Agulhas current is pushed further off shore, and the coastal waters along the southern coast become cooler.[41,59] This drop in temperature results in a different set of flora and fauna, exhibiting a high degree of endemism, occurring along the south east coastline which is classified as the warm temperate bio-geographical zone (Figure 2.1). The Agulhas current finally turns back on itself and flows eastward as the return Agulhas current.[59,60] The third bio-geographical zone is the cool temperate west coast which is markedly different from the east coast. The major current influencing this area is the Benguela current originating from a northerly deflection of the sub-Antarctic Western Drift current.[59] The Benguela current flows north up the west coast of South Africa, bringing with it cold water (Figure 2.1). Upwelling, another important phenomenon affecting the biogeography of the western coast, is caused by prevailing winds that blow the surface waters offshore, forcing water from the deep ocean to rise upwards and replace the retreating surface waters. The waters from the deeper reaches of the ocean are devoid of light and therefore cannot sustain plant life, resulting in a nutrient

rich environment.[59] The upwelling, bringing cold and nutrient rich water to the surface, creates an ideal environment for phytoplankton and seaweed populations, which in turn support food chains that culminate in productive fisheries.[59,60]

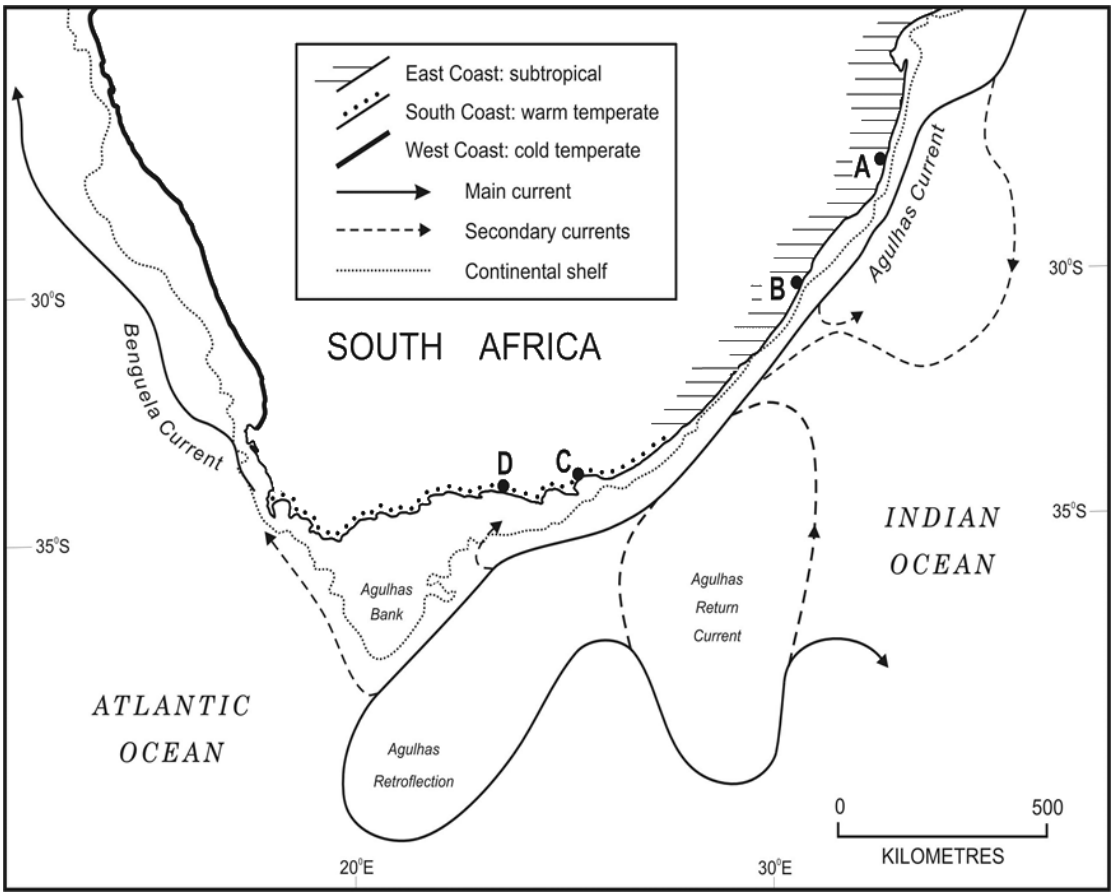

Figure 2.1: Map of the coastline of southern Africa depicting the ocean currents responsible of the three bio-geographical zones. The sites indicated relate to the areas where ascidian collections have been made (A = Sodwana Bay, B = Aliwal Shoal, C = Algoa Bay and D = Tsitsikamma Marine Reserve).[41]

2.1.2.1 Zoogeography of ascidians in South Africa

In 1971, Millar comprehensively reviewed the biological and taxonomic literature published on ascidians worldwide.[36] In his review, Millar estimated that 84 recognised species of ascidians occurred in the waters of South Africa. Of this population, Millar approximated that as many as half could be considered endemic to the region, and further stated that 39% were found in the warm, subtropical waters of the east coast, 35% in the warm temperate south coast waters, 22% in the cold temperate west coast waters and only 4% were ubiquitous.[36,39] The figures that Millar arrived at are in accordance with those obtained for other South African

marine fauna, however, the ascidian data reviewed was not collected with bio-geographical investigations in mind and as such the collection points along the coast were sporadic and for the most part focused on common ship routes. Thus statements such as those made by Millar, alluding to the geographic distribution and endemism of South African ascidians must be viewed with caution given that our knowledge of the true extent of South African ascidian population remains uncertain.[49]

Primo and Vasquez used modern statistical techniques to investigate the patterns of ascidian zoogeography of the southern African region. Their work included distribution data obtained from the descriptive taxonomic reports on South African ascidians, previously discussed in this chapter, along with other literature reports allowing the region to be expanded to include the littoral zones of Namibia and Mozambique as well as the West Wind Drift Islands[56] Due to the gaps in the knowledge of the ascidian diversity discussed previously the distribution of ascidians throughout the waters of southern Africa and because no new sampling was actively undertaken, it is once again with some caution that the results obtained by Primo and Vasquez can be accepted.[40,49,58] However, even with these factors in mind, some attention should still be given to the conclusions of Primo and Vasquez. Firstly, they concluded that the ascidian populations on the West Wind Drift islands were markedly different from those seem along the coast of southern Africa, and so were not considered in further classifications of bio-geographical zones. They also stated that that the population found on the subtropical east coast was for the most part different from those of the cold temperate west coast. In addition they proposed that the warm temperate Agulhas region along the south coast acted as a transitional zone between the subtropical and cold temperate biogeographical regions as they, contained ascidian species found in the two other areas.[56] They went on further to state that the southern African ascidian population exhibited 47% endemism, 25% Indo-Pacific and 13% cosmopolitan and that the colonial species dominated the tropical regions and solitary ascidians the colder regions.[56]

These conclusions, although more detailed, and with the added support of statistical proof, are by no means novel and at most simply add weight to classic observations on the general biogeography of the South African flora and fauna. These original and general studies commonly state that there is a high level of biodiversity in the warm regions opposed to the higher biomass observed in the cold regions. The south east temperate region has been shown to incorporate aspects of the other two regions, and has a rich population of filter feeders.[58,59]

2.1.2.2 Study site: Algoa Bay

The study site used for our investigation was Algoa Bay, situated in the south eastern warm temperate biogeographic coastal region of South Africa (shown as point C in Figure 2.1). The characteristic crescent shape of Algoa Bay protects the subtidal reefs present in the western sector of the bay from rough surf conditions, which helps to facilitate accessibility and collection of specimens from these reefs by SCUBA.[40] Algoa Bay is host to one of South Africa's major harbours, Port Elizabeth, which along with the anthropogenic influence of the surrounding Nelson Mandela metropole ensure a steady supply of nutrients that enrich the waters of the western sector of the bay. The nutrient rich warm temperate waters create an ideal habitat for filter feeders such as sponges and ascidians which are both abundant and ubiquitous in Algoa Bay.[58,59] The majority of the ascidians in our investigation were collected from dive sites in western Algoa Bay in 2004 as part of the National Cancer Institute's National Cooperative Drug Discovery Groups (NCDDG) program and had been kept continually frozen (-20 °C) since their collection.[44] Further selective collections of individual ascidian species were made (2011-2014) in Algoa Bay as the research described in this thesis evolved.

2.1.3 Previous investigations of the natural products chemistry of South African ascidians

Kashman and co-workers were the first to report the isolation of novel, bioactive metabolites from a South African ascidian species.[61] Polycitone A (**2.1**) and polycitrins A and B (**2.2** and **2.3**) were isolated from the ascidian *Polycitor* sp. collected in Sodwana Bay, South Africa (indicated as point A in Figure 2.1). The chemical structures of **2.1**-**2.3** were elucidated using standard NMR experiments, and further analysis through single crystal X-ray diffraction was required to confirm the structure of the highly symmetrical **2.1**.[61] In a subsequent investigation, polycitone A (**2.1**) and polycitrin A (**2.2**), along with methylated derivatives of both compounds were assayed against retroviral reverse transcriptases and cellular DNA polymerases. From this study the only compound with notable bioactivity was **2.1**, which was found to be a potent inhibitor of retroviral reverse transcriptases (*i.e.* of human immunodeficiency virus type 1, murine leukaemia virus and mouse mammary tumour virus) as well as cellular DNA polymerases (*i.e. Escherichia coli* DNA polymerase 1 and both *α* and *β* DNA polymerases).[62] This promising bioactivity provided the rationale for the total syntheses of **2.1** by Kreipl *et. al.*.[63]

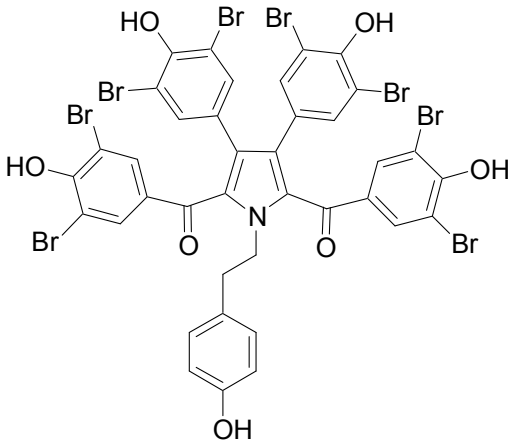

2.1

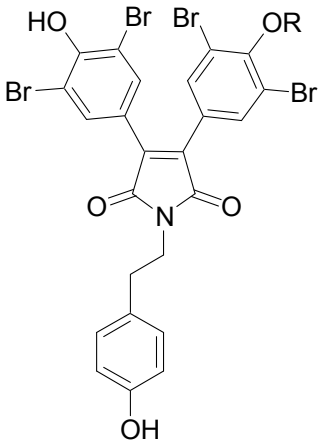

2.2 R = H
2.3 R = CH_3

Patil *et. al.* conducted a bioassay guided fractionation of a methanol extract of the ascidian *Lissoclinum* sp. that was collected from Aliwal Shoal, South Africa (indicated as B in Figure 2.1) as part of a collaborative marine invertebrate collection by Rhodes University and SmithKline Beecham (now Glaxo SmithKline).[64] This investigation targeted marine secondary metabolites inhibiting interleukin-8 (IL-8) receptors, and resulted in the isolation of the new lissoclin disulfoxide **2.4**.

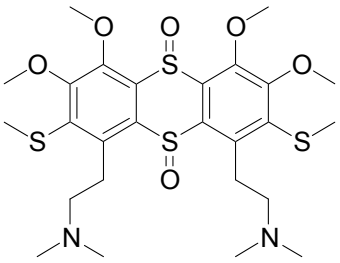

2.4

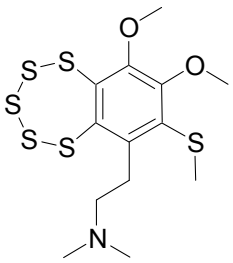

2.5

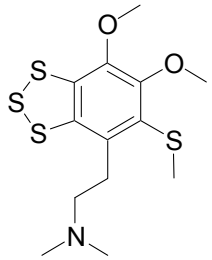

2.6

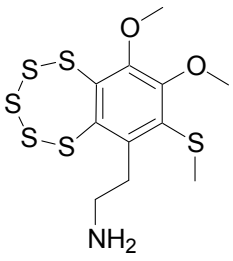

2.7

The role of IL-8 as a neutrophil granulocyte attractant and activator, links it to a number of inflammatory disorders such as rheumatoid arthritis and psoriasis.[64] Lissoclin disulfoxide (**2.4**) showed good inhibition activity against both IL-8 Rα and IL-8 Rβ receptors (IC_{50} = 0.6 μM and 0.82 μM respectively) as well as inhibitory activity against protein kinase C with an IC_{50} value of 1.54 μM.[64] In addition to the isolation of **2.4**, this South African ascidian also yielded three known cyclic polysulfides, namely N,N-dimethyl-5-(methylthio)varacin (**2.5**), and 3,4-dimethoxy-6-(2'-N,N-dimethylaminoethyl)-5-(methylthio)benzotrithiane (**2.6**) [both isolated previously from *Lissoclinum japonicum*[65]] and varacin (**2.7**) first isolated form *Lissoclinum vareau.*[64–66]

A group of acyclic amino alcohols were isolated as their acetate esters **2.8** – **2.11** from the ascidian *Pseudodistoma* sp. collected from the Tsitsikamma Marine Reserve, South Africa (labelled as point D in Figure 2.1). The detergent-like saponification products of **2.8** – **2.11** were proposed as being responsible for the anti-microbial activity observed for the *Pseudodistoma* sp. extract.[41,67]

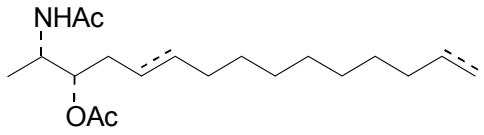

2.8 Δ^5, Δ^{13}
2.9 Δ^5

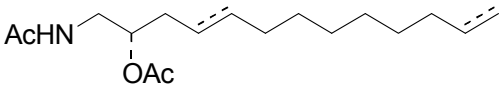

2.10 Δ^4, Δ^{12}
2.11 Δ^4

A second group of acyclic amines were isolated from another South African *Pseudodistoma* species, this time from Algoa Bay, South Africa. This ascidian was collected as part of a collaborative survey of the marine invertebrates and algae from the warm temperate coast of southern Africa by the Coral Reef Research foundation, the National Cancer Institute (USA) and Rhodes University.[41,68] Bioassay guided fractionation led to the isolation of four new nitrogenous metabolites, pseudodistamine (**2.12**), the unsaturated aliphatic amines **2.13** and **2.14** as well as the β-carboline alkaloid **2.15**.[68] The chemical structures of these compounds were elucidated using standard spectroscopic techniques and the absolute configuration of the single chiral centre in **2.12** was determined through preparation and NMR analysis of the Mosher's ester derivative of this compound. The absolute configuration of the chiral C-2 in the amines **2.13** and **2.14** were established after ozonolysis degradation to produce alanines which were further derivatised with Marfey's reagent and compared to derivatised *D*- and *L*-alanine standards using LC-MS.[68] Compounds **2.12** – **2.15** were all screened against the human tumour cell lines LOX (melanoma), A549 (non-small cell lung), SNB-19 (CNS) and OVCAR-3 (ovarian), however only **2.13** showed any cytotoxicity with an approximate IC_{50} value of 6.0 μM across all cancer lines.[68]

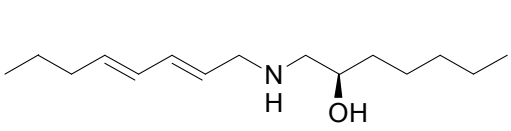

2.12

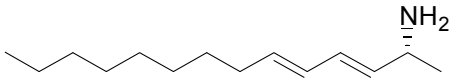

2.13

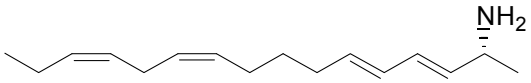

2.14

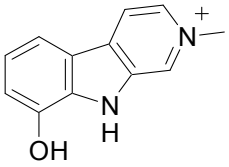

2.15

The two most recent studies into the chemistry of South African ascidians were both conducted by McPhail and co-workers, and involved ascidians from the same 2004 Algoa Bay collection (SAF2004) which has provided the ascidian material for this thesis.[53,54] The first of McPhail and co-worker's[53] investigations focused on a new species of *Lissoclinum* collected from Algoa Bay, South Africa. An organic extract of *Lissoclinum* sp. was shown to have potent cytotoxicity against lung cancer cells.[53] Through bioactivity guided fractionation of this extract a series of glycosylated polyketide macrolides, mandelalides A-D (**2.16** – **2.19**) were isolated.[23,53] The absolute configurations of the mandelalides were initially proposed from exhaustive NMR, and chiral GC-MS sugar analyses.[53] Mandelalides A and B (**2.16** and **2.17**) were bioassayed against mouse Neuro-2a neuroblastoma cells revealing IC_{50} values of 29 nM and 84 nM respectively and human NCI-H460 lung cancer cells yielding IC_{50} values of 12 nM and 44 nM respectively.[53] These potent cytotoxicity results against two different cancer cell lines highlighted the mandelalides as a promising family of compounds for further biological evaluation. However, the limited amounts of these compounds isolated in the preliminary study were a hindrance to further investigations of the mechanism of cytoxicity. As the most active member of the mandelalide series much interest has been paid to developing a total synthesis of **2.16** and its aglycone fragment.[69–71] The total synthesis of mandelalide A (**2.16**) by Willwacher *et al.* revealed small yet notable discrepancies between the NMR data of the synthetic, and natural occurring mandelelide A, most noticeably in terms of the ^{13}C chemical shifts of the C11 and C25 methyl carbons.[70] Willwacher *et al.* proposed that the flexible nature of the macrocycle may mean that the key ROESY correlations are observed even with configurations differing from those proposed for **2.16** by McPhail and co-workers.[70] In an attempt to clarify the configurational debate emerging around the structure of mandelalide A, a C11-epimer of mandelalide A was prepared, however noticeable differences in the spectral data between this epimer and the original published data for **2.16** prompted Willwacher *et al.* to conclude that there were further subtle but profound errors in the initial structure reported for mandelalide A.[70]

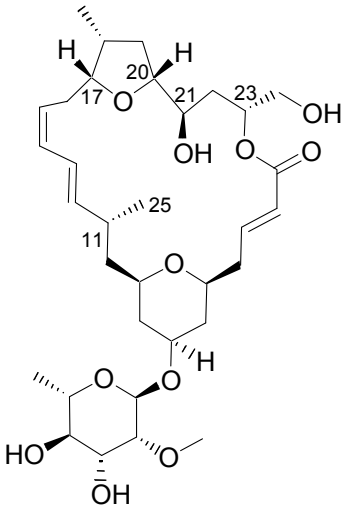

2.16

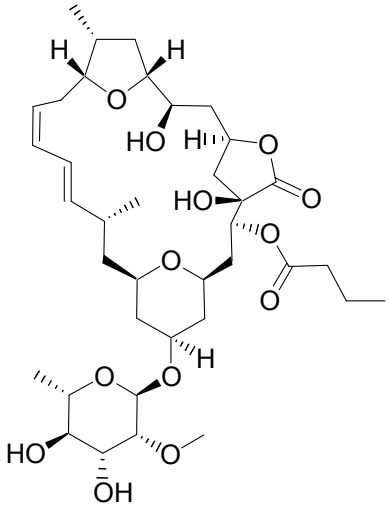

2.17

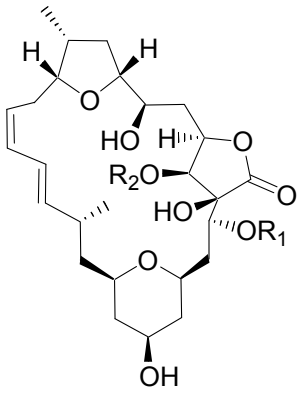

2.18 R_1 = $COCH_2CH_2CH_3$,
R_2 = OH
2.19 R_1 = $COCH_2CH_2CH_3$,
R_2 = $COCH_2CH_2CH_3$

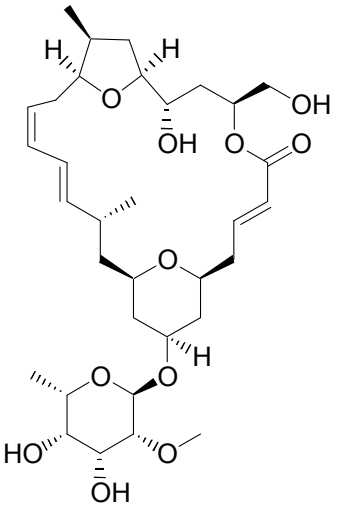

2.20

Just two months later, Ye and co-workers[71] reported another total synthesis of mandelalide A, this time including a reassignment of the stereochemistry of the macrolide moiety.[71] Similar inconsistencies in NMR data (*esp.* the chemical shifts of C11 stereo-center and the attached C25 methyl) were observed by Ye and coworkers, prompting the synthesis of a series of diastereomers of **2.16** and comparison of the NMR data of the synthetic diastereomers with those obtained for the naturally occurring secondary metabolite. From these investigations it was established that the correct structure of mandelalide A is **2.20** in which there is an inversion of the configuration not only at C23 but also C21 and at the oxymethine carbons (C17 and C20) of the tetrahydrofuran moiety when compared to the structure initially proposed for mandelalide A (**2.16**).[23,71] Interestingly, McPhail's original C11 *S* assignment was retained.[71] Ye and co-workers ended their investigation by submitting the synthetic

mandelalide A (**2.20**) into a panel of ten cancer cell lines and curiously reporting that no significant cytotoxicity was observed.[71] In order to unequivocally confirm the structure of mandelalide A, Ye and co-workers sent a small portion of synthetic **2.20** to Mcphail and co-workers. McPhail's group compared the synthetic mandelalide A with its naturally occurring counterpart using CD, NMR, and HPLC profiling (with and without co-elution with the natural product) and confirmed that the true structure of mandelalide A is **2.20**.[72] Interestingly, McPhail also noticed a minor contaminant in the synthetic sample of **2.20** and thus purified the synthetic **2.20** before submitting it into the original bioassay against human NCI-H460 lung cancer cells. Once again potent cytotoxicity was observed. McPhail postulates that the differences observed in bioactivity when **2.20** was tested by Ye and co-workers may be due in part to the impurity of the sample, as well as the type of activity tested *i.e.* mandelalide A may not be antiproliferative but rather cytotoxic to confluent cancer cells.[72]

Finally, the most recent Algoa Bay ascidian to be investigated by McPhail and co-workers was the new species *Synoicum globosum* Parker-Nance, 2012.[54] Four new brominated rubrolides (**2.21** – **2.24**) and two known rubrolides (**2.25** and **2.26**) were isolated *via* NMR-guided fractionation of a dichloromethane/methanol extract of *S. globosum*.[54] The rubrolides **2.21**-**2.26** were found to exhibit varying antibacterial activity in a range of pathogenic anti-bacterial assays.[54]

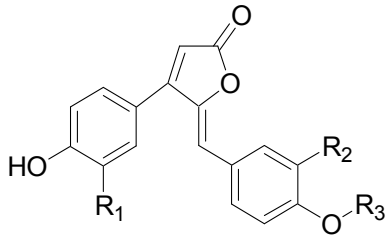

2.21 R_1 = H, R_2 = Br, R_3 = Me
2.22 R_1 = Br, R_2 = H, R_3 = H
2.23 R_1 = Br, R_2 = H, R_3 = Me
2.24 R_1 = Br, R_2 = Br, R_3 = H
2.25 R_1 = H, R_2 = H, R_3 = H
2.26 R_1 = H, R_2 = H, R_3 = Me

2.2 Screening techniques employed to identify nitrogenous metabolites in South African marine ascidians

The screens chosen to identify bioactive marine natural products will inevitably focus on a particular property whether biological, physical or chemical which the metabolites contained in the crude extract must possess to be regarded as being "of interest". Our interest in the chemistry of ascidians was focussed on the ability of ascidians to selectively concentrate metal ions by a phenomenon that is little understood. The initial aims of this study were to

attempt to detect intact organometallic complexes between nitrogenous marine natural products and selected metal ions in crude ascidian extracts and to also establish if metal concentration by ascidians was specific to certain taxonomic clades as opposed to the environment in which they may occur. With these aims in mind the following screens were sequentially employed; a literature survey to establish potential nitrogenous natural product chemical scaffolds that may be produced by South African ascidian genera; an NMR based screen to detect the presence of nitrogenous metabolites due to the prevalence of nitrogenous moieties in metal chelators;[30,47,73–75] the total metal concentration of both the intact ascidian and the organic extract to determine which ascidian species harboured high concentrations of metals which by their presence may indicate possible chelation opportunities; and finally a targeted LC-ICP-MS/ESI-MS investigation of selected South ascidian extracts deemed most likely to exhibit marine natural product metal chelation as a final conclusion to the preliminary screens described above.

2.2.1 MarinLit database survey

One of the most common difficulties for a natural products chemist when faced, as we were, with a sizeable and unique collection of marine organisms (the Algoa Bay ascidian collection contained 63 different ascidian specimens) is to determine which species to investigate with the greatest potential to yield new bioactive natural products. Since there is a paucity of studies of the chemical diversity of the South African ascidian populations, choosing ascidian species for study based on previous studies of ascidian chemistry from the southern African region would have been futile. However, many species in the same genus or family as those found in South African waters have been shown elsewhere around the world to produce a plethora of bioactive natural products, and so having an inventory of Algoa Bay ascidians (identified to the genus level) in hand an investigation of the contemporary global ascidian marine natural product literature was deemed a good starting point towards determining South African species most likely to produce natural products of interest.[2,31]

The marine natural products data base MarinLit[76] was utilised as an aid in the review of compounds isolated from particular ascidian genera. Care had to be taken during this survey as the taxonomy of ascidians is often changing with new techniques *e.g.* genomics being employed to add phylogenetic rigour to the more traditional taxonomic identification of ascidians based on consideration of morphological features only. The ongoing evolution of taxonomic methodology ensures continual renaming and reclassification of species, genera, or even families of ascidians even after literature publication under their previously associated synonym. In order to ensure a thorough analysis of the ascidian literature, all known synonyms obtained from the Ascidiacea World Database[77] were investigated, and incorporated into the set of results obtained for the modern classification of the genera. Figure 2.2 is a summary of the results obtained from the MarinLit survey. The ascidian

genera investigated are those reported to have species present in South Africa, these genera were grouped in to their parent suborders and families. In the case of some very prominent and well documented families, the remaining genera which are common in other locations, but not represented in South Africa were grouped under the title "other". For each genus surveyed the total number of publications listed in MarinLit were accounted for, and presented as either "MNP isolation papers" (show in blue in Figure 2.2), which report on the initial isolation and elucidation of ascidian marine natural products (MNP), or "non-MNP isolation papers" (shown in red in Figure 2.2) which document subsequent studies or reviews on the clinical, biological, ecological, synthetic, or stereochemistry or absolute configurations of ascidian metabolites. The second data set shown in Figure 2.2 depicts the number of isolated natural products contained in the MarinLit database that were related to each genus studied. These isolated natural products were further classed into two subsets, namely "nitrogenous compounds" shown in green, and "non-nitrogenous compounds" shown in purple. The reasoning behind this was because the initial aim of this thesis was to detect and isolate potential metal chelators from ascidians hence ascidians known to produce predominantly nitrogenous metabolites were of great interest due to the possible metal binding potential of their alkaloids.[30,47,73–75]

On initial review of these data obtained from the MarinLit survey it was obvious that some ascidian genera had markedly larger counts of papers and compounds published. Taken on face-value these results would imply that ascidians in these 'popular' genera are prolific producers of new secondary metabolites, however these high numbers should be treated with circumspection as they may rather reflect either a larger number of species in a particular genus or the accessibility, or even preferences, of different species to individual research groups which would bias their collection and further chemical investigations. Similarly, genera boasting a long history of study would also inevitably result in a larger publication output and thus record of isolated metabolites. Most importantly, the interpretation of Figure 2.2 should not ignore other less 'popular' genera whose chemical diversity is yet to be fully explored. In an attempt to account for the large discrepancies in the numbers recorded between well studied and less studied genera, Figure 2.2 contains two differently scaled axes. The axis at the bottom of Figure 2.2, running from left to right, relates to genera with a larger number of publication and/or compounds associated with it in MarinLit, whilst the axis at the top of Figure 2.2, running from right to left, accounts for the genera with a publication or compound count that is lower than twenty and is scaled so that differences between these genera can be compared more readily.

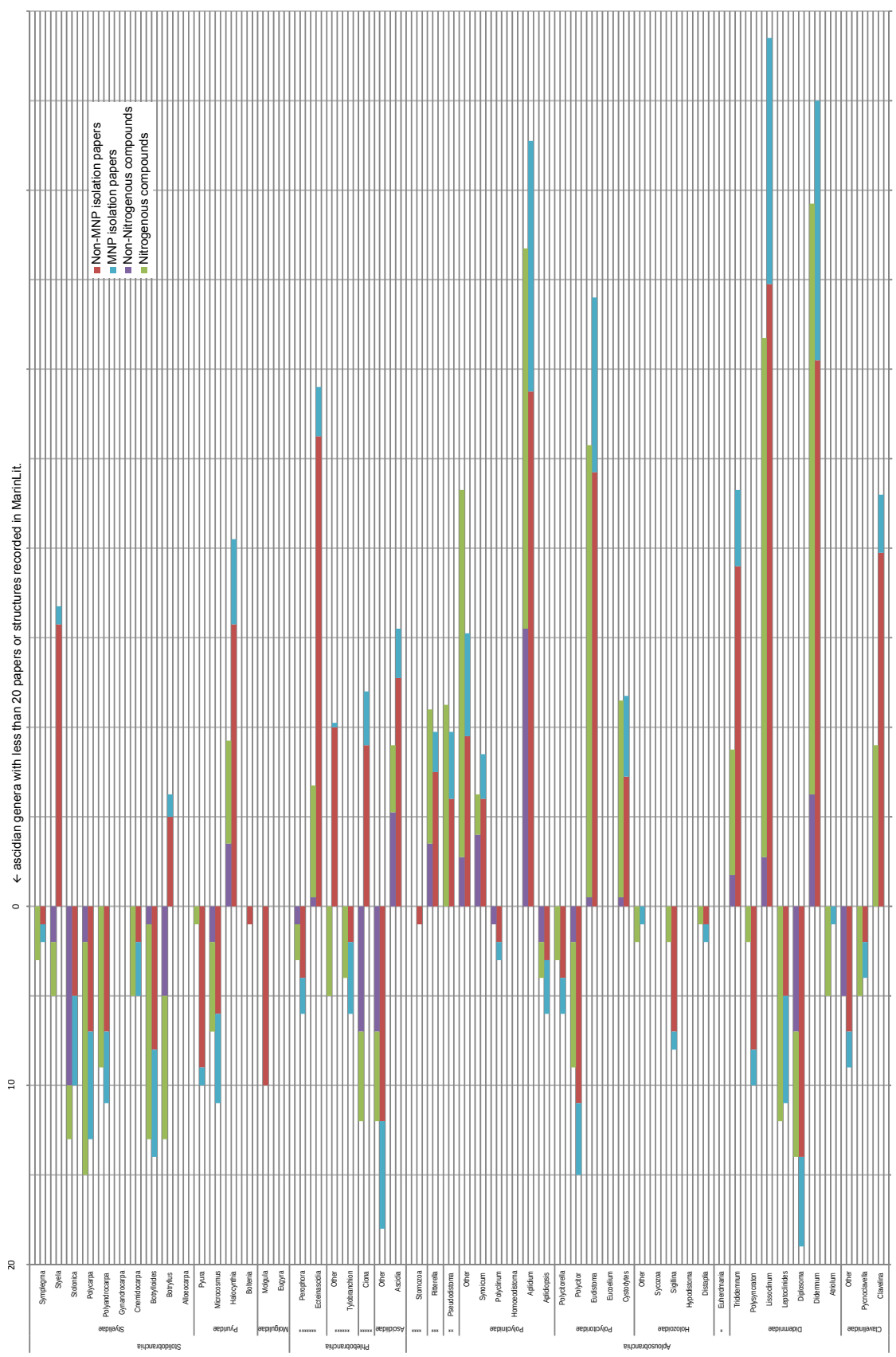

Figure 2.2: MarinLit survey results for South African ascidian genera. Total papers published per genus are displayed as marine natural product (MNP) isolation papers (blue) and non MNP isolation papers (red). Total marine natural product compounds are displayed as nitrogenous (green) and non-nitrogenous (purple). Ascidian genera with records over 20 are on the axis that reads from left to right, whilst those with records totalling less than 20 are plotted on the axis that reads right to left
(* = Euherdmaniidae: ** = Pseudodistomidae: *** = Ritterellidae: **** = Stomozoidae: ***** = Cionidae: ****** = Diazonidae: ******* = Perophoridae)

The MarinLit survey results displayed in Figure 2.2 were used to determine which ascidians from the South African collection were more likely to afford nitrogenous secondary metabolites in the screening protocols that followed this initial literature survey. Figure 2.2 shows that the MarinLit ascidian results are dominated by the suborder Aplousobranchia which is also the most well represented ascidian suborder in the waters off South Africa.[78] Not surprisingly the majority of the species chosen for screening were members of this suborder. The Aplousobranch genera that dominate the chemical literature (>100 publications or isolated secondary metabolites) include *Didemun*, *Lissoclinum*, *Eudistoma*, and *Aplidium*. These genera are well represented in South Africa and were an obvious choice to be included in our further screens. Aplousobranch genera such as *Clavelina, Tridemnum*, *Cystodytes*, *Synoicum* and *Pseudodistoma* produced moderate results (> 30 publications or isolated secondary metabolites), and because nitrogenous metabolites isolated dominated the secondary metabolite profiles of these genera they were also included in our further screens. The genera *Ritterella*, *Ascidia*, *Ecteinascidia*, and *Halocynthia* were not well represented in Algoa Bay, and so were excluded from the screens.

Conversely even though the genera *Pycnoclavella*, *Atriolum*, *Distaplia*, *Hypodistoma*, *Sigillina*, *Aplidiopsis* and *Botryllus* were the subject of only a few studies (<10) from the MarinLit survey (Figure 2.2), they are reasonably abundant in Algoa Bay and alkaloids dominate the secondary metabolites reported from these genera. Finally, the ascidian genera *Hypodistoma* and *Gynandrocarpa* had no records in MarinLit, and so would normally have been overlooked however the species *Hypodistoma vastum* and *Gynandrocarpa placenta* are very common species in Algoa Bay, and so were also included on the off chance that they would prove to be new reservoirs of nitrogenous secondary metabolites. The ascidian extracts subjected to further screening are listed in Table 2.1 together with the summarised screening results for these extracts.

2.2.2 ^{1}H-^{15}N HMBC NMR Screening

The first screen that was carried out, to confirm the presence of nitrogenous metabolites, was a general ^{1}H-^{15}N gHMBC NMR screen of the 20 ascidians selected from the results of the MarinLit survey. One of the aims of this thesis study was to detect and isolate potential metal chelators in ascidian extracts. Since nitrogeneous metabolites have previously been shown to complex with metals, a screen focused on highlighting ascidians whose extracts were rich in these metabolites was deemed appropriate.[30,47,73–75] The most efficient and cost effective method to detect nitrogen containing metabolites in a crude marine extract is LC-MS.[79] Unfortunately, the dearth of mass spectrometry facilities at Rhodes University was a significant challenge for our initial screening programme and was rectified later in the programme through collaboration with Professor Marcel Jaspars at the Marine Biodiscovery Centre at the University of Aberdeen. Fortuitously, in the period before being able to access

the MS facilities at the University of Aberdeen our research group had relatively unlimited access to the Rhodes University 600 MHz NMR, which was underutilised at the time when our screening programme was embarked upon, and hence a protocol was set up to employ this high powered analytical instrument for the detection of nitrogenous metabolites in crude ascidian extracts.

Table 2.1: Results from the screening of South African ascidian crude extracts. ^{1}H-^{15}N HMBC values are the numbers of distinct correlations observed. Tick marks indicate ascidian extracts where total metal analysis was conducted. Elements that produced significant peaks in the LC-ICP-MS/ESI-MS analysis are recorded. (The presence of a "–" indicates that the corresponding screen was not run on that particular ascidian sample)

Algoa Bay Ascidians				**Hits in Screens**		
Suborder	**Family**	***Species name***	**Sample Code**	**^{1}H-^{15}N HMBC**	**ICP-MS**	**LC-ICP-MS/ESI-MS**
Aplousobranchia	Clavelinidae	*Clavelina steenbrasensis*	TIC2011-036	-	✓	-
		Pycnoclavella filamentosa	SAF2004-058	1	✓	^{51}V, ^{75}As, ^{79}Br, ^{127}I
		Pycnoclavella narcissus	TIC2011-005	-	✓	-
	Didemnidae	*Atriolum marinense*	SAF2004-043	3	✓	^{127}I
		Didemnum leopardi	SAF2004-044	0	✓	-
		Didemnum sp.1	SAF2004-065	5	✓	^{63}Cu, ^{75}As, ^{79}Br, ^{127}I
		Didemnum sp.2	SAF2004-061	5	✓	^{63}Cu, ^{77}Se, ^{79}Br, ^{127}I
		Didemnum sp.3	SAF2004-031	2	-	-
		Didemnum sp.4	SAF2004-071	4	-	-
		Lissoclinum sp. nov.	TIC2011-035	-	✓	-
		Tridemnum cerebriforme	TIC2011-018	-	✓	-
		Leptoclinides sp.	SAF2004-015	2	✓	^{51}V, ^{75}As, ^{79}Br, ^{127}I
	Holozoidae	*Distaplia skoogi*	SAF2004-030	2	✓	^{51}V, ^{75}As, ^{79}Br, ^{95}Mo, ^{127}I
		Hypodistoma vastum	SAF2004-012	0	✓	-
		Sigillina sp.	SAF2004-051	2	✓	^{51}V, ^{63}Cu, ^{75}As, ^{79}Br, ^{127}I
	Polyclinidae	*Aplidiopsis tubiferus*	SAF2004-038	3	✓	^{75}As, ^{79}Br, ^{95}Mo
		Synoicum sp.	TIC2011-027	-	✓	^{63}Cu, ^{75}As, ^{79}Br, ^{127}I
		Aplidium sp.1	SAF2004-039	3	✓	^{51}V, ^{59}Co, ^{63}Cu, ^{75}As, ^{79}Br, ^{127}I
		Aplidium monile	TIC2011-032	-	✓	^{51}V, ^{75}As, ^{79}Br, ^{127}I
	Polycitoridae	*Polycitor* sp. nov.	SAF2004-068	4	✓	^{75}As, ^{79}Br, ^{127}I
		Eudistoma sp.1	SAF2004-028	2	✓	^{51}V, ^{59}Co, ^{63}Cu, ^{75}As, ^{79}Br, ^{127}I
		Eudistoma sp.2	SAF2004-037	3	✓	-
	Pseudodistomidae	*Pseudodistoma* sp.1	SAF2004-019	3	✓	-
		Pseudodistoma sp.2	SAF2004-022	1	✓	-
		Pseudodistoma sp.3	SAF2004-062	4	✓	-
Stolidobranchia	Styelidae	*Botryllus* sp.	TIC2011-026	-	✓	-
	Polyzoinae	*Gynandrocarpa placenta*	SAF2004-010	3	✓	-

Although both ^{14}N and ^{15}N exhibit nuclear magnetic moments (0.14 μ and -0.10 μ respectively), a crucial property for NMR analysis, the naturally abundant isotope, ^{14}N

(99.6%), has a spin quantum number of I = 1 and is therefore susceptible to quadrupolar relaxation resulting in the generation of broad and mostly unhelpful NMR signals.[80] However, the spin quantum number of ^{15}N is I = ½ resulting in a symmetrical, spherical charge distribution which is a more desirable property for an NMR investigation. However, the natural abundance of ^{15}N is only 0.4% and this characteristic coupled with a low relative magnetic moment makes the detection of non-^{15}N-enriched metabolites through conventional 1D NMR experiments impractical. Fortunately, the increase in sensitivity seen with the advent of inverse detection 2D NMR experiments *i.e.* indirect detection of a heteronucleus through the proton channel, has allowed the detection of ^{15}N without isotope labelling.[80] The 2D NMR experiment chosen for this screen was the heteronuclear multiple bond correlation (HMBC) capable of detecting ^{2}J and ^{3}J correlations between ^{1}H-^{15}N. Information obtained through analysis of HMBC data was believed to be more useful than that which would have resulted from analysis through the ^{1}H-^{15}N heteronuclear single quantum coherence (HSQC) experiments due to the potential of the HMBC experiment to detect primary, secondary and tertiary nitrogen moieties. The pulse program used was the same as that which would be employed for a standard ^{1}H-^{13}C gHMBC experiment, *i.e.* Bruker Topspin hmbcgplpndqf,[81] except that the second acquisition constant (CNST2) was changed from 145 Hz to 90 Hz which corrects the differences in coupling constant for the heteronucleus changing from carbon to nitrogen. The first and third gradient parameters were also corrected to 70% and 50.1% respectively.[81] Since the chemical shifts of the nitrogen resonances were unknown, a broad sweep width of 650 ppm was set and centred at O2= 200 ppm.

The combined results of the ^{1}H-^{15}N HMBC NMR screens of all 20 ascidian extracts are presented in Figure 2.3 as a single HMBC plot with all the individual ascidian extract ^{1}H-^{15}N HMBC NMR experiments overlaying each other allowing common correlations to appear more intense. The numbers of significant ^{15}N HMBC correlations, determined through the use of Bruker's Topspin oblique view,[81] are recorded in Table 2.1. Of the 20 ascidian extracts entered into this screen, only three extracts, namely SAF2004-044, SAF2004-012 and SAF2004-039, did not produce any significant ^{1}H-^{15}N HMBC correlations. Interestingly, thirteen ascidian extracts produced a pattern of common correlations from the proton resonances at δ_H 2.73 and 3.16 ppm to the nitrogen chemical shifts 36.9 and 51.3 ppm respectively, and within this set of ascidians, eleven extracts produced a third common correlation between δ_H 4.27 and δ_N 196.3 (Figure 2.3).

This pattern of correlations was initially proposed to be produced by a common guanidine [$HNC(NH_2)_2$] containing metabolite which would produce three distinct ^{15}N resonances. Ascidians have been found to be fairly prevalent producers of guanidine metabolites[82,83] however all attempts to isolate and characterise a metabolite of this class from the ascidian extracts under investigation were unsuccessful. The two common shielded correlations with proton resonances in the methylene window may also be attributed to aliphatic amines which are also fairly ubiquitous in the marine environment.[67,68]

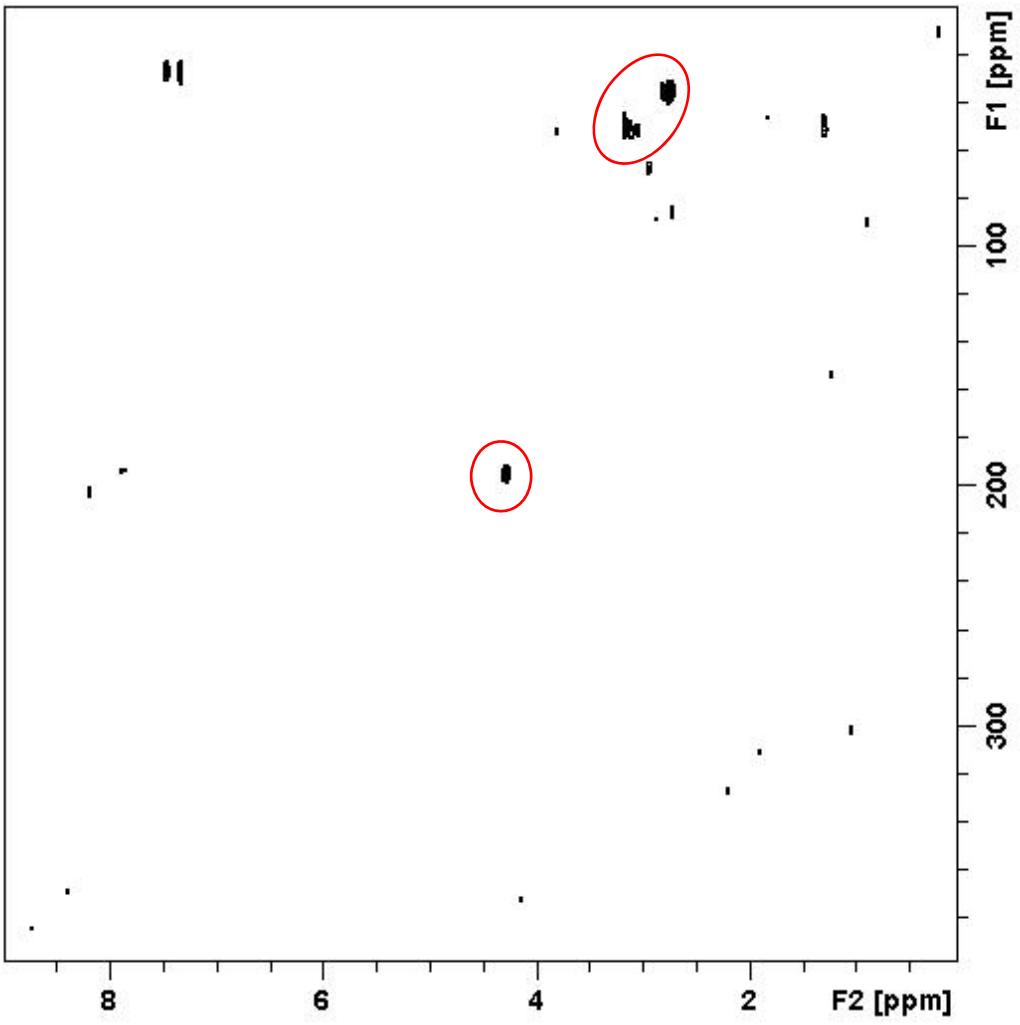

Figure 2.3: A region (F1 = δ 0.0-9.0 ppm; F2 = δ 0-400 ppm) of the stacked ^{1}H-^{15}N gHMBC spectra (DMSO-d6, 600 MHz) obtained for the 20 crude extracts of South African ascidians. The accompanying circles highlight the common correlations detected in most extracts.

2.2.3 Total Metal Ion Concentration Analysis

Following analysis of the data generated through the ^{1}H-^{15}N gHMBC NMR screen a subsequent collection of ascidians belonging to our selected South African genera of interest was made. The combined sample set from both collections was entered into the second investigation in which the total metal ion concentrations were established *via* ICP-MS. The ascidians collected after the ^{1}H-^{15}N gHMBC NMR screen were distinguished by the sample code prefix TIC2011. The results from the total metal concentration analyses are presented in depth in Chapter 3. The ICP-MS total metal analysis results obtained after nitric acid digestion of the organic extracts of each ascidian are presented in Figure 2.4. The metal concentrations are reported in mg of metal per kg of organic extract. Based on these metal concentrations thirteen ascidian extracts were chosen for further speciation analysis.

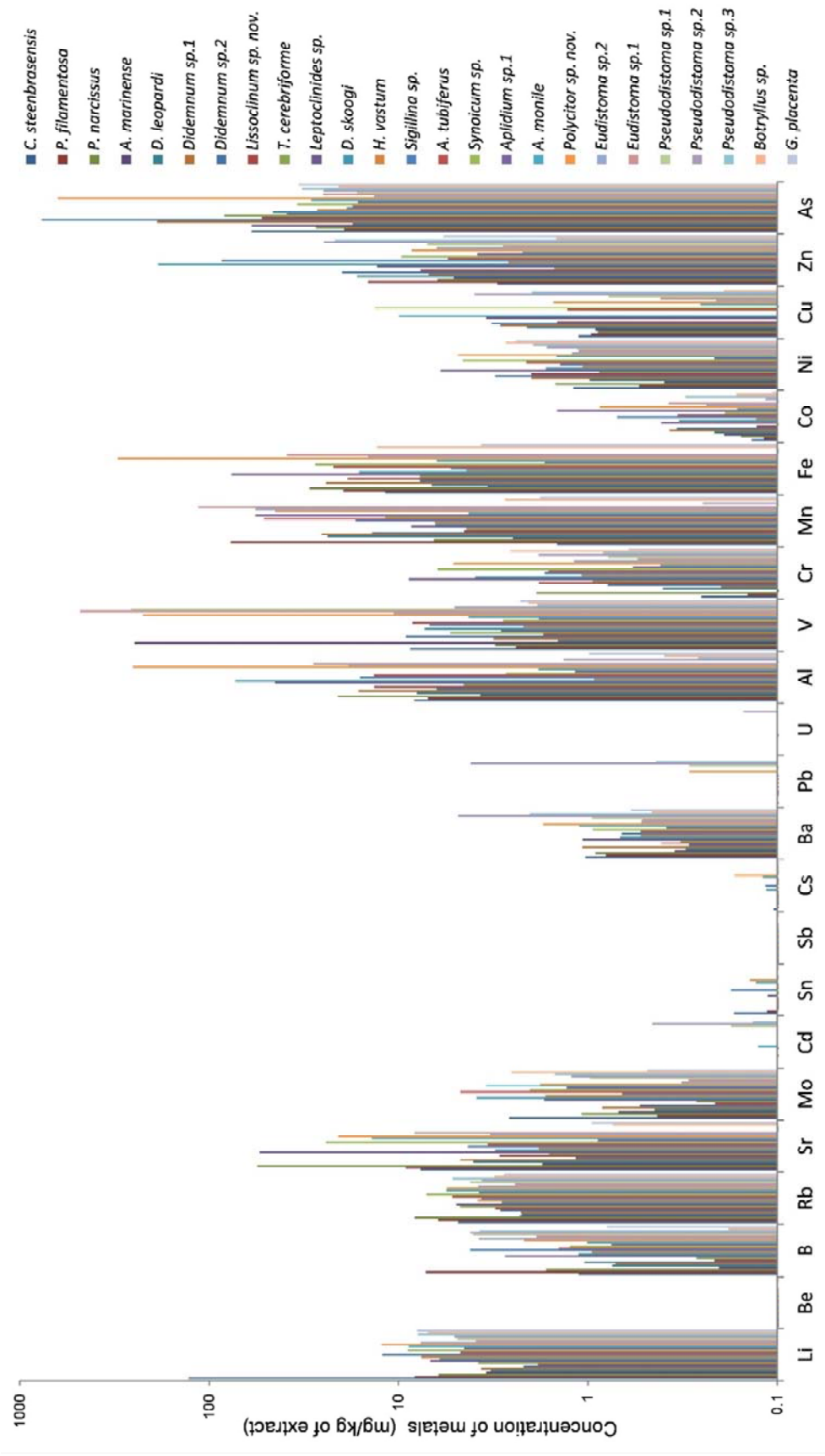

Figure 2.4: Concentrations (mg/kg) of metals in the organic extracts of 25 Algoa Bay ascidians. Values were obtained after HNO_3/H_2O_2 digests of the CH_2Cl_2/MeOH extracts of the respective ascidian specimens.

2.2.4 Speciation Analysis

Speciation studies were carried out on thirteen of the ascidian extracts which were flagged due to high levels of metals detected through total metal concentration analysis. The assumption we made was that the opportunity of detecting chelated species was greater in ascidians with high concentrations of metal ions. The speciation study utilised the unique arrangement of analytical equipment, present at the Marine Biodiscovery Centre (MBC) at the University of Aberdeen, which incorporated reversed-phase liquid chromatography (LC) with the parallel detection systems of inductively coupled plasma mass spectrometry (ICP-MS) and electrospray ionisation mass spectroscopy (ESI-MS). Jaspars and co-workers at MBC have reported success in the detection of metal and metalloid complexes through the use of LC-ICP-MS/ESI-MS (Figure 2.5).[45–47,75,84–90] The brief overview of this powerful analytical technique follows.

a)

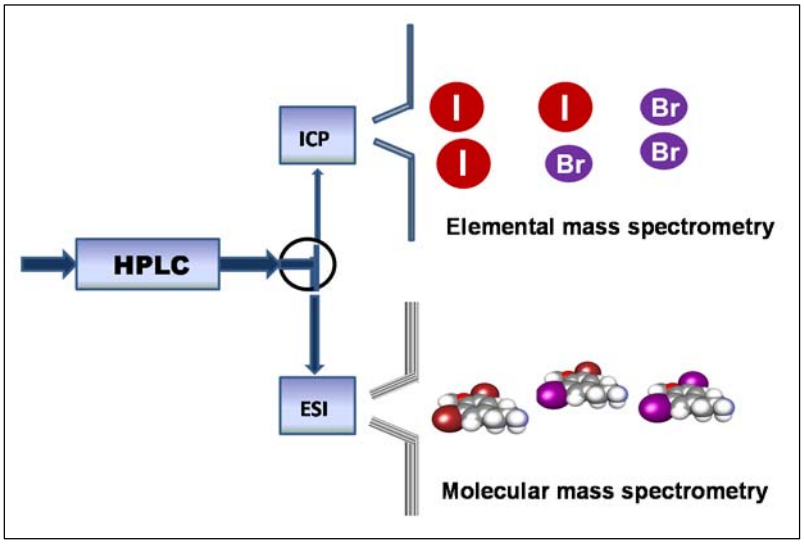

b)

Figure 2.5: Schematic diagram of the hyphenated LC-ICP-MS/ESI-MS technique (a) and the LC-ICP-MS/ESI-MS instrumentation used by the author in the Marine Biodiscovery Centre of Aberdeen University (b).

Inductively coupled plasma mass spectrometry (ICP-MS) is a popular analytical technique used to determine the elemental (metal ion) content of biological samples. ICP-MS has the capacity to measure multiple elements concurrently to an impressive part-per-billion (ppb) level of sensitivity.[75] However, this technique results in the complete destruction, atomisation and ionisation of the analytes making it an inherently elemental analysis technique and alone cannot give information regarding intact organic molecules for example incorporated in organo-metalic complexes. Liquid chromatography (LC) provides an opportunity to separate the organic components in complex matrices based on the varying retention times of different organic compounds on a particular chromatography column. If suitable standards are available the presence and concentrations of known compounds in biological samples can be determined directly from equivalent LC retention times. However, when dealing with crude extracts containing unknown and possibly novel secondary metabolites, where standards are not available, no conclusive molecular identifications of organo-metallic complexes can be made by coupling LC to ICP (LC-ICP-MS).[75]

Obtaining molecular information is essential for the determination of organo-metallic complexes that may be present in crude biological extracts. Electrospray ionisation mass spectrometry (ESI-MS) is a soft ionisation technique which is capable of ionising even unstable compounds and complexes without fragmentation.[75] ESI-MS may also be coupled with HPLC which aids in the identification of metabolites through chromatographic separation. When working with crude biological extracts it is difficult to identify possible metal containing complexes, as often one is searching blind, without prior knowledge of the polarity or mass signature of the complex.[75]

If these two powerful analytical techniques are used in parallel, invaluable elemental and molecular information is obtained. Using one HPLC system whose eluent is split between the ICP-MS and the ESI-MS ensures that the separated metabolites are analysed by both techniques simultaneously and has the added benefit of modifying the chromatography system to suit the properties of the analytes.[75] The LC-ICP-MS data pinpoints the retention times at which the elements of interest are found, whilst analysis of the ESI mass spectra produced at these retention times provides the crucial molecular information necessary in determining the structure of the compounds that may be associated with these elements *i.e.* as metal containing complexes.[75]

A common chromatography system used in the ESI-MS analyses of natural crude extracts is reversed-phase HPLC using methanolic solvent systems which offer effective solubility of a wide range of secondary metabolites and provide the solvent volatilty necessary for ESI-MS analysis.[75] The successful use of reversed-phase chromatography in parallel with ICP-MS and ESI-MS has been reported by the University of Aberdeen group in a number of studies in which arsenic containing biomolecules have been identified from a variety of sources

including cabbage, whelks, capelin fish and brown alga.[84–87] The covalent C-As bonds within these organo-arsenic compounds add stability and so they are not as likely to dissociate when exposed to reversed-phase (RP) chromatography as do metal chelates.[75] The detection of intact plant phytochelatin complexes with arsenic and mercury exposed to reversed-phase LC-ICP-MS/ESI-MS is a promising result showing that at least some biological metalloid and metal complexes are stable enough for detection through harsh reversed-phase chromatography.[88,89]

The first ascidian extract to be investigated by the Jaspars group using LC-ICP-MS/ESI-MS was *Lissoclinum patella*. *L. patella* afforded the cyclic peptides patellamides which have been shown through circular dichroism studies to complex copper.[45,46,73,90] In order to ensure that the copper complexes did not dissociate on chromatography Jaspars and co-workers ustilised a poly(methyl methacrylate) size-exclusion chromatography (SEC) column which reduced dissociation because there is little interaction between the analyte and the stationary phase.[75] Copper-patellamide complexes were successfully observed using SEC-ICP-MS/ESI-MS in an extract of *L. patella* that was spiked with copper however when the extract on its own, without the copper doping, was analysed no complexes were detected implying that these patellamides are not in fact complexed with copper in the ascidian.[75] Since this investigation involved previously established metal complexes it was a good starting point for the method development of SEC-ICP-MS/ESI-MS analyses of crude ascidian extracts.

Jaspars and co-workers subsequently used SEC-ICP-MS/ESI-MS to investigate a crude extract of the ascidian *Eudistoma gilboviride* which was found, through total metal concentration data, to contain high levels of iron. The data produced through SEC-ICP-MS/ESI-MS analysis revealed peaks at the same retention times in both the iron and bromine ICP-MS traces. Analysis of the ESI mass spectra recorded at these retention times identified a series of complexes involving Fe(II) and eudistomin H (**2.27**) and its analogues.[47] The authors state that although detection of intact iron complexes in the crude extract of *E. gilboviride* was successful, it is still not definitive proof that these complexes occur in the living ascidian, as there is a possibility that these complexes formed during the extraction process.[47] The successful SEC-ICP-MS/ESI-MS analysis of extracts of *L. patella* and *E. gilboviride* without dissociation of the metal complexes is a testament to the capabilities of SEC chromatography over RP chromatography. However, the negative aspect of using this SEC column is that without a customised buffered solvent system hydrophilic sites along the stationary phase result in chelate dissociation and prolonged retention of analytes.[75] The solvent system that was employed for the *L. patella* and *E. gilboviride* studies was accordingly 50 nM trimethylamine carbonate buffer at pH 8.8, which successfully eluted the majority of the metal complexes intact. The metal complexes that were retained on the column were subsequently eluted with a formic acid and methanol solvent system fortunately with marginal observed dissociation.[47,75]

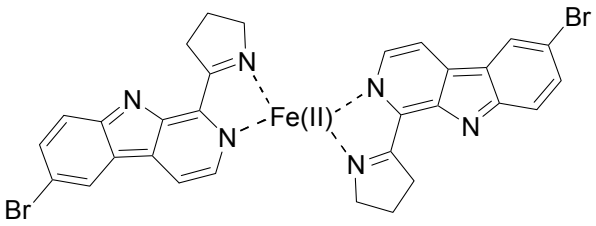

2.27

The trimethylamine buffer used by Wright *et al.* is unfortunately very unpleasant to work with due to a distasteful odour reminiscent of rotting fish. This property, along with the need for two separate solvent systems to ensure the complete elution of all metabolites, means that the use of a SEC column for the speciation of more than one ascidian extract is not practical, and to this end our investigation comprised of reversed-phase LC-ICP-MS/ESI-MS analysis. Any promising extract data obtained through this speciation analysis would be considered for subsequent SEC-ICP-MS/ESI-MS analysis.

For the speciation of the thirteen South African ascidian extracts the ICP-MS analyses focused specifically on the detection of V (*m/z* 51), Mn (*m/z* 55) Fe (*m/z* 57), Co (*m/z* 59), Cu (*m/z* 63), Zn (*m/z* 66), As (*m/z* 75), Se (*m/z* 77), Br (*m/z* 79), Mo (*m/z* 95) and I (*m/z* 127), whilst the ESI-MS simultaneously obtained mass data to aid in the identification of organic substituents. Ascidian crude extracts were prepared at Rhodes University following an established procedure (documented in Chapter 6) developed by Jaspars and co-workers in order to minimise metal contamination. Table 2.1 summarises the elements which were detected and produced peaks in the ICP-MS traces obtained from each ascidian extract. Unfortunately, although metals were detected in the LC-ICP-MS traces of a number of ascidian extracts the peaks produced were of low intensity, and were often insufficiently resolved to be considered for SEC-ICP-MS/ESI-MS analysis. Attempts were made to identify possible metal containing complexes at the retention times where metal ions detected by ICP-MS were coincident with the retention times of metabolites revealed by ESI-MS. However, because enhanced dissociation was increasingly likely following exposure to reversed-phase chromatography conditions, any organometallic complexes that had survived were potentially at very low concentrations thus resulting in small MS peaks which are always difficult to detect due to higher noise levels at low concentrations. During the LC-ICP-MS/ESI-MS analyses it soon became evident that this parallel mass analysis technique was particularly useful for identifying halogen (Br, I) containing secondary metabolites in the crude ascidian mixtures. Examples of these analyses are documented in the following section of this chapter.

2.3 Further analysis of selected ascidian extracts containing halogenated nitrogenous secondary metabolites

The following ascidian extracts produced promising results in the preliminary ^{1}H-^{15}N gHMBC NMR and LC-ICP-MS/ESI-MS screens, and were worked up accordingly when sufficient ascidian material was available to isolate the halogenated compounds. Where insufficient ascidian material was available to isolate the halogenated metabolites the screening results are noted, and potential ascidian extracts for further study are highlighted.

2.3.1 Distaplia skoogi - SAF2004-030

Specimen SAF2004-030 was a colony of the cream colour morph of *Distaplia skoogi* Michaelsen, 1934,[49,50] Aplousobranchia: Holozoidae,[49] (Figure 2.6). The ascidian *Distaplia skoogi* was collected using SCUBA at a depth of 25 m in White Sands, Algoa Bay, South Africa, in July 2004, and kept frozen until extraction.

Figure 2.6: *Distaplia skoogi*, collection specimen SAF2004-030 (left) and photographed at White Sands, Algoa Bay, South Africa (right, photograph by Dr. A. Oosthuizen).

2.3.1.1 Results from the ^{15}N HMBC screen

The ascidians SAF2004-030 (*Distaplia skoogi*) and SAF2004-051 (*Sigillina* sp.) are both from the family Holozoidae and their crude extracts both revealed distinct correlations from aromatic proton resonances (δ_H 7.25- 7.55) to nitrogenous functionalities (δ_N 20- 35) in the ^{15}N HMBC screen. Figure 2.7 depicts a region (F1 = δ 0.0-9.0 ppm; F2 = δ 0-200 ppm) of the ^{15}N HMBC spectrum obtained for the crude extract of *D.skoogi* clearly showing the correlations that flagged this extract for further study.

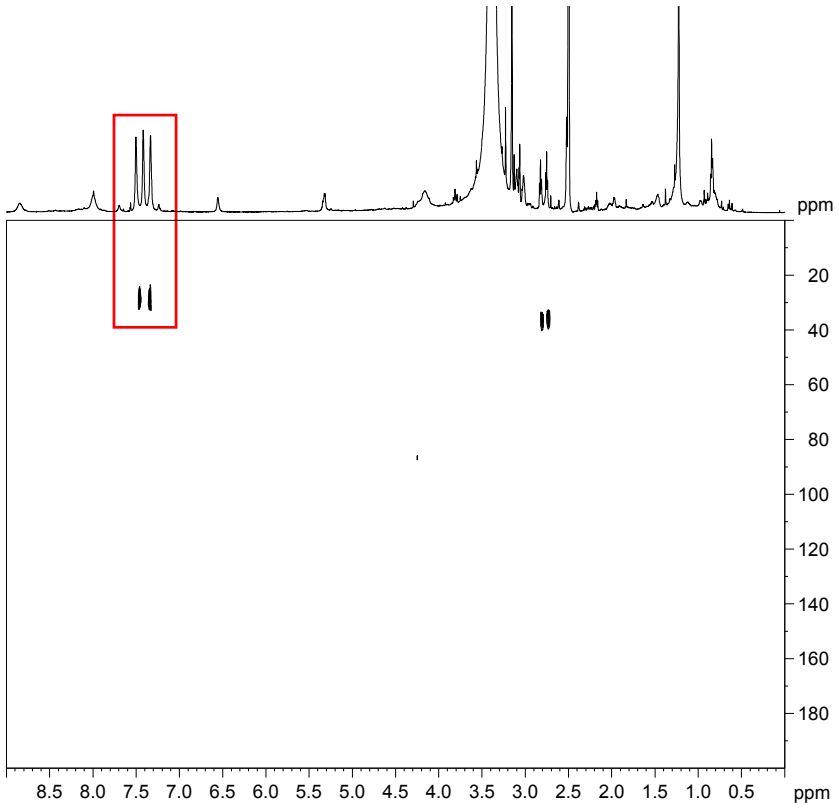

Figure 2.7: A region (F1 = δ 0.0-9.0 ppm; F2 = δ 0-200 ppm) of the ^{15}N HMBC spectrum (DMSO d-6, 600 MHz) obtained for the crude extract of *D. skoogi*.

2.3.1.2 Results from the LC-ICP-MS/ES-MS screen

Inspection of the LC-ICP-MS/ESI-MS data obtained for the crude extract of *D. skoogi* indicated the presence of relatively high levels of iodine, molybdenum, bromine, arsenic and vanadium in the extract (Figure 2.8). The intensities of the peaks found in the bromine (*m/z* 79) ICP-MS trace were markedly stronger that those observed for the other elements detected, suggesting the presence of significant amounts of one or more brominated metabolites and provided the rationale to continue and isolate and identify these brominated metabolites from the extract.

Figure 2.9 is a summary of the analysis of the LC-ICP-MS/ESI-MS data obtained for the crude extract of *D. skoogi* and reveals how this analysis was utilised to detect the presence of brominated metabolites. The bromine (*m/z* 79) ICP-MS trace is depicted in red, and the ESI-MS extracted ion chromatograms (EIC) of the brominated metabolites detected at selected retention times are shown in black [Figure 2.9(a)]. The ESI-MS spectra observed at selected

retention times coincident with the retention times of bromine peaks in the ICP-MS mass spectra are displayed in Figure 2.9(b).

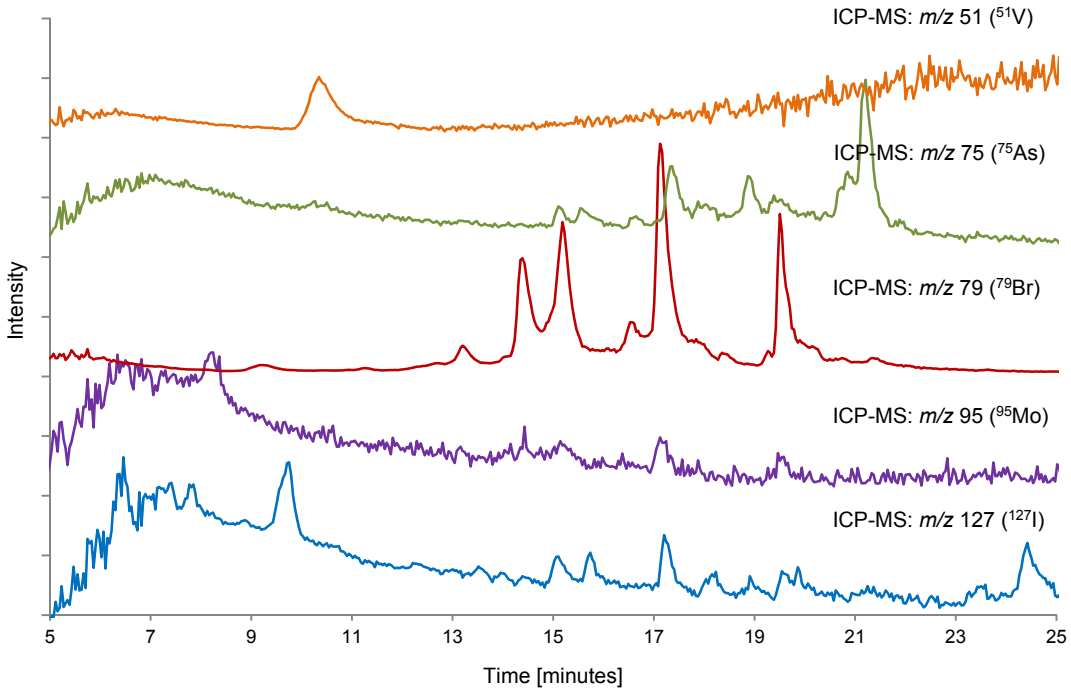

Figure 2.8: Selected LC-ICP-MS traces obtained for SAF04-030 (^{127}I blue trace, ^{95}Mo purple trace, ^{79}Br red trace, ^{75}As green trace and ^{51}V orange trace). Traces are vertically offset for clarity

The peak at retention time (T_R) 14.40 min in the bromine ICP-MS trace strongly overlaps with the ESI-MS EIC for *m/z* 211.9707 indicative of a brominated metabolite with this T_R in LC-ESI-MS. The ESI-MS mass spectrum at this T_R [14.40 min, Figure 2.9b)(i)] contained the ion cluster *m/z* 211.9706, 213.9686 in a 1:1 ratio which is characteristic of a monobrominated compound. The best fit simulation[91] resulted in the potential molecular formula of $C_8H_7ON^{79}Br$ [$(M+H)^+$ Δ 0.2 mmu] which was confirmed after isolation and structure elucidation (Section 2.3.1.3) to correspond to the bromo-oxindole **2.28**.

The major peak observed at T_R 17.13 min in the LC-Br-ICP-MS trace overlapped perfectly with the peak occurring at equivalent T_R in the LC-ESI-MS chromatogram which afforded a dominant ion cluster of *m/z* 589.9687, 591.9662, 593.9640 in a 1:2:1 ratio indicative of a dibrominated compound [Figure 2.9(b)(ii)]. Unfortunately attempts to isolate and identify this compound were unsuccessful. A point to note for possible further study is that at this T_R (17.13 min) peaks were observed in both the iodine (*m/z* 127) and molybdenum (*m/z* 95) ICP-MS traces obtained for *D.skoogi* (Figure 2.9). The intensities of these peaks were lower than that detected for bromine (*m/z* 79), however they may still imply a compound or number of compounds containing iodine, molybdenum and bromine.

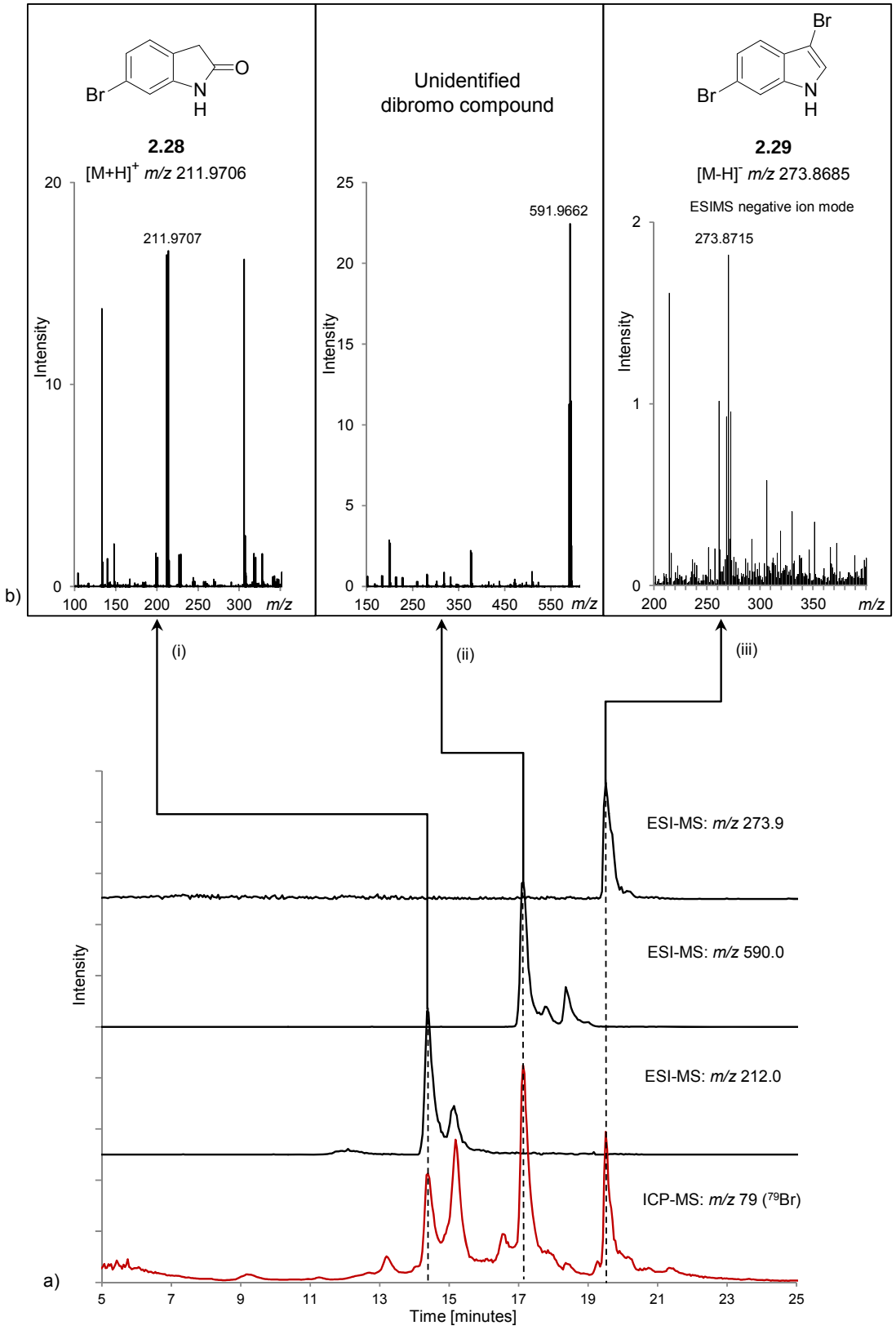

Figure 2.9: Halogenated metabolites detected in SAF04-030 extract by LC-ICP-MS/ESI-MS. a) Selected ICP-MS and ESI-MS EICs; b) ESI mass spectra and structures for (i) **2.28** at T_R 14.40 min, (ii) unidentified dibrominated compound at T_R 17.13 min, and (iii) **2.29** at T_R 19.50 min detected in ESIMS negative ion mode.

The third peak investigated in the Br-ICP-MS trace of *D. skoogi* had a T_R of 19.50 min. Attempts to obtain an extracted ion chromatogram (EIC) which overlapped with the Br-ICP-MS chromatogram were only successful in ESI in the negative ion mode. The negative ion ESI-MS EIC for *m/z* 272, was a good fit, and related to the ESI mass spectrum containing the 1:2:1 ratio isotope pattern at *m/z* 271.8735, 273.8715, 275.8694 suggesting the presence of a dibrominated metabolite [Figure 2.9(b)(iii)]. The [$(M-H)^-$] ion simulation[91] calculated for $C_8H_4N^{79}Br_2$ (Δ 3.0 mmu) resulted in the closest fit to the experimental data. The structure of this compound was later confirmed after isolation and structure elucidation to be 3,6-dibromoindole (**2.29**, Section 2.3.1.3).

*2.3.1.3 Isolation and structure elucidation of **2.28**, **2.29** and **2.30***

Due to the promising screening results, a larger portion of *D. skoogi* (SAF2004-030) was lyophilised and sequentially extracted with methanol followed by dichloromethane. The combined organic extracts were concentrated under reduced pressure before being subjected to a liquid-liquid partitioning between ethyl acetate and water. The nonpolar ethyl acetate partition was subjected to extensive normal phase DIOL HPLC, shown in Scheme 2.1, to yield the known compounds 6-bromo-2-oxindole (**2.28**), 3,6-dibromoindole (**2.29**), and 6-bromo-3-chloroindole (**2.30**).

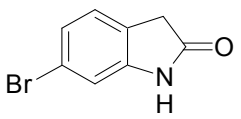

2.28

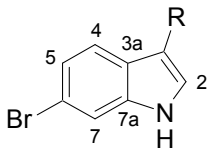

2.29 R = Br
2.30 R = Cl

The oxindole **2.28** was isolated as colourless needles with a melting point range of 216 - 219 °C. The molecular formula of **2.28** was established as $C_8H_6NO^{79}Br$ from HRESIMS, *m/z* 211.9710 (Δ 0.4 mmu) which implied six degrees of unsaturation. The IR spectrum contained a characteristic carbonyl band at 1643 cm^{-1}, as well as a strong band at 3435 cm^{-1}, indicating the possible presence of an amide.[80] The presence of a carbonyl moiety was further supported by a deshielded ^{13}C NMR resonance (δ_C 176.4) and thus accounted for one of the six double bond equivalents required by the molecular formula. The ^{13}C NMR spectrum also showed the presence of three aromatic methines (δ_C 126.0, 125.3 and 112.9), three aromatic quaternary carbon signals (δ_C 143.4, 124.0, 121.3) as well as a methylene carbon (δ_C 35.6), suggesting a monosubstituted bromo-oxindole chemical structure for **2.28** (Figure 2.10). Correlations observed in a 2-dimentional COSY NMR experiment between the aromatic protons δ_H 7.16 and 7.08 (J = 7.9 Hz) and the long range correlation between δ_H 7.16 and

7.03 (J = 1.5 Hz) suggested that the oxindole system was brominated at position 6 (Figure 2.11).

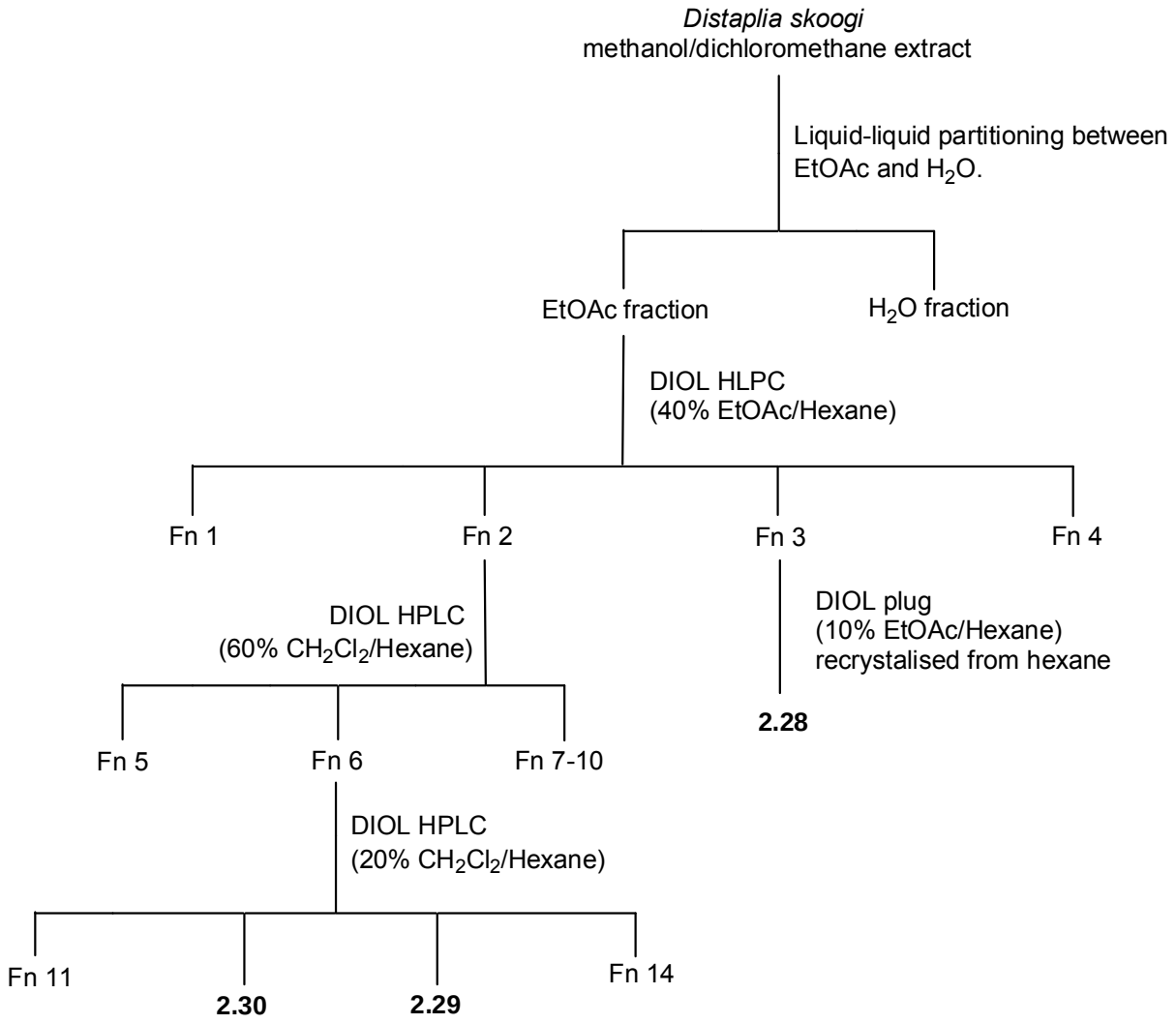

Scheme 2.1: Chromatography protocol used to isolate **2.28**-**2.30** from *Distaplia skoogi*

The distinctive, approximately 1:1 protonated molecular ion [$(M+H)^+$] isotope pattern [(*m*/*z* 214 (100), 212 (97)] in the ESI mass spectrum confirmed this substituent to be bromine. The ^2J and ^3J gHMBC correlations acquired for **2.28** (Table 2.2) unequivocally supported the proposed structure for **2.28**.

The oxindole **2.28** is commercially available[92] and has also been detected, using GC/MS, in extracts of the marine murex molluscs *Plicopurpura patula* and *Plicopurpura columellaris* (Mollusca: Gastropoda).[93] The presence of the same secondary metabolite in marine organisms from different phyla may indicate a common symbiotic microbial source for **2.28**.[94–96]

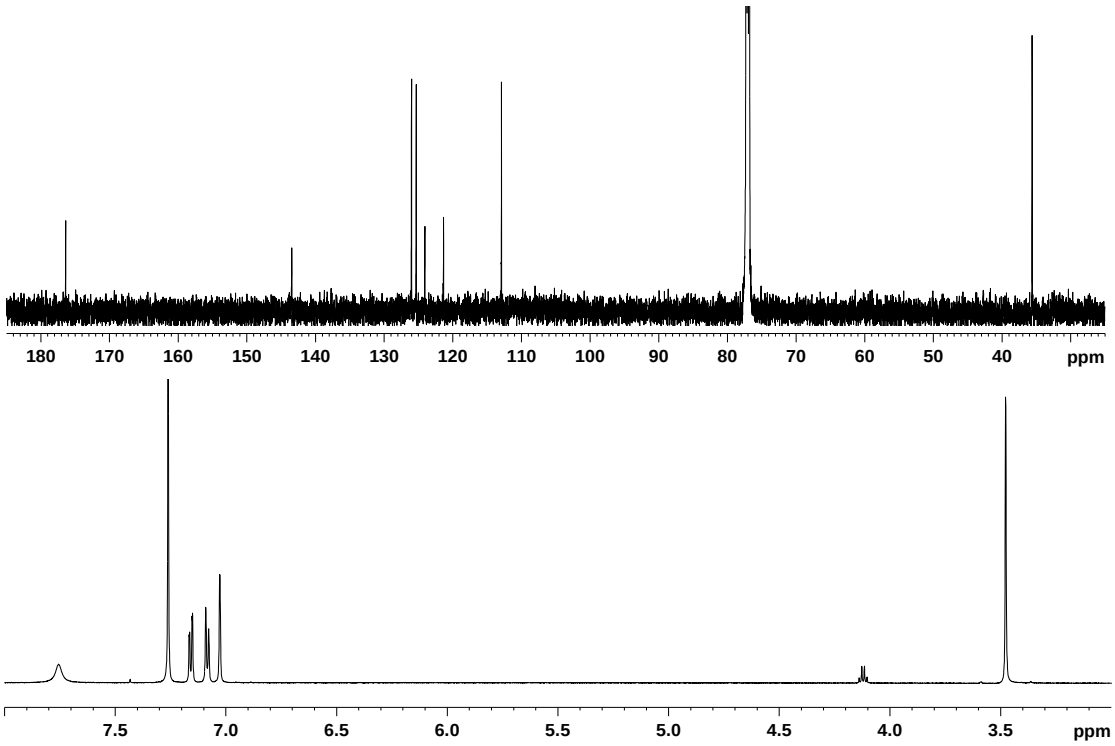

Figure 2.10: ^{1}H (600 MHz, $CDCl_3$) and ^{13}C (150 MHz, $CDCl_3$) NMR spectra obtained for the oxindole **2.28**.

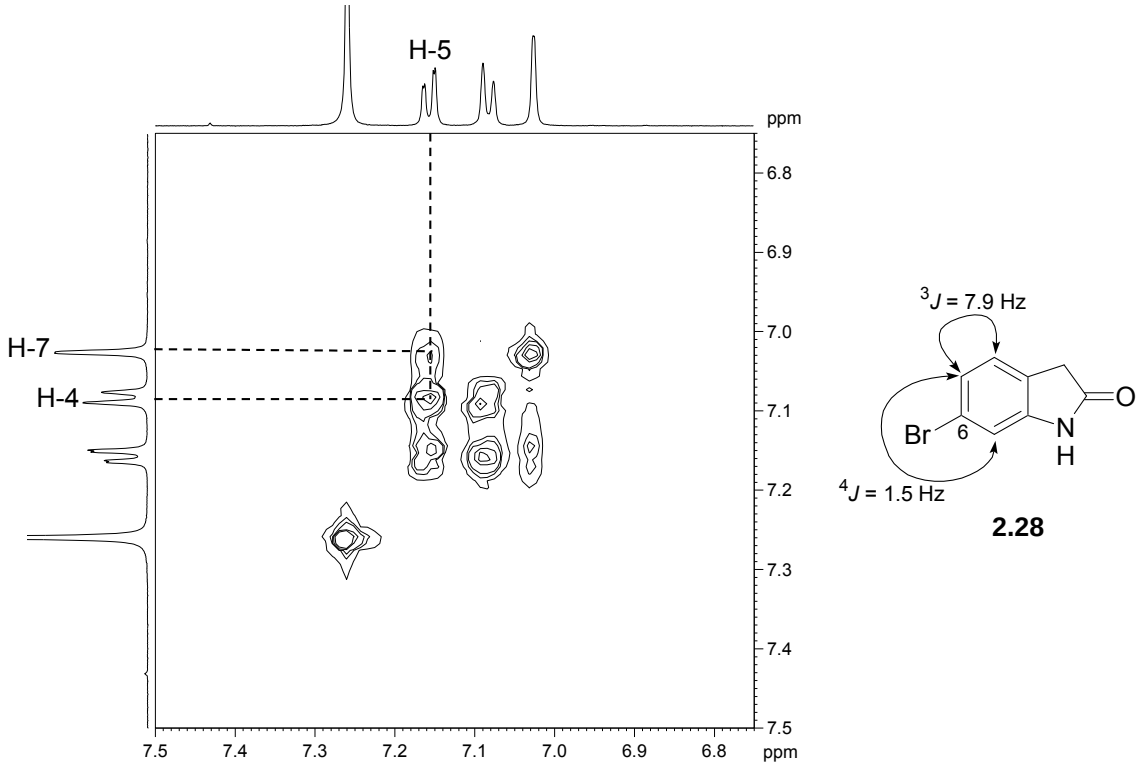

Figure 2.11: A region of the COSY spectra (F1 = 6.7 – 7.5 ppm) obtained for **2.28**. The accompanying structure illustrates the ^{3}J and ^{4}J COSY correlations used to determine the position of the bromine substituent.

Table 2.2: ^{1}H ($CDCl_3$, 600 MHz), ^{13}C ($CDCl_3$, 150 MHz) and 2D NMR data obtained for **2.28**

Position	δ_C ppm	δ_H ppm (int., mult., *J*/Hz)	COSY	HMBC[a]
1	-	7.76 (1H, br. s)		
2	176.4	-		
3	35.6	3.48 (2H, s)	H-4, H-5, H-7	C-2, C-3a, C-4, C-6, C-7, C-7a
3a	124.0	-		
4	126.0	7.08 (1H, d, 7.9)	H_2-3, H-5	C-3, C-6, C-7a
5	125.3	7.16 (1H, dd, 7.9, 1.5)	H_2-3, H-4, H-7	C-3a, C-7
6	121.3	-		
7	112.9	7.03 (1H, d, 1.5)	H_2-3, H-5	C-3a, C-5, C-6
7a	143.4	-		

[a] HMBC correlations are from the proton(s) stated to the indicated carbon.

Spectroscopic data (MS, NMR and IR) obtained for **2.29** were consistent with data reported for this compound, isolated from the ascidian *Distaplia regina* collected in Malakal Harbour, Palau.[97] The molecular formula of 6-bromo-3-chloroindole (**2.30**) was established as $C_8H_5N^{79}Br^{35}Cl$ from the appearance the deprotonated molecular ion $[(M-H)^-]$ at *m/z* 227.9215 (Δ 0.1 mmu) in the negative ion HRESIMS. A strong band at 3445 cm^{-1} in the IR spectrum was characteristic of a N-H stretching absorption.[80] The ^{13}C NMR and DEPT 135 spectra showed the presence of four aromatic methines (δ_C 123.9, 121.4, 119.7 and 114.4) and four quaternary carbons (δ_C 135.7, 124.4, 116.8, and 107.0) with typical heteroaromatic shifts, suggestive of a disubstituted indole system, which would account for the six degrees of unsaturation implied by the molecular formula. The IR spectrum also showed a band at 737 cm^{-1} suggesting that the indole ring was halogenated.[80] That this halogenation comprised both bromine and chlorine substituents was further supported by the presence of characteristic isotope peaks at *m/z* 228, 230, 232 $[(M-H)^-]$ in a 3:4:1 ratio in the ESI mass spectrum of **2.30**. Assignment of the ^{13}C chemical shifts of the two halogenated carbons in **3** was provided from a combination of gHMBC, HSQC and COSY NMR experiments. The position of the bromine and chlorine substituents at C-6 and C-3 on the indole ring in **2.30** was determined by initially comparing the ^{13}C chemical shift data of **2.30** with those of **2.29** (Table 2.3). The chemical shift of C-6 in **3** (δ_C 116.8) was consistent with that of C-6 in **2.29** (δ_C 116.8), while the downfield shift of C-3 (δ_C 107.0) in **3** compared to that of C-3 in **2.29** (δ_C 91.9) placed the chlorine substituent at this position in **2.30**.

Table 2.3: ^{1}H (600 MHz, $CDCl_3$) and ^{13}C (150 MHz, $CDCl_3$) NMR data obtained for compounds **2.29** and **2.30**.

	2.29		**2.30**	
Position	δ_C ppm	δ_H ppm (int., mult., *J*/Hz)	δ_C ppm	δ_H ppm (int., mult., *J*/Hz)
1	-	8.20 (1H, br. s)	-	8.08 (1H, br. s)
2	123.9	7.21 (1H, d, 2.6)	121.4	7.16 (1H, d, 2.6)
3	91.9		107.0	
3a	125.9		124.4	
4	120.5	7.44 (1H, d, 8.3)	119.7	7.50 (1H, d, 8.3)
5	124.0	7.31 (1H, dd, 8.3, 1.5)	123.9	7.30 (1H, dd, 8.3, 1.5)
6	116.8		116.8	
7	114.3	7.54 (1H, d, 1.5)	114.4	7.53 (1H, d, 1.5)
7a	136.0		135.7	

3-Chloro-6-bromoindole has not previously been isolated from an ascidian species, however, it has been shown to be produced, along with compound **2.29**, by the marine acorn worms *Ptychodera flava laysanica* and *Ptychodera flaval*.[98,99] Ascidians (Urochordata: Ascidiacea) and acorn worms (Hemichordata: Enteropneusta) are both marine detritus filter feeders, but phylogenetic analyses of the deuterostome phyla supported by cladistics analysis of morphological data confirms that these groups belong to two different clades.[100,101] Therefore the occurrence of compounds **2.29** and **2.30** in marine organisms from different phyla would again possibly suggest a common symbiotic marine microbial source for **2.29** and **2.30**.[94–96]

As part of our on-going investigation of the cytotoxicity of South African marine invertebrate and algal natural products to various cancer cell lines, **2.28**-**2.30** were screened against the metastatic MDA-MB-231 breast cancer cell line.[102,103] The IC_{50} values observed for **2.28**-**2.30** were 74.4 µM, 117.7 µM, 72.5 µM and respectively, indicating that these compounds are marginally cytotoxic to MDA-MB-231 breast cancer cells.[55] Compound **2.28** was previously found to be active against *Bacillus subtilis*, *Esherichia coli*, and *Staphylococcus aureus*.[97]

2.3.2 Aplidium monile - TIC2011-032

The ascidian *Aplidium monile* Monniot, F., 2001[49] Aplousobranchia: Polyclinidae, (Figure 2.12) was collected by SCUBA from a depth of 12 - 15 m at Bell Buoy dive site (33° 58.998' S 25° 41.622' E), Algoa Bay, South Africa, in November 2011 and given the voucher code TIC2011-032,.

Figure 2.12: *Aplidium monile* (TIC2011-032) collected from Bell Bouy dive site in Algoa Bay, South Africa. Photograph provided by Dr Shirley Parker-Nance.

2.3.2.1 Results from the LC-ICP-MS/ES-MS screen

The LC-ICP-MS/ES-MS data obtained for an extract of the ascidian *Aplidium monile* prepared using the extraction protocols adopted for preparing extracts for LC-ICP-MS/ES-MS screening revealed the possible presence of iodine, bromine, arsenic and vanadium containing compounds (Figure 2.13).

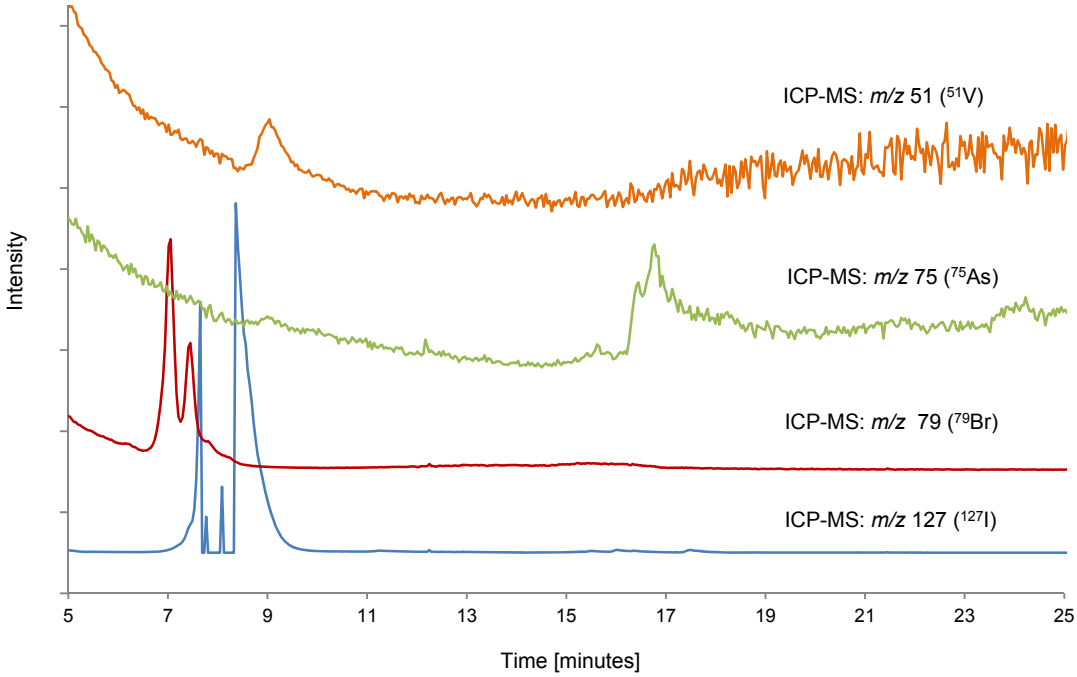

Figure 2.13: Selected LC-ICP-MS traces obtained for *Aplidium monile* (TIC2011-032) (^{127}I blue trace, ^{79}Br red trace, ^{75}As green trace and ^{51}V orange trace). Traces are vertically offset for clarity.

The bromine (*m/z* 79) ICP-MS trace aquired for the extract of *Aplidium monile* contained two major peaks at T_R 7.06 min and 7.46 min (Figures 2.13 and 2.14). The ESI-MS relating to T_R 7.06 min [Figure 2.14 (b)(i)] contains a major peak at *m/z* 309.9258 which had a distinct 1:2:1 (*m/z* 307.9283, 309.9258, 311.9235) isotope pattern indicating the presence of two bromine substituents. The best fit simulation[91] produced for this mass related to a $[(M+H)^+]$ molecular formula of $C_9H_{12}ONBr_2$ (Δ 0.2 mmu). Interestingly, even though a soft ionisation technique was used to acquire these data, evidence of some fragmentation was observed in the ESI-MS mass spectrum. The first fragment, with a dibromo- isotope pattern at *m/z* 290.9016 (relative intensity of 1), 292.8994 (2), and 294.8972 (1), correlated to a compound with a molecular formula of $C_9H_9OBr_2$ implying the loss of an ammonia ($[M+H-NH_3]^+$, Δ -17 amu) from the parent ion, a further loss of bromine ($[M+H-NH_3-Br]^+$, Δ -96 amu) resulted in the second fragment cluster at *m/z* 211.9831 (1) and 213.9810 (1) indicative of a monobrominated fragment. From these data it was believed the the compound detected at T_R 7.06 min was the tyramine analogue, 3,5-dibromo-4-methoxyphenethylamine (**2.31**).

The ESI-MS mass spectrum of the second major ^{79}Br-ICP-MS peak with the T_R 7.46 min [Figure 2.14 (b)(ii)] contained the major peaks *m/z* 355.9144 (1) and 357.9118 (1) suggesting a single bromine substituted metabolite. Once again there were secondary peaks, with the conserved bromine isotope patterns, at *m/z* 338.8879 (1) and 340.8855 (1) relating the the loss of ammonia ($[M+H-NH_3]^+$, Δ -17 amu) from the parent ion, and at *m/z* 211.9833 (1) and 213.9811 (1) suggestive of a similar structure to **2.31**. However the mass difference between the first and second fragment clusters was found to be -127 amu, characteristic of the loss of a labile iodine, which tentatively suggested that this tyramine derivative was 3-bromo-5-iodo-4-methoxyphenethylamine (**2.32**). The presence of iodine in this metabolite was further confirmed by the appearance of a small shoulder (almost completely obscured by a more dominant iodine containing metabolite) at T_R 7.46 min in the iodine (*m/z* 127) ICP-MS trace of this extract.

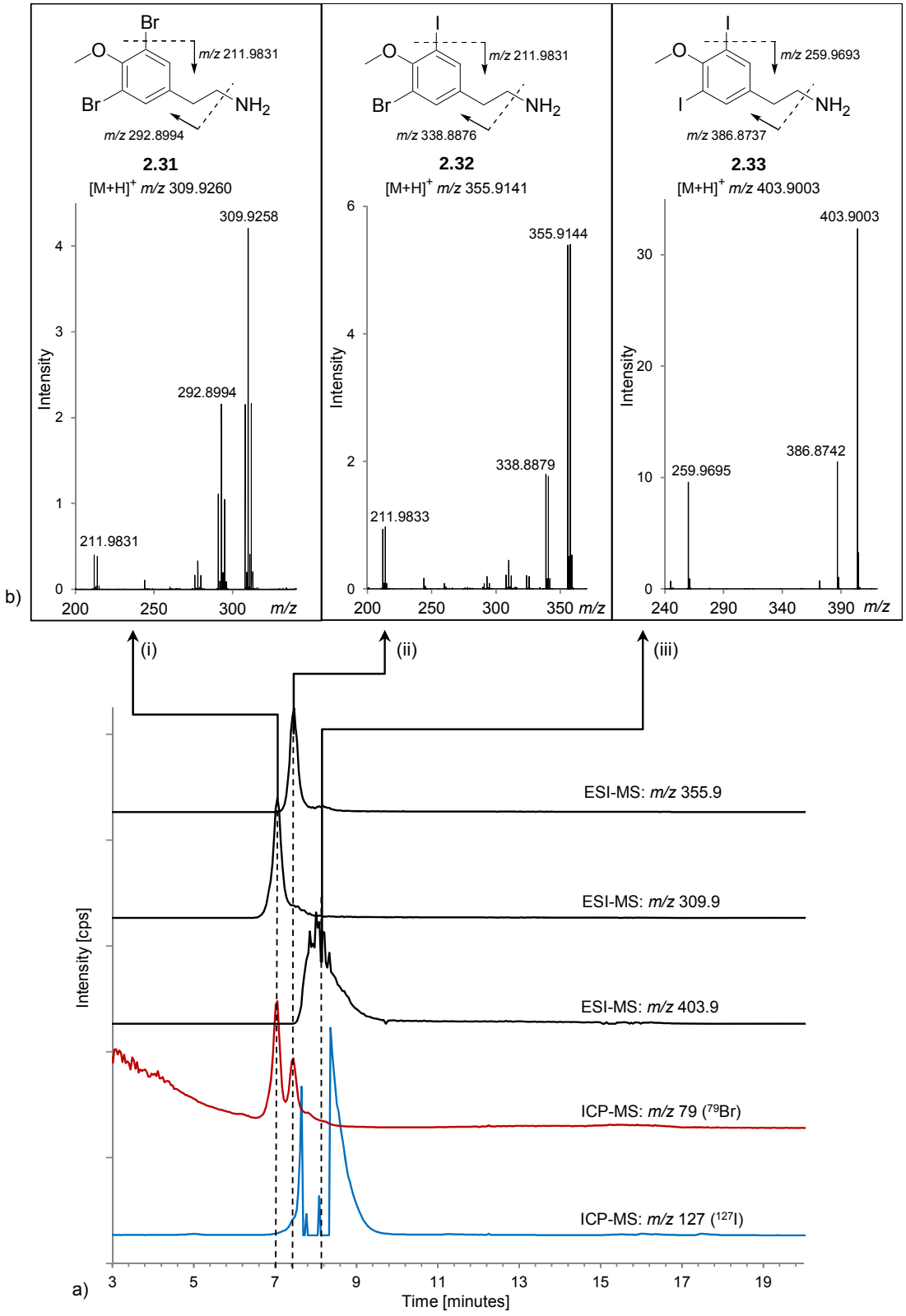

Figure 2.14: Halogenated tyramines detected in TIC2011-032 extract by LC-ICP-MS/ESI-MS. a) Selected ICP-MS and ESI-MS EICs; b) ESI mass spectra and structures for (i) **2.31** at T_R 7.06 min, (ii) **2.32** at T_R 7.46 min, and (iii) **2.33** T_R at 8.09 min.

The extract of *Aplidium monile* produced an iodine (*m/z* 127) ICP-MS trace with a peak between T_R 7.5 - 9.5 min that was of such magnitude that it saturated the detector resulting in the unusually shapped peak (T_R 7.5 - 9.5 min) observed in Figures 2.12 and 2.13. The ESI-MS relating to this retention time was dominated by a peak at *m/z* 403.9003 (Figure 2.14 b)(iii)). The EIC of *m/z* 403.9003 was a very good match to the iodine ICP-MS trace indicating that the compound with T_R 7.8 min is iodinated (Figure 2.14 a). As was observed with the brominated tyramine metabolites the ESI-MS for this dominant iodine containing compound had further peaks at *m/z* 386.8742 ($[M+H-NH_3]^+$, Δ -17 amu) and *m/z* 259.9695 ($[M+H-NH_3-I]^+$, Δ -144 amu), suggesting the presence of another halogentated tyramine, 3,5-diido-4-methoxyphenethylamine (**2.33**). The dominance of **2.33** in the extract of *A. monile* swamped the detection of potential vanandium or arsenic containing chelation complexes, and no further analysis of vanadium and arsenic data was pursued.

*2.3.1.3 Isolation and structure elucidation of **2.33***

To establish the structures of the halogenated tyramines in *A. monile* the remaining crude extract from the LC-ICP-MS/ESI-MS screen was partitioned between dichloromethane and aqueous methanol (70% aq. methanol). The ^{1}H NMR data acquired for the polar methanol partition contained, as expected, the resonances relating to the halogenated tyramine derivatives, as well as other prominent aromatic, and methylene signals of metabolites not detected in the initial analysis of the LC-ICP-MS/ESI-MS data. The investigation of the compounds giving rise to these latter resonances will be discussed further in Chapter 4.4.

Continuing with the attempted isolation of the halogenated tyramine derivatives, detected in the speciation analysis, the methanol partition fraction was fractionated using a C-18 Sep-Pak® cartridge (Waters,10 g). Seven fractions were collected based on the polarity of the solvents used to flush the cartridge (water, 10% acetonitrile$_{aq}$, 20% acetonitrile$_{aq}$, 40% acetonitrile$_{aq}$, 60% acetonitrile$_{aq}$, 80% acetonitrile$_{aq}$, and 100% acetonitrile). The fourth fraction produced a very simple ^{1}H NMR spectrum (Figure 2.15) with two methylene triplets at δ_H 3.14 (2H, *J* = 7.6 Hz) and 2.86 (2H, *J* = 7.6 Hz), a singlet at δ_H 3.81 (3H) indicative of a methoxy moiety, and an aromatic singlet at δ_H 7.77 relating to two chemically equivalent protons. These ^{1}H HMR data suggested either the presence of the dibromo- or diiodo-tyramine (either **2.31** or **2.33** respectively). The ^{13}C NMR spectrum supported the presence of an iodine substituent on an aromatic ring with the presence of a shielded resonance at δ_C 91.5 (Figure 2.15). That this compound was the anticipated diiodo-tyramine **2.33** and not **2.31** was confirmed from HRESIMS analysis which yielded the molecular formula $C_9H_{11}NOI_2$ (*m/z* 403.9000, $[(M+H)^+]$, Δ -0.3 mmu).

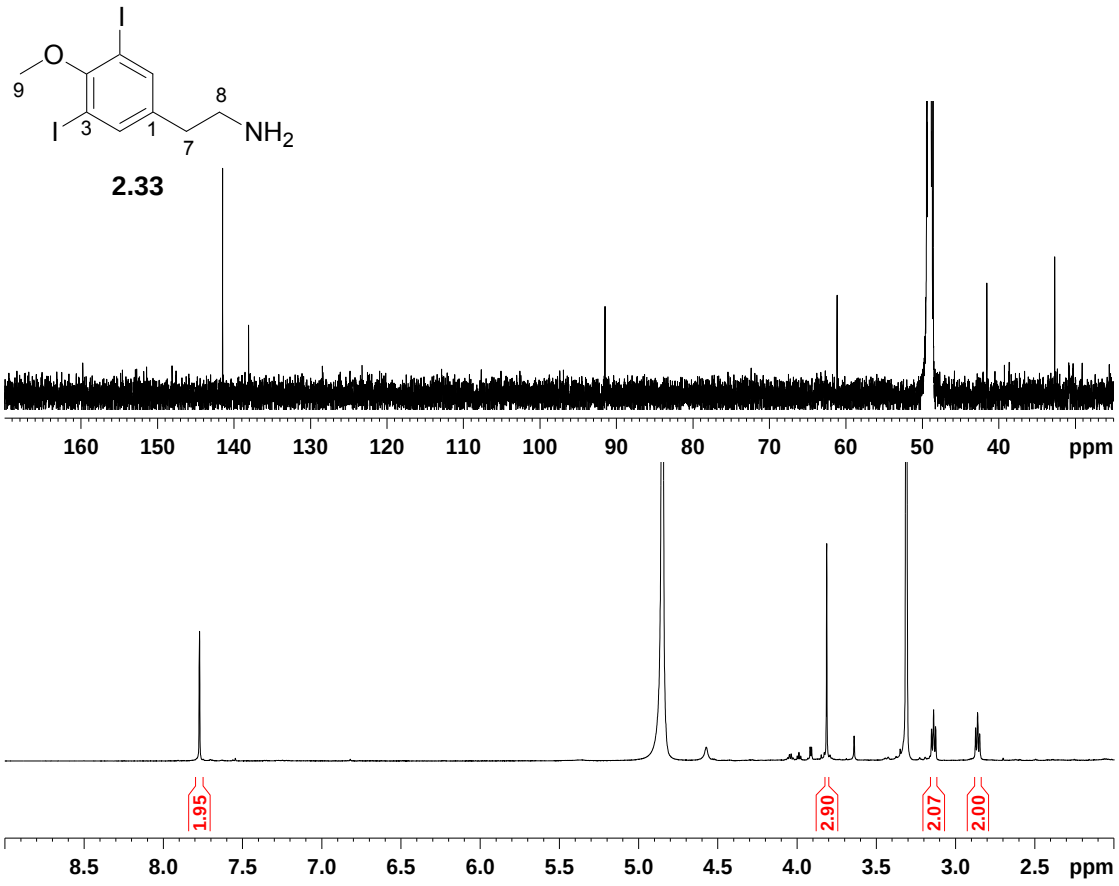

Figure 2.15: ^{1}H (600 MHz, MeOD) and ^{13}C (150 MHz, MeOD) NMR spectra obtained for the diiodo-tyramine **2.33**.

Table 2.4: ^{1}H (600 MHz, MeOD), ^{13}C (150 MHz, MeOD), COSY and gHMBC NMR data obtained for **2.33**.

	3,5-diiodo-4-methoxyphenethylamine (**2.33**)			
Position	δ_C ppm	δ_H ppm (int., mult., *J*/Hz)	COSY	HMBC[a]
1	138.1	-		
2	141.5	7.77 (1H, s)		C-3, C-4, C-5, C-6, C-7
3	91.5	-		
4	159.8	-		
5	91.5	-		
6	141.5	7.77 (1H, s)		C-2, C-4, C-5, C-7
7	32.7	2.86 (2H, t, 7.6)	H_2-8	C-1, C-2, C-6, C-8
8	41.6	3.14 (2H, t, 7.6)	H_2-7	C-1, C-7
9	61.1	3.81 (3H, s)		C-4

[a] HMBC correlations are from the proton(s) stated to the indicated carbon.

Standard 2D NMR experiments were carried out to confirm the arrangement of substituents on the benzene ring and unequivocally confirm the structure of **2.33** (Table 2.4). The key gHMBC correlations are displayed in Figure 2.16. The ^{3}J HMBC correlations from the methoxy protons (δ_H 3.81, H_3-9) and the aromatic protons (δ_H 7.77, 2H-2/6) both to the quaternary carbon resonance at 159.8 ppm established the position of the methoxy at C-4. The three bond HMBC correlation observed between the methylene protons at 2.86 ppm (H_2-7) and the aromatic methine at 141.5 ppm placed the amine chain at C-1. The ^{1}H and ^{13}C NMR shifts and key COSY and gHMBC correlations used to elucidate compound **2.33** are reported in Table 2.4.

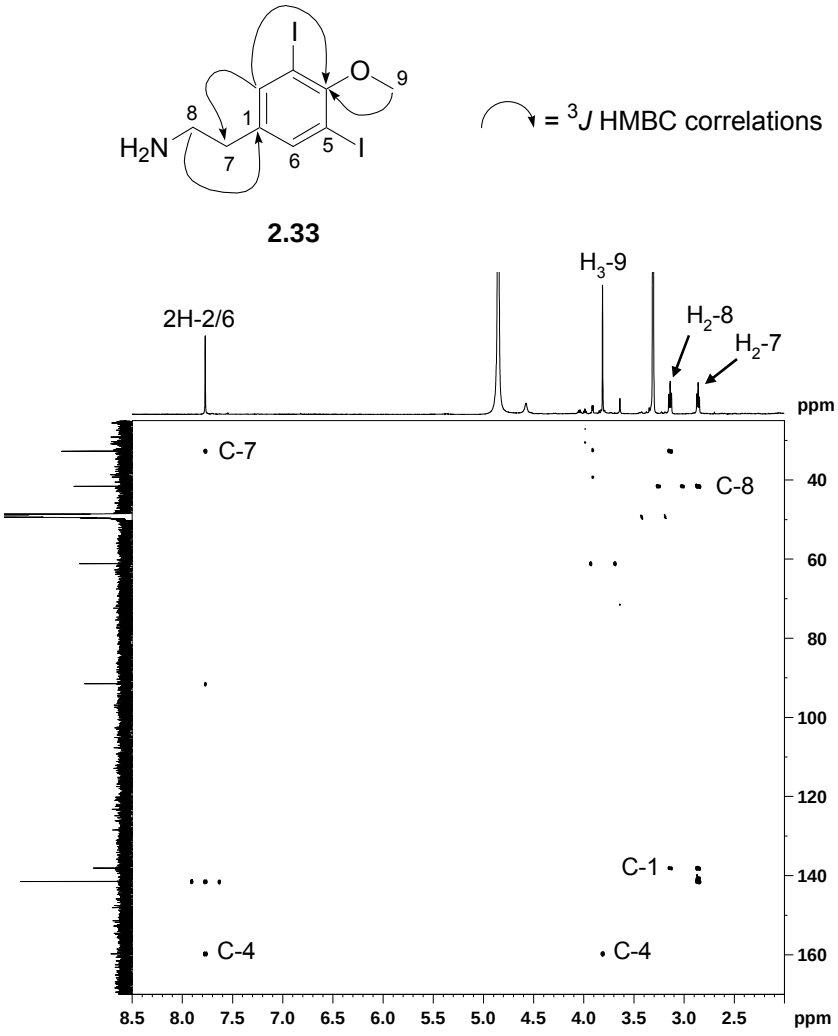

Figure 2.16: A region (F1 = δ 2.0-8.5 ppm; F2 = 20-170 ppm) of the gHMBC spectrum (MeOD, 600 MHz) of diiodotyramine **2.33**. The accompanying structure shows the key ^{3}J gHMBC correlatios used to elucidate the structure of **2.33**.

The ^{1}H NMR data obtained for the Sep-Pak® fractions five to seven were very similar to those observed for **2.33** however slight differences were seen when the chemical shifts of the aromatic proton singlets observed in the individual factions were compared (Figure 2.17). These slight shifts in chemical equivalence were believed to be due to the presence of

bromine substituents on the aromatic ring. However, when ^{13}C NMR data was acquired from fractions five to seven there were no observable shift in the resonance assigned to C-3 and C-5 (δ_C 91.5). In an attempt to isolate and elucidate the brominated derivatives detected during speciation analysis a larger scale extraction of TIC2011-032 was carried out. Unfortunately, the dominant iodinated compound **2.33** appeared to hinder the isolation of the other minor halogenated metabolites in the mixture due to major streaking of **2.33** during exhaustive attempts at HPLC purification of the different fractions.

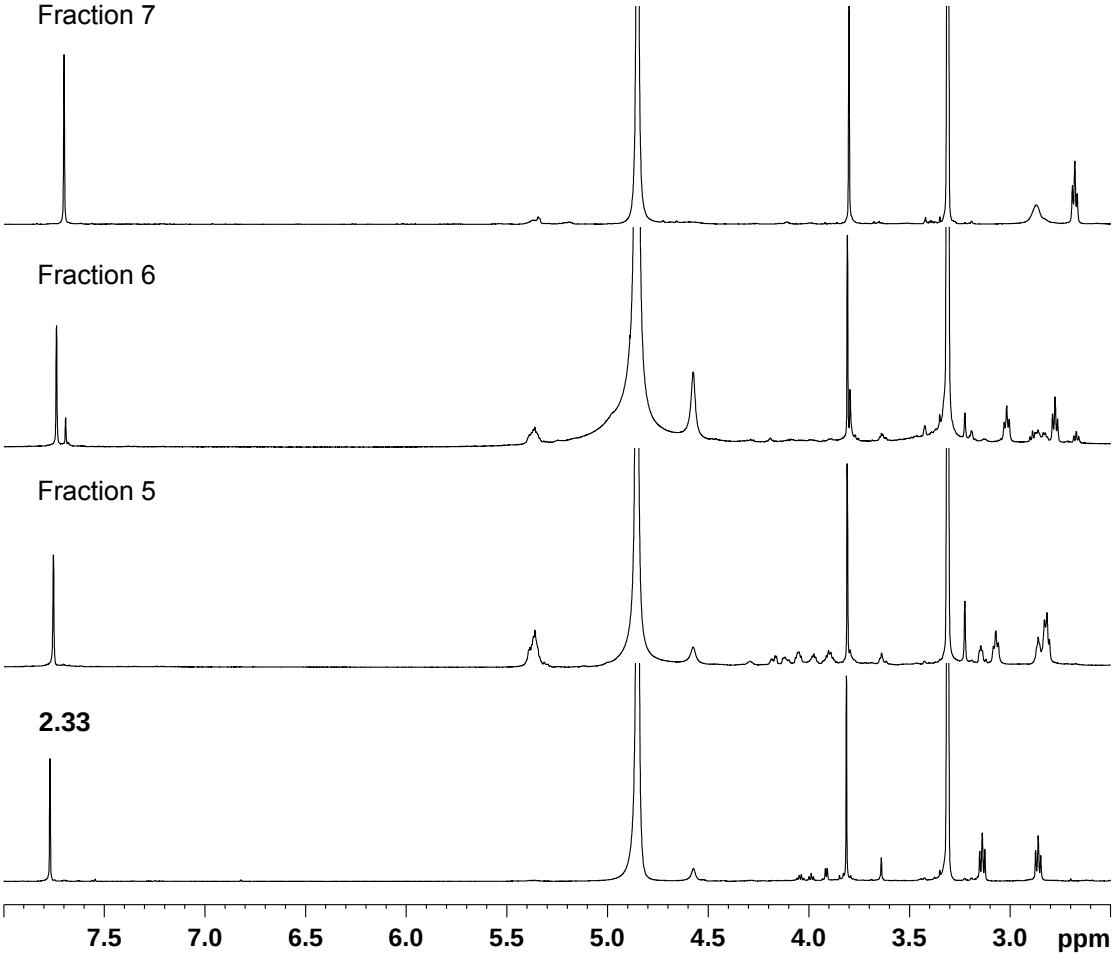

Figure 2.17: A stack plot of the ^1H NMR (MeOD, 600MHz) spectra obtained for **2.33** (bottom) and fractions five to seven produced from intial reversed-phase fractionation of the extract of *Aplidium monile*. Slight differences in the chemical shifts of resonances are believed to be due to differing halogenated substituents on the tyramine scaffold.

The first report on the isolation of 3,5-diiodo-4-methoxyphenethylamine (**2.33**) from a natural source was by Ireland and Sesin[104] who reported the isolation of **2.33** together with its urea derivative **2.34** from an unidentified species of *Didemnum* ascidian three decades ago.[104] Compound **2.33** was later isolated as the major compound in the Indonesian *Didemnum* sp. and the Palauan *Didemnum rubeum*.[105,106] More recently the ascidian *D. rubeum* was revisited and a series of iodinated tyramine derivatives were isolated including **2.33** and **2.34**

as well as seven new analogues **2.35**-**2.40**.[107] This is the first report of **2.33** from an African ascidian.

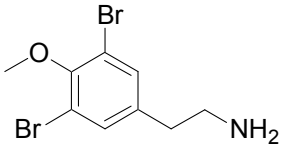

2.31

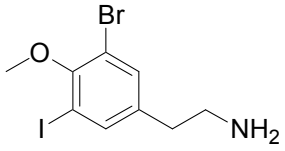

2.32

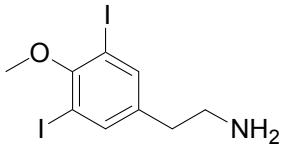

2.33

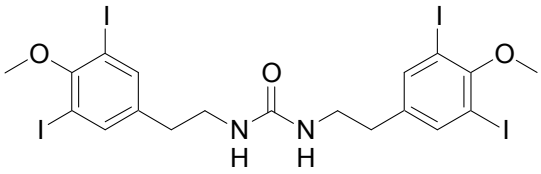

2.34

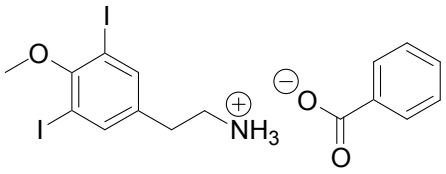

2.35

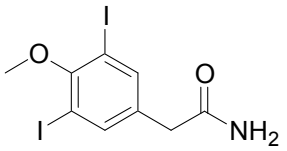

2.36

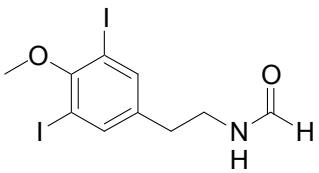

2.37

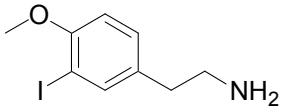

2.38

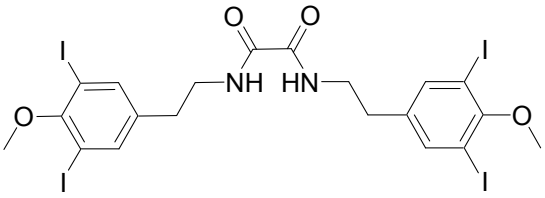

2.39

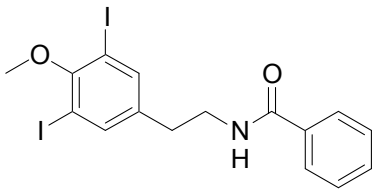

2.40

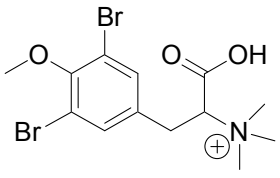

2.41

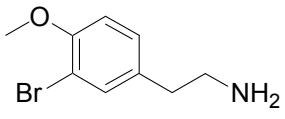

2.42

The dibrominated tyramine **2.31** appears to be less common, in the marine environment, than its iodo counterpart. The only reported isolation of **2.31** was by Ireland and co-workers[108] from the indonesian ascidian *Eudistoma* sp. however, related analogues of **2.31** such as the tetramethylated tyrosine derivative **2.41** and the monobromo-tyramine **2.42** have been isolated from the sponge *Verongula* sp. and the ascidian *Cnemidocarpa bicornuta* respectively.[108–110] In a synthetic and biolgical evaluation of a series of bromotyramines Schoenfeld *et al.* found **2.31** to exibit potent antifouling and cytotoxic properties.[111]

The C3 monohalogenation and C3, C5 dihalogenation pattern appears thus far to be ubiquitous in halogenated marine tyramines without exception and the C3, C5 dihalogenation pattern tentatively proposed for **2.30** and **2.31** would appear to be vindicated. Interestingly, albeit speculative, from high resolution mass data this appears to be the first case of an asicidian found to produce both the dibrominated (**2.31**) and diiodinated (**2.33**) tyramines, as well as the previously unreported bromo-iodo-tyramine **2.32** and is the first report of these compounds co-occurring in an African ascidian.

2.4 Parallel ICP-MS and ESI-MS as a tool to de-replicate known and discover new halogenated tyramines and tyrosines in South African marine ascidian extracts

In depth analysis of the LC-ICP-MS/ESI-MS data obtained from the screening of the 13 Algoa Bay ascidians resulted in the detection of halogenated tyramine metabolites from two additional ascidian extracts and suspected halogenated tyrosine metabolites from a further two ascidians. The use of LC-ICP-MS/ESI-MS analysis as a rapid dereplication technique for halogentated metabolites is further documented below.

2.4.1 Polycitor sp. nov. - SAF2004-068

The ascidian specimen SAF2004-068 (Figure 2.18) was an unknown species of *Polycitor* (Suborder: Aplusobranchia, Family: Polycitoridae) collected by SCUBA at a depth of 21 m from Haarlem Reef dive site, Algoa Bay, South Africa in July 2004. This colonial ascidian had a growth form consisting of multiple round lobes and was pale blue in colour with red orange zooids resulting in the common name of lucid polycitor ascidian. Organic extracts of *Polycitor* sp. nov. were entered into the ^{1}H-^{15}N HMBC screen, total metal concentration profile analysis, and LC-ICP-MS/ESI-MS analysis. The results of each screen are summarised in Table 2.1.

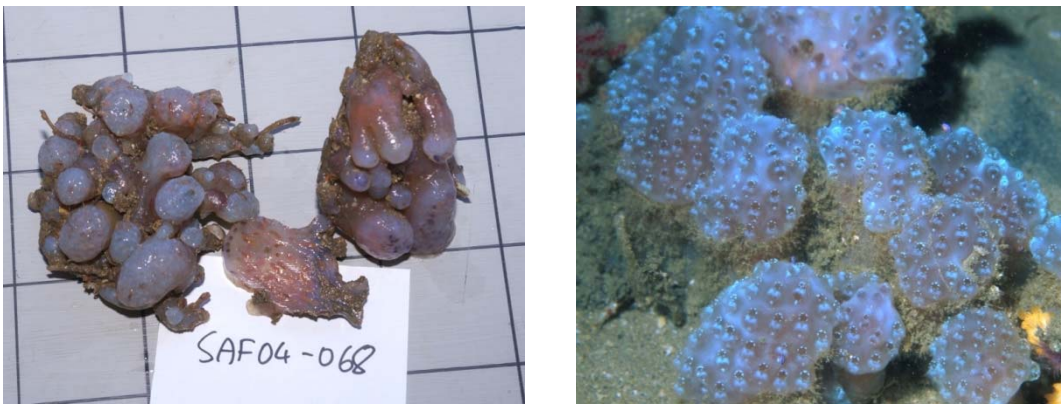

Figure 2.18: *Polycitor* sp. nov. collection specimen SAF2004-068 (left) and photographed at Algoa Bay, South Africa (right). Photograph credited to Coral Reef Research Foundation under contract to the National Cancer Institute (no. N02-CM-77249).

2.4.1.2 Results from the ^{1}H-^{15}N HMBC screen

The organic extract of *Polycitor* sp. nov. (SAF2004-068) was one of the eleven ascidian extracts that produced a common pattern of three correlations from the proton chemical shifts at δ_H 2.73, 3.16 and 4.27 ppm to the nitrogen resonances at δ_N 36.9, 51.3 and 196.3 respectively (Figure 2.3). In addition to these three common correlations a fourth clear correlation was seen from an aromatic proton resonance at δ_H 7.86 ppm to the downfield resonance at δ_N 196.3. The deshielded nature of these resonances found in the fourth correlation suggested the presence of an aromatic alkaloid in the extract of *Polycitor* sp. nov. which may have metal chelation potential.

2.4.1.3 Results from the LC-ICP-MS/ESI-MS screen

Analysis of the LC-ICP-MS/ESI-MS data obtained for the crude extract of the ascidian *Polycitor* sp. nov. (voucher code: SAF04-068) indicated the presence of iodine, bromine, arsenic and vanadium containing compounds (Figure 2.19). Attempts were made to establish the organic metabolites associated with these elemental data by investigation of the ESI-MS spectra obtained at the relevant retention times. Analysis of the bromine and iodine metabolites yielded the results presented below. Unfortunately, attempts to detect potential arsenic or vanadium containing metabolites were not successful.

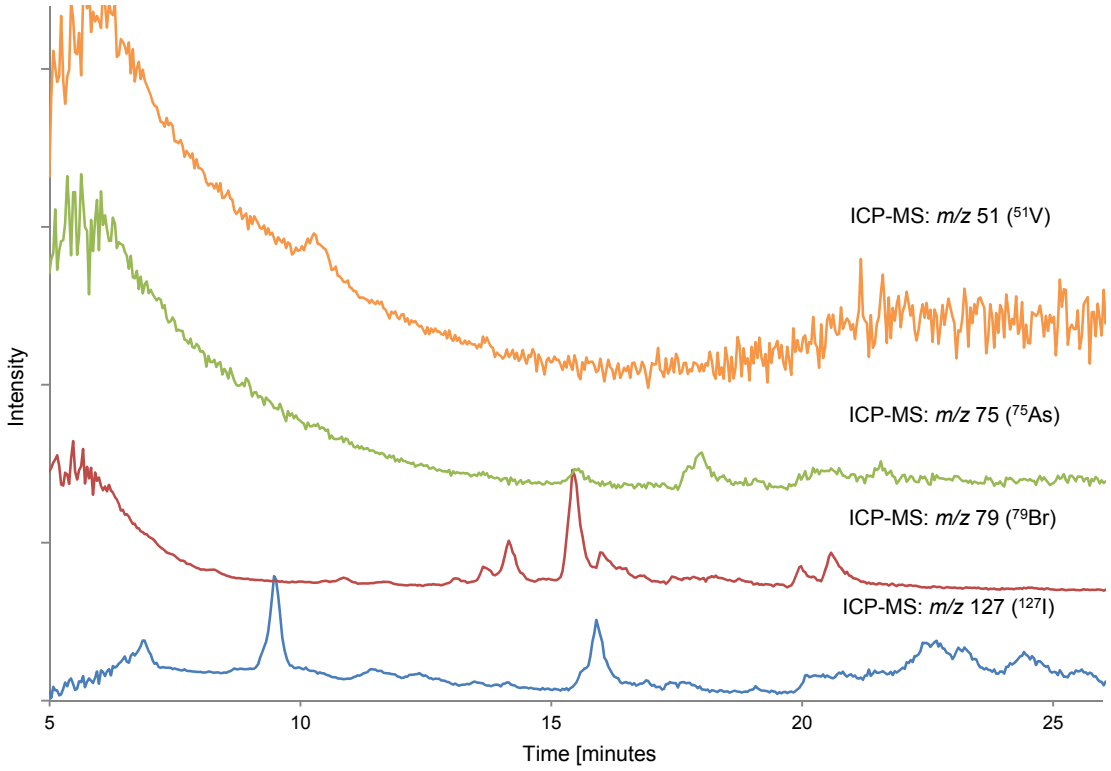

Figure 2.19: Selected LC-ICP-MS traces obtained for *Polycitor* sp. nov. (SAF2004-068); ^{127}I blue trace, ^{79}Br red trace, ^{75}As green trace and ^{51}V orange trace. Traces are vertically offset for clarity.

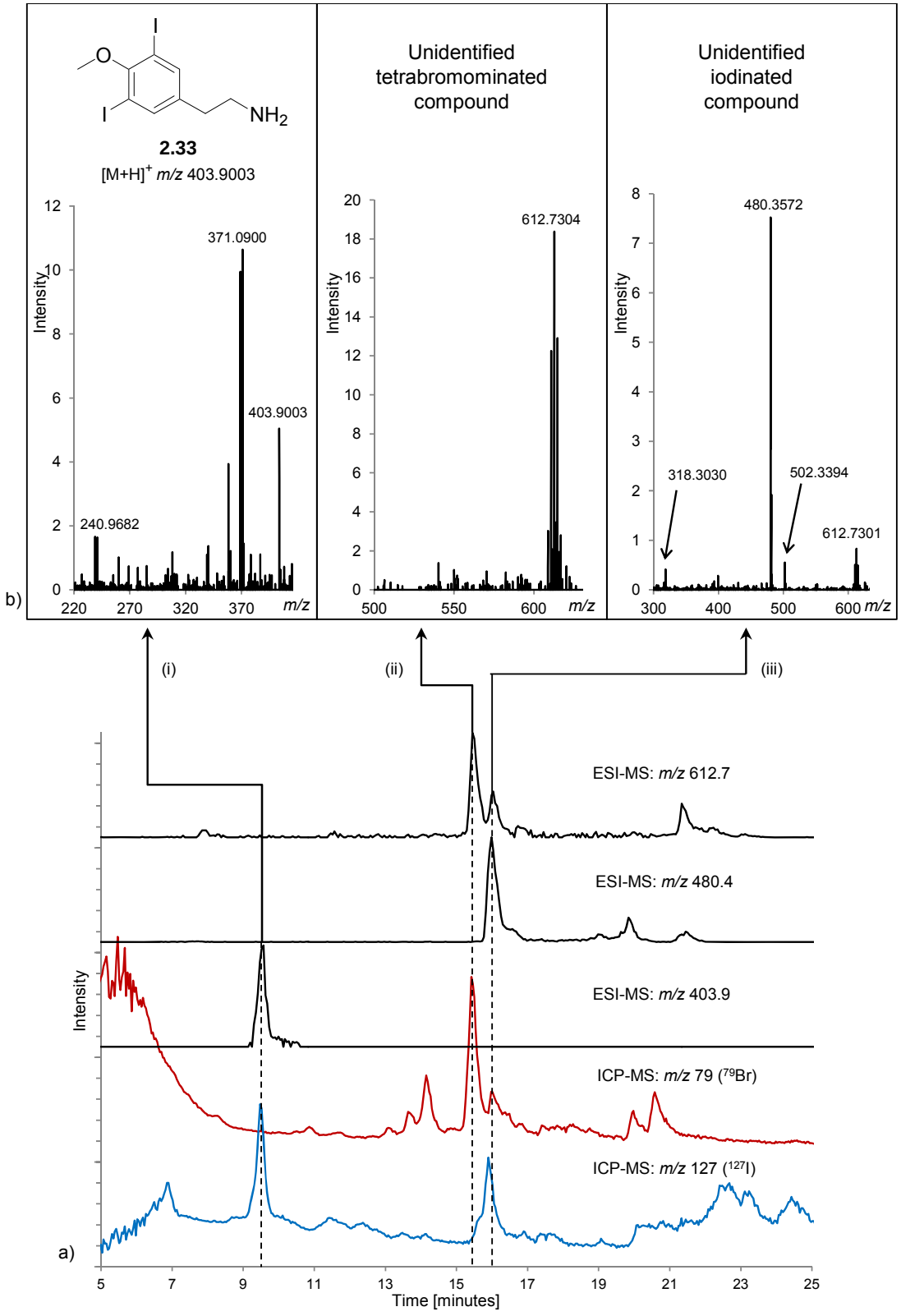

Figure 2.20: LC-ICP-MS/ESI-MS analysis of the extract of SAF2004-068 (*Polycitor* sp. nov.). a) Selected ICP-MS and ESI-MS EICs; b) ESI mass spectra for retention times of interest (i) 9.5 min, (ii) 15.4 min, and (iii) 15.9 min.

On inspection of the iodine (*m/z* 127) ICP-MS trace (Figure 2.19 and 2.19 a)), acquired for the organic extract of *Polycitor* sp. nov. the peaks at T_R 9.5 min and 15.9 min indicated the presence of iodinated metabolites at these retention times. The extracted ion chromatogram (EIC) of *m/z* 403.9003 (Figure 2.20 a) contained a peak at T_R 9.5 min, which correlates both in terms of mass and T_R to the diiodinated tyramine **2.33**, was also, as expected, congruent with a peak appearing at the same T_R in the ^{127}I ICP-MS trace. These data therefore suggest that **2.33** occurs in different species from both the Polycitoridae and Polyclinidae families occurring in Algoa Bay, South Africa.

The second peak in the ^{127}I ICP-MS of SAF2004-068 appeared at T_R 15.9 minutes and the ESI-MS produced at this retention time was dominated by the mono-isotope peak at *m/z* 480.3572. Unfortunately, the EIC produced for *m/z* 480.3572 was not a strong match and produced a peak apex that was shifted slightly to the right when compared to that in the I^{127} ICP-MS trace. Attempts to match EICs for the other ESI-MS peaks produced at this retention time were also unsuccessful. Therefore there was insufficient mass spectral evidence to speculate further on the structure of the iodine containing metabolite at T_R 15.9 mins.

The *Polycitor* sp. nov. ^{79}Br-ICP-MS contained a major peak at T_R 15.4 minutes which correlated with a similar T_R in the ESI-MS EIC for *m/z* 612.7304 (Figure 2.19 and 2.19 a). Inspection of the ESI-MS obtained at this retention time (Figure 2.20 b)(ii)) revealed an isotopic peak pattern at *m/z* 608.7347(1), 610.7328(4), 612.7304(6), 614.7285(4) and 616.7260(1) indicative of a tetra-brominated metabolite. The EIC for *m/z* 612.7304 was overlaid onto the bromine ICP-MS trace and giving a reasonable match (Figure 2.20 a). The molecular formula simulations[91] generated for the lowest isoptopic mass of *m/z* 608.7347 gave reasonablely similar *m/z* values for two molecular formulae; $C_8H_7O_4N_9Br_4$ ($[(M+H)^+]$ Δ -0.2 mmu) and $C_9H_{13}O_9N_2Br_4$ ($[(M+H)^+]$ Δ -0.7 mmu). Unfortunately, attempts at dereplication by matching these two molecular formulae to known formulae in available resources such as SciFinder and MarinLit yeilded no readily interpretable results and this species of Polycitor should be earmarked for further investigation. Regrettably, only a very limited amount of extract was available from the 2004 collection of SAF2004-068 and time and other resource constraints prevented further recollection and secondary metabolite isolation and structure elucidation investigations as part of this thesis study

2.4.2 Leptoclinides sp. - SAF2004-015

The ascidian with the sample code SAF2004-015 was a thin, upright, fan shaped colonial *Leptoclinides* species which was predominantly white with orange zooids (Figure 2.21). SAF2004-015 was collected by SCUBA from the White Sands dive site in Algoa Bay, South

Africa, from a depth of 21 m, in July 2004 and kept frozen until extraction for the aforementioned screens, the results of which will now be discussed.

Figure 2.21: *Leptoclinides* sp. collection specimen SAF2004-015 (left) and photographed underwater at Algoa Bay, South Africa (right, photograph supplied by Dr Shirley Parker-Nance.

2.4.2.1 Results from the ^{1}H-^{15}N HMBC screen

The results obtained for the crude organic extract of *Leptoclinides* sp. were unremarkable, with only two significant correlations produced from both the proton multiplets at δ_H 2.73 and 2.78 to the same nitrogen resonance at δ_N 36.9 ppm. The shielded nature of both the proton and nitrogen resonances involved in these correlations were indicative of resonances expected from an aliphatic amine.[80]

2.4.2.2 Results from the LC-ICP-MS/ESI-MS screen

Preliminary analysis of the LC-ICP-MS data obtained for the crude organic extract of the ascidian *Leptoclinides* sp. (Suborder: Aplousobranchia, Family: Didemnidae, voucher code: SAF04-015) revealed the presence of iodine, bromine, arsenic and vanadium containing compounds (Figure 2.22). Investigation of the corresponding LC-ESI-MS data was carried out in an attempt to identify the metabolites responsible for these elemental results.

The iodine (*m/z* 127) ICP-MS trace (Figures 2.22 and 2.23) obtained for *Leptoclinides* sp. had two major peaks appearing at T_R 9.5 and 16.0 min. The retention times of these peaks were very similar to those produced in the iodine ICP-MS trace of *Polycitor* sp. nov. (Figures 2.19 and 2.20), which tentatively implied common metabolites. Arising from similarities in T_R values the *m/z* values obtained at these retention times for the iodine elemental analysis of *Polycitor* sp. nov. were used as a starting point. The EIC for *m/z* 403.9003 was overlaid onto the I^{127} ICP-trace and the peak at T_R 9.5 min resulting in a reasonable match (Figure 2.23 a). The corresponding ESI-MS generated at this retention time did indeed display *m/z* 403.9003 as the major peak (Figure 2.23 b)(ii)). Once again the elemental and molecular information

would suggest that the tyramine, 2-(3,5-diiodo-4-methoxyphenyl)ethanamine (**2.33**), which had been isolated from a number of ascidians in the Didemnidae family,[104–107] was also present in this crude extract of *Leptoclindies* sp.. The use of an ion trap allowed for the analysis of the MSMS data for *m/z* 403.9003 which revealed one dominant peak at *m/z* 259.9695 and corresponded to the $[M+H-NH_3-I]^+$ (Δ -144 amu) fragmentation product as described previously.

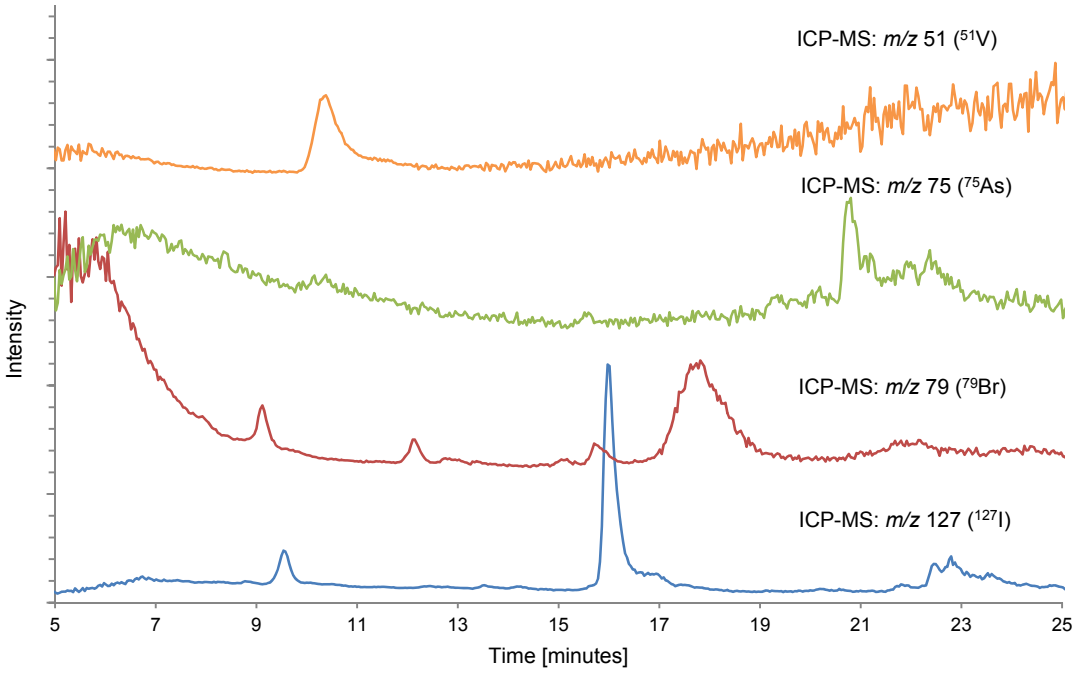

Figure 2.22: Selected LC-ICP-MS traces obtained for *Leptoclinides* sp. (SAF2004-015); ^{127}I blue trace, ^{79}Br red trace, ^{75}As green trace and ^{51}V orange trace. Traces are vertically offset for clarity.

Our initial analysis of the LC-ICP-MS/ESI-MS data generated at T_R 15.9 min from the extract of *Polycitor* sp. nov. (documented in the previous section) also did not yield any readily interpretable results. However, the successful identification of **2.33** at T_R 9.5 min in both the *Leptoclinides* sp. and *Polycitor* sp. nov. extracts motivated us to investigate the second common iodinated metabolite in the *Leptoclinides* sp. extract with T_R 15.9 min. The *Leptoclinides* sp. ESI-MS mass spectrum between T_R 15.9 and 16.1 mins was accordingly investigated.

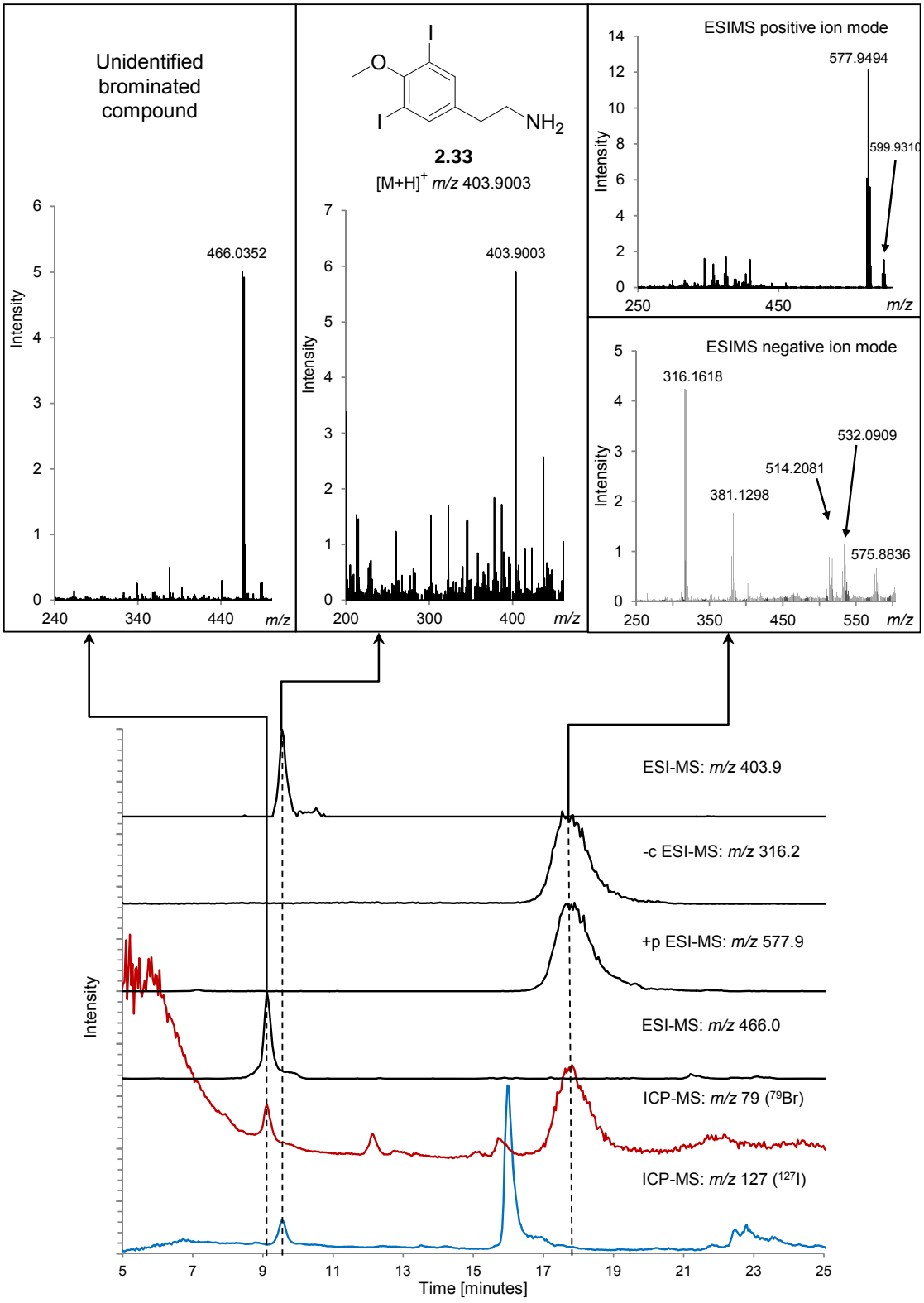

Figure 2.23: LC-ICP-MS/ESI-MS results obtained for the extract of *Leptoclinides* sp. (SAF2004-015). a) Selected ICP-MS and ESI-MS EICs; b) ESI mass spectra for retention times of interest (i) 9.1 min, (ii) 9.5 min, and (iii) 17.7 min.

No distinct major mass peak was observed in this T_R time frame and only a series of *m/z* peaks of moderate intensity were present. The EICs corresponding to each of these *m/z* values were consecutively extracted and overlaid onto the ^{127}I LC-ICP-MS trace. Unfortunately, none of the EICs where strong matches, and so the *m/z* value that might correspond to the elemental data produced could not be interpreted with any confidence. The failure to obtain even a suggested *m/z* value in either of the data sets obtained may also suggest that the unknown iodinated metabolite with T_R 15.9-16.1 min is not successfully ionised by the soft ES ionisation technique.

The *Leptoclinides* sp. LC-ICP-MS bromine (*m/z* 79) trace contained an intense and broad peak with a retention time ranging from 16.9 – 18.7 minutes as well as a minor peak at T_R 9.1 min (Figures 2.22 and 2.23 a). The ESI-MS spectrum corresponding to T_R 9.1 min contained the intense peaks as *m/z* 466.0352 and 468.0331 with a distinct 1:1 isotope ratio indicative of a mono-brominated compound. It was therefore not surprising that the EIC generated for *m/z* 466.0355 overlaid perfectly with the peak observed at the same retention time in the bromine ICP-MS trace for *Leptoclinides* sp. (Figure 2.23). The two simulations generated with the smallest Δmmu afforded molecular formulas $C_{31}H_{15}Br$ ($[(M+H)^+]$ Δ -0.3 mmu) and $C_{17}H_{17}O_6N_5Br$ ($[(M+H)^+]$ Δ 0.2 mmu), the former is far less probable. Searches of the marine natural product literature (MarinLit) and general chemical literature (SciFinder) did not yield any known compounds with molecular formula consistent with the predicted formulae and no chemical structure could proposed from these limited mass data.

The ESI-MS for the T_R range 16.9-18.7 min (Figure 2.23) contained a series of peaks with distinctive bromine isotope patterns at *m/z* 575.9517(1), 577.9494(2), 579.9471(1) and *m/z* 597.9333(1), 599.9310(2), 601.9290(1) indicating the presence of possibly a dibromo-metabolite. The EIC of the major peak (*m/z* 577.9494) matched the bromine ICP-MS trace excellently (Figure 2.23). Attempts, through molecular ion simulations and database searches, were made to identify the di-brominated metabolite assuming that the *m/z* 577.9494 value related to the $[(M+H)^+]$ ion, however no known marine natural products with molecular masses consistent with these data were found. Interestingly, when the negative ion channel of the ESI-MS of T_R 16.9-18.7 min was utilised, as a routine check in these analyses, a wealth of molecular ion adducts were observed (Figure 2.23). Regrettably, because of a paucity of material in hand no further attempts were made to isolate these individual brominated compounds.

As a final note on the LC-ICP-MS/ESI-MS data obtained for the extract of *Leptoclinides* sp.. We were continually cognisant of the aim of the project to find nitrogenous ascidian metabolites chelating to metal ions and our attempts at proposing a structure for the chemical structure of the metabolite responsible for the distinct peak at T_R 10.38 min in the elemental LC-ICP-MS analysis of vanadium (*m/z* 51, Figure 2.22) will be discussed briefly. The ESI-MS generated at this retention time revealed two major peaks at *m/z* 211.14 and 333.21,

however, the EICs for these mass values were not exactly coincident with the peak observed in the ^{51}V ICP-MS trace thus it was deemed unlikely that these two peaks represent vanadium containing organometallic complexes.[112]

2.4.3 Didemnum sp.2 - SAF2004-061

The ascidian specimen collected by SCUBA at a depth of 18 m at White Sands reef, Algoa Bay, under the voucher code SAF2004-61 was a colony of the purple encrusting ascidian *Didemnum* sp.2 (Family: Didemnidae, Suborder: Aplusobranchia, Figure 2.24).

Figure 2.24: *Didemnum* sp.2 collection specimen SAF2004-061 (left) and photographed underwater at Algoa Bay, South Africa (right). Photograph credited to Dr Shirley Parker-Nance.

2.4.3.1 Results from the ^{15}N HMBC screen

The extract of *Didemnum* sp.2 (SAF2004-061) also gave the common pattern of correlations from the protons at δ_H 2.73, 3.16 and 4.27 to the nitrogen resonances at δ_N 36.9, 51.3 and 196.3 respectively (Figure 2.3). The ^{1}H-^{15}N HMBC spectra obtained for *Didemnum* sp.2 further revealed two more correlations from δ_H 3.09 and 4.12 ppm to δ_N 53.6 and 374.4 ppm respectively.

2.4.3.2 Results from the LC-ICP-MS/ESI-MS

Analysis of the LC-ICP-MS/ESI-MS data obtained for the crude organic extract of the ascidian *Didemnum* sp.2 (SAF04-061) indicated the presence of iodine, bromine, selenium and copper containing compounds (Figure 2.25). Unfortunately, the peaks observed in the selenium and copper LC-ICP-MS traces were of low intensity, and none of the attempts to extract molecular information from the corresponding ESI-MS data were possible. The detection and tentative structure elucidation from mass data of two halogenated metabolites within this extract is discussed here.

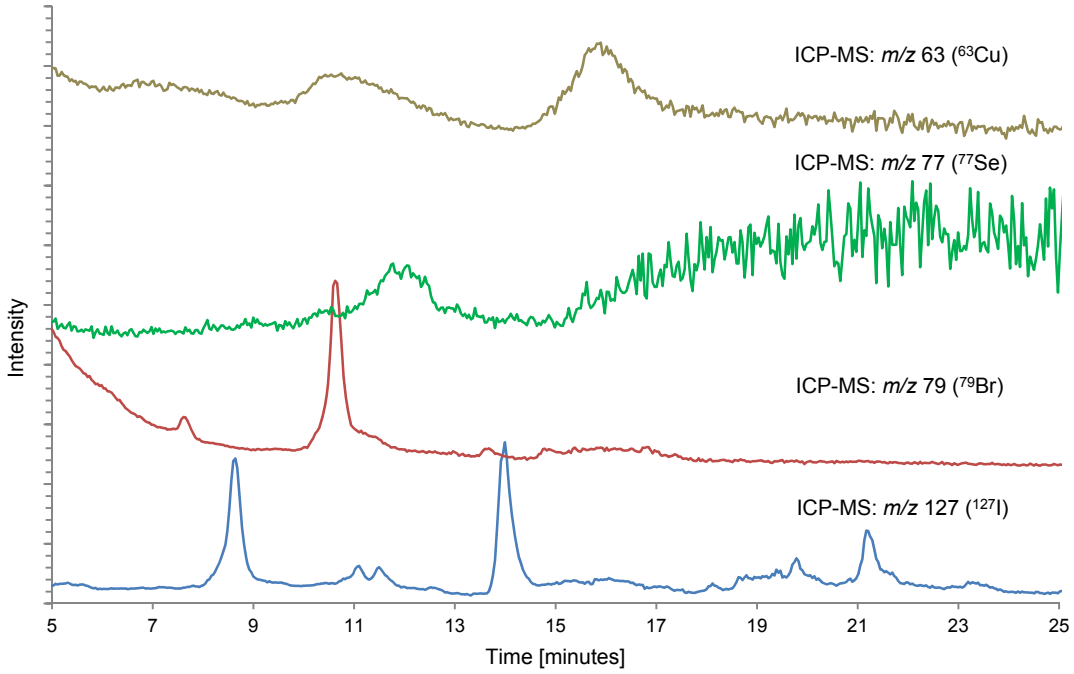

Figure 2.25: Selected LC-ICP-MS traces obtained for *Didemnum* sp.2 (SAF04-061); ^{127}I blue trace, ^{79}Br red trace, ^{77}Se green trace and ^{63} Cu brown trace. Traces are vertically offset for clarity.

The iodine (*m/z* 127) ICP-MS trace (Figure 2.25 and 2.26) obtained for *Didemnum* sp.2 revealed two major peaks appearing at T_R 8.64 and 13.99 min. Unfortunately, none of the major peaks seen in the ESI-MS obtained at 13.99 min had EIC retention times that matched the iodine ICP-MS trace, therefore no further analysis was carried out.

The correlating ESI-MS obtained at 8.64 min (Figure 2.26) contained two major peaks at *m/z* 364.0401 and 237.0949 (Figure 2.26 b) (i)). Although the major peak at this retention time was *m/z* 237.0949 the extracted ion chromatograph for this mass did not match that obtained for the elemental ^{127}I ICP-MS suggesting that this was not an iodinated metabolite. The EIC for the less intense peak at *m/z* 364.0401 was however a perfect match to the ^{127}I ICP-MS trace (Figure 2.26 a)). The mass difference of 126.9452 amu between these two major peaks is indicative of the loss of labile iodine adding further support for the presence of iodine in the compound with a molecular ion at *m/z* 364.0401. The closest fit simulation[91] generated corresponded to the molecular ion formula $C_{13}H_{19}O_3NI$ (Δ -0.3 mmu). Submitting these mass data in to the MarinLit data base did not yield any iodinated metabolites. In an attempt to extract more information from these data the MSMS for *m/z* 364.0401 was analysed and showed three major peaks at *m/z* 304.9661, 258.9609, and 178.0620 (Figure 2.26 b) (ii)).

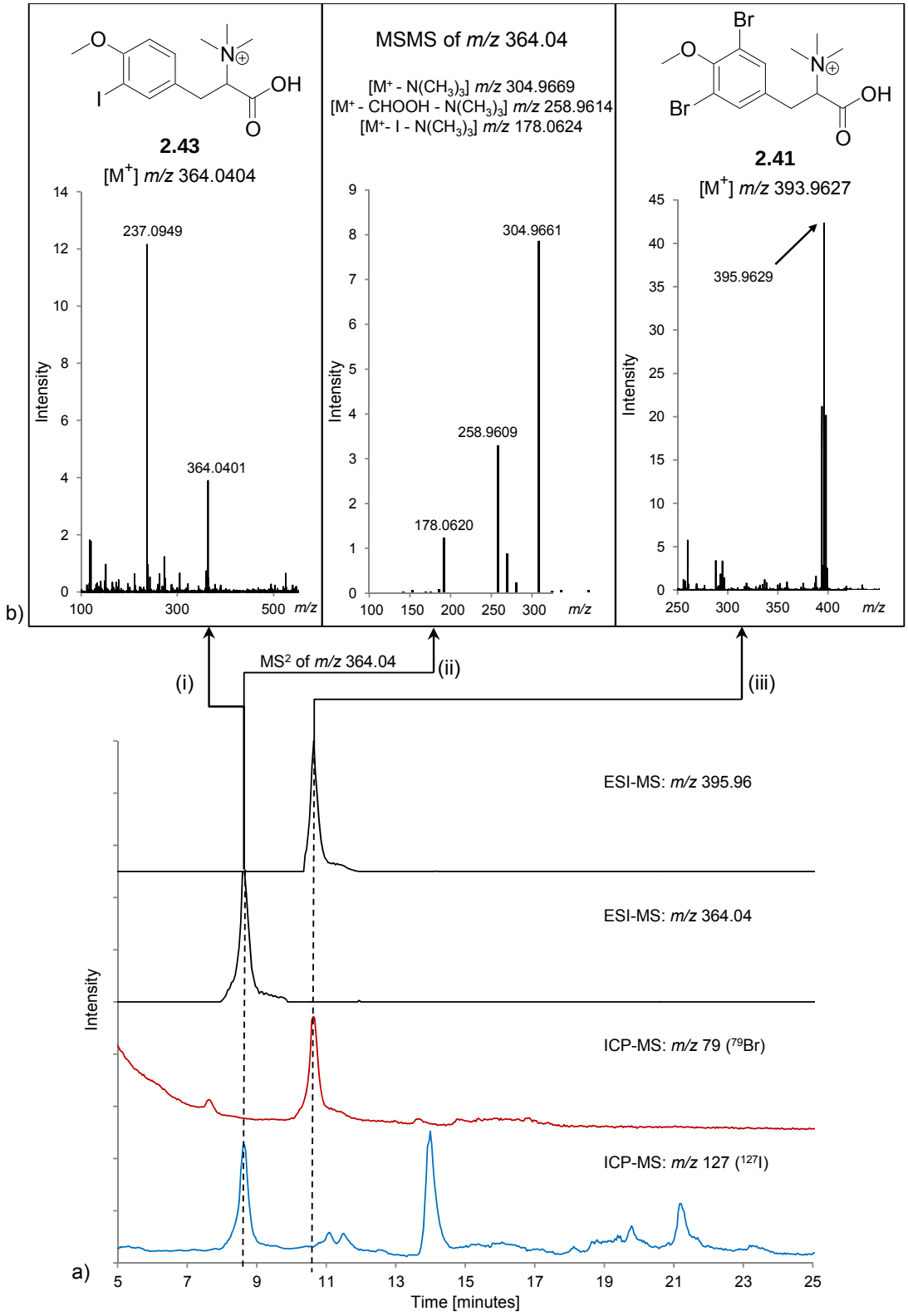

Figure 2.26: LC-ICP-MS/ESI-MS results obtained for the extract of *Didemnum* sp.2 a) Selected ICP-MS and ESI-MS EICs; b) ESI mass spectra for retention times of interest (i) 8.6 min (ii) the MS^2 spectrum acquired for *m/z* 364.04 and (iii) ESI-MS for T_R 10.6 min.

The mass difference between the parent ion (*m/z* 364.0401) and the fragment peak at *m/z* 304.9661 (Δ 59.0740 amu) in the MSMS suggested the loss of a trimethylamine [$N(CH_3)_3$] moiety. The remaining fragment peaks observed in the MSMS are also both indicative of the loss of this trimethylamine, along with a further loss of carboxylic acid group in the case of *m/z* 258.9609 (Δ 105.0792 amu), and an iodine rather in the case of *m/z* 178.0620 (Δ 185.9781). The formation of similar fragments, albeit through the loss of differing functional groups, was seen with the tyramine derivatives **2.31**-**2.33** detected in TIC2011-032 (*Aplidium monile*). The structure of the iodinated compound with in this current extract (SAF2004-061, *Didemnum* sp.2) was therefore tentatively proposed to be that of the tetramethylatedtyrosine derivative **2.43** ([M^+] *m/z* 364.0404, Δ 0.3 mmu).

The *Didemnum* sp.2 ICP-MS trace relating to the occurrence of bromine (*m/z* 79) (Figures 2.25 and 2.26) generated one major peak appearing at the retention time of 10.64 minutes. The ESI-MS for this retention time (Figure 2.26 b) (iii)) clearly showed a major compound with an isotope pattern at *m/z* 393.9650 (1); 395.9629 (2); 397.9607 (1) that implied the presence of a molecular ion with two bromine functionalities. The EIC of *m/z* 395.9629 was a good match to bromine ICP-MS trace (Figure 2.26). The simulation generated, for this isotope pattern, which produced smallest mass difference corresponded to the molecular ion formula $C_{13}H_{18}O_3NBr_2$ (Δ 0.2 mmu), indicating a brominated metabolite with a similar scaffold to that detected in the iodine analysis. A MarinLit search relating to these data yielded one dibromo-metabolite, **2.41** ([M^+] *m/z* 393.9627, Δ -0.2 mmu), whose mass data matched the dibromo compound detected in the extract of *Didemnum* sp.2. Compound **2.41** was first isolated by Albrizio *et al.* from the Caribbean Verongida sponge *Aiolochroia crassa* (reported under the synonymised name of *Pseudoceratina crassa*).[109] The anti-fouling and anti-parasitic properties of compound **2.41** were subsequently investigated and **2.41** was found to be inactive in both cases.[113,114] The structure of **2.41** is consistent with the structure predicted through MSMS fragmentation data for the iodinated compound **2.43**. Unfortunately, due to the small quantity of *Didemnum* sp.2 obtained in the original collection made in 2004, no attempt at the isolation and elucidation of these halogenated metabolites were carried out.

2.4.4 Aplidium sp. - SAF2004-039

The ascidian specimen with the collection code SAF2004-039 was an undescribed *Aplidium* sp. (family: Polyclinidae, suborder: Aplousobranchia) collected from a depth of 12 m at Roman Rock dive site in Algoa Bay, South Africa in July 2004. This colonial ascidian had an irregular cushion like growth form and was tan in colour with purple zooids creating a mottled appearance throughout (Figure 2.27).

Figure 2.27: *Aplidium* sp. collected by SCUBA from Roman Rock reef, Algoa Bay, South Africa. Collection specimen SAF2004-039 (left) and photographed underwater at Algoa Bay, South Africa (right). Photograph credited to Dr Shirley Parker-Nance.

2.3.6.1 Results from the ^{1}H-^{15}N HMBC screen

The ^{1}H-^{15}N HMBC data obtained for the crude organic extract of *Aplidium* sp. (SAF2004-039) revealed only the three correlations from the protons at δ_H 2.73, 3.16 and 4.27 ppm to the nitrogen resonances at δ_N 36.9, 51.3 and 196.3 respectively which were common to eleven of the extracts screened (Figure 2.3).

2.3.6.2 Results from the LC-ICP-MS/ESI-MS analysis

The elemental LC-ICP-MS data obtained for the crude extract of *Aplidium* sp. (SAF2004-039) indicated the presence of the elements iodine, bromine, arsenic, copper, cobalt and vanadium (Figure 2.28). The traces for arsenic (*m/z* 75) and copper (*m/z* 63) although weak, appear at a similar retention time. The two major isotopes of copper (^{63}Cu [~70%] and ^{65}Cu [~30%]) would create a molecular ion isotope pattern in the ESI-MS that would be fairly recognisable, and would help with the identification of a copper-natural product complex if such a complex existed in the extract. However, no such pattern was observed in the LC-ESI-MS chromatogram at the equivalent retention time in the LC-ICP-MS chromatogram.

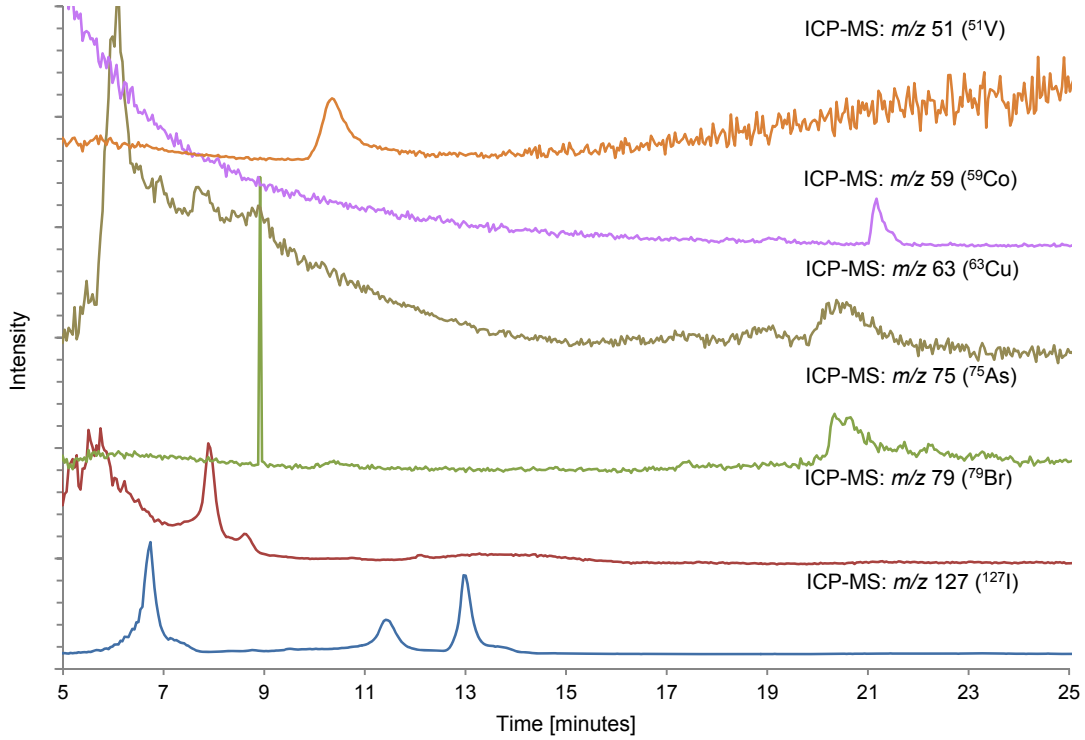

Figure 2.28: Selected LC-ICP-MS traces obtained for *Aplidium* sp.(SAF2004-039); ^{127}I blue trace, ^{79}Br red trace, ^{75}As green trace; ^{63}Cu brown trace; ^{59}Co pink trace; ^{51}V orange trace. Traces are vertically offset for clarity.

The iodine (*m/z* 127) LC-ICP-MS trace obtained for *Aplidium* sp. revealed major peaks at T_R 6.73, 11.45 and 13.00 minutes (Figures 2.28 and 2.29). The peaks with T_R of 6.74 min in the ESI-MS chromatogram (Figure 2.29 b)(i)) afforded dominant mass peak at *m/z* 307.9780. The closest fit simulation generated for *m/z* 307.9780 corresponded to the molecular ion formula of $C_9H_{11}O_3NI$ (Δ 0.4 mmu; $[M+H]^+$). MSMS analysis of this molecular ion yielded a fragment ion (*m/z* 261.9716), which represents a mass difference of 46.006 amu with the parent ion. These MSMS data would imply that the major fragment observed at *m/z* 261.9716 corresponds to the loss of a carboxylic acid group $[M+H-CHOOH]^+$ supporting the presence of a carboxylic acid moiety in **2.44** and accounting for one of the five degrees of unsaturation implied by the molecular formula. A tri-substituted benzene ring would account for the remaining four degrees of unsaturation and accommodate an iodine, hydroxyl and a 2-amino-propanoic acid substituent consistent with 2-iodo-tyrosine (**2.44**).

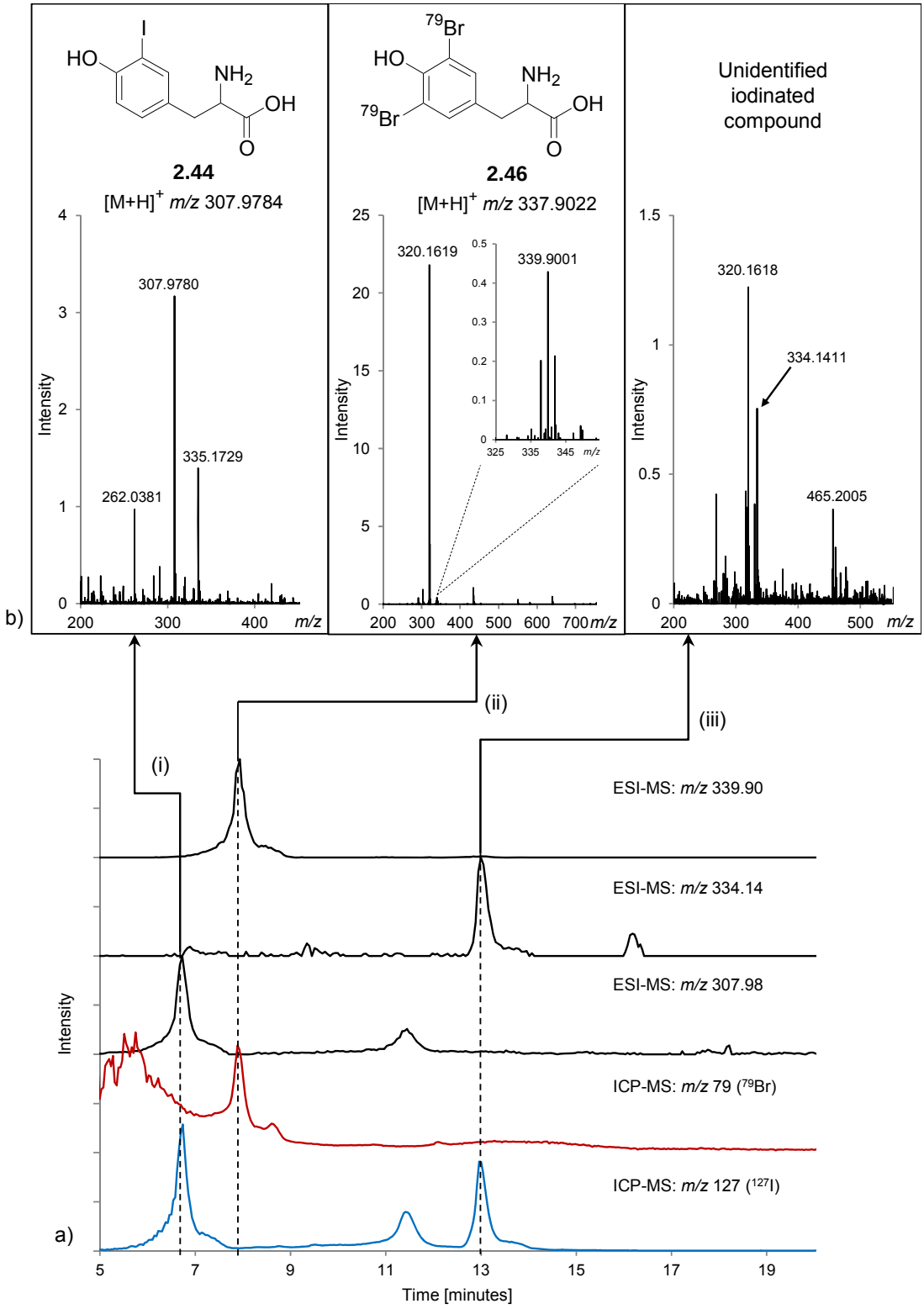

Figure 2.29: LC-ICP-MS/ESI-MS results obtained for the extract of *Aplidium* sp. (SAF2004-039); a) Selected ICP-MS and ESI-MS EICs; b) ESI mass spectra for retention times of interest (i) 6.73 min (ii) .7.90 and (iii) 13.00 min.

Early histochemical studies by Kennedy[115] and later Barrington and Thorpe[116] into the distribution of high levels of iodine in the organs of a number of tunicates, reported the occurance of monoiodotyrosine (**2.44**) and diiodotyrosine (**2.45**) in the endostyle, blood, tunic and gonads however, compounds **2.44** and **2.45** were not isolated in these studies. A recent review by Gribble reports the detection of iodinated tyrosines in marine algae, spoges and gorgonians.[117]

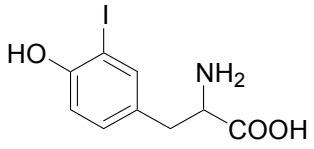

2.44

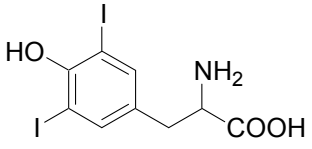

2.45

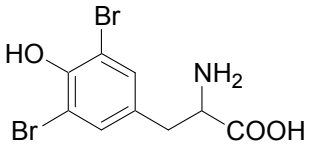

2.46

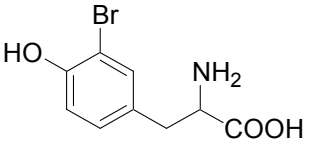

2.47

The *Aplidium* sp. LC-ICP-MS trace relating to bromine (*m/z* 79) (figures 2.28 and 2.29 a)) had a single clearly distinct peak at T_R 7.90 min. Our first inspection of the ESI-MS for this retention time [Figure 2.29 b)(ii)] revealed a dominant mono-isotopic peak at *m/z* 320.1619 which could not be the molecular ion for a compound containing one or more bromine atoms. After a closer analysis of the other peaks in the mass spectrum an isotopic pattern comprising three peaks at *m/z* 337.9022 (1); 339.9001 (2) and 341.8980 (1) was observed which we proposed corresponded to the $[M+H]^+$ of a dibromo metabolite. The best fit simulations obtained for the *m/z* 337.9022 was $C_9H_{10}O_3N^{79}Br_2$ (Δ -0.04 mmu; $[M+H]^+$) which was similar to the molecular formula established for **2.44** differing only in the presence of two bromine atoms instead of a single iodine atom. Unfortunately, the intensity of this molecular ion peak was too low to obtain the MSMS spectrum and any fragmentation data. However, some useful data was obtained through the ion mapping functionality. The product ions mapped for the monoisotopic parent ions *m/z* 337.90 ($^{79}Br_2$) and 341.90 ($^{81}Br_2$) were *m/z* 292 (Δ 45.9 mu) and 296 (Δ 45.9 mu) respectively which once again would suggest the presence of a carboxylic acid moiety in the parent ion and lead us to tentatively propose a 2,5-dibromotyrosine structure for **2.46**. There is no record of the isolation of **2.46** from a marine source in the database MarinLit,[76] **2.46** however the monobromo analogue **2.47** has been reportedly detected in sponges, molluscs and gorgonians.[117]

A complex ESI-MS spectrum (Figures 2.29) was acquired for the third prominent peak (T_R13.00 min) in the ^{127}I ICP-MS chromatogram The extracted ion chromatograph which overlaid best with the elemental ^{127}I peak was *m/z* 334.1411. However attempts at establishing the iodine containing molecular ion formula through calculated simulations all yielded mass values which differed significantly from the experimental mass (Δ mmu > 20) and no tentative structure could be proposed.

2.5 Concluding remarks

Although disappointed that we were unable to find evidence of metal-alkaloid chelation in the cohort of Algoa Bay ascidian extracts which we had selected for further study, we were able to conclusively show the value of LC-ICP-MS/ESI-MS to rapidly identify a plethora of iodinated and brominated metabolites in six *i.e.* nearly half of the 13 extracts screened. This discovery would suggest that brominated and/or iodinated tyrosine and tyramine metabolites are far more common in Algoa Bay ascidians than was previously known. We also realised that the metal ion concentrations and their distribution in 25 different Algoa Bay ascidians, which we had obtained in our screening regime, provided a unique record of metal ion assimilation in these organisms. Further statistical interrogation of the metal ion concentration data to identify amongst others possible patterns of metal ion concentration by different species in the same genus, and temporal and spatial differences in metal ion hyper-accumulation by Algoa Bay ascidians are presented in the following Chapter. We return to our interest in metal ion chelation in ascidians by describing in Chapter 4 our approach to establishing the chelation of vanadium ion with the nucleosides which were also isolated from *Aplidium monile* from Algoa Bay.

Chapter Three:
Trace Metal Concentration Analysis of Algoa Bay Ascidians

3.1 Metals in the marine environment

Metals in the marine environment originate from either terrestrial sources through river inputs, atmospheric deposition, or hydrothermal sources.[118] The persistence of a particular metal ion in the marine environment is related to its chemistry, natural abundance, and anthropogenic significance.[118] Numerous metals have biological significance thus marine organisms, in common with terrestrial organisms, have developed mechanisms to acquire, retain and use metals from the surrounding environment, mostly in trace amounts, and a delicate balance of metals is often required in order for an organism to remain healthy.[75] Investigating the levels of metals in marine organisms can thus not only establish the health of an organism but also the reef system as a whole.

3.2 Metals and ascidians

The discovery of high levels of vanadium in the ascidian *Phallusia mamillata* by Henze led to numerous investigations into the accumulation of vanadium in ascidians which are discussed in greater detail in Chapter 4.[119,120] The ability of ascidians to not only tolerate but actively concentrate a range of metals was reviewed by Monniot in 1978.[121] This review detailed high levels of metals including Sn, Mn, Ti, Cr, Fe, Nb and Ta within taxonomically and geographically diverse ascidian species.[121] Since this report relatively few additional studies have investigated the accumulation of a wide range of metals within ascidians. The investigations that reported other metals, apart from vanadium, often investigated metal concentrations within particular ascidian body parts such as the tunic, blood plasma, and branchial basket but did not quantify the total metal content of the ascidian species as a whole.[122,123] The results of two recent investigations into the metal concentrations measured in whole specimens of different ascidian species are presented in Table 3.1 along with the limited values reported by Monniot.[75,121,124] The first of these recent studies was conducted by Baker and co-workers and investigated the levels of vanadium, manganese and nickel in ten Antarctic ascidians.[124] More recently Jaspars and co-workers reported the concentrations of sixteen transition metals in eleven ascidians from the Great Barrier Reef.[75] In both these reports the ascidians investigated were found to accumulate metals in concentrations far greater than the surrounding sea water.[75,124] The ability for ascidians to tolerate high concentrations of a wide range of metals could make them potentially good candidates for biomonitoring programs concerned with the early detection of metal pollutions in reef ecosystems.

Table 3.1: Previously reported ascidian metal concentration data. Values are reported in parts per million (ppm) unless otherwise stated.[75, 121, 124]

	Li	Ti	V	Cr	Mn	Fe	Co	Ni	Cu	Zn	As	Se	Rb	Nb	Mo	Cd	Sn	Ba	Ta	U
Ciona intestinalis[a,5]																	10^6			
Microcosmus sulcatus[a,5]																	10^7			
Styela plicata[a,5]														250			10^8		540	
Ciona sp.[5]					120															
Eudistoma ritteri[5]		1512	471	144																
Pyura stolonifera[5]						5100														
Molgula manhattensis[5]														98						
Aplidium sp. 1[8]			40		19			1.0												
Aplidium sp. 2[8]			54		9			13.0												
Ascidia sp.[8]			567		48			2.0												
Pyuridae sp.[8]			18		13			7.0												
Distaplia colligans[8]			26		8			1.0												
Distaplia cylindrica[8]			1455		1			7.0												
Synoicum sp. 1[8]			17		33			2.0												
Synoicum sp. 2[8]			79		25			4.0												
Synoicum adareanum[8]			40		3			1.0												
Leptoclinides sp.[2]	0.9		31	0.7	13	52	0.3	1.5	5.9	23	8.9	1.0	1.1		0.6	0.2		5.2		3.4
Aplidium sp.[2]	1.8		970	9.0	43	480	0.8	7.3	4.7	24	9.5	1.8	1.6		1.6	0.2		5.6		1.6
Didemnum sp. 1[2]	1.4		2050	4.2	19	270	0.3	3.0	5.2	8.2	11	1.6	2.5		1.6	0.7		6.3		2.5
Didemnum sp. 2[2]	2.1		82	1.7	3.4	220	0.3	3.3	7.1	20	120	4.9	3.5		1.7	1.6		1.1		1.5
Didemnum sp. 3[2]	2.7		0.7	1.4	2.5	29	0.2	0.9	0.8	7.1	1.6	0.2	0.5		0.2	0.2		0.2		0.2
Didemnum sp. 4[2]	0.5		0.7	7.4	11	97	0.2	3.6	1.5	0.2	4.6	1.0	1.9		0.7	0.5		8.6		1.8
Didemnum sp.5[2]	0.3		0.2	1.0	1.3	14	0.1	2.0	1.5	0.1	6.0	0.3	0.3		0.5	0.0		4.9		2.9
Didemnum sp.6[2]	0.3		0.7	1.2	0.9	14	0.2	1.8	1.6	0.3	4.5	0.2	0.5		0.4	0.2		10		3.9
Lissoclinum patella[2]	1.6		0.4	0.8	3.1	43	0.1	1.7	4.1	4.3	6.7	0.7	2.4		0.3	0.5		3.4		1.8
Polysyncraton sp.[2]	1.2		0.9	2.8	8.7	160	0.3	1.9	3.2	7.0	8.7	1.1	1.5		1.0	1.1		6.3		3.1
Polycarpa sp.[2]	1.5		6.2	5.4	19	100	0.3	5.6	15	5.7	15	2.1	2.2		4.6	0.2		7.2		0.9

[a] Values reported for the concentration of tin are the orders of magnitude by which the ascidian concentration is greater than that of the surrounding seawater.

3.3 Marine invertebrates and environmental monitoring

The use of sessile marine organisms as bioindicators for environmental stresses such as metal pollution have long been considered to have a critical role in sustaining the health of reef ecosystems. Rainbow and Philips proposed five criteria to identify marine study organisms suitable for a biomonitoring programme. The marine organism chosen should be; first, capable of passively accumulating metals in high concentrations; second, sedentary; third, reasonably abundant in the site of interest; fourth, simple to identify and fifth; large enough to provide sufficient material for analysis.[125] A good biomonitoring candidate would also be a species that is able to grow in healthy, nonpolluted areas (thus providing a point of reference) as well as being able to tolerate the variable environments characteristic of metal polluted sites.[125] Following these principles some marine filter feeders have successfully become bio-indicators for metal pollution in their reef ecosystems. The mussel *Mytilus galloprovincialis* was the bio-indicator species used to assess the metal pollution of the coastal waters off Galicia.[126] A Mediterranean-based study of a number of potential sponge bioindicators established that the ability of *Crambe crambe* to accumulate copper and lead, the concentrations of which varied in a consistent manner with seasonal, spatial and temporal changes, making it a sound bio-indicator for these metals.[127] An extensive 12 year study into the levels of a range of metals in the Mediterranean sponge *Spongia officinalis* also revealed spatial and temporal variation in metal concentrations which indicated an improvement in the health of the area since the establishment of a sewage plant which appeared to markedly reduce the concentration of heavy metals over the study period.[128]

There are only two reports of ascidians as good candidates for metal ion biomonitoring programmes. The first report investigated the metal accumulation ability of two ascidians (*Ciona intestinalis* and *Microcosumus sulcatus*) common to the Saronicos gulf of the Aegean Sea. From the high concentration of metals detected in these two species, the authors concluded that *C. intestinalis* could be used as an indicator for iron pollution and *M. sulcatus* as an indicator for selenium, chromium, zinc and cobalt pollution.[129] The second report stated that the detection of elevated levels of vanadium, copper, lead and cadmium in the ascidians *Microcosmus squamiger*, *Microcosmus exasperates*, *Herdmania pallida*, *Phallusia arabica*, and *Styela canopus* from Thoothukudi on the South East Indian coast implied that these ascidians could be used as bioindicator species for metals in seawater.[130] Metal accumulating ascidians are sessile, abundant, often found in large colonies, and capable of surviving in healthy and polluted waters which are all important criteria which satisfy Rainbow and Philips[125] guidelines for establishing good biomonitoring agents. However, these guidelines are based on the assumption that the marine invertebrates studied are passively accumulating metals which can therefore be directly related back to the health of the surrounding environment.[125,131] Paradoxically, the investigations into metal hyperaccumulation in ascidians, at least for the most part, tend to conclude that the unusually high levels of trace metals in these organisms are brought about through mechanisms which

are far from passive.[75,124,132] In particular, Wright *et al.*[75] have provided a simplified overview of the active cellular mechanisms used by marine organisms to actively transfer metal ions across hydrophobic cell membranes against a concentration gradient *via* transfer ligands. The transfer of metal ions from transfer ligands to internal ligands within the cell generates a kinetic trap which prevents large scale expulsion of metal ions from the cell and enables hyperaccumulation of these ions within the cell.[75]

Our current study was aimed at determining the concentrations of a 24 different metals in 25 selected specimens from a unique collection of ascidians made from Algoa Bay in 2004 and 2011 and to further explore the metal ion data thus obtained through statistical analysis in an attempt to establish if there were any statistically significant correlations between metal accumulation patterns and ascidian families (phylogenetic correlation), the reefs from which the ascidians were collected (spatial correlation) and the year in which the ascidians were collected (temporal correlation). To the best of our knowledge this is the largest and most extensive investigation of metal concentrations in a group of different ascidians occurring in the same area.

3.4 ICP-MS analysis on South African ascidians

The ICP-MS total metal concentrations were measured for triplicate samples of the whole dried ascidian samples as well as crude organic extracts of each species. The 24 different metals assayed were Li, Be, B, Rb, Sr, Mo, Cd, Sn, Sb, Cs, Ba, Pb, U, Al, V, Cr, Mn, Fe, Co, Ni, Cu, Zn, As, and Se (Section 2.2.4 details the theory of ICP-MS as a highly sensitive elemental analysis technique). Due to the sensitivity of ICP-MS and to ensure accuracy to reflect only naturally occurring concentrations great care was taken to ensure that minimal contamination occurred during the preparation of ascidian samples for analysis. All laboratory equipment used, including glassware, spatulas, falcon tubes, adaptors, *etc.* were acid washed using 10% nitric acid, and thoroughly rinsed with Millipore water. When preparing the organic extracts, only HPLC grade methanol and dichloromethane were used.

All of the species studied were compound ascidians therefore the samples prepared were all taken from the same colony. For each ascidian species three representative samples (approximately 1.5 g wet weight) of the frozen colony were lyophilised, ground into a powder and stored at -20°C until digestion and total metal analysis. These triplicate samples will be referred to as whole ascidian samples from this point on. Further representative samples (at least 5 g wet weight) of the frozen ascidian species were used to prepare organic extracts using HPLC grade methanol and dichloromethane. Extractions were carried out in the normal way excepting that all glassware and tools *e.g.* spatulas used were acid washed, an ice-water bath was used when sonicating the material, and when a rotary evaporator was needed to dry the extract, an acid washed splash head adaptor was used which was gently heated with a

heat gun to ensure that no water vapour within the shaft or adaptor could condense and run back into the sample flask causing contamination. The crude ascidian extracts were stored at -20°C until digestion and ICP-MS analysis. These ascidian extracts will be referred to as crude organic extracts from this point on. The spent ascidian material remaining after the sequential extraction process was lyophilised and divided into three samples that were made available for total metal analysis as the need arose. Throughout sample preparation, all masses were recorded to four decimal places to ensure accurate calculation of total metal concentrations.

Digestions and total metal ICP-MS analyses were performed by the author with assistance from Dr Andrea Raab at the Marine Biodiscovery Centre (MBC) at the University of Aberdeen. Subsamples of approximately 100 mg of the triplicate whole ascidian samples and the crude organic extracts were made for each species for digestion. These subsamples were digested in a microwave (CEM) with 1 mL of concentrated nitric acid and 2 mL of hydrogen peroxide. After digestion each sample was made up to 25 mL with Millipore water, and stored at 4°C until ICP-MS analysis. Digests of five samples of reference material (whole egg, IAEA 140, TORT-2, DOLT-4 and DORM-3) were made following the same procedure. Eight calibration standards were made incorporating all the metals investigated, at varying concentrations. Since high concentrations of iron and vanadium were expected in the ascidian samples the seventh and eighth calibration standards were doped with these metals to ensure accurate measurement at high concentrations. Throughout the analysis ^{73}Ge was used as the internal standard.

Once the ICP-MS data were collected for all the samples, the metal concentrations obtained for the five reference samples were compared with those reported in the literature to ensure a reasonable recovery and accuracy.

3.4.1 Results of metal concentration studies in Algoa Bay ascidians

The total metal analysis results for the triplicate whole, dried ascidian samples are presented as an averaged value for each species in Tables 3.2 and 3.3, and Figure 3.1. The results obtained for the organic extracts were used to determine which ascidian extracts to investigate using LC-ICP-MS/ESI-MS, the results of which are documented in Section 2.3.

If Tables 3.2 and 3.3 are taken at face value it is not possible to identify any obvious patterns within the metal concentration data presented in these two tables. Due to the vast difference in the metal concentrations across the different metals, a logarithmic scale is used in the bar chart in Figure 3.1 to try and provide a relative and quantifiable perspective.

Table 3.2: Transition metal concentrations of 25 Algoa Bay ascidian species and oceanic concentrations[97] of the metals measured in ppm (mg of metal per kg of whole dry ascidian or mg per kg of seawater). Ascidian metal concentration values are averages of the triplicate measurements of whole dry ascidian samples after HNO_3/H_2O_2 digestion.

	Mo		Cd		Pb		V		Cr		Mn		Fe		Co		Ni		Cu		Zn	
Ascidian Species	**mean**	**sd**	**mean**	**sd**	**mean**	**sd**	**mean**	**sd**	**mean**	**sd**	**mean**	**sd**	**mean**	**sd**	**mean**	**sd**	**mean**	**sd**	**mean**	**sd**	**mean**	**sd**
Botryllus sp.	1.51	0.44	0.26	0.06	3.29	0.18	28.06	15.82	9.79	1.23	67.60	7.82	2910.70	317.81	0.92	0.06	3.17	0.31	3.63	0.70	26.51	5.74
Gynandrocarpa placenta	3.71	0.29	0.81	0.06	0.77	0.15	3.43	0.03	1.52	0.47	27.36	5.70	289.54	55.71	0.31	0.08	3.18	0.28	5.45	0.57	21.35	2.91
Clavelina steenbrasensis	2.82	0.17	0.21	0.02	0.90	0.11	30.16	8.01	3.93	0.37	18.78	1.12	1038.66	71.28	0.48	0.02	1.57	0.12	2.04	0.13	31.73	3.25
Pycnoclavella filamentosa	1.11	0.04	0.54	0.09	2.57	0.11	12.03	2.67	10.18	0.91	136.69	19.16	2411.78	294.82	1.05	0.24	2.49	0.74	7.68	9.85	19.65	1.74
Pycnoclavella narcissus	1.00	0.01	0.38	0.10	2.70	0.42	11.51	0.35	11.35	0.21	56.98	2.42	3251.95	28.62	1.29	0.07	3.50	0.05	10.75	1.87	103.28	8.61
Atriolum marinense	2.34	0.09	0.51	0.07	0.40	0.08	3531.44	859.60	1.13	0.57	7.75	2.98	290.00	158.32	0.28	0.09	0.58	0.22	2.73	0.64	125.52	23.37
Didemnum leopardi	2.27	0.23	0.16	0.02	1.59	0.37	3.70	0.35	2.23	0.31	41.11	2.09	753.90	90.46	0.34	0.03	1.04	0.10	1.43	0.08	37.76	0.13
Didemnum sp. 1	1.11	0.05	5.42*	1.22	4.29	1.15	12.53	1.67	9.47	4.29	134.18	50.19	3235.42	1541.11	1.38	0.56	4.30	1.63	5.50	2.08	40.34	7.31
Didemnum sp. 2	1.72	0.05	0.60	0.12	1.71	0.34	9.82	1.03	5.34	0.92	54.06	13.71	1519.96	271.55	0.73	0.03	2.18	0.16	1.85	0.42	39.36	5.10
Lissoclinum sp.	2.91	0.14	0.50	0.03	0.90	0.16	9.03	2.61	3.27	0.72	22.89	3.40	785.41	199.55	0.41	0.06	1.36	0.24	1.78	0.12	87.91	7.14
Leptoclinides sp.	2.62	0.51	0.25	0.02	1.54	0.01	4.29	0.66	3.81	0.76	33.09	13.67	912.14	37.74	0.32	0.01	1.82	1.16	1.27	1.34	14.98	2.03
Tridemnum cerebriforme	1.02	0.05	0.31	0.03	0.95	0.57	3.00	0.54	1.60	0.45	13.14	3.41	486.70	129.12	0.22	0.03	0.93	0.10	1.12	0.07	24.59	1.19
Distaplia skoogi	3.88	0.48	0.92	0.03	0.47	0.02	18.41	2.11	1.74	0.10	12.63	1.14	164.25	38.27	0.42	0.02	1.52	0.43	3.38	0.29	78.21	4.83
Hypodistoma vastum	3.28	0.20	0.17	0.02	1.01	0.08	194.55	29.17	0.66	0.07	30.94	4.39	242.16	23.33	0.25	0.02	0.51	0.08	1.35	0.04	23.05	2.42
Sigillina sp.	0.91	0.21	0.18	0.03	1.16	0.13	9.53	3.53	2.00	0.58	23.49	2.34	972.96	347.34	0.31	0.08	1.25	0.35	2.18	0.74	19.06	2.01
Eudistoma sp. 1	1.17	0.14	0.27	0.07	3.21	0.49	4658.40	586.92	8.24	0.46	127.53	7.80	2631.81	271.52	1.10	0.09	2.63	0.55	2.47	0.08	36.01	1.02
Eudistoma sp. 2	2.03	0.32	0.36	0.09	3.42	0.77	95.56	13.40	9.04	1.69	133.38	21.55	2807.58	229.00	1.23	0.14	3.28	0.19	2.81	0.32	30.22	3.71
Polycitor sp.	1.64	0.20	0.26	0.06	4.32	2.14	388.28	146.99	10.15	3.75	295.65	68.87	3684.54	1891.95	1.12	0.15	2.22	0.25	1.46	0.12	32.06	3.59
Aplidium sp	8.10	0.85	0.88	0.08	1.73	0.45	7.58	0.59	6.08	0.98	191.65	33.08	1663.91	285.01	0.85	0.12	1.77	0.16	3.61	0.09	38.29	2.23
Aplidium monile	3.66	1.18	0.51	0.06	1.38	0.14	6.77	2.75	5.62	0.38	42.07	15.75	1562.47	152.07	0.75	0.02	2.24	0.17	4.36	0.62	52.10	13.34
Aplidiopsis tubiferus	1.08	0.17	0.32	0.02	6.04	0.75	22.20	8.87	10.92	1.83	136.10	10.58	3281.75	533.86	1.10	0.17	3.16	0.40	2.48	0.39	24.56	3.87
Synoicum sp.	2.85	0.28	0.36	0.05	0.67	0.05	2.09	0.22	2.23	0.19	34.93	11.05	655.29	62.52	0.44	0.02	1.78	1.02	17.57	1.06	60.92	1.96
Pseudodistoma sp. 1	1.37	0.14	0.59	0.23	0.26	0.15	1694.81	421.50	3.08	1.05	0.02	0.00	0.18	0.04	0.08	0.02	0.66	0.12	2.85	0.40	61.44	6.08
Pseudodistoma sp. 2	8.94	6.59	1.11	0.70	1.42	1.38	3.76	2.61	8.80	7.17	0.26	0.05	1.14	1.32	0.35	0.26	1.99	0.44	10.46	5.63	163.10	106.99
Pseudodistoma sp. 3	8.01	2.71	0.96	0.12	1.92	0.68	5.34	1.26	11.36	4.04	0.51	0.26	1.87	0.46	0.79	0.12	4.22	0.38	4.81	0.58	102.43	10.03
Oceanic concentrations (ppm)[97]	**1.0×10^{-2}**		**7.0×10^{-5}**		**2.7×10^{-6}**		**2.0×10^{-3}**		**2.1×10^{-4}**		**2.0×10^{-5}**		**3.0×10^{-5}**		**1.2×10^{-6}**		**4.8×10^{-4}**		**1.5×10^{-4}**		**3.5×10^{-4}**	

* Indicates measurements shown to be influencing outliers which were subsequently adjusted for PCA.

Table 3.3: Non-transition metal concentrations of 25 Algoa Bay ascidian species and oceanic concentrations[97] of the metals measured in ppm (mg of metal per kg of whole dry ascidian or mg per kg of seawater). Ascidian metal concentration values are averages of the triplicate measurements of whole dry ascidian samples after HNO_3/H_2O_2 digestion

	Li		Be		B		Rb		Sr		Sn		Sb		Cs		Ba		U		Al		As	
Ascidian Species	**mean**	**sd**	**mean**	**sd**	**mean**	**sd**	**mean**	**sd**	**mean**	**sd**	**mean**	**sd**	**mean**	**sd**	**mean**	**sd**	**mean**	**sd**	**mean**	**sd**	**mean**	**sd**	**mean**	**sd**
Botryllus sp.	5.60	0.22	0.12	0.01	41.09	4.23	5.94	0.60	1549.61	248.42	0.38	0.10	0.04	0.01	0.43	0.04	15.09	1.16	0.70	0.09	2158.09	231.23	6.89	1.32
Gynandrocarpa placenta	2.28	0.10	0.02	0.00	41.36	1.51	3.38	0.36	133.09	6.04	0.11	0.02	0.02	0.01	0.04	0.02	1.47	0.40	0.30	0.01	242.85	63.01	15.51	3.26
Clavelina steenbrasensis	62.74*	4.05	0.05	0.01	83.78	5.15	7.42	0.43	249.51	3.50	0.09	0.01	0.02	0.00	0.26	0.05	19.27	3.19	0.24	0.01	1085.29	70.96	19.98	2.83
Pycnoclavella filamentosa	5.98	0.13	0.30*	0.35	61.50	0.66	4.15	0.49	0.00	0.00	0.12	0.02	0.06	0.00	0.31	0.04	24.93	0.85	0.54	0.06	1633.49	296.91	5.18	0.22
Pycnoclavella narcissus	8.78	0.38	0.19	0.02	60.68	2.36	11.85	0.54	286.49	128.86	0.16	0.01	0.03	0.00	0.72	0.07	10.42	0.57	0.39	0.04	3423.27	139.91	13.61	1.70
Atriolum marinense	1.84	0.29	0.03	0.01	47.26	5.67	3.61	0.62	2526.81	729.17	0.13	0.02	0.03	0.00	0.11	0.04	9.54	1.31	6.75	2.22	353.48	187.27	103.81	9.70
Didemnum leopardi	2.14	0.26	0.04	0.00	71.05	0.60	2.46	0.18	2755.98	2965.79	0.09	0.02	0.01	0.00	0.15	0.02	10.37	0.60	3.92	0.08	932.92	111.67	3.92	0.26
Didemnum sp. 1	4.40	1.44	0.13	0.07	37.54	1.37	6.84	2.89	1500.54	617.71	0.19	0.05	0.05	0.01	0.51	0.28	12.15	0.93	0.83	0.12	2444.39	1360.70	52.58	3.53
Didemnum sp. 2	4.09	0.66	0.07	0.01	89.87	10.21	4.28	1.00	987.22	1496.01	0.14	0.02	0.04	0.00	0.31	0.07	13.52	2.45	3.21	0.70	1759.64	288.23	246.46	77.95
Lissoclinum sp.	2.94	0.34	0.06	0.01	75.20	3.48	3.54	0.40	5661.17	788.24	0.14	0.04	0.06	0.00	0.24	0.05	15.14	1.54	12.02	0.90	948.72	233.92	11.92	0.33
Leptoclinides sp.	3.11	0.16	0.03	0.00	95.38	12.54	2.64	0.18	1178.82	1018.86	0.52*	0.76	0.04	0.01	0.19	0.01	20.02	5.73	6.14	0.85	1047.95	101.55	3.30	0.39
Tridemnum cerebriforme	2.39	0.37	0.03	0.01	78.08	7.82	3.02	0.17	0.00	0.00	0.15	0.02	0.07	0.12	0.09	0.02	10.43	1.05	3.05	0.10	673.82	132.46	10.83	1.26
Distaplia skoogi	3.33	0.17	0.01	0.00	77.02	1.80	7.58	0.29	237.86	16.21	0.05	0.02	0.02	0.00	0.05	0.00	2.25	0.42	0.57	0.07	181.46	29.74	19.74	0.49
Hypodistoma vastum	3.65	0.33	0.03	0.00	81.24	3.28	3.76	0.21	181.40	31.18	0.08	0.03	0.04	0.00	0.08	0.00	1.49	0.27	1.05	0.03	132.60	14.61	12.78	0.51
Sigillina sp.unknown	3.19	0.29	0.04	0.02	54.08	2.43	3.52	0.47	301.92	45.24	0.09	0.02	0.01	0.00	0.14	0.05	2.71	0.65	0.18	0.04	646.31	200.98	5.95	0.71
Eudistoma sp. 1	4.71	0.52	0.12	0.01	51.40	7.13	4.90	0.25	1710.67	188.00	0.11	0.01	0.08	0.01	0.40	0.02	14.76	1.77	1.55	0.16	1641.86	97.34	8.30	0.03
Eudistoma sp. 2	6.30	1.75	0.15	0.04	57.24	14.78	7.86	1.08	1300.06	391.56	0.18	0.03	0.03	0.01	0.53	0.08	12.37	0.71	0.60	0.13	2662.54	792.86	6.11	0.25
Polycitor sp.	4.67	0.05	0.09	0.03	49.21	3.23	5.47	0.18	1072.43	313.37	0.12	0.01	0.08	0.01	0.33	0.07	15.18	4.54	0.71	0.11	1494.66	313.59	93.67	30.97
Aplidium sp.	4.80	0.47	0.08	0.01	75.44	3.82	5.73	0.08	902.20	218.65	0.18	0.01	0.05	0.02	0.32	0.01	7.39	1.57	0.91	0.31	1459.44	223.76	10.28	0.25
Aplidium monile	5.74	0.35	0.08	0.02	80.52	10.14	7.42	1.24	1023.60	579.23	0.07	0.02	0.02	0.00	0.32	0.05	28.20	7.80	1.00	0.72	1545.81	236.28	13.81	1.84
Aplidiopsis tubiferus	5.26	0.66	0.13	0.03	41.18	3.30	6.49	1.01	1933.13	220.49	0.22	0.05	0.06	0.01	0.47	0.11	16.87	2.57	0.68	0.08	2280.10	440.69	4.63	0.48
Synoicum sp.	5.31	0.19	0.04	0.01	101.08	6.49	6.82	0.20	230.41	6.97	0.08	0.04	0.02	0.00	0.17	0.01	14.59	2.35	0.38	0.05	695.82	55.91	15.46	0.95
Pseudodistoma sp. 1	4.34	0.16	0.00	0.00	108.12	2.18	4.60	0.03	0.18	0.00	0.00	0.00	0.00	0.00	0.01	0.00	2.00	0.63	0.24	0.06	0.07	0.02	15.62	0.57
Pseudodistoma sp. 2	3.72	0.78	0.05	0.01	69.10	6.70	4.27	0.35	0.70	0.93	0.16	0.05	0.04	0.04	0.09	0.09	5.65	7.11	0.50	0.14	0.39	0.38	13.25	4.74
Pseudodistoma sp. 3	3.75	0.55	0.07	0.02	63.77	1.62	6.07	0.62	0.33	0.30	0.20	0.04	0.08	0.04	0.27	0.06	5.86	4.41	0.72	0.06	0.96	0.18	11.85	0.60
Oceanic concentrations (ppm)[97]	**1.8×10^{-1}**		**2.1×10^{-7}**		**4.5**		**1.2×10^{-1}**		**7.8**		**5.0×10^{-7}**		**2.0×10^{-4}**		**3.1×10^{-4}**		**1.5×10^{-2}**		**3.2×10^{-3}**		**3.0×10^{-5}**		**1.2×10^{-3}**	

* Indicates measurements shown to be influencing outliers which were subsequently adjusted for PCA

Figure 3.1: Metal concentrations in ppm (mg/kg dry weight) of 25 Algoa Bay ascidians. Values are an average of the ICP-MS measurements after NO_3/H_2O_2 digestion of the representative triplicate samples of ground dried ascidians.

Even with this acknowledgement of a widely varying sense of scale, it is easy to overlook certain metals, such as Be, Sn, Sb, Cs, and Co, which are found only at low concentrations (< 1 ppm). These "low concentration" metals may still be of some importance. It is possible that the ascidians could still be considered to be bioaccumulating these "low concentration" metals as their concentrations within the ascidians may be significantly higher than the surrounding seawater concentrations.[133] A measure of the degree to which the ascidians are accumulating the metal ions relative to the surrounding seawater would therefore be far more useful in any attempts to determine any patterns in the unique data set (the first of its kind from an African ascidian population) which we had in hand. Unfortunately, at the time that the ascidian collections were made it was unbeknown to us that a metal ion analysis would be carried out several years later on these Algoa Bay ascidians and accordingly no seawater samples were collected from the relevant dive sites at the time of the collection. Investigations into the literature relating to metal concentrations in Algoa Bay yielded some results relating to metal concentrations in water samples collected within river estuaries[134,135] at coastal sites near sewage outfalls[136] as well as in Port Elizabeth Harbour.[137] Although these reports are interesting, they do not include all 24 metals which were measured in this present study, and they are mostly from sites where the metal concentrations are expected to be very high, as opposed to those concentrations expected at the relatively pristine open water collection sites which are further off shore. For these reasons, the oceanic metal concentrations (Tables 3.2 and 3.3) used to determine the bioconcentration factors for the metals in the ascidians are those values reported by Nozaki[133] in a review of the open water oceanic elemental distribution in the North Pacific. Regrettably there have been no similar studies made in the Indian Ocean that we could access for our purposes.

$$\text{Bioconcentration Factor} = \frac{[\text{metal}] \text{ in whole ascidian (ppm)}}{[\text{metal}] \text{ in seawater}^{133} \text{ (ppm)}}$$

The bioconcentration factors calculated for each of the metal concentration measurements are presented in Figure 3.2. There are still vast differences in the calculated bioconcentration factors between different ions, with some concentrations for example of Li and B appearing to be only an order of magnitude higher than the general values reported for seawater, while other metals such as Al and Fe were concentrated by several orders of magnitude higher than seawater by some species (Figure 3.2). However, as expected even though a logarithmic scale is still required to view the data, the use of a bioconcentration factor helps to establish which of the "low concentration" metals the ascidians are actively concentrating, for example Be, Cd, Sn and Co.

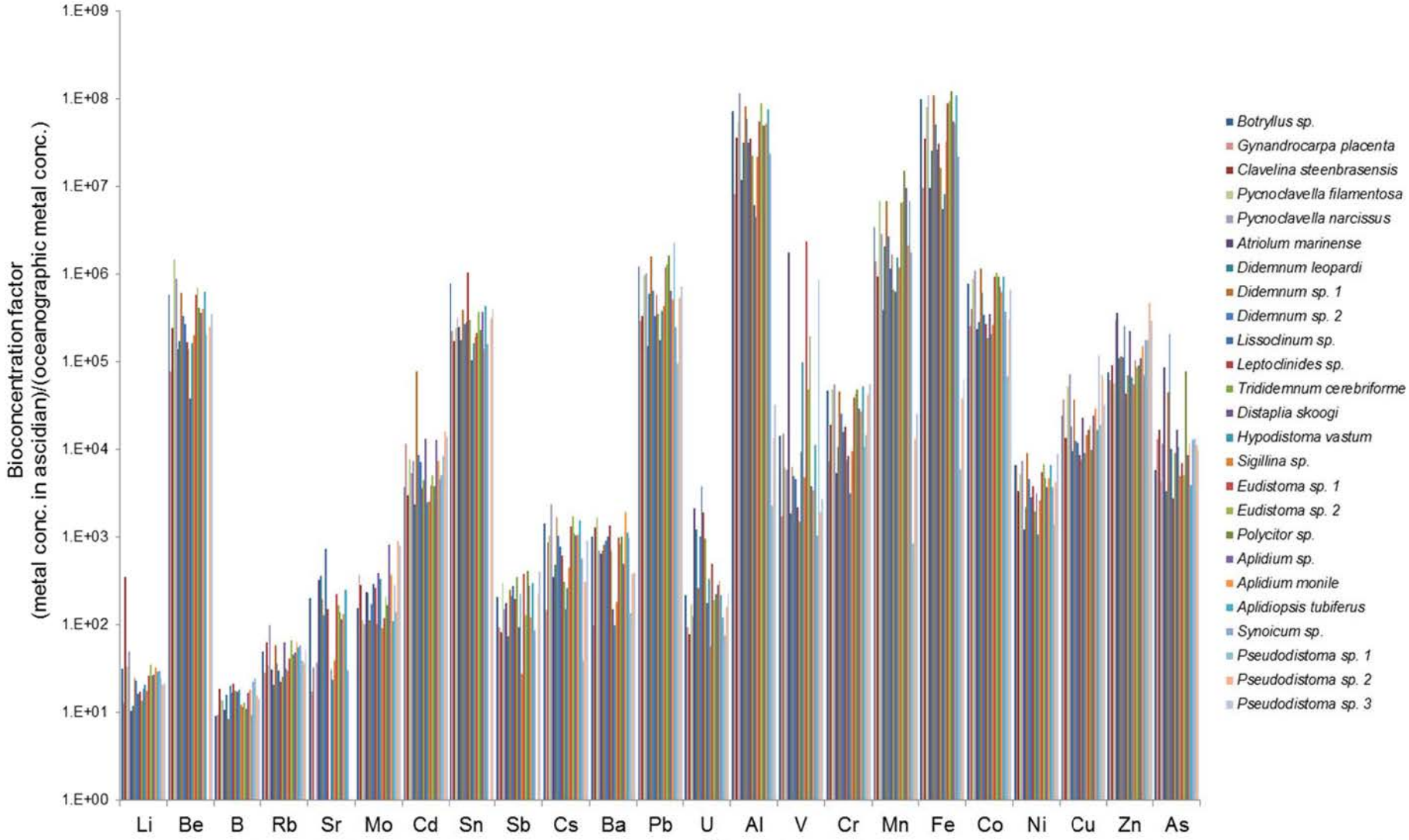

Figure 3.2: Metal bioconcentration factors (relative to oceanic concentrations[97]) of 25 Algoa Bay ascidians. Values are calculated from the average of the ICP-MS measurements after NO_3/H_2O_2 digestion of the representative triplicate samples of ground dried ascidians.

The magnitude and relative complexity of this data set made it difficult to observe clear patterns without further statistical analysis. Although knowing the metal concentrations in a particular species of ascidian is interesting, what would be far more beneficial would be to be able to confidently identify patterns within these data which might, firstly for example, identify quantifiable differences between different collection sites possibly indicative of unknown localised areas of metal pollution. Secondly, since our collection of ascidians was comprised of species collected in 2004 and 2011, it would also be interesting to establish if certain metals are more abundant in the ascidians relative to the year collected. A third question that could be asked would be: are certain taxonomic groups *i.e.* families of ascidians accumulating a specific metal preferentially over others, and are groups of metals being concentrated together in different species from the same taxonomic families. In an attempt to address these interesting questions the data set was investigated using multivariate statistical analyses.

3.4.1.1 Multivariate analysis – Correlation matrix

One approach to establishing patterns or reducing the dimensionality of a large data set with many variables is through principal component analysis (PCA). In essence PCA identifies which variables differ most between the individual cases.[138] In other words PCA re-expresses the data according to a set of factors where the greatest amount of variability is shown. In this way the measured variables are grouped into the factors based on their correlations with each other (grouped into same factor) as well as the variance between them (grouped into different factors), thus it is expected that the majority of the data set may now be accounted for and explained using fewer factors, or principal components.[138] Plotting the weightings of the principal components against each other will then help to show any patterns that can be used to explain the majority of the data set, and may further establish key trends that can help predict the results of a new set of measurements. Therefore PCA can be used to establish relationships between cases and variables.[138] In this present study the variables are the metal concentrations measured in the whole dry ascidian samples, which are the cases. Since PCA does not test anything, but rather identifies sources of grouping and variability in a data set, it is a good tool to use in exploring the metal concentration data which we had in hand. In particular our aim was to establish if there are any patterns relating to metal ion concentrations at the different dive sites, over the two different years of collections, and within certain taxonomic families of ascidians.

The first step was to establish if the data set was indeed appropriate for PCA. The metal concentration data set certainly has multiple variables, but if there are no correlations between them, the variables cannot be grouped into factors as no relationship will be apparent. On the other hand, if the variables are all strongly correlated to one another then there is no need for PCA analysis as there is probably only one underlying factor that can

explain the data set.[138] In other words, PCA analysis will be useful for a data set which has correlating variables that can be grouped into factors as well as a level of variance between said variables so that patterns and trends may become apparent when the established factors are compared. The best approach to use to determine if the data set is appropriate, is to create a correlation matrix of the variables.[138] Table 3.4 is the correlation matrix obtained for the ascidian metal concentrations. The numbers expressed in this matrix are the correlation coefficients (*r* values) calculated, and those that are marked red were shown to be significant with a probability (*p* value) of less than 0.05. Negative values indicate an inverse correlation, for example the correlation between Pb and B is -0.59 which would imply that an ascidian with a relatively high concentration of Pb will have a low concentration of B and *vice versa*. The correlation matrix obtained for the data shows a number of significant correlations ($p < 0.05$; marked in red) between metal concentrations, as well as a level of variance which satisfies the need for PCA to establish the underlying factors and patterns in the data. Interestingly, vanadium and arsenic are not significantly correlated to any metals, and the accumulation of vanadium and arsenic in the ascidians appeared to be independent of any other metal.

Although the calculated bioconcentration factors facilitated in visualising the degree to which the ascidians accumulate metals relative to the surrounding seawater, there was no difference in the correlation matrices (or the subsequence PCA) results obtained for the factored measurements compared to that of the non-factored measurements which would imply that the relationships between the metal concentrations within the ascidians are independent of the seawater concentrations.

Table 3.4: Correlation matrix of the triplicate whole dry ascidian metal concentration data for the 24 metals measured. Correlations marked in red are significant at $p < 0.05$.

	Li																							
Be	0.01	Be																						
B	0.16	-0.27	B																					
Rb	0.30	0.34	-0.07	Rb																				
Sr	-0.14	-0.02	-0.18	-0.19	Sr																			
Mo	-0.03	-0.18	0.17	-0.01	-0.15	Mo																		
Cd	-0.09	0.11	-0.27	0.19	0.00	0.09	Cd																	
Sn	-0.07	0.10	-0.03	-0.02	-0.01	0.00	0.03	Sn																
Sb	-0.13	0.23	-0.25	-0.04	0.11	-0.07	0.04	0.18	Sb															
Cs	0.11	0.59	-0.39	0.70	0.13	-0.26	0.24	0.21	0.27	Cs														
Ba	0.26	0.39	0.00	0.16	0.21	-0.32	-0.08	0.18	0.23	0.45	Ba													
Pb	-0.08	0.45	-0.59	0.32	0.12	-0.31	0.24	0.22	0.44	0.73	0.35	Pb												
U	-0.18	-0.17	0.14	-0.44	0.71	-0.07	-0.11	0.19	0.12	-0.16	0.15	-0.24	U											
Al	0.08	0.58	-0.33	0.62	0.16	-0.38	0.20	0.22	0.16	0.94	0.47	0.67	-0.12	Al										
V	-0.09	-0.04	-0.15	-0.14	0.17	-0.17	-0.09	-0.12	0.11	-0.06	-0.04	-0.04	0.14	-0.09	V									
Cr	0.00	0.57	-0.41	0.50	-0.04	-0.10	0.20	0.21	0.43	0.77	0.38	0.78	-0.30	0.62	-0.06	Cr								
Mn	-0.08	0.38	-0.40	0.18	0.09	-0.15	0.15	0.05	0.37	0.51	0.29	0.72	-0.22	0.53	0.03	0.51	Mn							
Fe	0.03	0.57	-0.49	0.49	0.14	-0.39	0.21	0.17	0.28	0.86	0.46	0.85	-0.22	0.89	0.00	0.70	0.78	Fe						
Co	0.01	0.65	-0.50	0.62	0.04	-0.21	0.35	0.14	0.37	0.92	0.40	0.81	-0.29	0.85	-0.01	0.83	0.69	0.88	Co					
Ni	-0.03	0.48	-0.47	0.52	-0.11	0.01	0.45	0.35	0.27	0.70	0.19	0.62	-0.32	0.57	-0.17	0.75	0.34	0.57	0.77	Ni				
Cu	-0.05	0.42	0.11	0.39	-0.27	0.27	0.17	-0.04	-0.16	0.14	0.00	-0.08	-0.28	0.10	-0.14	0.13	-0.08	0.02	0.15	0.28	Cu			
Zn	-0.10	-0.09	0.07	0.19	0.07	0.59	0.14	-0.13	-0.13	-0.11	-0.28	-0.29	0.16	-0.21	0.17	-0.03	-0.33	-0.28	-0.15	-0.03	0.43	Zn		
As	-0.05	-0.06	0.06	-0.07	0.10	-0.11	0.11	-0.05	0.07	0.04	0.02	-0.01	0.16	0.09	0.11	-0.03	0.10	0.06	0.07	-0.03	-0.13	0.07	As	
Se	-0.06	-0.13	0.04	0.27	-0.16	0.23	0.27	-0.15	-0.17	-0.14	-0.25	-0.21	-0.15	-0.15	-0.08	-0.16	-0.21	-0.18	-0.07	0.11	0.21	0.27	0.00	Se

3.4.1.2 *Multivariate analysis – Principal component analysis*

Principal component analysis (PCA) was carried out on the ascidian metal concentration data set based on correlations. Since PCA aims to establish variance in a data set, this analysis may give added unsubstantiated weight to variables with large measurement values, thus potentially missing patterns resulting from those measurements with lower values.[138] In order to overcome this challenge, the original data set was standardised to give equal weighting and validity to all variables. When PCA is performed on raw non-standardised data it is based on covariance as opposed to correlations, which is when the data set is standardised. The ascidian metal concentration data was indeed very varied, and even with the calculation of a bioconcentration factor, in an attempt to standardise the raw data, there were still vast differences between the metal concentration factors measured. For this reason PCA was carried out based on correlations rather than covariance.

Since 24 metals were measured the maximum number of factors that could be used to explain the data set was 24. The eigenvalues of these PCA generated factors as well as the percentages of the data set which could be accounted for by each factor are recorded in Table 3.5. Since our aim was to reduce the number factors required to explain the data set efficiently, the next step in our analysis was to decide how many of the PCA generated factors to retain, and how many to ignore.

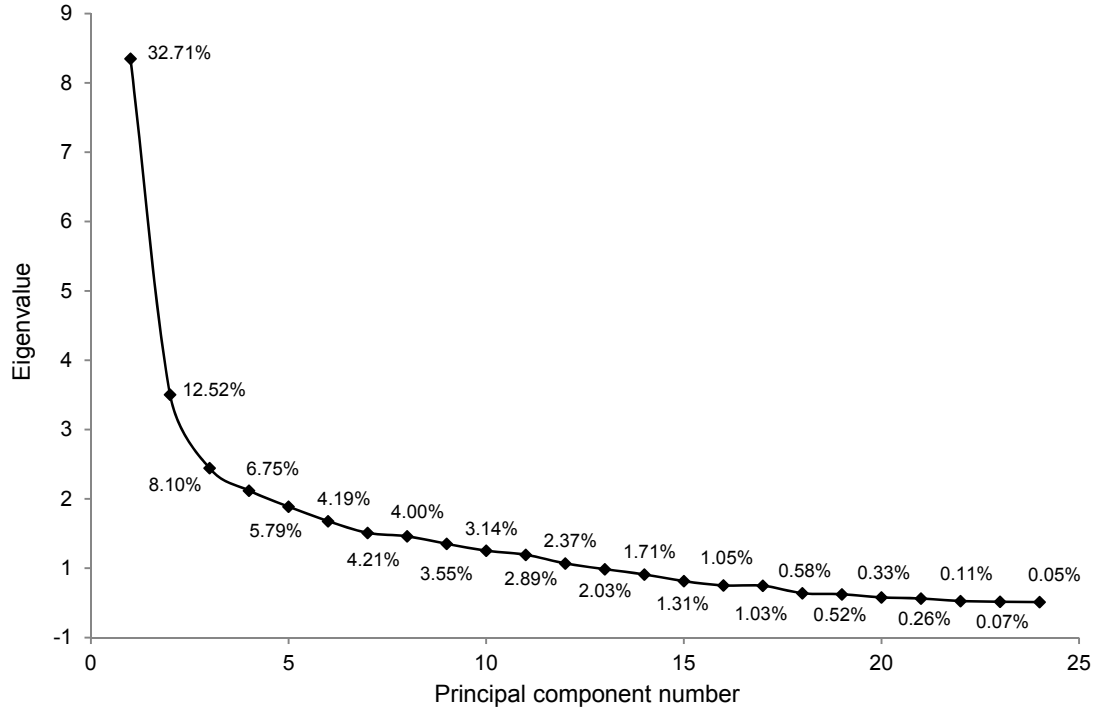

Figure 3.3: Scree plot of the principal components calculated for the ascidian metal concentration data. Points are labelled with the percentage value of the data that can be explained by the related principal component.

A common method for deciding on the number of factors to retain is by plotting a scree plot (Figure 3.3).[138] The points on the curve that appear before the break, or elbow of the curve, after which the curve levels out, are the factors that one would go forward with.[139,140] However, in this case there was not a clear break in the curve, and so it was difficult to decide which factors to ignore. For this reason, Kaiser's criterion was used to establish which principal components to continue with. Kaiser's criterion states that factors with an eigenvalue above 1 are significant.[141]

Table 3.5: PCA eigenvalues of correlation matrix and related statistics. Components highlighted in red are retained following Kaiser's criterion.

	Eigenvalue	% Total Variance	Cumulative Eigenvalue	Cumulative %
1	7.850571	32.71071	7.85057	32.7107
2	3.003319	12.51383	10.85389	45.2245
3	1.944684	8.10285	12.79857	53.3274
4	1.619947	6.74978	14.41852	60.0772
5	1.388797	5.78665	15.80732	65.8638
6	1.179509	4.91462	16.98683	70.7784
7	1.010144	4.20893	17.99697	74.9874
8	0.961153	4.00480	18.95812	78.9922
9	0.852058	3.55024	19.81018	82.5424
10	0.753396	3.13915	20.56358	85.6816
11	0.693998	2.89166	21.25757	88.5732
12	0.569398	2.37249	21.82697	90.9457
13	0.486729	2.02804	22.31370	92.9738
14	0.409946	1.70811	22.72365	94.6819
15	0.314395	1.30998	23.03804	95.9918
16	0.252131	1.05054	23.29017	97.0424
17	0.247466	1.03111	23.53764	98.0735
18	0.139915	0.58298	23.67756	98.6565
19	0.124453	0.51855	23.80201	99.1750
20	0.079414	0.33089	23.88142	99.5059
21	0.063090	0.26288	23.94451	99.7688
22	0.027368	0.11403	23.97188	99.8828
23	0.016211	0.06755	23.98809	99.9504
24	0.011908	0.04962	24.00000	100.0000

Table 3.5 shows the eigenvalues of each factor along with the percentage of the variance that is explained by each factor. With these data, one would continue with the first seven factors (highlighted red), which would have a cumulative percentage of 74.98% of the variance explained. Normally seven components would be a large number of components to investigate and Table 3.5 shows that the eigenvalues of the components three to seven are fairly small in comparison to the first two components. The third principal component,

although small, is on the elbow of the scree plot and incorporating it would explain over 50% of the data set, thus our most thorough statistical investigations of the data set focused on establishing patterns in the data that could be explained by the first three factors generated.

The results of the PCA showed that the variables had been grouped into factors which displayed the most variance between each other and it was of interest to establish the weighting that each factor had on the metals measured.[138] These variable factor loadings are shown in Table 3.6. The higher the loading score of a metal the more emphasis it had on the particular factor. An alternative view is that the factor within which a metal has its highest score will be the factor that best explains the results obtained for that metal variable.[138] The PCA factor loading for each variable (Table 3.6) showed that eleven of the 24 metal variables had strong factor weightings (>0.50) in the first principal component, which accounted for 32.71% of the variance in the total data set. Thus, the concentrations of these eleven metals within the ascidian cases will influence the case weightings for the first principle component.

Table 3.6: Factor loading scores of the metal variables obtained from principal component analysis. Red font indicates strong weightings (>0.5).

	Factor 1	Factor 2	Factor 3	Factor 4	Factor 5	Factor 6	Factor 7
Li	-0.04	-0.12	-0.58	0.29	0.15	-0.08	-0.19
Be	-0.67	-0.12	-0.05	0.20	-0.09	0.33	0.11
B	0.52	-0.11	-0.37	0.40	-0.14	-0.05	-0.31
Rb	-0.58	-0.57	-0.17	0.28	0.22	-0.06	0.00
Sr	-0.06	0.57	0.45	0.43	0.14	-0.10	0.29
Mo	0.31	-0.53	0.34	0.03	-0.33	0.13	-0.21
Cd	-0.30	-0.32	0.43	-0.14	0.11	-0.46	0.01
Sn	-0.23	0.14	0.07	0.10	-0.70	-0.28	-0.05
Sb	-0.39	0.31	0.27	-0.17	-0.30	0.23	-0.39
Cs	-0.93	-0.05	-0.01	0.24	0.06	-0.05	0.03
Ba	-0.48	0.32	-0.30	0.46	-0.13	0.05	-0.07
Pb	-0.87	0.18	0.08	-0.24	-0.04	0.00	0.02
U	0.28	0.58	0.43	0.52	-0.14	-0.14	0.08
Al	-0.88	0.04	-0.10	0.26	0.13	-0.14	0.08
V	0.06	0.28	0.29	-0.02	0.43	0.48	-0.06
Cr	-0.85	-0.11	0.07	-0.03	-0.17	0.16	-0.13
Mn	-0.70	0.22	0.03	-0.29	0.09	0.11	-0.15
Fe	-0.93	0.14	-0.04	-0.01	0.14	-0.02	0.04
Co	-0.97	-0.08	0.08	0.00	0.08	0.01	-0.05
Ni	-0.76	-0.34	0.19	-0.08	-0.23	-0.17	0.01
Cu	-0.12	-0.69	0.06	0.30	-0.10	0.30	0.10
Zn	0.24	-0.49	0.58	0.38	0.07	0.25	-0.10
As	-0.02	0.18	0.22	0.13	0.37	-0.26	-0.70
Se	0.16	-0.55	0.23	-0.04	0.24	-0.35	0.08

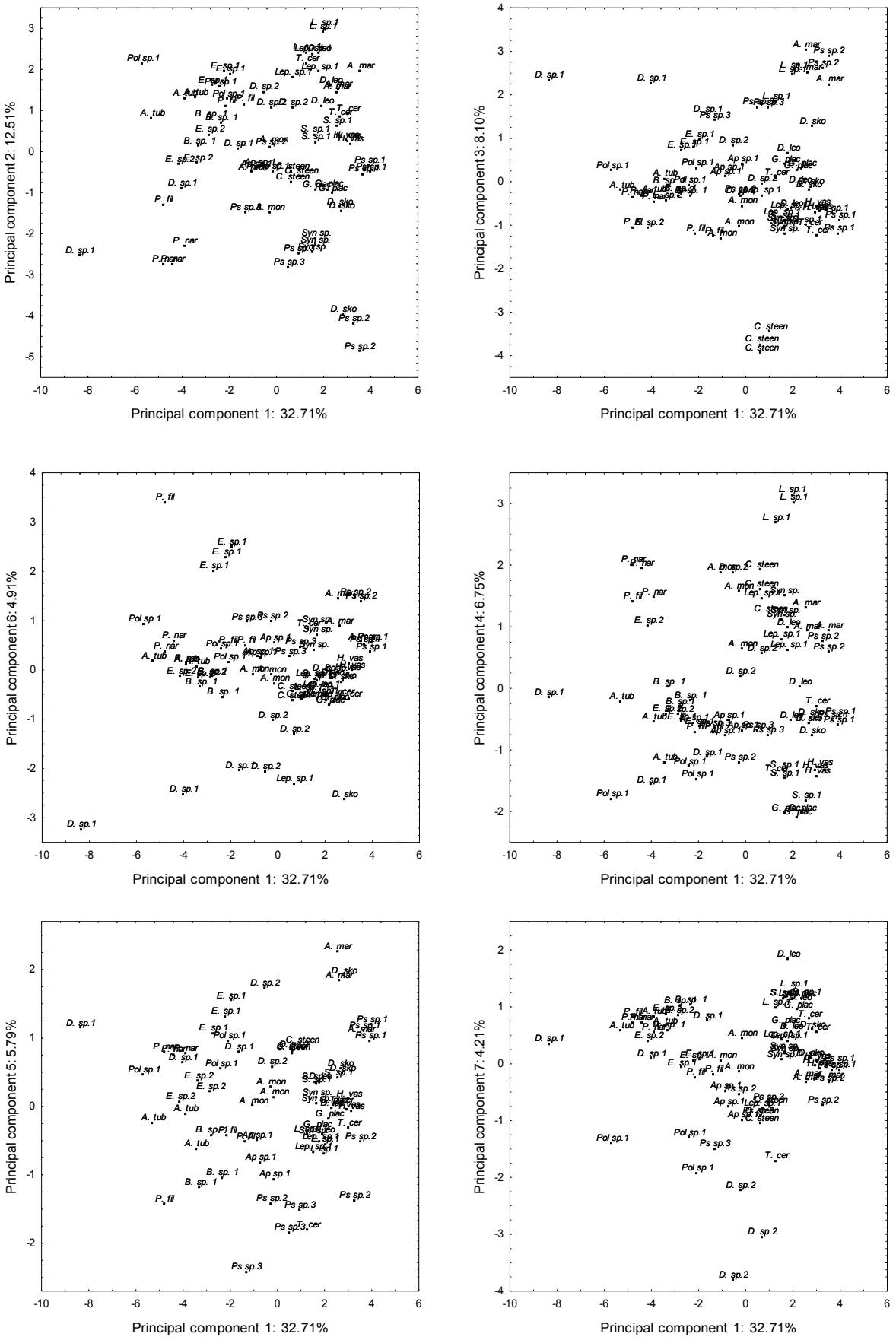

Figure 3.4: Principal component analysis results displayed as case factor loading plots of principal component 1 against each of the other retained principal components 2 to 7. Data points are labelled with abbreviated ascidian species names.

A visual representation of how the principal components are able to group the ascidian cases is shown in Figure 3.4 with a series of factor loading plots where cases are plotted based on their factor weightings for principal component one against each of the other retained principal components. At this stage we concluded that these plots are "busy" and do not reveal any obvious grouping of the ascidian cases. On investigation of the case factor loading plots generated from the principal component three against principal component one the *Clavelina steenbrasensis* (*C. steen*) samples appeared to be well separated from the other ascidians (Figure 3.4). The metal variables with reasonable factor weightings for factor three are Li (-0.58) and Zn (0.58). Since *C. steenbrasensis* has a low score for principal component three, it is reasonable to state that the concentrations recorded for Zn maybe much lower than the other ascidians or the concentration of Li is higher in *C. steenbrasensis* compared to the other ascidians. Revisiting the raw data in Tables 3.2 and 3.3 reveal that *C. steenbrasensis* has a zinc concentrations of 31.73 ppm which was not markedly lower that than of other ascidians. However, the lithium concentration was significantly larger (62.74 ppm) in *C. steenbrasensis* which is approximately 12 times higher than the Li concentrations recorded for the other ascidians in the study. This high Li concentration explained why this species appeared to be well isolated from the rest of the data set in the factor plot of PC 1 vs PC 3.

It was necessary for us at this point to evaluate the validity of the high lithium concentration obtained for *C. steenbrasensis*. Consequently, on further investigation of the data set we established that the high concentrations of Li were measured in all of the three samples of *C. steenbrasensis* assayed and that the concentrations of the other metals measured were not unreasonably different from trends observed in other ascidian species in our data set, thus providing significant support for the validity of the result obtained. It was also unclear why such a high concentration of lithium would be present in only one of the ascidian species especially since lithium has been shown to be a crucial trace metal in the development of ascidian embryos, with particular emphasis on the early development of the nervous system and larval tail.[142] Biological investigations have shown that over exposure of ascidian eggs and blastomeres to lithium chloride resulted in clear development anomalies, emphasising the need for controlled regulation of the uptake of this trace metal.[142]

In terms of the PCA results it was also of interest for us to see the effect which the high concentration of lithium in only one ascidian species had on the third principal component. It would appear that the variance explained by the third principal component was dominated by the result of only one ascidian and the relationship between the concentrations of lithium in the remaining ascidians was not being reflected. Since the PCA was based on correlations the effect of this unusual lithium measurement on the correlation analysis was investigated. The correlation between lithium and the other metals in the study was investigated further and in order to explain the method used to critically analyse these data the correlation between lithium and iron will be presented here as a representative example.

Regression Summary for Dependent Variable Li: R= 0.03066581 R²= 0.00094039				
	b	**Std.Err. b**	**t(73)**	**p-value**
Intercept	34.4926	11.2529	3.0652	0.0030
Fe	0.0307	0.1170	0.2621	0.7939

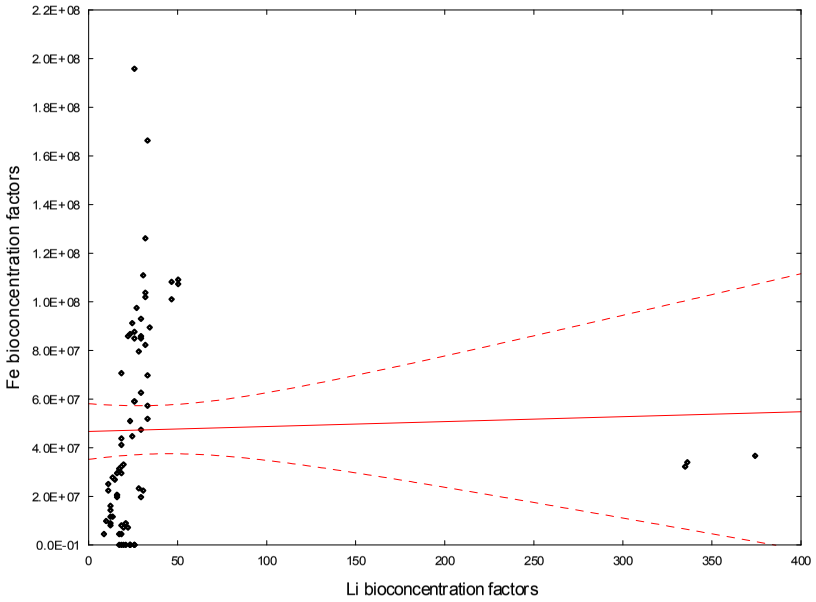

Regression Summary for Dependent Variable Li: R= 0.70373382 R²= 0.49524130				
	b	**Std.Err. b**	**t(70)**	**p-value**
Intercept	16.3086	1.1768	13.8578	0.0000
Fe	0.7037	0.0849	8.2873	0.0000

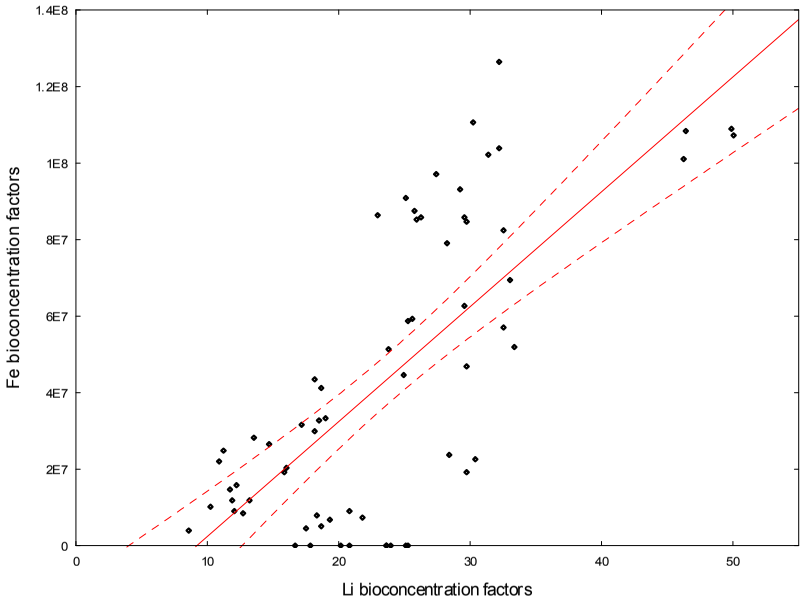

Figure 3.5: Correlation curves from Li vs. Fe with influencing data points (a) and without influencing data points (b). Regression lines are shown in red with a 95% confidence interval. The accompanying tables report the results of the multiple regression analyses performed.

The regression analysis performed between lithium and iron showed that there was no correlation between the concentrations of these metals (r = 0.0307). However, Figure 3.5 illustrates the correlation and regression results in a simple scatter plot, and it is clear to see that the data points relating to the three *C. steenbrasensis* samples are distinct outliers which may be having an effect on the overall regression results.

In order to determine whether these data points are influencing the correlation results, a residual analysis was performed, and the Cook's distance of the all the data points were measured to determine the most prominent outliers.[143,144] Cook's distance judges the contribution of each data point towards the determination of the least squares estimate in linear regression.[143,144] Data points which result in higher than average (for the data set tested) Cook's distance values can be considered to be outliers that may have an adverse effect or influence on the regression analysis results.[143,144] The residual analysis of lithium against iron using Cook's distance to determine outliers clearly showed that the three data points corresponding to the *C. steenbrasensis* samples were outliers, with Cook's distances of 1.86, 1.56 and 1.53 which were markedly larger than mean Cook's distance of 0.007 produced in this analysis.

Figure 3.5(b) shows the regression analysis results of lithium against iron with the *C. steenbrasensis* lithium data points removed. There is a dramatic difference in the regression analysis results, with a correlation coefficient of r = 0.7037 (shown by the solid red line) which has a significance within the confidence interval of $p < 0.05$ (red dashed lines). With the influencing outliers removed the true relationship between the metals is now apparent. It is important to note that the correlation and regression analyses of lithium against iron has been used here as an example to illustrate the dataset influencing outliers in the lithium data, however, lithium showed similar results against other metals, where the true correlation was only seen once the outliers were removed from the analysis.

Since the PCA analysis is based on correlations, it was important that the true relationship between the metals was being investigated. It was therefore fortuitous that these outliers in the lithium readings were revealed when investigating the case weightings in relation to the third principal component. It was believed that lithium was not the only metal to have influencing data points that would possibly result in false correlation values, and therefore subsequently affect the results of the PCA. Hence a systematic investigation of each of the metals was carried out using regression analysis and Cook's distance of the residuals to determine the most prominent outliers in each of the metal variable data sets. The regression analyses were then rerun with these outliers removed and if distinct changes in the r or p values calculated were seen then these outliers were deemed influencing data points.

The metals which contained influencing data points were Li, Be, Cd, and Sn. These outliers are indicated in Tables 3.1 and 3.2 by asterisks. The validity of the original readings is unclear however these data points were adjusted so that the PCA carried out would be based on the correlations that resulted from the majority of the readings, and not those skewed by unexplainable outliers. Unfortunately, the calculations involved in PCA do not allow for missing data and PCA will exclude any cases with incomplete data sets from the analysis.[138] For this reason, simply removing the influencing data points was not the correct approach to take and the influencing data points were therefore adjusted to give the average value of the remaining data points in the set. If, as in the case of Be, there was only one influencing data point (*Pycnoclavella filamentosa* sample 3), the influencing data point was adjusted to be the averaged value obtained for the two other samples assayed for that species.

Once all the influencing data points where established and adjusted a new correlation matrix was made (Table 3.7). This correlation matrix shows that the corrected metals *i.e.* Li, Be, Cd and Sn now have significantly stronger correlations to other metals than before they were corrected (shown in red in Table 3.7). Strong and significant direct correlations were seen between Be and Cs (0.97), Fe and Al (0.94) and Cs and Al (0.94) indicating that these pairs of metal are commonly present together in elevated levels in the ascidians investigated. Interestingly, the correlation results for the outlier corrected data once again show that the concentration of vanadium and arsenic are not significantly correlated to concentrations of any other metals.

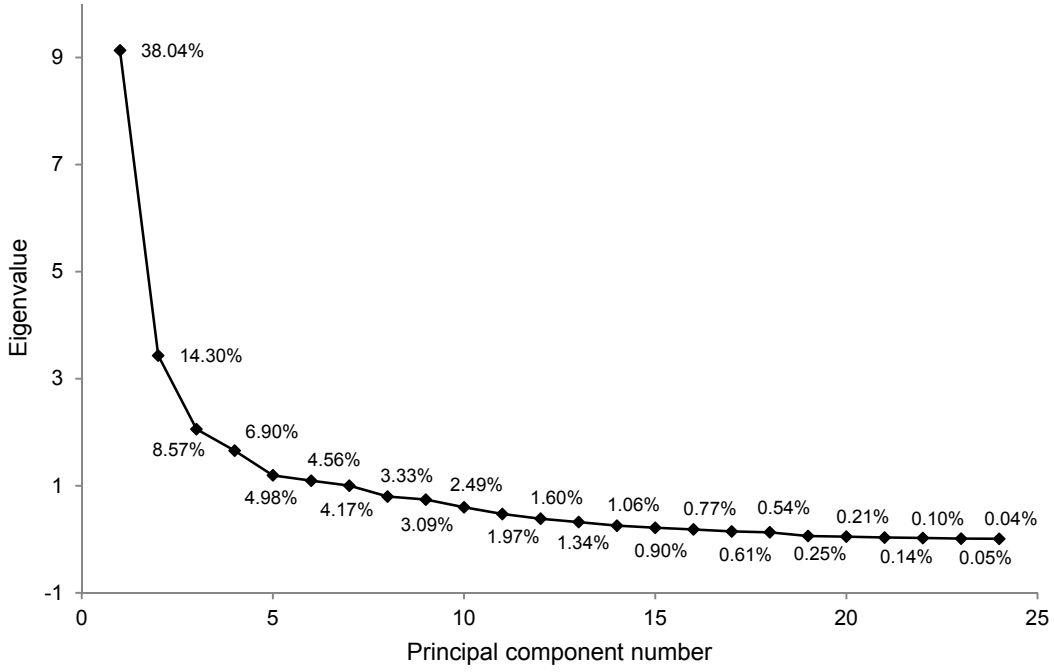

Figure 3.6: Scree plot of the principal components calculated for the ascidian metal concentration data where the influencing data points have been corrected. Points are labelled with the percentage value of the data that can be explained by the related principal component.

Table 3.7: Correlation matrix of the triplicate whole dry ascidian metal concentration data for the 24 metals measured with significant outliers corrected. Correlations marked in red are significant at $p < 0.05$.

	Li	Be	B	Rb	Sr	Mo	Cd	Sn	Sb	Cs	Ba	Pb	U	Al	V	Cr	Mn	Fe	Co	Ni	Cu	Zn	As	Se
Be	0.80																							
B	-0.05	-0.44																						
Rb	0.80	0.66	-0.07																					
Sr	-0.18	0.09	-0.18	-0.19																				
Mo	-0.19	-0.22	0.17	-0.01	-0.15																			
Cd	-0.13	-0.18	0.05	0.07	-0.18	0.78																		
Sn	0.28	0.54	-0.51	0.21	0.15	-0.04	-0.05																	
Sb	0.09	0.29	-0.25	-0.04	0.11	-0.07	-0.08	0.31																
Cs	0.79	0.97	-0.39	0.70	0.13	-0.26	-0.22	0.53	0.27															
Ba	0.38	0.40	0.00	0.16	0.21	-0.32	-0.35	0.12	0.23	0.45														
Pb	0.46	0.74	-0.59	0.32	0.12	-0.31	-0.27	0.51	0.44	0.73	0.35													
U	-0.44	-0.22	0.14	-0.44	0.71	-0.07	-0.11	-0.03	0.12	-0.16	0.15	-0.24												
Al	0.75	0.90	-0.33	0.62	0.16	-0.38	-0.30	0.47	0.16	0.94	0.47	0.67	-0.12											
V	-0.13	-0.02	-0.15	-0.14	0.17	-0.17	-0.08	-0.16	0.11	-0.06	-0.04	-0.04	0.14	-0.09										
Cr	0.67	0.80	-0.41	0.50	-0.04	-0.10	-0.02	0.50	0.43	0.77	0.38	0.78	-0.30	0.62	-0.06									
Mn	0.37	0.51	-0.40	0.18	0.09	-0.15	-0.15	0.25	0.37	0.51	0.29	0.72	-0.22	0.53	0.03	0.51								
Fe	0.70	0.89	-0.50	0.53	0.14	-0.40	-0.31	0.50	0.24	0.90	0.47	0.81	-0.22	0.94	0.01	0.68	0.69							
Co	0.72	0.91	-0.50	0.62	0.04	-0.21	-0.11	0.49	0.37	0.92	0.40	0.81	-0.29	0.85	-0.01	0.83	0.69	0.90						
Ni	0.50	0.69	-0.47	0.52	-0.11	0.01	0.15	0.53	0.27	0.70	0.19	0.62	-0.32	0.57	-0.17	0.75	0.34	0.60	0.77					
Cu	0.38	0.18	0.11	0.39	-0.27	0.27	0.34	-0.02	-0.16	0.14	0.00	-0.08	-0.28	0.10	-0.14	0.13	-0.08	0.05	0.15	0.28				
Zn	-0.05	-0.04	0.07	0.19	0.07	0.59	0.65	-0.08	-0.13	-0.11	-0.28	-0.29	0.16	-0.21	0.17	-0.03	-0.33	-0.29	-0.15	-0.03	0.43			
As	-0.10	-0.03	0.06	-0.07	0.10	-0.11	0.08	0.00	0.07	0.04	0.02	-0.01	0.16	0.09	0.11	-0.03	0.10	0.04	0.07	-0.03	-0.13	0.07		
Se	-0.03	-0.15	0.04	0.27	-0.16	0.23	0.37	-0.18	-0.17	-0.14	-0.25	-0.21	-0.15	-0.15	-0.08	-0.16	-0.21	-0.18	-0.07	0.11	0.21	0.27	0.00	

Once again the next step in analysing this corrected data set was to establish the number of principal components to keep for further analysis. The scree plot in Figure 3.6 was once again difficult to interpret with no clear elbow and thus Kaiser's criterion (Table 3.8) was used as an alternative method to resolve this impasse. Table 3.8 shows that the first seven components accounting for a cumulative 81.5% of the total variance in the data set have eigenvalues which are greater than or equal to one which through Kaiser's criterion would deem them significant to explore further.[141]

Table 3.8: Eigenvalues of the correlation matrix and related statistics for the ascidian metal concentration data where the influencing data points have been corrected. Components highlighted in red are retained following Kaiser's criterion.

	Eigenvalue	% Total variance	Cumulative eigenvalue	Cumulative %
1	9.13	38.04	9.13	38.04
2	3.43	14.30	12.56	52.34
3	2.06	8.57	14.62	60.91
4	1.66	6.90	16.27	67.81
5	1.19	4.98	17.47	72.78
6	1.09	4.56	18.56	77.34
7	1.00	4.17	19.56	81.51
8	0.80	3.33	20.36	84.84
9	0.74	3.09	21.10	87.93
10	0.60	2.49	21.70	90.42
11	0.47	1.97	22.17	92.39
12	0.38	1.60	22.56	94.00
13	0.32	1.34	22.88	95.33
14	0.25	1.06	23.13	96.39
15	0.22	0.90	23.35	97.29
16	0.18	0.77	23.53	98.06
17	0.15	0.61	23.68	98.67
18	0.13	0.54	23.81	99.21
19	0.06	0.25	23.87	99.47
20	0.05	0.21	23.92	99.68
21	0.03	0.14	23.96	99.82
22	0.02	0.10	23.98	99.91
23	0.01	0.05	23.99	99.96
24	0.01	0.04	24.00	100.00

Table 3.9 shows the factor coordinates generated from the PCA of the outlier corrected ascidian metal concentration data. The values shown in red are the stronger factor weights for each metal variable. Thus it was easy for us to see that the factors with the strongest weighting were factors 1 and 2 with thirteen metals and eight metals respectively showing strong weightings. The only metal variables with reasonable weightings with factor 3 are Sr

(0.51) and Zn (0.52) which both had stronger weightings with factor two. The other retained factors also only had one or two strong weightings across the variables and thus may not produce insightful results with further analyses. Interestingly although factor 5 had a weighting of 0.71 for vanadium it would seem that only the results of this metal are explained by factor 5. Since vanadium concentration was still not correlated with any of the other metal concentrations (Table 3.7) even after the influencing outliers were removed, it would appear that vanadium concentrations in ascidians are not related in any way to the concentration of any of the other metals in this study. Chapter 4.1 will explore the vanadium concentrations of Algoa Bay ascidians in more detail.

Table 3.9: Factor coordinates of the outlier-corrected ascidian metal concentration data variables based on correlations. Red font indicates strong weightings (>0.5).

	Factor 1	Factor 2	Factor 3	Factor 4	Factor 5	Factor 6	Factor 7
Li	-0.77	-0.32	-0.35	-0.25	-0.00	0.09	-0.11
Be	-0.95	-0.09	0.05	-0.16	0.00	-0.06	-0.08
B	0.50	-0.13	-0.42	-0.41	-0.19	0.43	0.06
Rb	-0.62	-0.54	-0.23	-0.28	0.12	-0.11	0.04
Sr	-0.06	0.51	0.51	-0.48	-0.11	-0.24	0.02
Mo	0.31	-0.64	0.42	0.10	-0.26	0.19	-0.05
Cd	0.24	-0.72	0.48	0.07	-0.01	0.18	0.09
Sn	-0.58	0.03	0.35	0.17	-0.32	-0.26	0.13
Sb	-0.36	0.25	0.39	0.25	-0.10	0.44	-0.15
Cs	-0.95	-0.05	0.02	-0.22	-0.01	-0.05	0.03
Ba	-0.47	0.32	-0.16	-0.36	-0.26	0.32	-0.10
Pb	-0.85	0.18	0.13	0.27	0.01	0.02	-0.01
U	0.29	0.50	0.48	-0.53	-0.22	-0.04	0.05
Al	-0.90	0.06	-0.10	-0.27	0.02	-0.08	0.13
V	0.07	0.24	0.25	-0.12	0.71	0.02	-0.51
Cr	-0.85	-0.14	0.15	0.12	-0.08	0.18	-0.12
Mn	-0.65	0.20	0.08	0.27	0.15	0.29	0.03
Fe	-0.94	0.12	-0.05	-0.06	0.10	-0.07	0.04
Co	-0.96	-0.08	0.09	0.02	0.10	0.06	0.03
Ni	-0.75	-0.33	0.19	0.18	-0.10	-0.09	0.11
Cu	-0.12	-0.68	-0.10	-0.25	-0.06	0.06	-0.21
Zn	0.23	-0.60	0.52	-0.38	0.11	0.00	-0.19
As	-0.00	0.14	0.22	-0.20	0.43	0.41	0.65
Se	0.17	-0.52	0.02	-0.03	0.27	-0.28	0.33

The results of the PCA of the outlier corrected metal concentration data were easier to interpret once displayed as a factor loading plots using the first two principal components (Figure 3.7-3.9). Only the first two principal components established in the PCA will be used here to discuss the results because according to Table 3.9 these factors contained strong weightings for majority of the metal variables. The factor loading plots showing the

relationship of the other seven retained components to each other did not result in clearly interpretable patterns and thus will not be presented here, but can be viewed in Appendix A.

Plotting the case (ascidian samples) weightings for principal component 1 (PC 1) against principal component 2 (PC 2) with the ascidian samples displayed as icons based on their taxonomic families showed some level of grouping (Figure 3.7). The grouping of ascidian families in the PC 1 vs PC 2 factor plot will be discussed briefly here. The stolidobranch ascidian family Styelidae (blue circles) was only represented by two species in this investigation namely *Botrylus* sp. and *Gynandrocarpa placenta*. The factor weighting of the data points relating to these species placed them quite distinctly apart from each other (Figure 3.7). This may be because, although they are in the same family, *Botrylus* sp. and *Gynandrocarpa placenta* are placed into separate subfamilies Botryllinae and Polyzoinae respectively. This taxonomic distinction may result in differing metal concentrations however, analysis of a larger number of these stolidobranch ascidians would be necessary to properly establish any phylogenetically related metal concentration trends. All of the other Algoa Bay ascidians included in this investigation belong to families within the suborder Aplousobranchia.

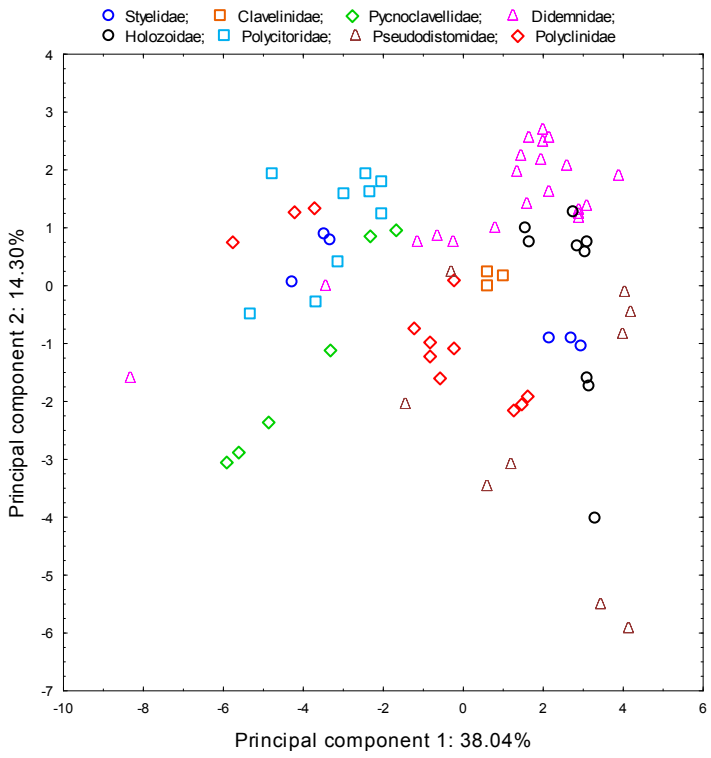

Figure 3.7: Principal component analysis results displayed as case factor loading plots of principal component 1 against principal component 2. Data points are shown as different icons based on taxonomic families.

The families Clavelinidae (red squares) and Pycnoclavellidae (green diamonds) have recently been found, through phylogenetic relationships using mitochondrial DNA data to be taxonomically similar enough to be placed in the same family.[145] However, in this analysis we allocated different icons to the two historically different genera and labelled them as the previous family synonyms to facilitate the observation of patterns. Interestingly there was no clear grouping of the Clavelinidae and Pyconclavellidae (previous synonym) samples based on the metal ion data (Figure 3.7) which may be solely due to the fact that only three species were used to represent this family which was not a large enough number to give a true representative result.

The family Didemnidae (pink triangles) appear to be grouping with high scores for both PC 1 and PC 2. Interestingly the 3 samples of *Didemnum* sp. 1 are all inconsistent with the other samples of this family, and are randomly scattered. A point to note is that on analysing the metal correlation data for influencing outliers the samples of *Didemnum* sp.1 often appeared to have larger than average Cook's distance values however, there were no significant changes in the regression analysis if these data points were removed, thus the correcting of the data obtained for *Didemnum* sp.1 was not warranted because these are not influencing outliers. This does however help to explain why the factor scores for *Didemnum* sp. 1 were not consistent with the other didemnid samples.

Within the family Holozoidae (black circles) the data relating to both *Sigillina sp.* and *Hypodistoma vastum* appear in a similar area of the scatter plot presented in Figure 3.7 whilst data relating to *Distaplia skoogi* is distinctly separated. The random positioning of each of the triplicate data points relating to *D. skoogi* would suggest that there was variation in the metal content measured across this colony suggesting that this particular sample or genus of Holozoidae may be unusually inconsistent in terms of its metal content profile.

The data points relating to ascidians within the Polycitoridae family (blue squares) all appeared relatively well grouped together in the PC 1 vs PC 2 factor loading scatter plot (Figure 3.7). However, these data points are not distinctly separated from the other families which once again may be due to the limited number of Polycitoridae species assayed impacting negatively on us being able to observe any interpretable patterns for this family.

The data points corresponding to the Pseudodistomidae family are randomly scattered in Figure 3.7. Additionally there appears to be distinct differences between the triplicate ascidian samples measured indicating inconsistency within the metal concentration fingerprint of these colonies of Pseudodistomidae species.

The Polyclinidae family (red diamonds) seem to have an interesting pattern where the data obtained for the two species within the genus *Aplidium* are positioned fairly close to each

other in the scatter plot, whilst the *Synoicum* sp. data grouped further to the right and *Aplidiposis tubiferus* data points appear to be shifted to the left side of the PC 1 vs PC 2 factor loading scatter plot (Figure 3.7). It is not clear why the Polyclinidae data was grouped in this way.

The interpretation of these data was difficult as the samples investigated were representative of a relatively large number of ascidian families and in most cases the data were obtained from only three or four species per family meaning that statistically significant patterns of metal concentration within different families, if they existed, were not easily discerned. The family Didemnidae contributed the greatest number of species to our data set and, with one notable exception (*Didemnum* sp.1) as discussed above, provided the clearest evidence of a possibly phylogenetic related trend in metal ion accumulation in Algoa Bay ascidians.

Plotting the case weightings for principal component 1 vs principal component 2 with the cases grouped based on dive site (Figure 3.8) and based on year of collection (Figure 3.9) do not show any definitive patterns. Plots generated for all the other factors are just as homogeneous, implying that neither the year nor dive site has an influence on the concentrations of metals concentrated in the ascidian species.

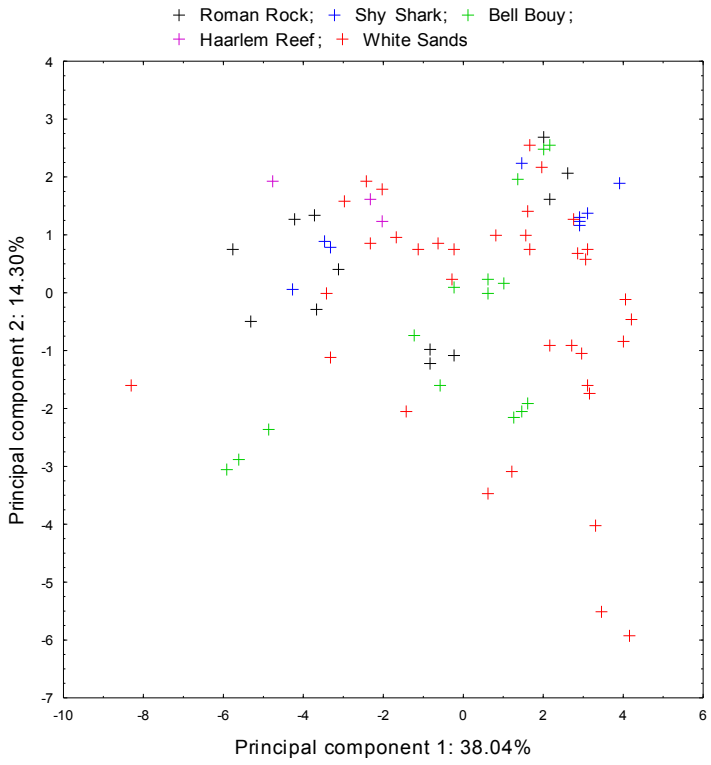

Figure 3.8: Principal component analysis results displayed as case factor loading plots of principal component 1 against principal component 2. Data points are shown as different icons based on the dive sites from where ascidian samples were collected.

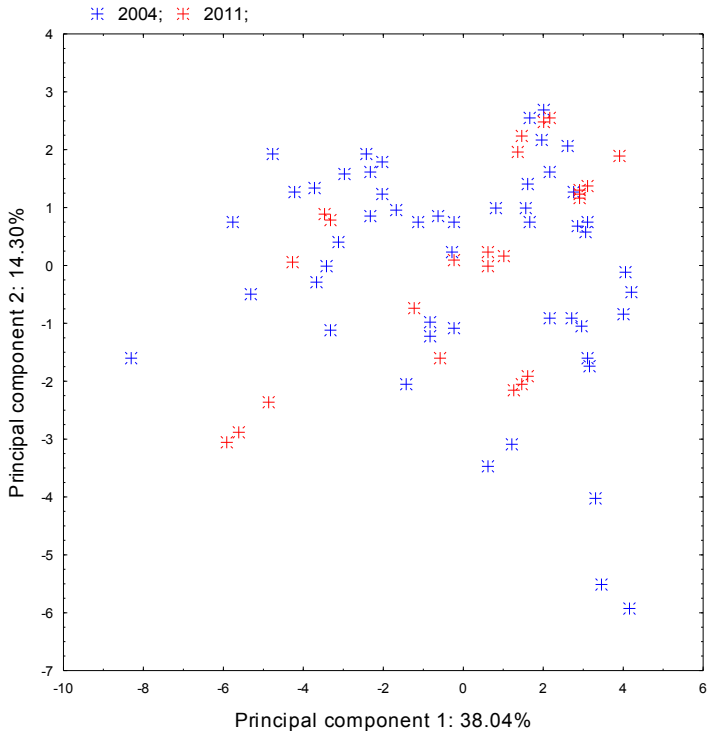

Figure 3.9: Principal component analysis results displayed as case factor loading plots of principal component 1 against principal component 2. Data points are shown as different icons based on the year of collection.

The rationale behind displaying the PCA results based on collection location and year was because both of these variables would potentially indicate a change in the metal concentrations found in the surrounding seawater. The homogenous nature of the data in factor loading scatter plots in Figures 3.8 and 3.9 indicated that the accumulation of different metals in this set of ascidian samples is not related to the collection location or year. This suggests that the concentrations of the metals contained in the surrounding seawater are not necessarily a strong influencing factor of the metal concentration profile of ascidians. This adds weight to the belief that ascidian species actively accumulate a variety of metals from the surrounding seawater and are not simply a sink for metals passively accumulated in filter feeding. This observation also indicated that Algoa Bay ascidians could not be considered as suitable environmental metal biomonitoring organisms as there were no observed pattern which linked the site of collection to the metals accumulated by the ascidians (the collection sites on the western periphery of Algoa Bay were spread over an area > 20 km^2). The presence of elevated levels of a particular metal in an invertebrate does not warrant its use as a bioindicator and extensive long term studies on the temporal and spatial relationships of the metals in the environment and the invertebrate are necessary to confirm that the concentrations detected in the invertebrate are in fact directly related to the health of the surrounding reef.[127,128,131]

As a cautionary note, as was discussed with the interpretation of the PCA results in which we attempted to find a possible phylogenetic link between ascidian families and metal ion accumulation patterns, the absence of a possible spatial and temporal correlation with metal ion accumulation in Algoa Bay ascidians concluded from this study may be a reflection of the relatively small sample size and thus not truly representative.

3.5 Concluding Remarks

The initial purpose of the large scale collection of ascidians from Algoa Bay in 2004 was the discovery of new bioactive secondary metabolites with potential pharmaceutical applications and not to analyse the metal concentrations with an aim of possibly identifying a potential bioindicator candidate for the future environmental monitoring of Algoa Bay. However, our later investigation of this unique collection of ascidians for bioactive metal – marine natural product complexes described in Chapter 2, coupled with the subsequent emergence of significant taxonomic data around this collection, provided, as a spin-off from the main goal of the project, an opportunity to acquire a dataset that afforded the concentrations of 24 different metals in 25 different Algoa Bay ascidian species. Therefore, our goal described in this Chapter was to retrospectively critically evaluate this unique database to discern if there were any potential phylogenetic, temporal and spatial correlations between metal concentrations and selected Algoa Bay ascidians. While we were unable to find any evidence to support temporal and spatial correlations between these selected Algoa Bay ascidian species and metal distribution, through the principal component analysis of the data which we had at hand we were able to provide some evidence to support a phylogenetic relationship between metal concentration and Algoa Bay ascidians. This preliminary investigation could warrant a larger, more in depth future study to further support, or refute, this initial observation.

Chapter Four:

Aplidium monile -

Isolation of nucleosides and vanadyl complexation studies

4.1 Vanadium in ascidians

Since Henze's 1911[119] discovery of unusually high levels of vanadium together with an organic chromogen in the blood of the ascidian *Phallusia mamillata*, both chemists and biologists alike have been curious about the biological reason why, and the mechanism of how, particular ascidains are able to hyper-accumulate vanadium.[119,120] Early investigations of the metal content of ascidians showed high levels of vanadium to be localised in vacuolated blood cells, termed vanadocytes, in the blood of phlebobranchs whereas the evolutionarily more advanced stolidobranchs preferentially accumulated iron in blood cells which were termed ferrocytes.[146] The aplousobranchs which were believed to be positioned in between the two ascidian suborders in terms of evolutionary progress were found to concentrate either iron or vanadium.[120,146,147] These findings, along with the fact that at the time vanadium was considered a rare metal, led many early investigators to falsely predict that vanadium was used in oxygen transportation in phlebobranch ascidians. It was erroneously proposed that since Phlebobranchs, like other ascidians, are primitive chordates that understanding the transition from vanadium as an oxygen carrier over to iron could hold the key to discovering how respiration in higher order chorates evolved.[120]

The blood of ascidians is made up of approximately nine to eleven variable blood cells that can be classified as either hemoblasts, leukocytes, lymphocytes, vacuolated cells, nephrocytes, or pigment cells depending on their morphology.[148] It is the vacuolated cells that accumulate vanadium and they are commonly referred to a vanadocytes, however there are still further morphological differences as well as vanadium accumulating abilities that distinguish the vacuolated cells further into groups of morula cells, signet ring cells, compartment cells, and small compartment cells respectively.[148] Interestingly, ascidian blood cells are actively amoeboid and are all able to leave the vascular system and penetrate the tunic therefore bearing little resemblance to the blood of higher order chordates such as vertebrates.[149] The presence of a circulating biological fluid and the fact that oxovanadium can undergo redox reactions to take up or release oxygen, does not prove that vanadium within the blood of ascidians has the primary role of oxygen transportation.[38,120,150] Ascidians are sessile and do not expend a great deal of energy. Accordingly, the oxygen transfer directly from the ascidian's branchial sac to the surrounding body parts during periods of filter feeding, when there is a constant water flow, is believed to be sufficient for respiration and cell function.[132,150] However, there is some evidence that vanadium in the blood system may be involved in the release of oxygen for respiration during extended periods of anoxia.[132,151] These periods of oxygen deprivation may occur when ascidians tightly close their siphons during low tides especially when growing in intertidal regions. Throughout this anoxic period, the branchial sac which is filled with seawater will act as an oxygen reservoir, however, as the partial pressure of oxygen in the trapped seawater decreases the need for oxygen to be transported around the body in a metal-bound form may arise.[132,151] The biological

significance of high levels of vanadium in the blood of some ascidian species is therefore still questionable.[38,120,132,151]

Like most transition metals, vanadium most commonly occurs in the marine environment as an oxyanion. The majority of the vanadium in seawater will persist in the V(V) oxidation state as vanadate (HVO_4^{2-}), however, in anoxic environments reduction may occur to produce unstable hydroxide species of vanadyl (VO^{2+}) with vanadium in the V(IV) oxidation state.[118] The oxidation state of vanadium accumulated within ascidians appears to be related to phylogeny with phlebobranch ascidians concentrating the majority of vanadium in the V(III) oxidation state, in the form of aqua-sulphato ions $[V(III)SO_4(H_2O)_5]^+$, often alongside much lower concentrations (~10%) in the V(IV) state, whilst Aplousobranchia ascidians exclusively contain vanadium (IV) in the form of vanadyl (VO_2^+), and finally stolidobranch ascidians do not commonly contain elevated levels of vanadium.[120,147] In the case of accumulation by both Aplousobranchia and Phlebobranchia ascidians vanadate present in seawater enters the ascidian's branchial sac and is absorbed and reduced to the less stable V(IV) and/or V(III) for storage in the vanadocytes.[148] A number of different blood cells have been found to house vanadium in varying concentrations and the term vanadocyte is a common name given to all vanadium containing blood cells. Since V(III) is only stable under very acidic conditions numerous investigations have focused on determining the compounds or proteins present that are effective in reducing vanadate as well as chelating to, and thus stabilising and storing, V(III).[38,120] This evidence led to a focussed search towards finding auxiliary compounds present in the blood of ascidians that were responsible for vanadium reduction and storage.[38]

4.1.1 Tunichromes

Kustin and co-workers[152] established that green and yellow chromagens, which they called tunichromes, were contained in the vanadium rich ascidians *Phallusia nigra* (synonum *Ascidia nigra*) and *Ciona instenalis*. Tunichromes were also found in the iron accumulating *Molgula manhattensis* and were shown to successfully reduce both metals.[152,153] The early studies of tunichromes found them to be very unstable, highly reactive and either subject to decomposition on exposure to air and water, or strongly retained by a variety of solid phase chromatography packing materials.[152,154] Furthermore, attempts to stabilise the tunichromes through acetylation before purification were unsuccessful.[154] These setbacks led Kustin and co-workers to develop an unusual extraction and purification process where all stages of these two processes were carefully conducted with degassed solvents under inert, dry and anaerobic conditions. As a result, some five years later, the definitive structures of the brightly coloured tunichromes from the vanadium rich blood of *P. nigra* were established as the hydrodopamine derived tripeptides, **4.1** - **4.3**.[155] Using the same anhydrous and anaerobic isolation protocols three other tunichromes (**4.4** - **4.6**) were isolated from the

vanadium rich blood of *Phallusia mamillata*.[149] The basic structure of tunichromes **4.4** - **4.6** differed from those isolated from *P. nigra* only by the saturation of the C-11 to C-12 bond.[29,149] A further two tunichromes containing only two dopamine residues, linked by either glycine (**4.7**) or leucine (**4.8**) were isolated from the iron rich stolidobranch *Mogula manhattensis*.[156]

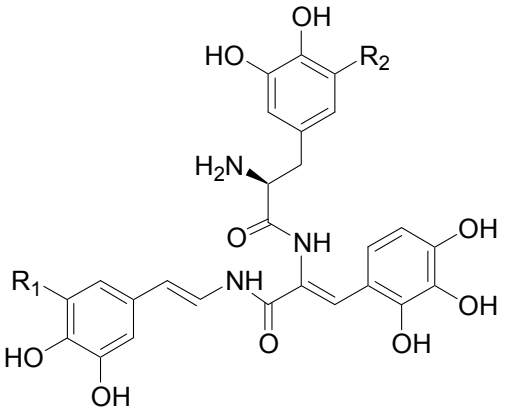

4.1 $R_1 = R_2 = OH$
4.2 $R_1 = OH$; $R_2 = H$
4.3 $R_1 = R_2 = H$

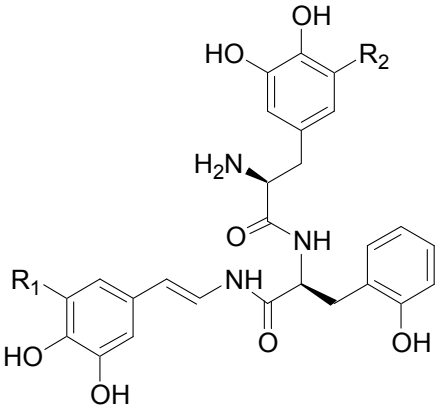

4.4 $R_1 = R_2 = OH$
4.5 $R_1 = OH$; $R_2 = H$
4.6 $R_1 = H$; $R_2 = OH$

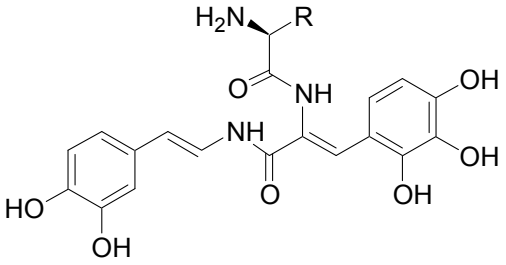

4.7 R = H
4.8 R = i-butyl

The catechol and or pyrogallol moieties present in tunichromes provided strong evidence in support of the predicted involvement of tunichromes in the reduction and chelations of vanadium in phlebobranchs and iron in stolidobranchs.[38,154] However, further investigations to test these predictions were initially impossible owing to the complicated isolation procedures and instability of tunichromes. It was only after Kim *et al.* developed an isolation procedure where the tunichromes in the extracted ascidian blood were temporarily stabilised throughout the purification stage as *tert*-butyldimethylsilyl (TBDMS) and *tert*-butyloxycarbonyl (Boc) ethers (the ether protecting groups were subsequently removed after purification in the usual manner[38,149,154]) that this method allowed for the isolation of even trace amounts of tunichromes in numerous other ascidians as well as facilitating the production of synthetic tunichromes in large enough quantities for detailed metal reduction and chelation studies.[38]

Subsequent studies on the purified tunichromes found that while tunichromes strongly chelate with vanadium and are able to reduce V(V) to V(IV) at biologically relevant conditions, they

cannot reduce vanadyl further to V(III) in aqueous solutions.[38,120,157–159] There are also a number of other biologically common compounds including glutathione, cysteine, NADH, and NADPH which are capable of reducing V(V) to V(IV), clearly suggesting that tunichromes are not the only source of reducing agents available.[120] The presence of tunichromes has been widely studied in a number of vanadium accumulating phlebobranchs as well as iron accumulating stolidobranchs, however no tunichromes have been reported for the vanadium rich aplousobranchs.[38,120,160,161] The lack of tunichromes in aplousobranchs implies that either the primary biological role of tunichromes is not to reduce and concentrate metals such as iron and vanadium, or that aplousobranch ascidians have evolved a different mechanism for concentrating vanadium which does not require the presence of tunichromes.[38]

The strongest piece of evidence against the role of tunichromes in vanadium accumulation and reduction in ascidians is that although both vanadium and tunichromes are concentrated in the blood of phlebobranch ascidians, studies have shown that majority of vanadium is stored as V(III) in the green/grey signet ring cells whilst tunichromes occur exclusively in the bright yellow green morula cells.[162] This separation of V(III) and tunichromes between two different cells indicates that the primary biological role of tunichromes is not the production and maintenance of V(III) in the blood of phlebobranchs. Although the biological role(s) of tunichrome in ascidians remain uncertain they have been shown to be involved in the crosslinking of fibres in the structural formation of the tunic, in defence mechanisms, and in wound healing.[38,163]

4.1.2 Vanabins - Vanadium associated proteins involved in vanadate reduction

After over 100 years of research into the accumulation of vanadium in ascidians it is only within the last decade that some headway has been made. An important development made recently was Michibata and co-workers' discovery of a series of vanadium binding proteins termed vanabins (Figure 4.1).[164] To date five vanabins have been found with vanabins 1-4 being present in the vanadocytes and vanabinP present in the blood plasma of *Ascidia sydneiensis samea*.[120] The first vanabins were identified using anion exchange chromatography and atomic absorption spectroscopy. All of the vanabins were found to be rich in cysteine and lysine residues and to have a molecular mass of between 10-20 kDa.[75,164,165] The positioning of 18 cysteine residues within the amino acid chains appeared to be well conserved for vanabins 1-4.[120,165,166] Michibata's group identified the genes which encoded vanabin 1 and 2 and through cloning and recombinant gene expression using *E. coli* they were able to conduct numerous studies into the properties of vanabins.[167] The solution structure of vanabin 2 was subsequently determined using multidimensional NMR experiments. Vanabins have a novel bow-shaped structure where four α-helices are stabilised by the disulphide bonds between the 18 cysteine residues (Figure 4.1).

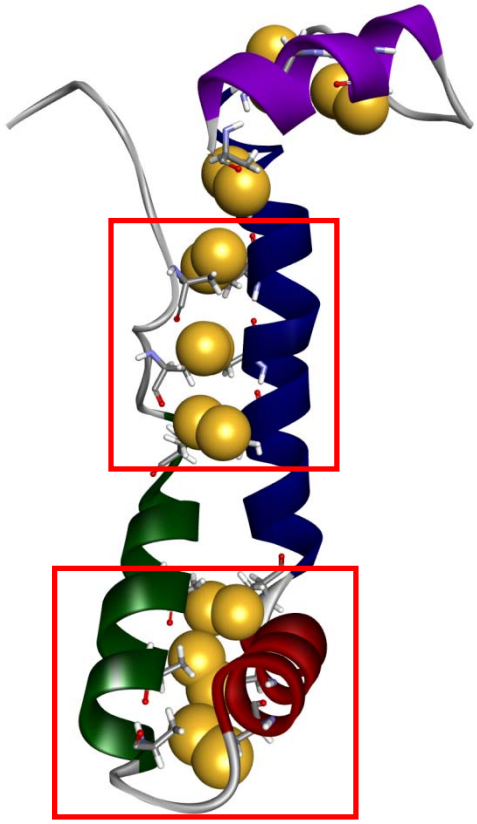

Figure 4.1: The structure of vanabin 2 (Protein Data Bank ID: 1VF1)[168,169] with the sulphur atoms (yellow) of the nine disulphide bridges enlarged for easy identification. The areas within the red rectangles encompass sites targeted by Michibata and co-workers in directed mutagenesis experiments.[148,170]

Vanabins 1 and 2 were shown to bind up to 20 vanadyl ions and through electron paramagnetic resonance studies as well as ^{15}N HSQC NMR titration studies, it was established that the VO^{2+} ions were localised in a region of the protein where basic amino acids such as lysine and arginine were present.[164,168] These experiments, along with recent site specific mutation studies, confirm that the amine functionalities on lysine and arginine residues are critical for metal binding whilst the highly conserved cysteine residues appear to have little association with vanadyl ions.[164,168,171]

Generally, disulphide bonds are not commonly found in cytoplasmic proteins as the environment within the cells would result in the reduction of cysteine residues.[168] However, the rare disulphide bond containing intracellular proteins such as thioredoxin and glutathione have been linked to redox processes.[168] Michibata and coworkers therefore postulated that the role of the disulphide linkers between the 18 cysteines in vanabins 1-4 are involved in the reduction of vanadate. Michibata and co-workers propose that the vanabin catalyse the

reduction of V(V) to V(IV) through a redox cascade; fuelled by the electron transfer when disulphide bonds are cleaved and then reform.[148] Further evidence for the involvement of the disulphide linked cysteines in the formation of vanadyl has recently been established after site directed mutagenesis experiments on the cysteine residues of vanabin 2 effectively neutralised V(V) reduction.[170] Vanabins are therefore involved in both the reduction of V(V) to V(IV) and the storage and transport of V(IV) within the vanadocyte.[170] The presence of vanabins within phlebobranch ascidians is thought to be fairly ubiquitous, however, no evidence supporting the production of vanabin by vanadium rich aplousobranchs has been reported in the literature.[164,170,172]

4.1.3 The role of cellular acidity and sulphates in the maintenance of V(III)

Many early reports noted that a strongly acidic solution was present on lysis of ascidian blood cells and vanadium accumulation was often found in low pH conditions in ascidians.[148,173,174] Although the accumulated V(III) would be more stable under these acidic conditions, there are a number of conflicting reports providing contradictory pH values for the solution resulting from the lysis of ascidian blood cells and so it was difficult to determine if the reported pH values were the result of redox reactions or lysis of the ascidian blood cells.[38,148] Michibata and co-workers used a microelectrode and non-invasive electron spin resonance (ESR) techniques on intact blood cells of three *Ascidia* species and were able to determine that the most acidic cells were indeed those that contained V(III).[148] Vanadium accumulation has also commonly been reported in conjunction with high levels of sulphates.[175–177] Through nonintrusive X-ray absorption spectroscopy (XAS) studies Frank *et al.* were able to determine that vanadium was predominantly coordinated as $[V(III)SO_4(H_2O)_{4\text{-}5}]^+$ in the signet ring cells of *A. cerotodes*.[175–177] The acidity of the signet ring cells and the vanadium/sulphate interaction finally explains how such high concentrations of the unstable V(III) are maintained in phlebobranch ascidians. How vanadium is reduced to the V(III) is unfortunately still unclear although it has been postulated that cysteine is involved in this process which is once again supported by the high levels of sulphur common in the blood cells of vanadium accumulating ascidians.[148]

4.2 Presence of vanadium in Algoa Bay ascidians

Chapter 3 describes the total metal analysis of twenty five carefully selected Algoa Bay ascidians. The results described in this Chapter show that South African ascidian species, in common with ascidians elsewhere, are capable of bioaccumulating a variety of metals from the marine environment. Notably, the PCA presented in Chater 3 revealed that dispite numerous correlations between the concentrations of metals investigated, none of the other metal concentrations correlated significantly with high concentrations of vanadium (Table 3.3). What this possibly means is that high levels of vanadium in an ascidian is not related to high or low levels of any of the other metals investigated which in turn may imply that the

mechanisms used in the accumulations of vanadium are distinct from those employed in the process of concentrating other metals.

The introduction to this chapter detailed numerous successful investigations that have contributed towards a growing understanding of the accumulation and maintenance of vanadium within the blood of ascidians. The most thoroughly studied ascidian suborder in terms of vanadium accumulation and reduction, and accordingly the best understood, is the suborder Phlebobranchia.[120] Our interest however lies in the suborder Aplousobranchia which are abundantly represented on the reefs of Algoa Bay and relatively understudied when it comes to the process of vanadium accumulation. What little is known about the vanadium chemistry of aplousobranchs ascidians is also distinctly different to that of the phlebobranchs *i.e.* aplousobranchs accumulate only V(IV) and not V(III), no vanadium reducing tunichromes have been found in the blood of aplousobranchs, and there is no current evidence towards the presence of the vanadium binding vanabins in aplousobranchs.[120,147,148,160,171] These differences all add weight to Swinehart's early prediction that the differences in vanadium oxidation state may suggest that aplousobranchs evolved to accumulate vanadium independently from phlebobranch ascidians potentially resulting in a completely different mechanism used for accumulation and even a distinctly different biological use for vanadium.[173] It was therefore deemed necessary to explore the vanadium concentration results obtained for twenty five Algoa Bay ascidians (23 aplousobranchs and 2 stolidobranchs).

4.2.1 Total vanadium concentrations in 25 Algoa Bay ascidians

The triplicate average vanadium concentrations measured for whole freeze dried ascidian samples as well as organic extracts (not in triplicate) of the corresponding 25 ascidians collected from Algoa Bay are shown in Figure 4.2. Vanadium concentrations were determined using ICPMS after sample digestion with nitric acid, as detailed in Chapter 3. The ascidian species with the highest concentration of vanadium were *Eudistoma sp.1* (4658.4 ppm), *Atriolumn marinense* (3531.4 ppm), *Pseudodistoma sp.1* (1694.8 ppm), *Polycitor sp.* (388.3 ppm) and *Hypodistoma vastum* (194.6 ppm). With the exception of *Eudistoma* none of the genera from the Algoa Bay collection which resulted in exceptionally high vanadium concentrations have been previously investigated. Vanadium accumulation in ascidians belonging to the genus *Eudistoma* have been fairly well studied. Levine reported a vanadium concentration of 471 ppm in the body of *Eudistoma ritteri*. A pH of 1.5 was reported for the body tissue and tunic fluid of *E. ritteri* and believed to be the result of sulphuric acid present in the ascidian however proof that the acid was associated with the vanadium was not conculsive.[174] Ciereszko *et. al.* found 200 ppm vanadium in *E. olivaceum* however the level of vanadium in *E. capsulatum* was below the detection limit.[178] Swinehart *et al.* established the vanadium concentration of *E. psammion*, *E. diaphanes*, *E. molle*, and *E. ritteri* to be 130 ppm, 25 ppm, 1000 ppm, and 320 ppm respectively.[173] The oxidation state of vanadium

found in all of the *Eudistoma* species investigated by Swinehart *et al.* was V(IV) and these researchers noted that many of these species possessed acidic tunics.[173] A recent study by Jaspars and co-workers of the metal ion content of an organic extract from *E. gilboviride* found a relatively low concentration of 19 ppm of vanadium.[47]

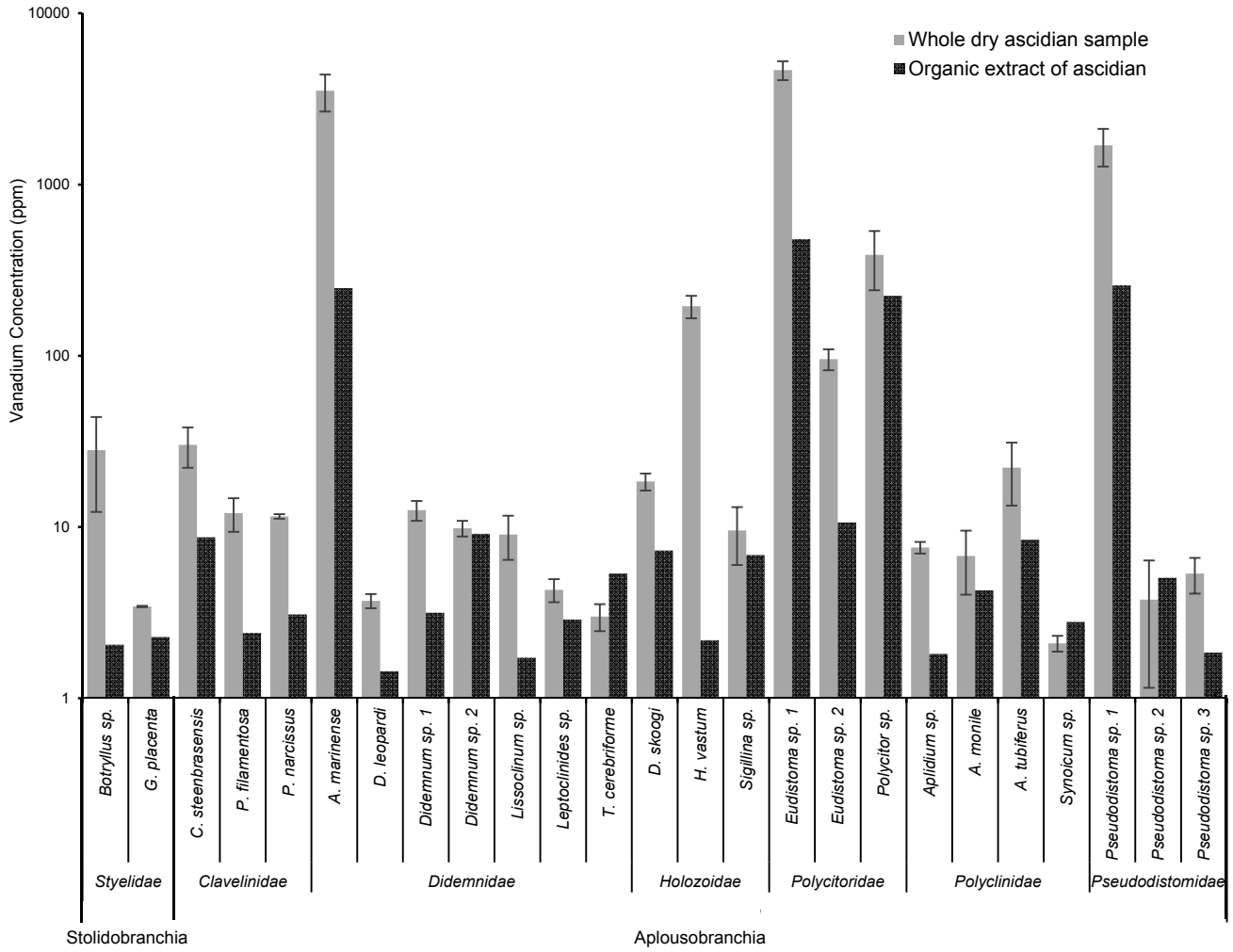

Figure 4.2: Concentrations in ppm (mg of metal per kg of organism or extract) of vanadium in 25 Algoa Bay ascidians. Values were obtained from NO_3/H_2O_2 digests of either triplicated samples of whole dry ascidian (error bars indicate standard deviation) or single samples of CH_2Cl_2/MeOH extracts of ascidian and are displayed in grey and black respectively.

Although all of the other ascidian species represented in Figure 4.2 exhibited markedly lower concentrations of vanadium (< 100 ppm) the oceanic concentration of vanadium is only 2.0 ppb[133] which means that even the ascidian with the lowest recorded concentration of vanadium, *Synoicum sp.* (2.1 ppm), is able to accumulate vanadium in concentrations that are a thousand times greater than that of the surrounding seawater.

This shows that even though only three of the ascidian species studied could be termed vanadium hyper-accumulators with vanadium concentrations above 1000 ppm, the concentrations of vanadium recorded in all of the ascidians studied were distinctly greater than that of the surrounding seawater. Ascidians from the suborder Aplousobranchia have previously been found to contain high concentrations of vanadium.[147] However ascidians belonging to the order Stolidobranchia are believed to have lost their ability to accumulate vanadium in their evolutionary development, however in our study the stolidobranch *Botryllus sp.* was found to contain vanadium at a concentration of 28.1 ppm which, although low, is certainly comparable to many of the vanadium accumulating aplousobranchs that formed part of our study (Figure 4.2). This could imply that not all stolidobranchs have lost their ability to accumulate vanadium.

The concentrations of vanadium found in the organic extracts of each ascidian species are also presented in Figure 4.2. It was promising to see that for the most part species with high vanadium concentrations in the whole organism also had relatively high levels of vanadium in the organic extracts produced from these ascidians. This congruency may indicate the presence of organo-vanadium compounds in the extracts which prompted us to investigate the presence of these compounds in selected extracts with LC-ICP-MS/ESI-MS. As mentioned previously in Chapter 2, the organic ascidian extracts chosen for LC-ICP-MS/ESI-MS were selected based on the results obtained for all of the metals tested not only vanadium. Figure 4.2 depicts the vanadium (*m/z* 51) ICP-MS traces obtained for all of the ascidian extracts selected for LC-ICP-MS/ESI-MS analysis. It was very surprising that the ^{51}V-ICP-MS traces obtained for the ascidians with the greatest concentrations of vanadium, *Eudistoma sp.1* (4658.4 ppm), *Atriolumn marinense* (3531.4 ppm), *Pseudodistoma sp.1* (1694.8 ppm) and *Polycitor sp.* (388.3 ppm) did not contain prominent vanadium peaks (Figure 4.3). A possible explanation of this observation may be that the vanadium species present in the whole ascidian and organic extracts are highly polar compounds that elute early in the chromatography gradient and the vanadium signal would thus be obscured in the region of the ICP-MS trace that is dominated by noise from inorganic salts. In the case of ascidians of the genus *Eudistoma* there are literature precedents which indicate a link between the presence of high levels of vanadium and an acidic, sulphur rich environment where vanadyl is present as a sulphate or hydroxyl anion.[173,174]

Of further interest was that the vanadium (*m/z* 51) ICP-MS traces obtained for the other ascidians investigated resulted in fairly board peaks at two different retention times of 9.05 and 10.30 minutes. The presence of peaks at similar retention times may indicate the presence of a similar vanadium species across the ascidian extracts. Unfortunately, no clear molecular ions of possible organo-vanadium complexes could be identified at the corresponding retention time in any of the ESI-MS spectra suggesting that these complexes if they did exist do not survive the LC-ICP-MS/ESI-MS protocols we had in place.

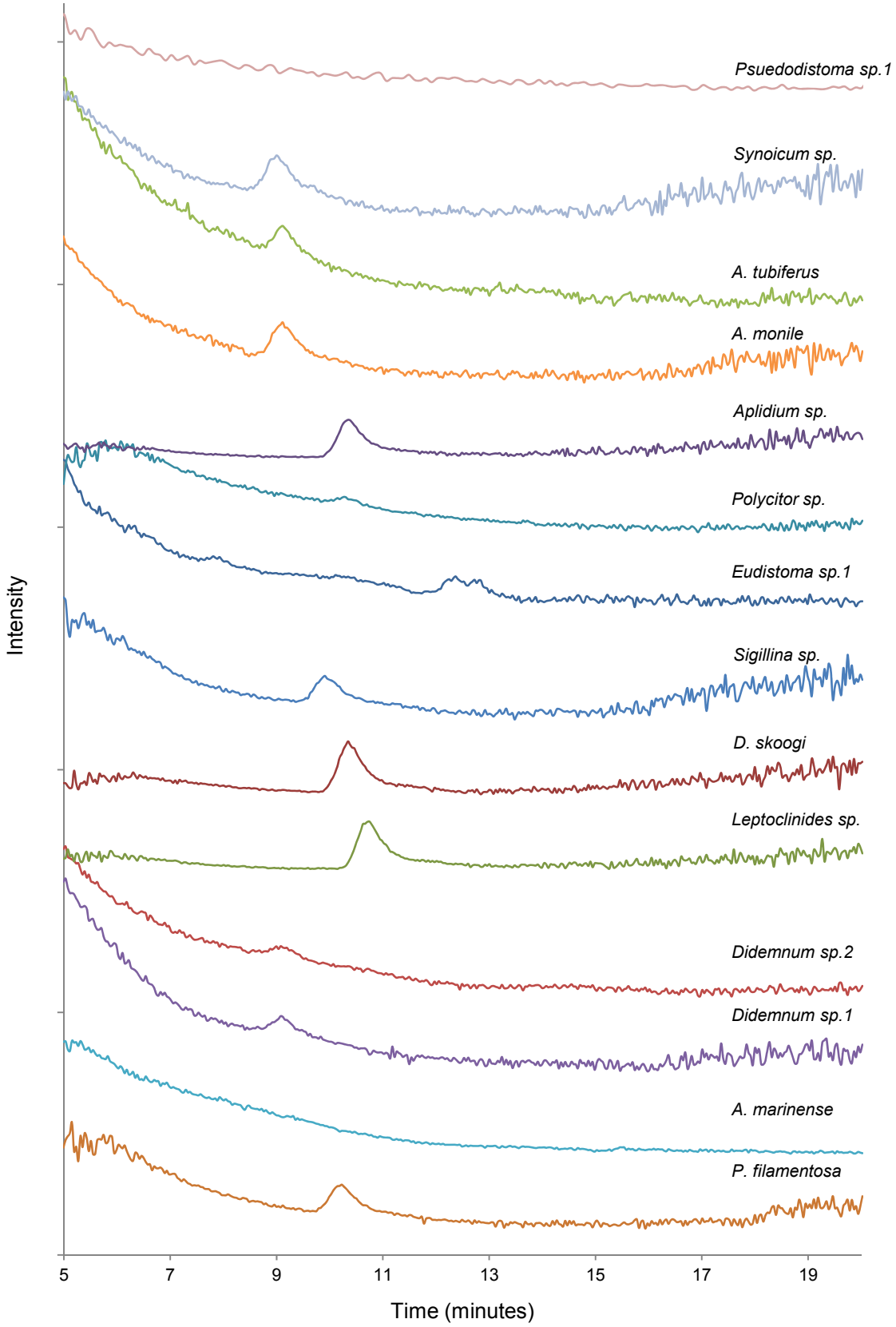

Figure 4.3: Vanadium (^{51}V) LC-ICP-MS traces obtained for the MeOH/CH_2Cl_2 extracts of selected Algoa Bay ascidians. Traces are vertically offset for clarity.

It became increasingly evident to us that our LC-ICP-MS/ESI-MS strategy was not going to provide us with evidence of organo-vanadium complexes in the Algoa Bay ascidians and we returned to the literature to explore vanadium complexation with various biomolecules. Given our discovery of nucleoside metabolites in *Aplidium monile* through the inital NMR studies of the Algoa Bay extracts described in Chapter 2.3.2 and their isolation and identification discussed here in Section 4.4, our attention was drawn to a significant body of work around the complexation of vanadium with nucleosides.[179–183]

4.3 Nucleosides as metal ion chelators

Nucleosides consist of either a pyrimidine base in the case of cytidine (**4.9**), thymidine (**4.10**) and uridine (**4.11**), or a purine base in the case of guanosine (**4.12**), ionosine (**4.13**) and adenosine (**4.14**), attached to either five carbon ribose or deoxyribose sugars.[184] Nucleosides form an integral part of the structure of the phosphorylated nucleotides which are the building blocks for RNA and DNA making them key components of all living cells.[184] Not surprisingly the biochemical role of both natural and synthetic nucleosides and their analogues have been widely studied. Numerous studies have successfully proven that nucleosides readily interact with metal cations including gold, ruthenium, lead, mercury, magnesium, calcium, strontium, barium, manganese, cobalt, nickel, zinc, and cadmium.[185–188] Of interest to us in the context of this thesis, however, is the interaction between nucleosides and vanadium.

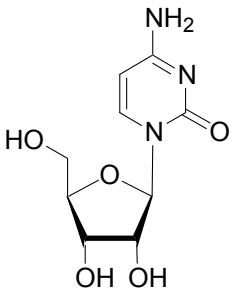

4.9

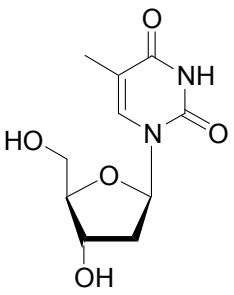

4.10

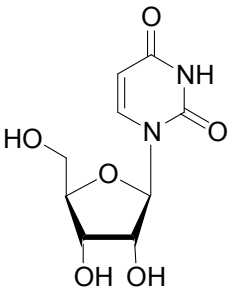

4.11

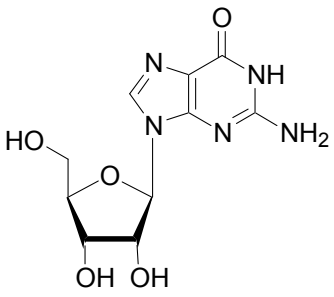

4.12

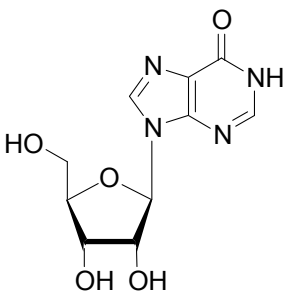

4.13

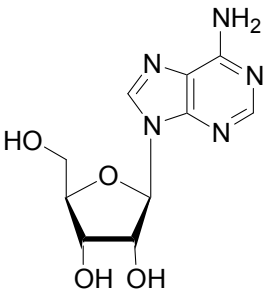

4.14

4.3.1 Vanadium chelation by nucleosides

The interaction of nucleosides and vanadium has been a topic of great interest to many researchers due to the ability of vanadium to inhibit ribonuclease activity by direct enzyme interaction *via* either the metal cation or the nucleoside-vanadium complexes.[181,189] Although nucleoside complexes with both vanadate and vanadyl ions are possible in biological systems, investigations into the stability and structure of nucleoside-vanadium complexes have only thus far been conducted for the vanadate ion.[189–193] Nucleoside-vanadate investigations have used ^{51}V NMR spectroscopy in combination with common nuclei NMR spectroscopy, circular dichroism and potentiometric analyses to successfully detect and characterise complexes.[180,192,193] The uridine and adenosine based studies established that the major nucleoside-vanadate complex formed in biologically analogous systems was in a 2:2 metal:ligand ratio. Paradoxically, the minor 1:1 metal:ligand complex was shown to be the more potent inhibitor of ribonuclease.[192,193] In the case of the adenosine-vanadate study the most stable complexes which formed were $V_2Ad_2^{n-}$ which were found to persist over the wide pH range of 3.5 to 10.0. Between pH 5.5 and 8.0 almost 75% of the vanadate is bound in these complexes with the -2 charged state predominating. Spectroscopic analysis of this dimeric structure revealed that vanadium was pentacoordinated with one of the two coordinated ribose vicinal oxygens from each adenosine moiety bridging the two vanadium atoms.[192] The investigation into the uridine-vanadate counterpart yielded similar results with the $V_2Ur_2^{2-}$ complex present as the major species.[193] The exact geometry of these adenosine-vanadate and uridine-vanadate complexes were later established by X-ray crystal structure analysis.[183,194] Figure 4.4 depicts a simplified representation of the structure established through X-ray crystallography of the 2:2 vanadate-adenosine complex.[181,183] A great deal of research has been carried out to understand the chemical structure and properties of vanadate-nucleoside complexes and their role in the inhibition of ribonuclease and as a result these systems are now well understood.[181] Studies into the interactions between nucleosides and vanadyl are unfortunately rare and usually qualitative in nature with limited information provided about the stability or structures of the complexes formed.[190] The vanadyl accumulating aplousobranch ascidians dominated our study of Algoa Bay ascidians therefore providing us with the rationale to investigate the relatively little studied binding ability and stability of vandyl-nucleoside complexes.

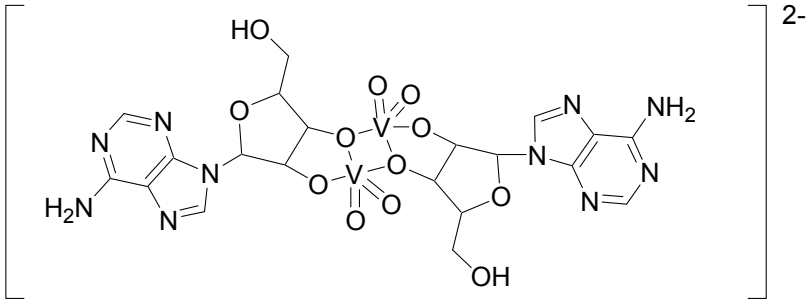

$V_2Ad_2^{2-}$

Figure 4.4: The structure of the major 2:2 vanadate-adenosine complex determined by X-ray crystallography.[183]

4.3.2 The distribution of nucleosides and their derivatives in ascidians

Nucleosides and their derivatives are commonly found in a vast array of marine organisms and a recent review by Peng and co-workers details the more unusual nucleosides discovered in the marine environment.[184] The following discussion will focus only on those nucleosides isolated or detected in ascidians.

The isolation of nucleosides and their derivatives are well documented in aplousobranch ascidians.[184] Within the Didemnidae family the nucleosides thymidine (**4.10**) and uridine (**4.11**) have been isolated alongside 2'-deoxynucleosides (**4.15**-**4.18**) from *Atriolum robustum*,[195] *Didemnum psammatodes*[196] and *Tridemnum cereum*.[197] The tubercidin derived 7-deaza-5'-deoxyadenosine nucleoside (**4.19**) was isolated with its brominated (**4.20**) and iodinated (**4.21**) analogues from *Didemnum voeltzkowi*,[198] whilst the Okinawan didemnid *Diplosoma* sp. yielded a similar iodinated tubercidin-like nucleoside (**4.22**) which possessed an uncommon sugar unit.[199]

Within the Polycitoridae family the only genus from which nucleosides have been isolated is *Eudistoma*. The common nucleosides **4.12** and **4.14** were isolated from the Brazilian ascidian *E. vannamei*[196] whilst **4.10** and **4.14** were isolated from a Micronesian *Eudistoma* species.[200] The new nucleoside derivative, 3-deazainosine (**4.23**) was isolated along with the known nucleosides **4.13**-**4.15** and **4.18** form the Egyptian ascidian *E. laysani*.[201]

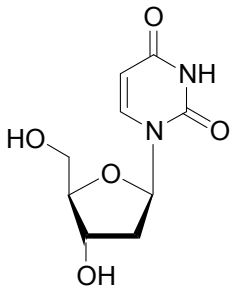

4.15

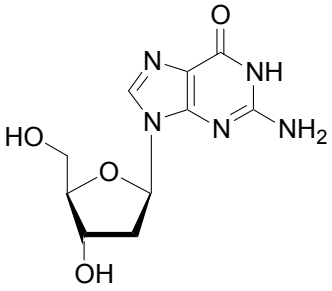

4.16

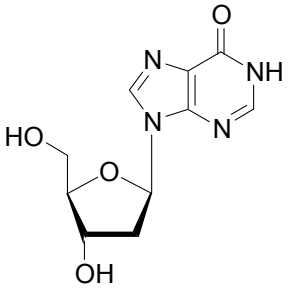

4.17

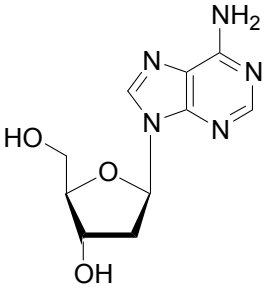

4.18

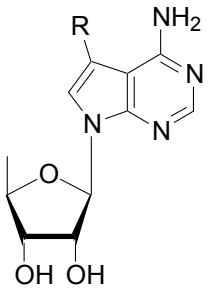

4.19 R = H
4.20 R = Br
4.21 R = I

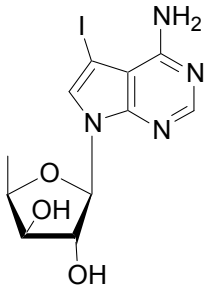

4.22

The genus of ascidian which is most commonly reported to contain nucleosides is *Aplidium* belonging to the Polyclinidae family.[31] Thymidine (**4.10**) was detected in the Antarctic species *A. falklandium, A. fuegiense, A. meridianum* and *A. millari*.[202] The nucleosides **4.10**, **4.11** and **4.14** were isolated from *A. constellatum* collected in the South China Sea.[203] Thymidine-5'-carboxylic acid (**4.24**) and 2'-deoxyuridine-5'-carboxylic acid (**4.25**) were isolated from the Mediterranean ascidian *Aplidium fuscum* and are the only nucleosides with a 5'-carboxylic acid functionality reported in the marine environment.[184,204] The known nucleosides **4.10** and **4.11** and 2'-deoxynucleosides **4.15** and **4.17** as well as 7-deazainosine (**4.26**) were isolated form the South Australian ascidian *A. pantherinum*.[205]

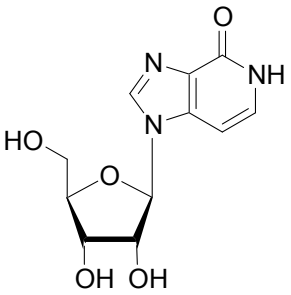

4.23

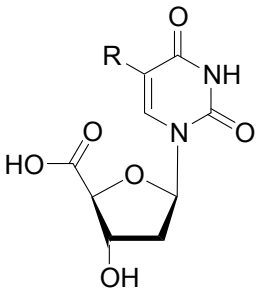

4.24 R = Me
4.25 R = H

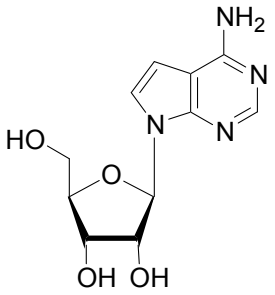

4.26

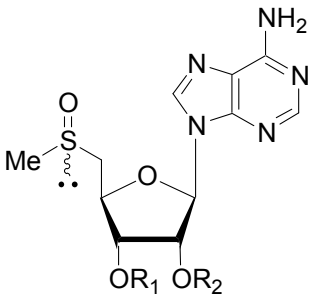

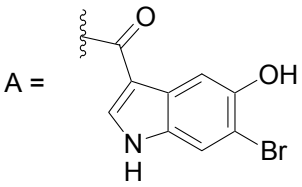

4.27 R_1 = A; R_2 = H
4.28 R_1 = H; R_2 = A
4.29 R_1 = A; R_2 = H (epimer of **4.27** at sulphur atom)
4.30 R_1 = H; R_2 = A (epimer of **4.28** at sulphur atom)

From the chemical literature there appears to be a tenuous phylogenetic relationship between the presence of nucleosides in concentrations high enough to be detected and isolated from the general mix of primary metabolites. Lopes and co-workers established a detection protocol using ESI-MSMS to screen ascidian extracts for common nucleosides **4.10**-**4.14**.[196] They proposed that the protocol developed could be employed to use nucleosides as chemotaxonomic markers to identify specific ascidian species, however, regrettably they failed to provide any guidelines as to what the presence of a particular nucleoside of group of nucleosides in an ascidian species could mean in terms of phylogeny.[196]

From the literature detailed above all of the ascidians with nucleoside isolates belong to the Aplousobranchia ascidian suborder which appears to be rich in nucleosides and their derivatives. A recent study on the chemistry of *Herdmania momus* yielded the epimeric methylsulfinyladenosine nucleoside derivatives **4.27**-**4.30**.[206] This report along with the isolation of **4.11** from *Botryllus schlosseri*[196] are the only reports of nucleosides and their derivatives being isolated from stolidobranch ascidians.[184] Interestingly, there have not been any reports of nucleoside isolation from phlebobranch ascidians.[184] This note on a phylogenetic relationship is based only on the published ascidian-nucleoside literature. However, nucleoside isolations may not regularly be reported as nucleosides are primary metabolites which form the building blocks of RNA and DNA and therefore are present in all

living organisms. With this in mind, the number of ascidian studies where nucleosides have been detected or isolated may therefore be far greater than what has been detailed above.

The presence of nucleosides in concentrations which are elevated enough for them to be detected and isolated using classical natural products techniques may allude to a secondary biological function of nucleosides within ascidians, unrelated to DNA and RNA production. Interestingly, cytidine (**4.9**) has never been reported as an ascidian isolate which is curious as if the nucleosides are only involved in primary metabolic processes involving RNA and DNA, all of the common nucleosides **4.9**-**4.14** would presumably be present and available for isolation. This adds weight to the idea that the nucleosides isolated from ascidians are involved in a secondary biological process. In an early report detailing the isolation of 2'-deoxy-nucleosides from *T. cereum*, Dematté *et al.* argued that the nucleosides isolated were not artefacts produced through the breakdown of RNA and DNA during extraction and isolation.[197] Dematté *et al.* firstly reiterated that on breaking down, the bonds between the deoxyriboses and the bases of DNA would cleave before the bonds in the phosphorous-diesters thus the production of nucleosides at elevated levels detected in ascidians from DNA or the phosphorylated nucleotides is unlikely.[197] Their second argument related to the fact that the uracil base is a component of RNA and as such would only be associated with a ribose sugar, thus, the isolation of 2'-deoxyuridine (**4.15**) cannot be due to the degradation of DNA.[197] The same principle would apply with the isolation of 2'-deoxyinosine (**4.17**) as the hypoxanthine base is only associated with tRNA.[184]

The elevated levels of nucleosides in ascidians may also indicate a role in the production of more complex secondary metabolites such as the inosine derived shimofuridins A-G (**4.31**-**4.37**) form the Okinawan ascidian *Aplidium multiplicatum*[207] and the adenosine derived **4.38** and **4.39** from the Australian didemnid *Atriolum robustum*.[195] These are the only reports of the isolation of complex secondary metabolites, which are clearly derived from nucleosides, from ascidian species. Since the majority of the compounds, **4.15**-**4.26**, are simple nucleoside derivatives which are commonly isolated alongside the nucleosides **4.10**-**4.14** this may provide evidence of a secondary biological function for this former cohort of compounds. The possibility of other biological functions for nucleosides in ascidians coupled with the previously discussed metal chelation ability and a paucity of nucleoside vanadyl complex studies of nucleosides prompted us to begin a preliminary investigation into the stability of nucleoside-vanadyl complexes.

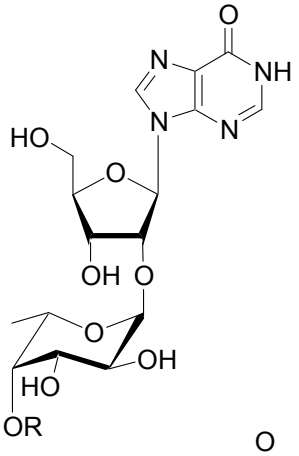

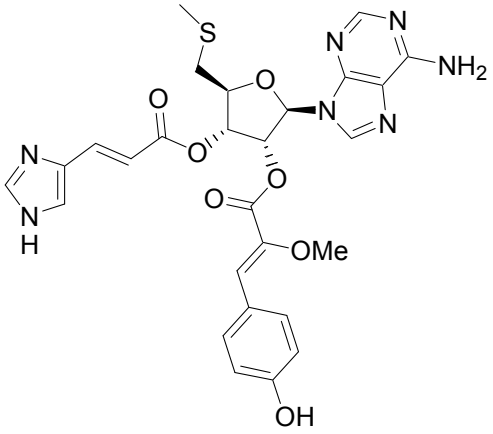

4.38

4.31 R =

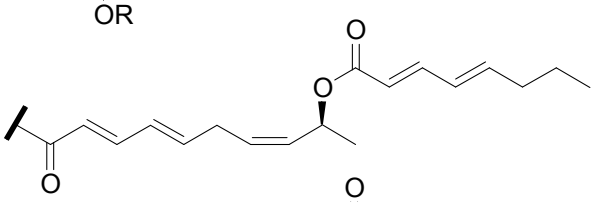

4.32 R =

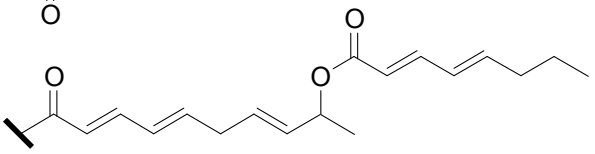

4.33 R =

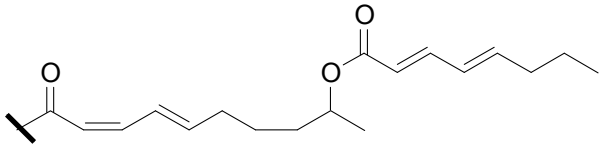

4.34 R =

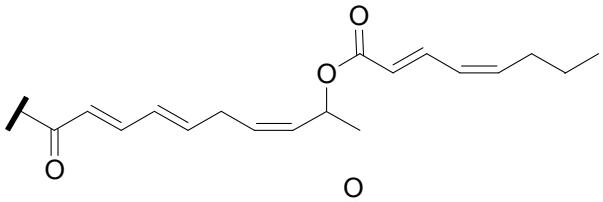

4.35 R =

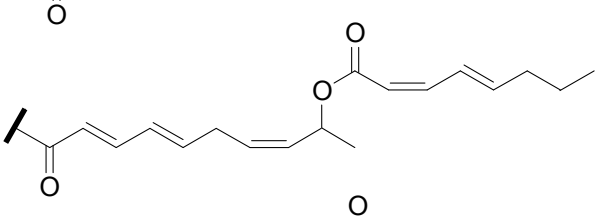

4.36 R =

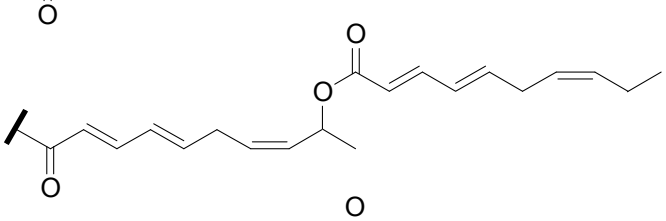

4.37 R =

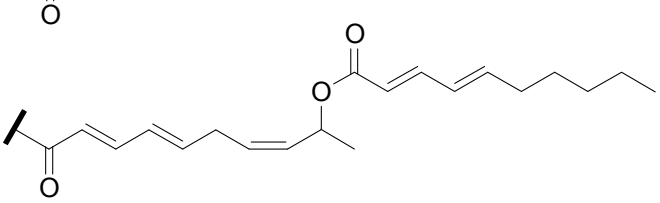

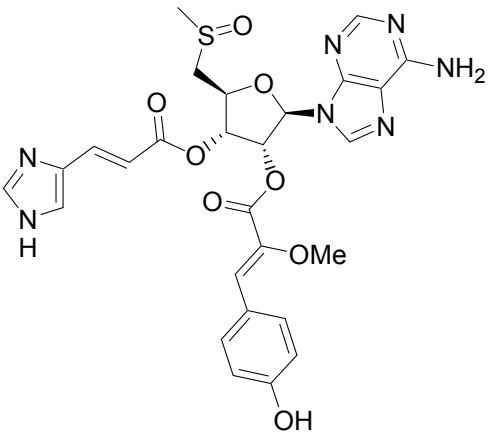

4.39

4.4 Isolation and structure elucidation of nucleosides from *Aplidium monile*

Aplidium monile Monniot, F., 2001[49] (Figure 4.5) is an aplousobranch ascidian belonging to the Polyclinidae family.[49] This compound ascidian grows in soft, cushion shaped colonies which have an overall pink colour with paler zooid apertures arranged in botryllid-like irregular double rows.[49] Colonies of *Aplidium monile* have been reported along the east coast of South Africa from Sodwana Bay to Algoa Bay.[49,78] The sample of *A. monile* investigated in our study was collected, under the voucher code TIC2011-032, from a depth of 12 - 15 m at Bell Buoy Reef, Algoa Bay, South Africa, in November 2011. The results obtained from the LC-ESI-MS/ICP-MS screen of the extract of *A. monile* are documented in Chapter 2.3.2 along with the successful isolation of the diiodotyramine **2.33**. This section will detail the isolation and characterisation of a series of nucleosides form a larger scale extraction of *A. monile*.

Figure 4.5: *Aplidium monile* (TIC2011-032) collected from Bell Bouy Reef, Algoa Bay, South Africa. Photography provided by Dr S. Parker-Nance.

Scheme 4.1 illustrates the chromatography protocol for the large scale (262.6 g wet mass of ascidian colony) methanol extract of *A. monile*. The initial solid phase extraction with a C-18 Sep-Pak® cartridge (Waters,10 g) yielded seven fractions reflecting the polarity of the solvent used to flush the cartridge (water, 10% acetonitrile$_{(aq)}$, 20% acetonitrile$_{(aq)}$, 40% acetonitrile$_{(aq)}$, 60% acetonitrile$_{(aq)}$, 80% acetonitrile$_{(aq)}$, and 100% acetonitrile). ^{1}H NMR spectra were acquired for each of the seven fractions and are reproduced in Figure 4.6. The ^{1}H NMR spectrum obtained for fraction two contained numerous peaks in the aromatic (δ_H 7.0-8.5) and oxymethine (δ_H 3.5-6.5) regions of the spectrum and was thus chosen for further fractionation. Fraction two was subsequently subjected to several rounds of reversed-phase semi-preparative HPLC as detailed in Scheme 4.1 to yield the nucleosides **4.10**, **4.11**, **4.13**, **4.15**, **4.17** and **4.40.**

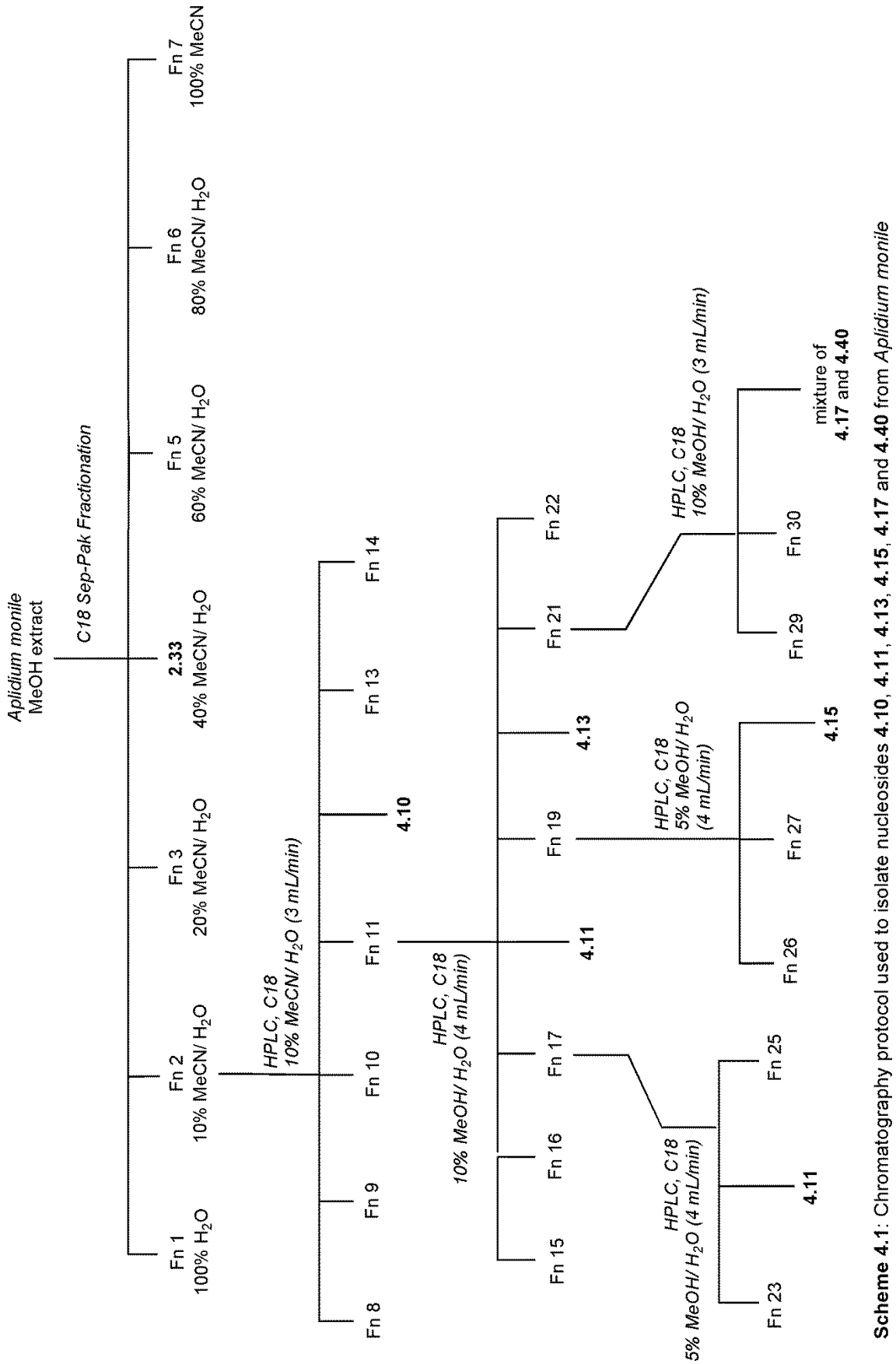

Scheme 4.1: Chromatography protocol used to isolate nucleosides **4.10**, **4.11**, **4.13**, **4.15**, **4.17** and **4.40** from *Aplidium monile*

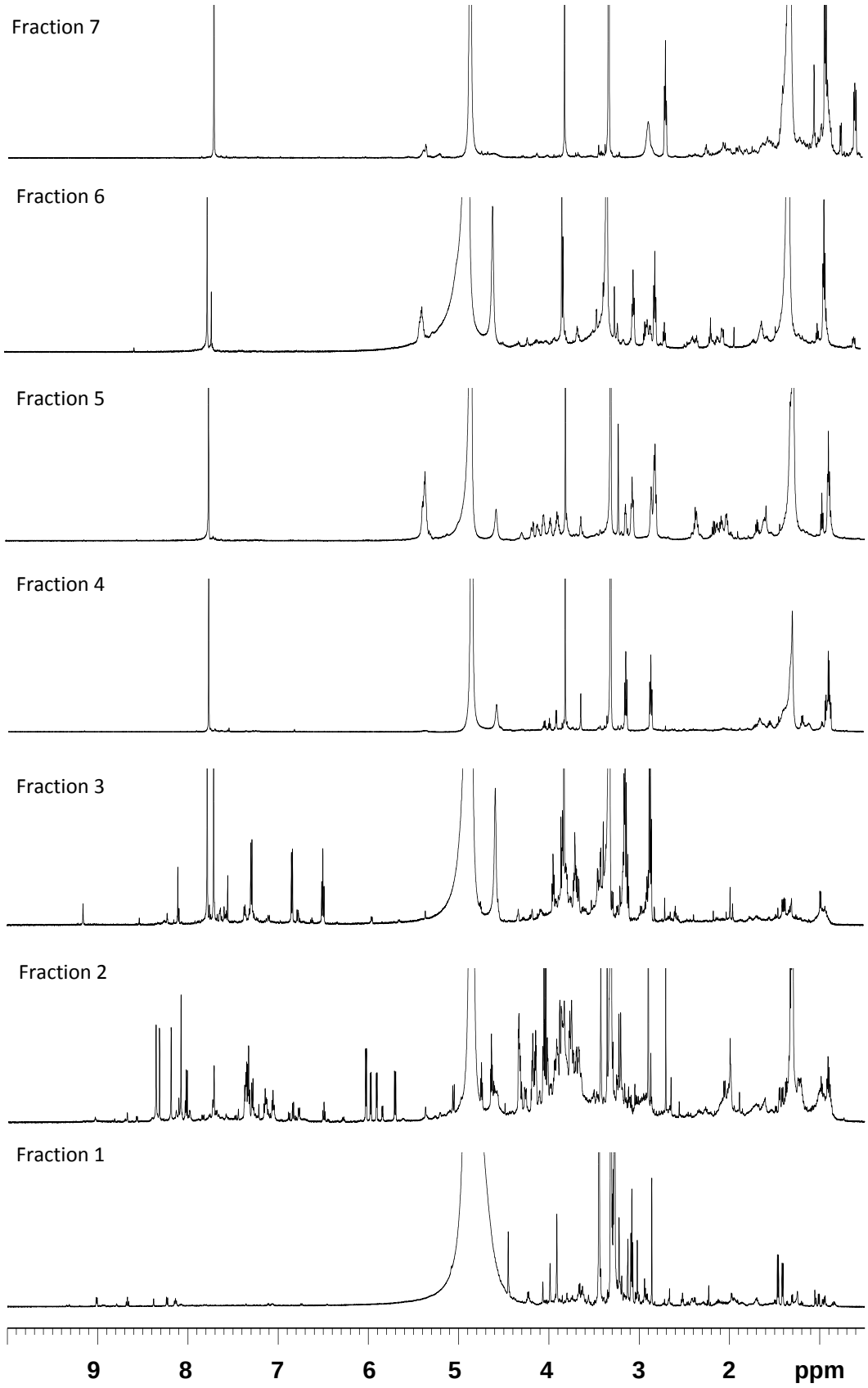

Figure 4.6: ^{1}H NMR (600 MHz, MeOD) data obtained for fractions 1-7 after reversed phase fractionation of the methanol extract of *A. monile*.

The HRESIMS data obtained for compound **4.10** (*m/z* 243.0988) indicated a molecular formula of $C_{10}H_{15}N_2O_5$ ($[M+H]^+$ calc., 243.0981, Δ 0.7 mmu) which implied five degrees of unsaturation. The characteristic broad bands at 3464 and 3403 cm^{-1} in the IR spectrum of **4.10** revealed the presence of hydroxyl groups whilst the band at 3237 cm^{-1} was suggestive of an amide moiety. The presence of bands at 1640 and 1619 cm^{-1} in the IR spectrum along with resonances at δ_C152.5 and 166.6 in the ^{13}C NMR spectrum suggested the presence of two carbonyl moieties which would account for two of the five degrees of unsaturation. The deshielded resonances in the ^{13}C spectrum (δ_C 111.5 and 138.2) and aromatic proton resonance [δ_H 7.83 (s)] suggested a highly substituted aromatic system. Three bond gHMBC correlations from the aromatic proton [δ_H 7.83 (s)] to both carbonyl resonances (δ_C 152.5 and 166.6) as well as the methyl proton shift (δ_H 1.88) with ^3J HMBC correlations to the carbonyl resonance (δ_C 166.6) and the olefinic resonance (δ_C 138.2) established the structure of the thymine component of **4.10**.

Five deshielded resonances in the ^{13}C NMR spectrum (δ_C 41.2, 62.6, 72.2, 86.3 and 88.8) of **4.10** and the corresponding proton shifts [δ_H 2.23 (2H, m), 3.73 (1H, dd, *J* = 12.0, 3.6 Hz) and 3.80 (1H, dd, *J* = 12.0, 3.1 Hz), 4.40 (1H, dt, *J* = 6.2, 3.3 Hz), 6.29 (1H, t, *J* = 6.7 Hz), and 3.90 (1H, dt, *J* = 3.4, 3.5 Hz)] implied a sugar functionality. Correlations observed in the two-dimensional COSY NMR experiment from the deshielded proton resonance [δ_H 6.29 (1H, t, *J* = 6.7 Hz)] through to the methylene protons [δ_H 3.73 (1H, dd, *J* = 12.0, 3.6 Hz) and 3.80 (1H, dd, *J* = 12.0, 3.1 Hz)] indicated a contiguous five carbon chain with chemical shifts characteristic of a 2'-deoxyribose unit. Three bond gHMBC correlations from the proton signal (δ_H 6.29) to the carbonyl (δ_C 152.5) and aromatic (δ_C 138.2) resonances indicated that the 2'-deoxyribose moiety was connected to the base at C-1' and unequivocally established **4.10** as the nucleoside thymidine. The structure elucidation of **4.10** gave us the first indication of the presence of a diverse array of related nucleosides in the *A. monile* extract.

The structures of the other common nucleosides **4.11**, **4.13**, and **4.15** were determined through direct comparison of the ^1H and ^{13}C NMR data obtained with those published in the literature (Figures 4.7 and 4.8 and Table 4.1). Standard two dimensional NMR experiments were used to confirm structures where necessary.

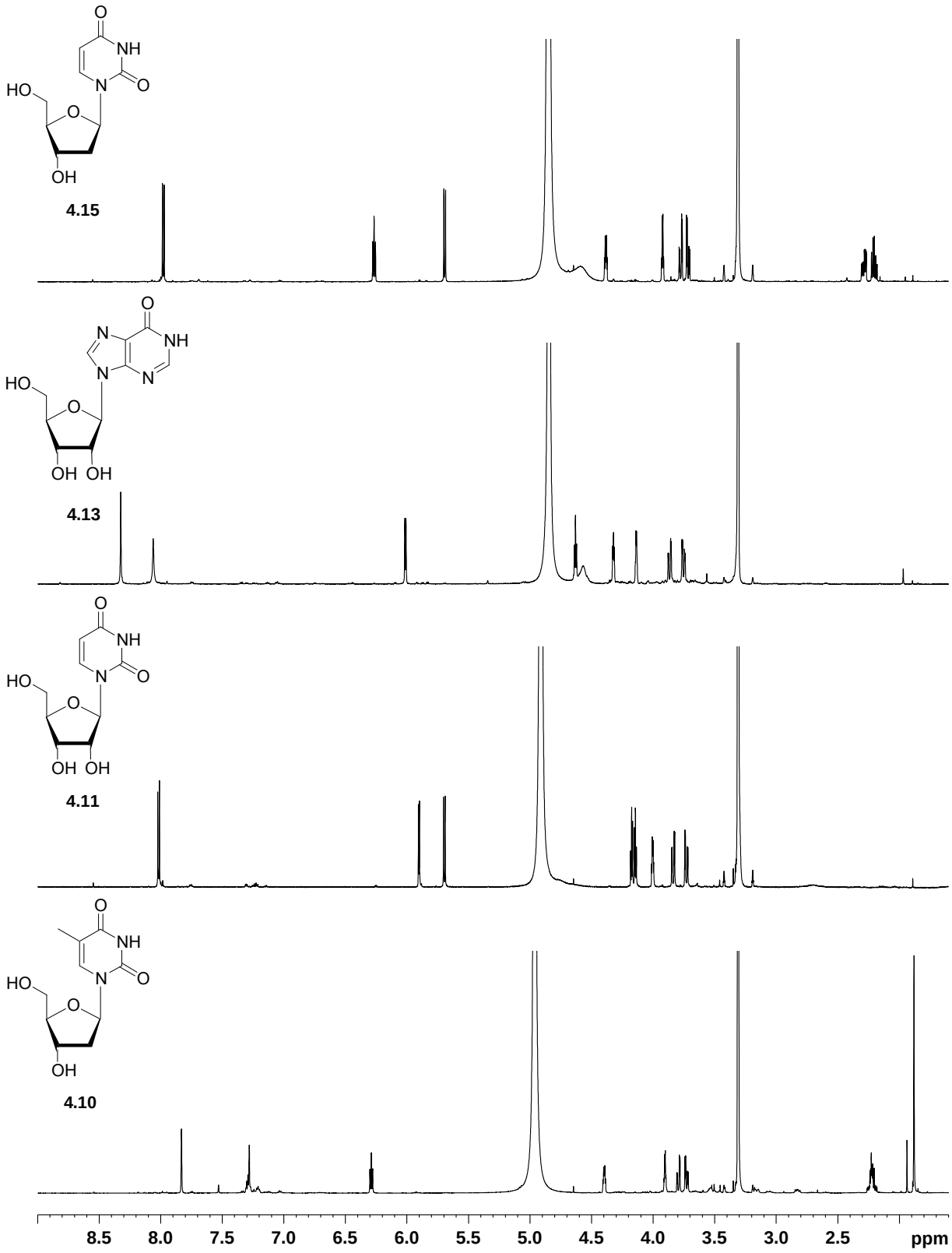

Figure 4.7: ^{1}H (MeOD, 600 MHz) NMR spectra of the known nucleosides **4.10**, **4.11**, **4.13** and **4.15** isolated from *A. monile*.

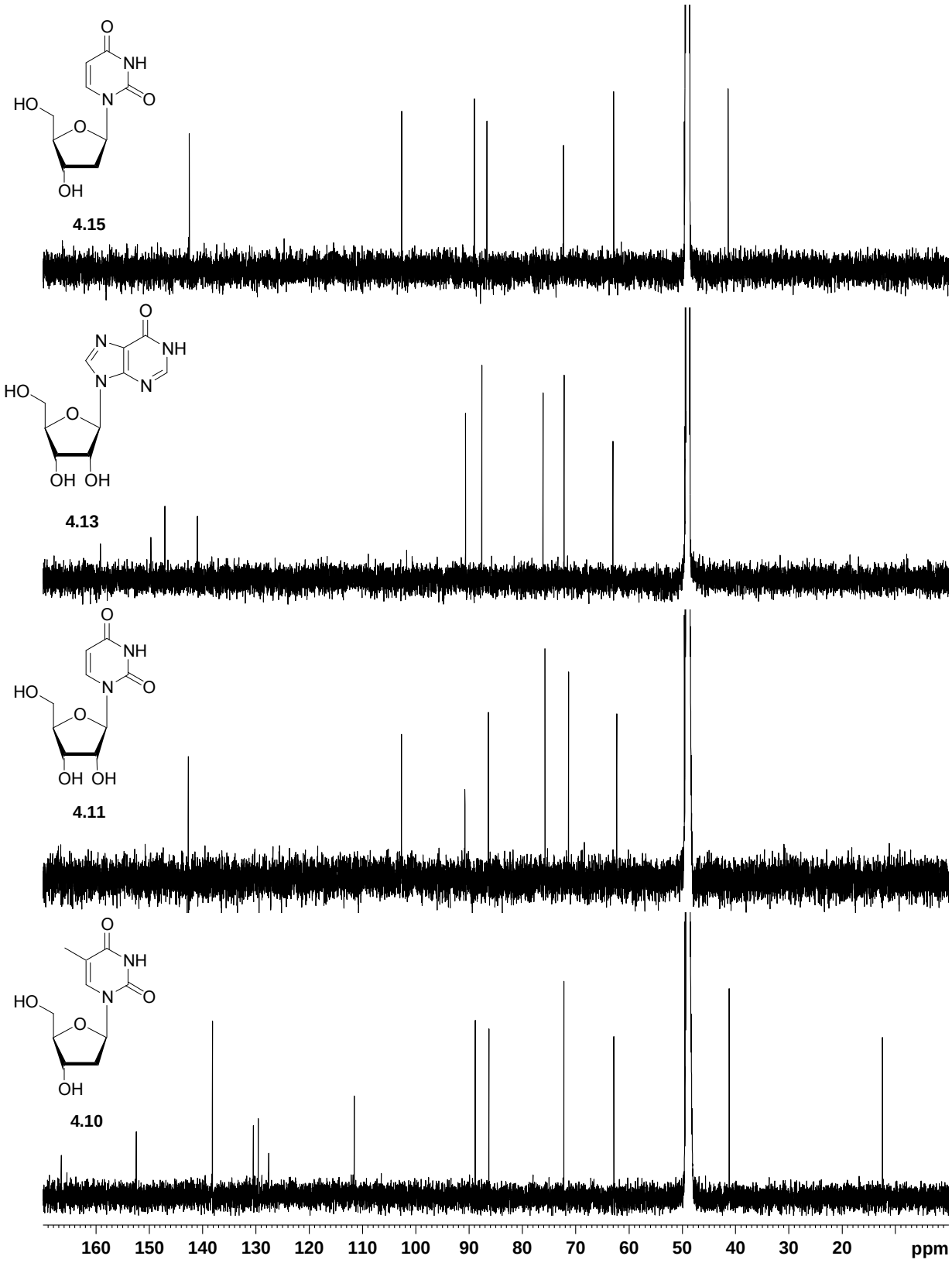

Figure 4.8: ^{13}C (MeOD, 150 MHz) NMR spectra obtained from the known nucleosides **4.10**, **4.11**, **4.13** and **4.15** isolated from *A. monile*.

Table 4.1: ^{1}H (MeOD, 600 MHz) and ^{13}C (MeOD, 150 MHz) NMR data obtained for nucleosides **4.10**, **4.11**, **4.13**, and **4.15** isolated form *A. monile* along with the relevant NMR data reported in the chemical literature.

	4.10				**4.11**				**4.13**				**4.15**		
	^{13}C		^{1}H		^{13}C		^{1}H		^{13}C		^{1}H		^{13}C ǂ	^{1}H	
		Lit.[68]		Lit.[68]		Lit.[75]		Lit.*		Lit.*		Lit.*			Lit.[61]
Position	δ_C (ppm)	δ_C (ppm)	δ_H (ppm)	δ_H (ppm)	δ_C (ppm)	δ_C (ppm)	δ_H (ppm)	δ_H (ppm)	δ_C (ppm)	δ_C (ppm)	δ_H (ppm)	δ_H (ppm)	δ_C (ppm)	δ_H (ppm)	δ_H (ppm)
1	N		-		N		-		N		-		N		
2	152.5	152.4	-		152.7	152.7	-		147.1	147.2	8.06	8.06	152.3		
3	N				N				N		-		N		
4	166.6	166.4	-		166.6	166.0	-		149.7	149.7	-		166.4		
5	111.5	111.5	-		102.7	102.8	5.70	5.70	126.1	125.9	-		102.6	5.69	5.69
6	138.2	138.2	7.83	7.80	142.7	142.9	8.02	8.00	159.2	159.2	-		142.5	7.98	7.98
7	12.4	12.3	1.88	1.88					N		-				
8									141.0	141.1	8.32	8.34			
9									N		-				
1'	86.3	86.3	6.29	6.27	90.8	90.1	5.90	5.90	90.7	90.7	6.01	6.02	86.6	6.27	6.26
2'	41.2	41.2	2.23	2.23	75.7	75.7	4.17	4.18	76.1	76.3	4.63	4.63	41.4	2.29	2.24
														2.20	
3'	72.2	72.2	4.40	4.40	71.3	71.9	4.14	4.15	72.2	72.2	4.32	4.32		4.38	4.36
4'	88.8	88.8	3.90	3.90	86.3	86.7	4.00	4.00	87.7	87.5	4.14	4.14	72.3	3.92	4.0-3.6
5'	62.9	62.9	3.73	3.71	62.3	62.7	3.73	3.73	63.0	63.2	3.75	3.75	89.0	3.78	4.0-3.6
			3.80	3.81			3.84	3.84			3.87	3.87	62.9	3.72	

* NMR data obtained from nucleoside standards

ǂ No literature data available

The ^{1}H and ^{13}C NMR spectra acquired from the final fraction (fraction 31), afforded from the chromatography protocol depicted in Scheme 4.1 are reproduced in Figure 4.9. On inspection of the ^{1}H NMR peak integration data the consistency of the values obtained implied that these data related to a single compound and the elucidation of the structure of the suspected single compound using the spectroscopic techniques available to us (1D and 2D NMR and IR) was commenced. The IR spectrum obtained for fraction 31 contained characteristic bands at 3438 and 1638 cm^{-1} indicative of hydroxyl and carbonyl moieties respectively. The presence of mid-field resonances in the ^{1}H NMR [δ_H 2.44(1H, ddd, 13.6, 6.2, 3.3), 2.74 (1H, ddd, 13.6, 7.5, 6.2), 3.73 (1H, m), 3.74 (1H, m), 3.81 (1H, dd, 12.1, 3.4), 3.85 (1H, dd, 12.3, 2.9), 4.04 (1H, dt, 3.4, 3.3), 4.10 (1H, dt, 3.1, 3.1), 4.29 (1H, dd, 4.9, 3.6), 4.56 (1H, dt, 6.0, 2.9), 4.60 (1H, t, 5.5), 5.83 (1H, d, 5.8), and 6.45 (1H, t, 6.79)] and the ^{13}C NMR spectra (δ_C 41.8, 63.2, 63.3, 72.3, 72.7, 75.5, 86.6, 87.4, 89.6, 90.3) supported the IR data by suggesting the presence of numerous oxymethine groups. The two dimensional COSY NMR data (Figure 4.10 and Tables 4.2 and 4.3) were used to establish the presence of two ribose moieties in fraction 31, one of which was a 2'-dexoyribose.

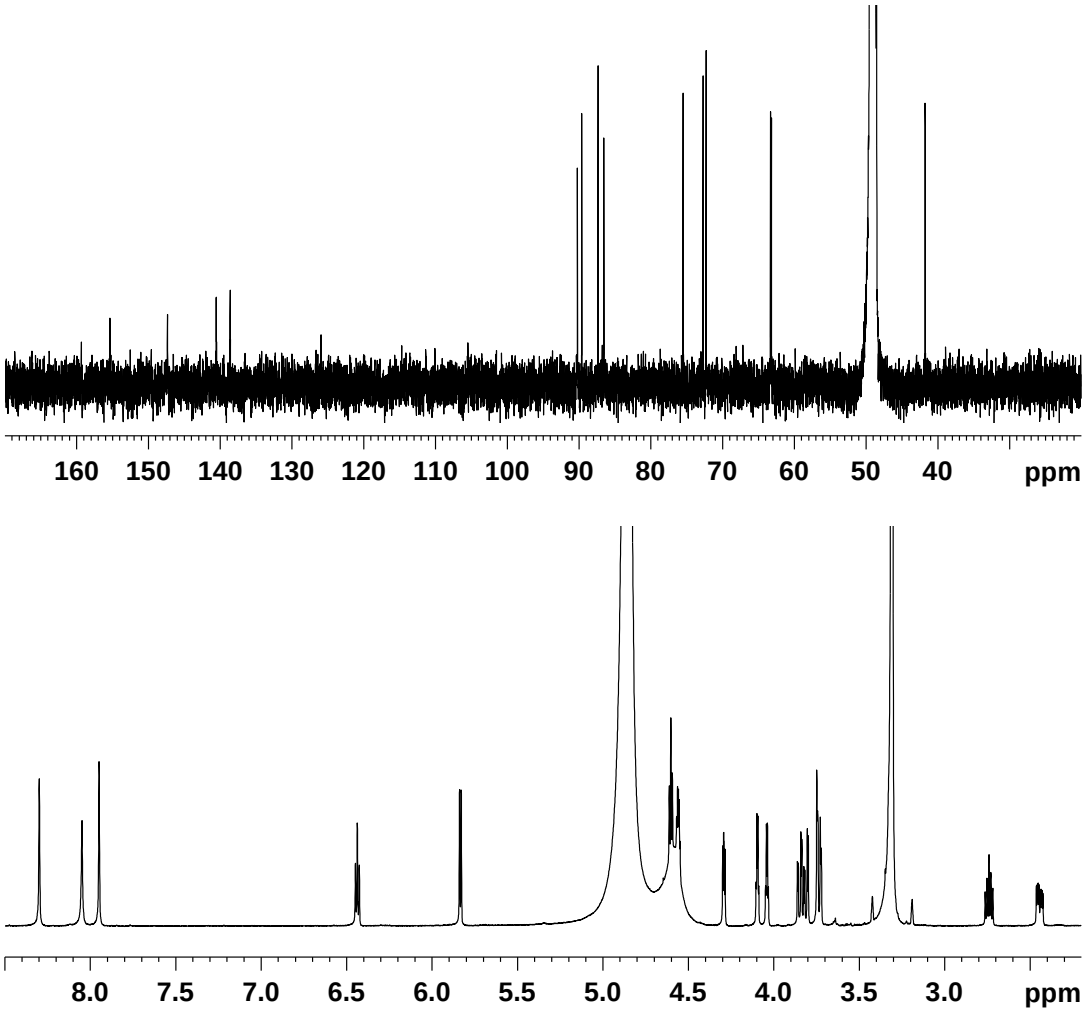

Figure 4.9: ^{1}H (MeOD, 600 MHz) and ^{13}C (MeOD, 150 MHz) NMR spectra obtained for the mixture of **4.17** and **4.40** from *A. monile*.

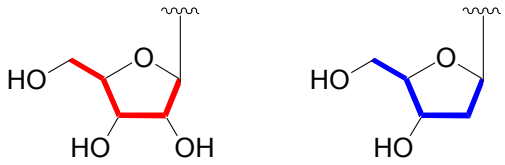

Ribose moieties present in fraction 31 with bold coloured bonds indicating COSY correlations

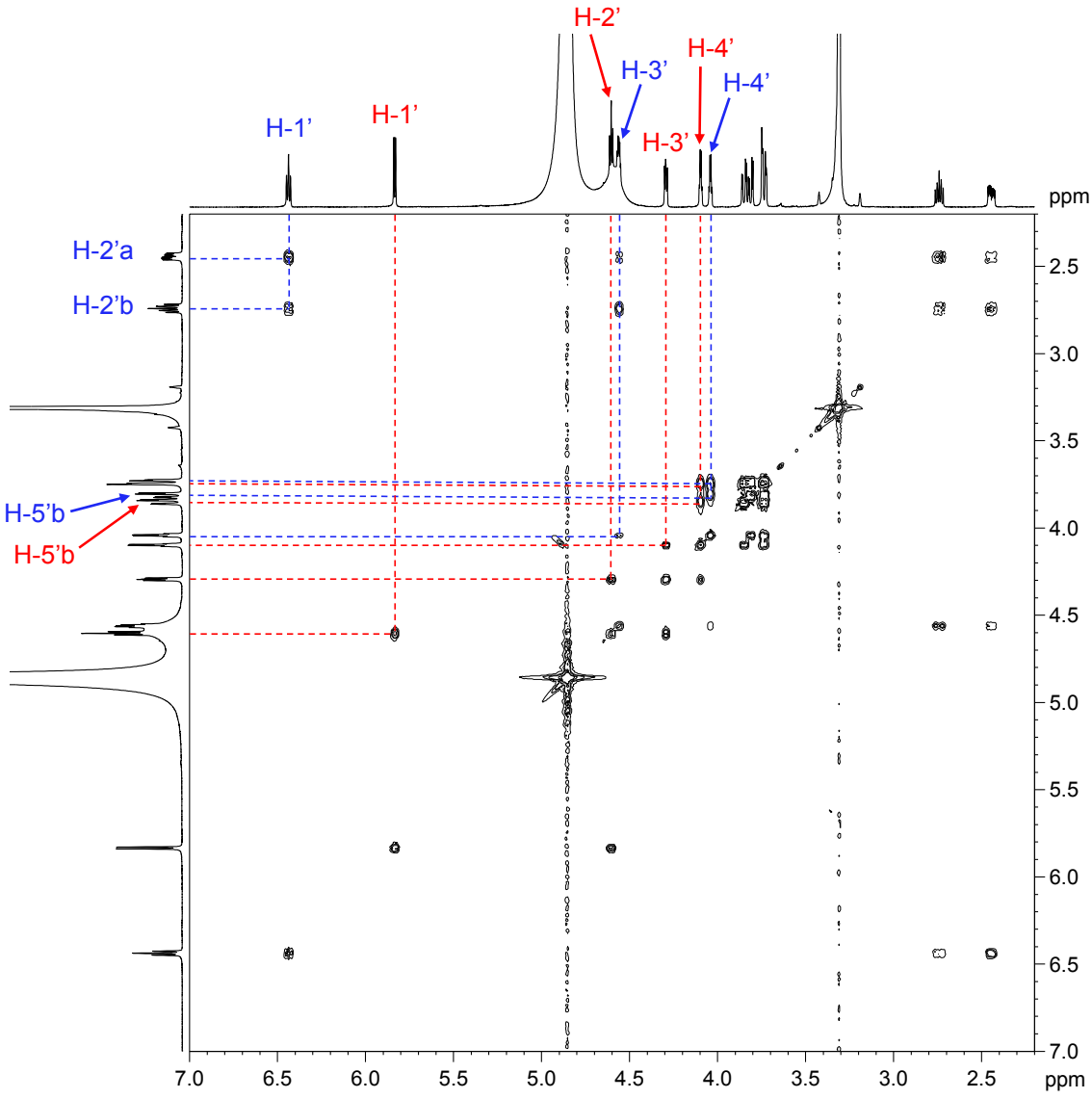

Figure 4.10: A region of the COSY spectrum (F1 = δ 2.0-7.5 ppm) obtained for fraction 31. The dashed lines indicate the correlations used to establish the presence of two distinct ribose moieties shown in the accompanying figure.

The presence of the ribose moieties along with the deshielded resonances in the ^{1}H NMR spectrum [δ_H 7.95 (1H, s), 8.05 (1H, s) and 8.3 (1H, s)] and ^{13}C NMR (δ_C 118.4, 126.1, 138.6, 140.5, 147.3, 149.7, 152.6, 159.5 and 159.8) spectra implied that fraction 31 also contained heteroaromatic functionalities similar to those seen in the nucleosides **4.10**, **4.11**, **4.13** and **4.15**. Thorough investigation of the two-dimensional NMR data obtained eventually established that fraction 31 was in fact an inseparable mixture of two compounds and did not contain a single compound as originally proposed.

The ^{3}J HMBC correlations (Table 4.2) between the aromatic proton resonance at 8.05 ppm and the carbonyl (δ_C 159.8) and heteroaromatic (δ_C 149.7) carbons as well correlations between the aromatic proton (δ_H 8.30) and quaternary aromatic carbons (δ_C 126.1 and 149.7) were indicative of a hypoxanthine base moiety such as that found in compound **4.13**. The gHMBC correlations between the proton at 6.45 ppm and the carbons at 140.5 and 149.7 ppm connected the 2'-deoxyribose sugar to the hypoxanthine base establishing the structure to be 2'-deoxyinosine (**4.17**). The NMR data relating to **4.17** is presented in Table 4.2.

The second compound in fraction 31 afforded 3 bond HMBC correlations between the aromatic resonance at δ_H 7.95 and the two carbonyl carbons at δ_C 152.6 and 159.5 in addition to a two bond correlation with the aromatic resonance at δ_C 118.4. HMBC correlations were also observed between δ_H 5.83 and δ_C 138.6 and 152.6 (Table 4.3) confirming the position of the ribose sugar on the nitrogenous base. These NMR data suggested that this compound was a C-5 substituted uridine derivative. The chemical shift of C-5 (δ_C 118.4) indicated that the substituent at C-5 was an amine group thus prompting us to propose a 5-aminouridine structure (**4.40**) for the second compound in Fraction 31. Further support for our structural assignment was provided by the ^{13}C NMR data reported for synthetic 5-aminouridine which correlates well with the data reported here for **4.40** isolated from *A. monile*.[208] Compound **4.40** has not previously been isolated form the marine environment[184]

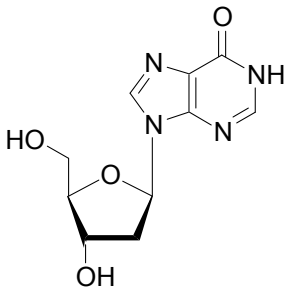

4.17

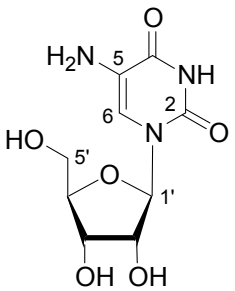

4.40

Various attempts to separate compounds **4.17** and **4.40** with reversed phase semi-preprative and analytical HPLC were unsuccessful and only served to reduce the quantity of these

compounds available for further study. All attempts to obtain reasonable high resolution mass spectral data on the inseparable mixture of **417** and **4.40** were unfortunately unsuccessful.

Table 4.2: ^{1}H (MeOD, 600 MHz), ^{13}C (MeOD, 150 MHz) and 2D NMR data obtained for **4.17**

Position	δ_C ppm	δ_H ppm (int., mult., *J*/Hz)	gHMBC[a]	COSY
1				
2	147.3	8.05 (1H, s)	C-4, C-6	
3				
4	149.7			
5	126.1			
6	159.8			
7				
8	140.5	8.3 (1H, s)	C-4, C-5	
9				
1'	86.6	6.45 (1H, t, 6.79)	C-4, C-8	H-2'a, H-2'b
2'a	41.8	2.44 (1H, ddd, 13.6, 6.2, 3.3)	C-1'	H-1, H-2'b, H-3'
2'b		2.74 (1H, ddd, 13.6, 7.5, 6.2)		H-1', H-2'a, H-3'
3'	72.7	4.56 (1H, dt, 6.0, 2.9)		H-2'a, H-2'b, H-4'
4'	89.6	4.04 (1H, dt, 3.4, 3.3)	C-2'	H-3', H-5'a, H-5'b
5'a	63.2	3.73 (1H, m)	C-3'	H-4', H-5'b
5'b		3.81 (1H, dd, 12.1, 3.4)	C-3'	H-4', H-5'a

[a] HMBC correlations are from proton(s) stated to indicated carbons

Table 4.3: ^{1}H (MeOD, 600 MHz), ^{13}C (MeOD, 150 MHz) and 2D NMR data obtained for **4.40**

Position	δ_C ppm	δ_H ppm (int., mult., *J*/Hz)	gHMBC[a]	COSY
1				
2	152.6			
3				
4	159.5			
5	118.4			
6	138.6	7.95 (1H, s)	C-2, C-4, C-5	
1'	90.3	5.83 (1H, d, 5.8)	C-2, C-6, C-2'	H-2'
2'	75.5	4.60 (1H, t, 5.5)	C-1'	H-1', H-3'
3'	72.3	4.29 (1H, dd, 4.9, 3.6)	C-5'	H-2', H-4'
4'	87.4	4.10 (1H, dt, 3.1, 3.1)		H-3', H-5'a, H-5'b
5'a	63.3	3.74 (1H, m)	C-3'	H-4', H-5'b
5'b		3.85 (1H, dd, 12.3, 2.9)	C-3'	H-4', H-5'a

[a] HMBC correlations are from proton(s) stated to indicated carbons

4.5 Metal chelation studies using potentiometic titrations with commercially available nucleosides and vanadium

In order to determine whether the nucleosides **4.10**-**4.14** were potentially involved in the accumulation and stabilisation of vanadyl (VO^{2+}) in aplousobranch ascidians an investigation into the stability of nucleoside-vanadyl complexes will be described here. Potentiometric experiments have successfully determined the organometallic complex speciation of oxovanadium (IV) or vanadyl across biological pH ranges as well as the relative stability of the complexes formed.[209,210] Since little work has been done to establish the stability of nucleoside-vanadyl complexes within biological environments, a potentiometric study of the system was deemed necessary in order to gain a better understanding of the stability of such a system.

When vanadyl (VO^{2+}) is in aqueous solution it is susceptible to hydrolysis and may form insoluble species. Figure 4.11 depicts a model, based on the vanadyl stability constants established by Henry *et al.*,[211] showing the speciation products which would be present across the pH range of 2 to 14. This model clearly illustrates that above pH 6 the majority of the free vanadyl will be present as insoluble hydroxides. In order to establish if the nucleosides **4.10**-**4.14** are capable of forming stable complexes with vanadyl the protonation constants for each nucleoside would need to be established first. The nucleoside protonation constants were determined using potentiometric titrations with a glass electrode and are presented in Table 4.4.

Throughout the potentiometric study titrations were controlled using Tiamo 2.0 software following a method used successfully by Tshentu and co-workers.[209,210] Nucleosides **4.10**-**4.14** were purchased from Sigma-Aldrich. Calibration of the glass electrode across a strong acid-base reaction used the Gran-method[212] and the computer program GLEE[213] to determine the standard potential E^o of the electrode. All appropriate calculations were based on the ionic product of water (pK_w) to be 13.76 at 25.0 ± 0.1 ^oC in 0.10 M sodium chloride.[214] The protonation constants for the nucleosides and oxovanadium(IV) complexes were determined by potentiometric titrations of approximately 25 mL solutions. All solutions were prepared using freshly boiled and degassed deionised milli-Q water to ensure the removal of dissolved oxygen and carbon dioxide. The ligand concentration of 1 mM was used and initial metal-to-ligand ratios of 1:1 were later changed to 1:10 to avoid precipitation. Titrations were performed over the pH range of 2 to 11 under a continuous flow of purified nitrogen using 0.1 M hydrochloric acid (1 mL) and sodium hydroxide (0.1 M). The ionic strength of the titration solutions was kept constant at 0.10 M sodium chloride. The data obtained from the potentiometric titrations of the nucleosides and the oxovanadium-nucleoside mixtures were used to calculate the protonation and stability constants.

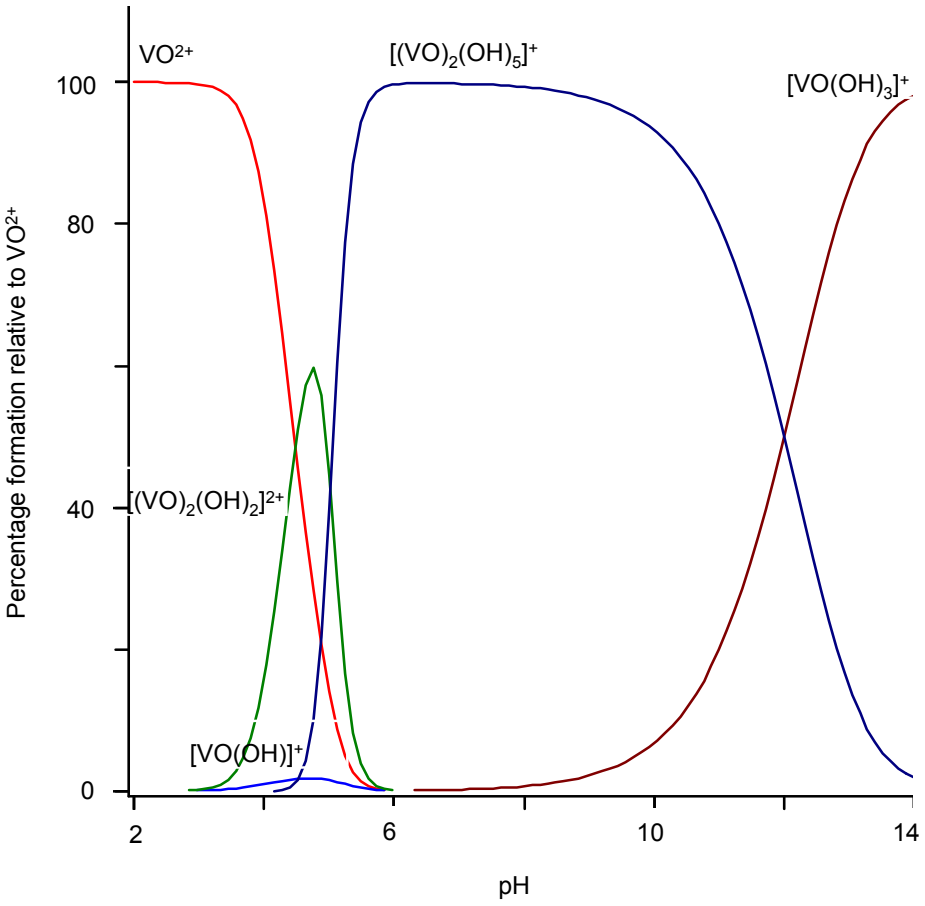

Figure 4.11: Speciation distribution as a function of pH for aqueous vanadyl (VO^{2+}) showing the hydroxyl products formed at certain pH values. Model created using the computer program HySS.[215]

The computer program HYPERQUAD[216] was used to calculate the concentration stability constants from the potentiometric titration data. HYPERQUAD generates a model titration curve based on the concentrations of the species involved in the titration. This HYPERQUAD model works on the principal that for each chemical species $M_pL_qH_r$, where M, L, and H represent metal, ligand and proton respectively, in the equilibrium solution there is a chemical constant that can be expressed as $\beta_{pqr} = [M_pL_qH_r]/[M]^p[L]^q[H]^r$.[216] HYPERQUAD will then fit the experimental data to the model and refine the protonation and/or stability constants of each chemical species. Since this is an iterative refinement it is important that the initially predicted stability constant values entered produce a reasonable fit of the experimental data to the model. For this reason the hydrolysis model of the oxidovanadium(IV) system (Figure 4.11) was included in the model *i.e.* $[VO(OH)_3]^-$ ($\log\beta_{10\text{-}3}$ = -18.0) and $[(VO)_2(OH)_5]^-$ ($\log\beta_{20\text{-}5}$ = -22.0), $[VO(OH)]^+$ ($\log\beta_{10\text{-}1}$ = -5.94) and $[(VO)_2(OH)_2]^{2+}$ ($\log\beta_{20\text{-}2}$ = -6.95).[211]

The protonation constants obtained for the nucleosides **4.10**-**4.14** are shown in Table 4.4. From these results the pyrimidine based nucleosides **4.10** and **4.11** have two potential sites where protonation occurs across the pH range of 2-11. The first of which is a hydroxyl group

on the sugar moiety and the other the N-3 position on the pyrimidine base. The purine based nucleosides **4.12**-**4.14** also have two sites of potential protonation, once again a hydroxyl and the N-1 position on the purine base, whilst **4.12** and **4.14** contain a third protonation site due to the presence of an amine substituent on the purine base. Establishing the protonation constants associated with these sites was necessary in order to determine if the nucleosides are capable of forming stable complexes with the vanadyl ion at a pH which is biologically relevant.

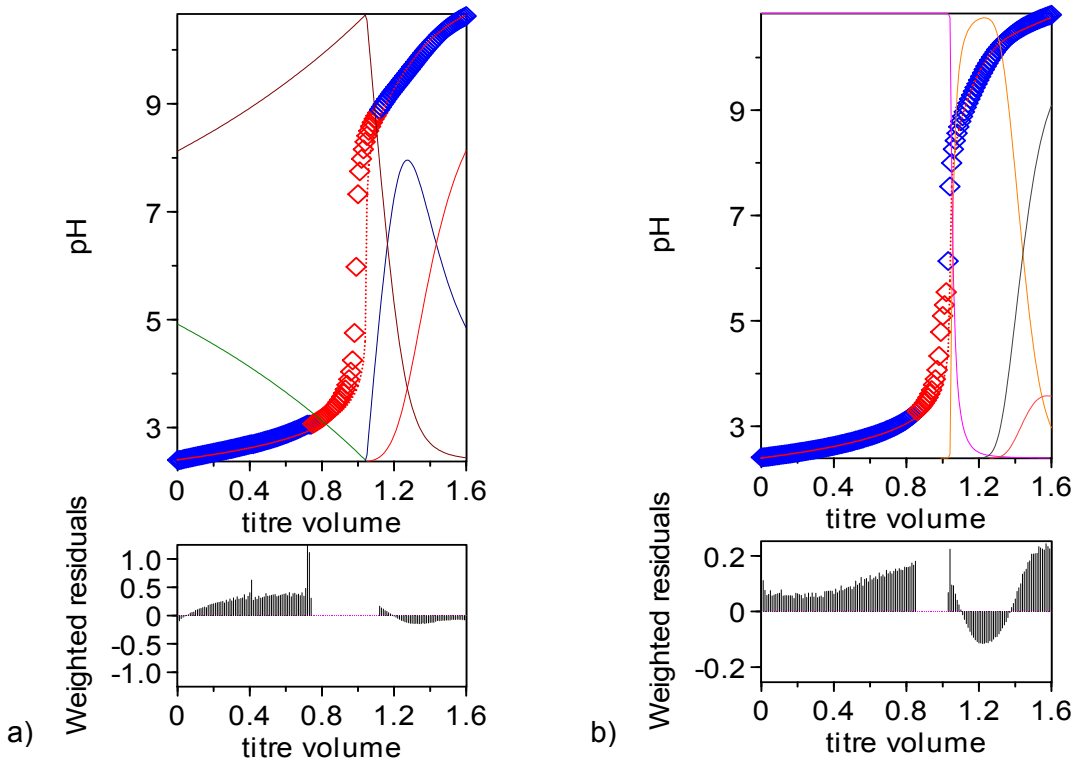

Figure 4.12: Titration and fitted curves of a) guanosine (**4.12**) protonation and b) VO-guanosine complexation systems. Experimental data points are shown as blue and red diamonds whilst the calculated model is shown by the dashed red line. The other lines represent species and were not defined.

The results obtained for the studies involving guanosine (**4.12**) shall be shown as a representative example. Figure 4.12 depicts the experimental and calculated titration curves for the guanosine protonation studies [Figure 4.12 a)] alongside the titration curves for the vanadyl-guanosine studies [Figure 4.12 b)]. The curve in Figure 4.12 a) show that the experimental data (blue diamonds) are a very good fit to the calculated model (dashed red line) which established the protonation constants of guanosine to be log*K* 9.6, 2.30 and 8.87. The red diamonds observed over the end point of the titration curve represent data points that were excluded from the refinement and model calculation as these points are often found

unreliable as large shifts in pH occur even with small changes in titre volume at the end point of a titration. Guanosine (**4.12**) protonation constants of log*K* 9.22 and 2.11, relating to protonation of the base, have been reported by Sigel *et al.*[217] which are in line with the constants determined here (log*K* 9.6 and 2.30) however we were able to establish a third protonation constant for the hydroxyl of **4.12** with a log*K* 8.87 which has not been previously reported.

With the protonation constants of guanosine determined the computer program HySS[215] was used to simulated the species of guanosine that would be expected throughout a pH range of 2 to 11 (Figure 4.13). From this simulation one can see that at a high pH of 2 to 4 the nucleoside **4.12** would be present as either the protonated or neutral species. The neutral guanosine species persists over the wides pH range of 3 to 8 after which deprotonation occurs (Figure 4.13).

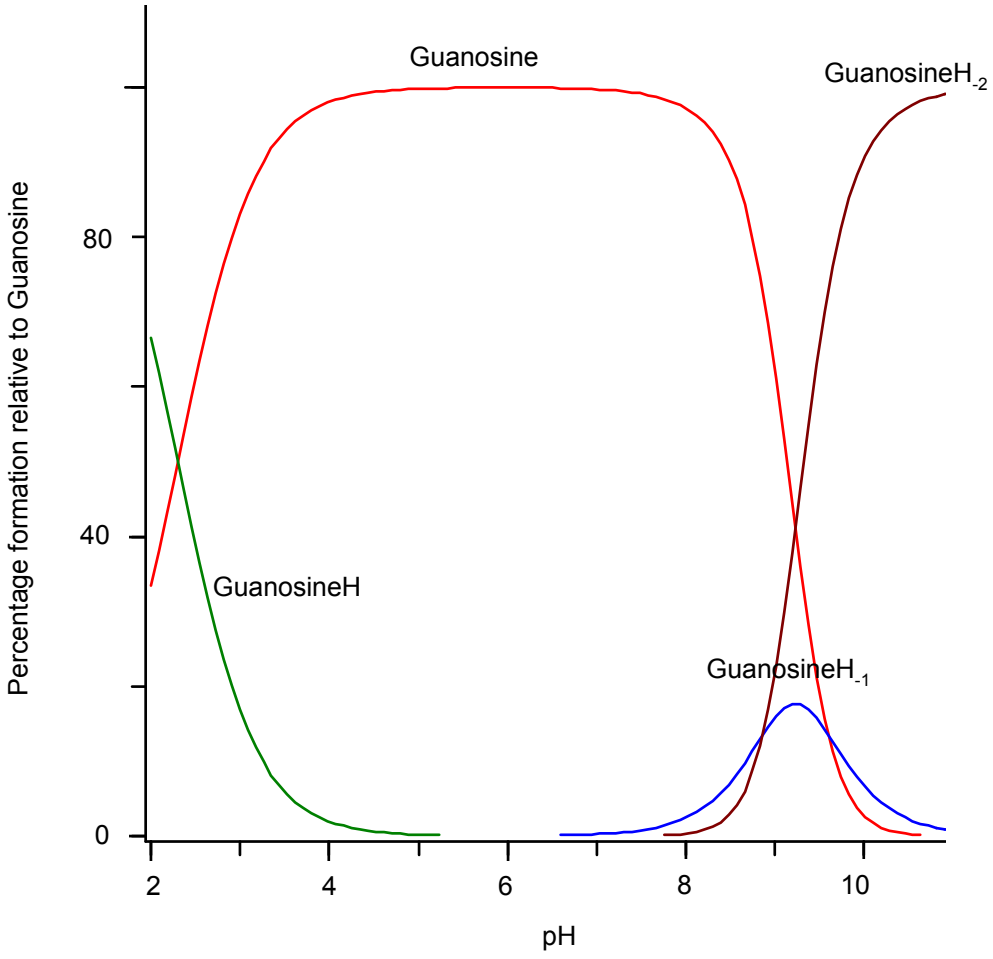

Figure 4.13: Species distribution as a function of pH simulated form the protonation constants determined for aqueous guanosine (**4.12**). Model created using the computer program HySS.[215]

Table 4.4: Logarithms of the protonation (log*K*) and stability constants (log*β*) for the VO^{2+}-L complexes at 25(±0.1)°C; *I* = 0.10 M (NaCl). L = thymidine, uridine, guanosine, inosine and adenosine, and L^{3-} implies that we consider cumulative association on a nucleoside that is deprotonated at three sites (one at the hydroxyl group and another at the NH group on the base, while in the case of adenosine and guanosine the NH_2 group on the base which can be protonated in acidic solutions is considered deprotonated).

Constant	4.10 Thymidine		4.11 Uridine		4.12 Guanosine		4.13 Inosine		4.14 Adenosine	
(VO^{2+},L^{3-},H)	log*β*	log*K*	log*β*	log*K*	log*β*	log*K*	log*β*	log*K*	log*β*	log*K*
(0, 1, 1)	9.54(2)	9.54(2)	9.12(2)	9.12(2)	9.6(1)	9.6(1)	*	*	*	*
(0, 1, 2)	20.32(2)	10.78(2)	19.89(2)	10.77(2)	18.47(6)	8.87(6)	8.63(2)	8.63(2)	11.04(1)	11.04(1)
(0, 1, 3)	**	**	**	**	20.77(4)	2.30(4)	**	**	14.69(1)	3.65(1)
(1, 1, 0)$	13.6(3)	13.6(3)	10.9(3)	10.9(3)	19.9(3)	19.9(3)	12.2(2)	12.2(2)	10.8(6)	10.8(6)
(1, 1, 1)$	#	-	13.9(3)	-	30.9(1)	-	17.8(4)	-	16.2(6)	-

*Protonation constant not determined due to it being higher than the pH range studied (*i.e.* assumed non-deprotonated)
**Protonation constant not determined due to the lack of the particular functional group.
#Stability constant not determined for the particular nucleoside.
$In modelling (1, 1, 0) it was assumed that there are no deprotonation of the ligand while (1, 1, 1) assumes that the neutral ligand binds and takes up a proton in another site.
– Not presented since it is not clear which of the groups on the nucleoside protonates during the complexation.

The first protonation constant determined for thymidine (**4.10**) log*K* 9.54 is similar to that established by Al-Flaijj *et al.*[218] (log*K* 9.50) however no second protonation constant, relating to the hydroxyl, was reported in the literature for direct comparison with that obtained in our study (log*K* 10.78). The protonation constants established for uridine (**4.11**), log*K* 9.12 and 10.77 are reasonably similar to those obtained by Crans and co-workers[193] (log*K* 9.0 and 12.6).

The only protonation constant determined for inosine (**4.13**) was log*K* 8.63 which was consisted with previous reports of log*K* 8.76[217] and 8.65[219] all other protonation constants relating to **4.13** were too high to be determined with the method employed here. Finally the protonation constants obtained for adenosine (**4.14**) were log*K* 11.04 and 3.64 which were consistent with those determined by Crans and co-workers[192] (log*K* 12.00 and 3.67). Unfortunately the constant relating to the amine substituent on the purine base of **4.14** was too large to be determined accurately in the pH range used.

Once the protonation constants for the nucleoside ligands were determined potentiometric titrations investigating vanadyl-nuceoside complexation were carried out. Analysis of the results obtained revealed that vanadyl-nucleoside system was complicated and conclusions drawn from the data would be limited. From our results the nucleosides appear to associate with the vanadyl ion with varying stability constants. In the theoretical model used in this analysis and reported in Table 4.4 the system relating to (1, 1, 0) it was assumed that the nucleoside ligand involved is not deprotonated at any site, whilst the (1, 1, 1) system assumes that the neutral nucleoside ligand binds to the vanadyl and takes up a proton in another site. This was assumed because the nucleoside species that would be available to complex the the vanadyl at the pH ranges studies were most likely not deprotonated (Figure 4.13). Unfortunately with the data at hand the protonation constants (log*K*) of the vanadyl-nucleoside complexes were not determined for the (1, 1, 1) system as it is not clear which sites on the nucleoside were protonated during the complexation. Due to the difficulty in determining protonation and stability constants for the vanadyl-nucleoside complexes formed no predictions can be made as to the structure of the complex, or even the nucleoside functionalities involved in the vanadyl complexation. However, from the results in Table 4.4 a comparison can be made between the nucleosides based on their ability to associate with the vanadyl ion to form a stable complex. The stability constants obtained from the vanadyl-guanosine titration data [Figure 4.12 b)] are the largest (logβ 19.9 and 30.9) across the series and would imply that **4.12** is the most likely of the nucleosides to bind to vanadyl forming a stable complex. It is however with some caution that any conclusions as to the nature of such systems or their presence in aplousobranch ascidians are made. The results of the potentiometric studies are difficult to interpret and although it appears that complexation occurs, evidence towards even a basic structure of the systems involved were not apparent.

It must also be noted that further influencing factors would be involved in a biological system which have not been considered in this experiment.

4.6 Conclusion

The accumulation of vanadium by certain species of ascidians has long been of interest to biologists and chemists. Although the recent discovery of a group of vanadium binding proteins, vanabins, in phlebobranch ascidians has helped to explain the presence of such large concentrations of vanadium in this suborder of ascidian, research towards understanding the mechanisms used by vanadium accumulating aplousobranchs is limited. The isolation of nucleosides **4.10**, **4.11**, **4.13**, **4.15**, **4.17** and **4.40** from the aplousobranch *Aplidium monile* prompted us to investigate the vanadyl binding properties of nucleosides commonly present in high quantities in ascidian extracts. The results obtained from the potentiometric complexation studies with commercially available nucleosides and oxovanadium (IV) revealed that nucleosides are capable of binding to vanadyl ions in aqueous media with guanosine (**4.12**) appearing to form the most stable complex. However, we concluded that the structure of the vanadyl-nucleoside complex is complicated and from the data obtained from the potentiometric experiments we were not able to shed any light on the structure of the complexes that clearly formed in solution nor establish exactly which nucleoside functional groups were involved in complexation with vanadyl.

Chapter Five:

Atriolum marinense & *Clavelina* sp. - Isolation of a common styrene oligomer

5.1 Bioassay on HP-20 fractions

In previous studies conducted by our research group, crude extracts of *Clavelina* sp. and *Atriolum marinense* were found to exhibit potent cytotoxicity towards oesophageal cancer cells in screening assays conducted at the University of Cape Town. Attempted isolation and identification of the compounds responsible for this activity were unfortunately unsuccessful, possibly because of the relatively low sensitivity of the NMR facilities (400 MHz) available at Rhodes University at that time. Following the arrival of a 600 MHz NMR spectrometer at Rhodes University it was deemed appropriate to revisit these two ascidian species and attempt the isolation and characterisation of the metabolites responsible for the oesophageal cancer cell toxicity.

a)  b) 

Figure 5.1: Colonies of (a) *Atriolum marinense* and (b) *Clavelina* sp. both photographed in Algoa Bay, South Africa by Dr Shirley Parker-Nance.

The ascidian, *Atriolum marinense* Kott, 2001[40,220] (Sub-order: Aplousobranchia, Family: Didemnidae) is cream to peach-orange in colour and has characteristic small, upright, flask shaped colonies which have a common apical cloacal opening (Figure 5.1a).[40,220] Specimens of *A. marinense* were previously reported as *Atriolum robustum*[34,40,220] but have subsequently been correctly described as a new and separate species by Kott, 2001.[220] The genus Atriolum is a small genus of the family Didemnidae with currently only six species described worldwide.[40] *Atriolum marinense* is the only species of this genus to be found outside of Australian waters, with a wide distribution including New Caledonia, South Africa and the Mozambique Channel.[40] *A. marinense* is found throughout Algoa Bay, South Africa, occurring at depths of 12 to 24 m.[40] For this investigation, a specimen of *A. marinense* was collected using SCUBA in November 2011 from the Algoa Bay dive site, known as Shy Shark reef.

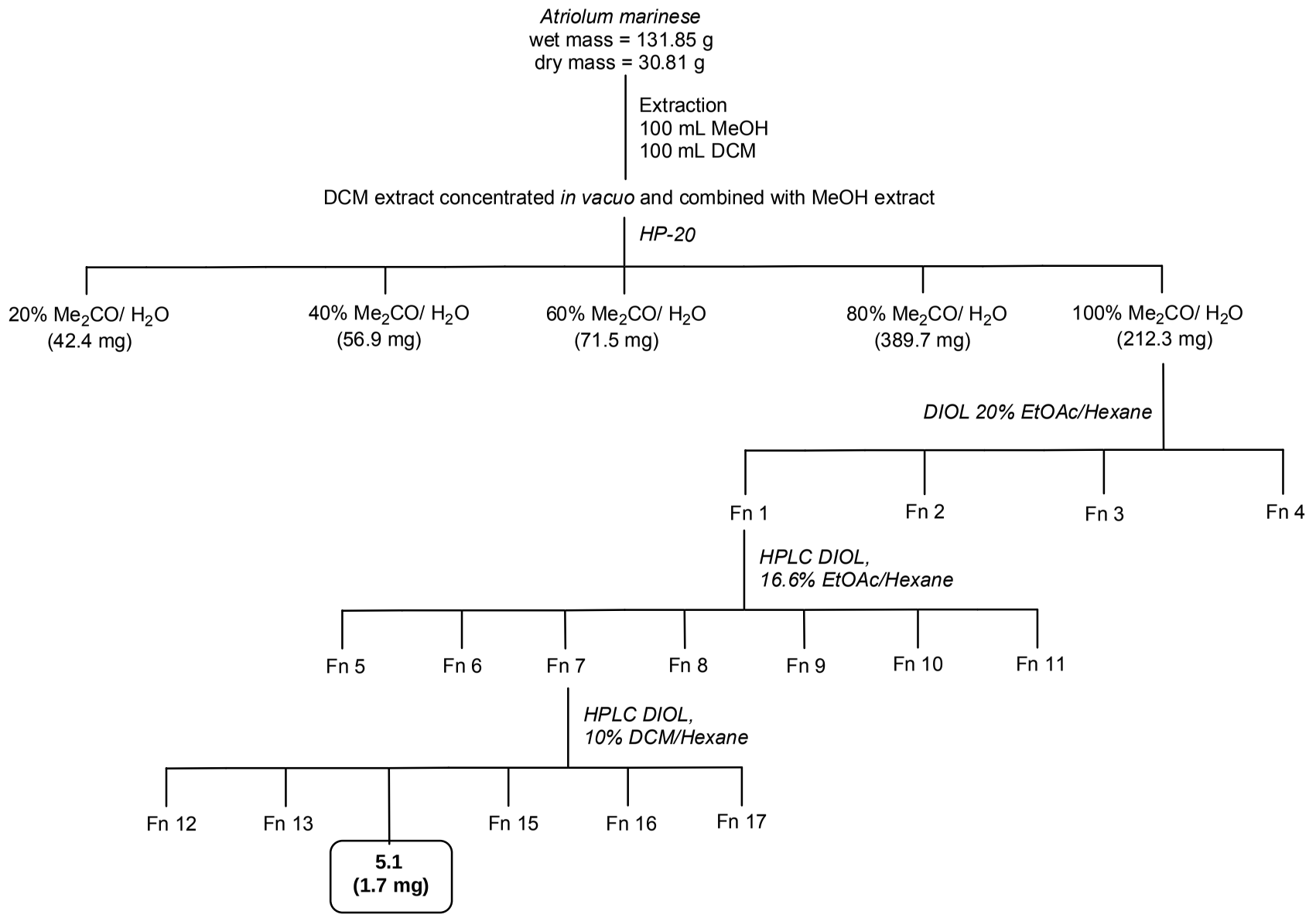

Scheme 5.1: Chromatography protocol used to isolate styrene trimer **5.1** from *Atriolum marinense*.

The delicate blue ascidian commonly known as Lori Bell's clavelina is a new species of Clavelina which shall be referred to as *Clavelina* sp. and is depicted in Figure 5.1(b). *Clavelina* sp. has also been found at depths between 17 and 24 m on low profile reefs off the South African coastal towns of Port Alfred and East London.[78] The sample of *Clavelina* sp. investigated here was allocated the voucher code SAF2004-029 and was collected using SCUBA from a depth of 21 m at White Sands reef, Algoa Bay in 2004.

Lyophilised samples of both species were sequentially extracted with equal volumes of methanol and dichloromethane. During this extraction process, the dichloromethane and methanol extracts were kept separate, and before HP-20 fractionation, the dichloromethane extract was concentrated under reduced pressure. This was necessary as dichloromethane is immiscible with water and if the solvent was not removed before the aqueous dilutions that are involved in cyclic loading (Section 5.3) the extract onto the HP-20 resin the organic metabolites would not be adsorbed by the resin. Once all of the dichloromethane had been removed, the remaining solid extract was taken up in acetone and combined with the methanol extracts and cyclic loaded onto the HP-20 resin. The HP-20 beads were washed thoroughly with water before being sequentially stripped with aqueous acetone mixtures of decreasing polarity (20%, 40%, 60%, 80% acetone/water and 100% acetone), to afford five fractions (Scheme 5.1).

At the time this work was repeated in 2013 access to the oesophageal cancer screens was no longer available to us and subsamples of approximately 1 mg of each of the five HP-20 fractions obtained for both ascidian species were instead assayed against breast cancer cells at concentrations of 50 µg/mL and 5 µg/mL. In the assay the percentage viability of the breast cancer cells after exposure to the HP-20 fractions were measured and are illustrated in Figure 5.2.

The results yielded from the fractions of *A. marinense* suggested that the 80% acetone$_{(aq)}$ fraction was the most cytotoxic with less than 50% cell viability even at the lower concentration of 5 µg/mL. The other acetone$_{(aq)}$ fractions of *A. marinense* were only cytotoxic against the cells at a higher concentration of 50 µg/mL. Interestingly and inexplicably, the HP-20 column wash (methanol/dichloromethane) of *A. marinense* appeared to promote the growth of the cancer cells at both concentrations assayed (Figure 5.2).

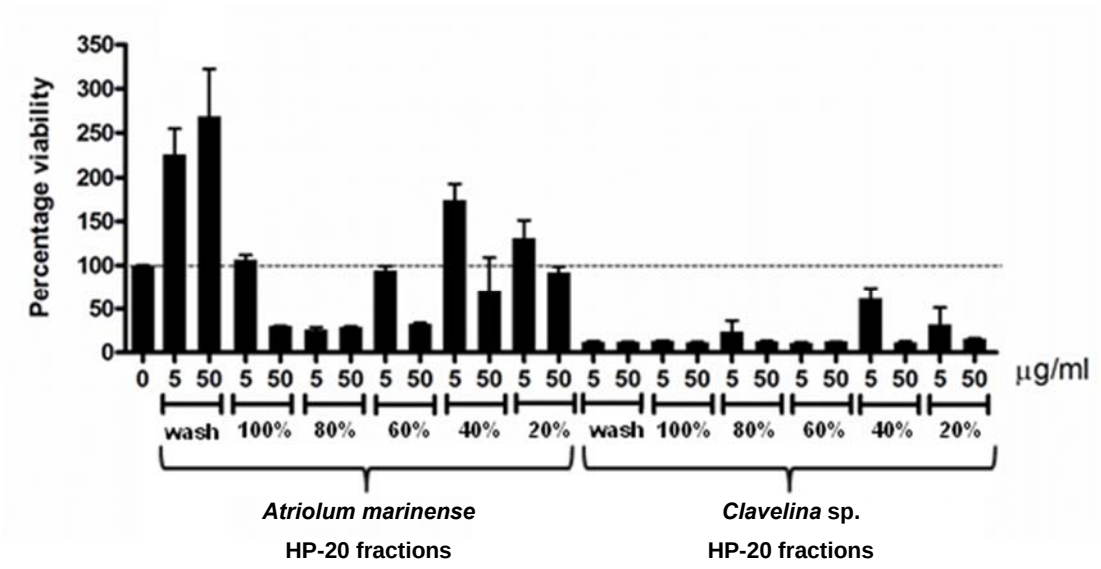

Figure 5.2: Percentage viability of breast cancer cells on exposure to 50 µg/mL and 5 µg/mL of the acetone$_{(aq)}$ fractions of *A. marinense* and *Clavelina* sp. eluted from the respective HP-20 columns (in each case the wash fraction was eluted using 1:1 methanol/dichloromethane).

The HP-20 fractions obtained for the extract of *Clavelina* sp. were all markedly more cytotoxic than the *A. marinense* fractions in the breast cancer cell screens. All of the *Clavelina* sp. fractions assayed showed cytotoxicity against the breast cancer cells even at the lower test concentration of 5 µg/mL. The more non-polar HP-20 fractions of *Clavelina* sp. (60%, 80%, 100% acetone$_{(aq)}$ and wash) appeared to be very active with less that 30% cell viability resulting from the assay with 5 µg/mL concentrations of the fractions.

These promising bioassay results prompted further investigation of the most cytotoxic chromatography fractions from both species. The ^{1}H NMR spectra acquired for each of the five *A. marinense* and *Clavelina* sp. fractions eluted off of the HP-20 column are illustrated in Figures 5.3 and 5.4 respectively. From these promising bioassay results the spectra obtained for the 80% acetone$_{(aq)}$fraction of *A. marinense* and the 60%, 80%, 100% acetone, and wash fractions of *Clavelina* sp. were of greatest interest. Unfortunately, with the exception for the 100% acetone$_{(aq)}$fractions of both ascidian species, the ^{1}H NMR spectra produced by these particular fractions did not reveal the presence of major compounds with deshielded resonances ($\delta_H > 4.5$) characteristic of many bioactive secondary metabolites.

At the outset we proposed that compounds responsible for the cytotoxicity were probably a very active minor compound(s) occurring in all the HP20 chromatography fractions making bioassay guided chromatography difficult. The NMR data suggested that most active non polar fractions were dominated by what appeared to be structurally unremarkable fatty acid glycerides.

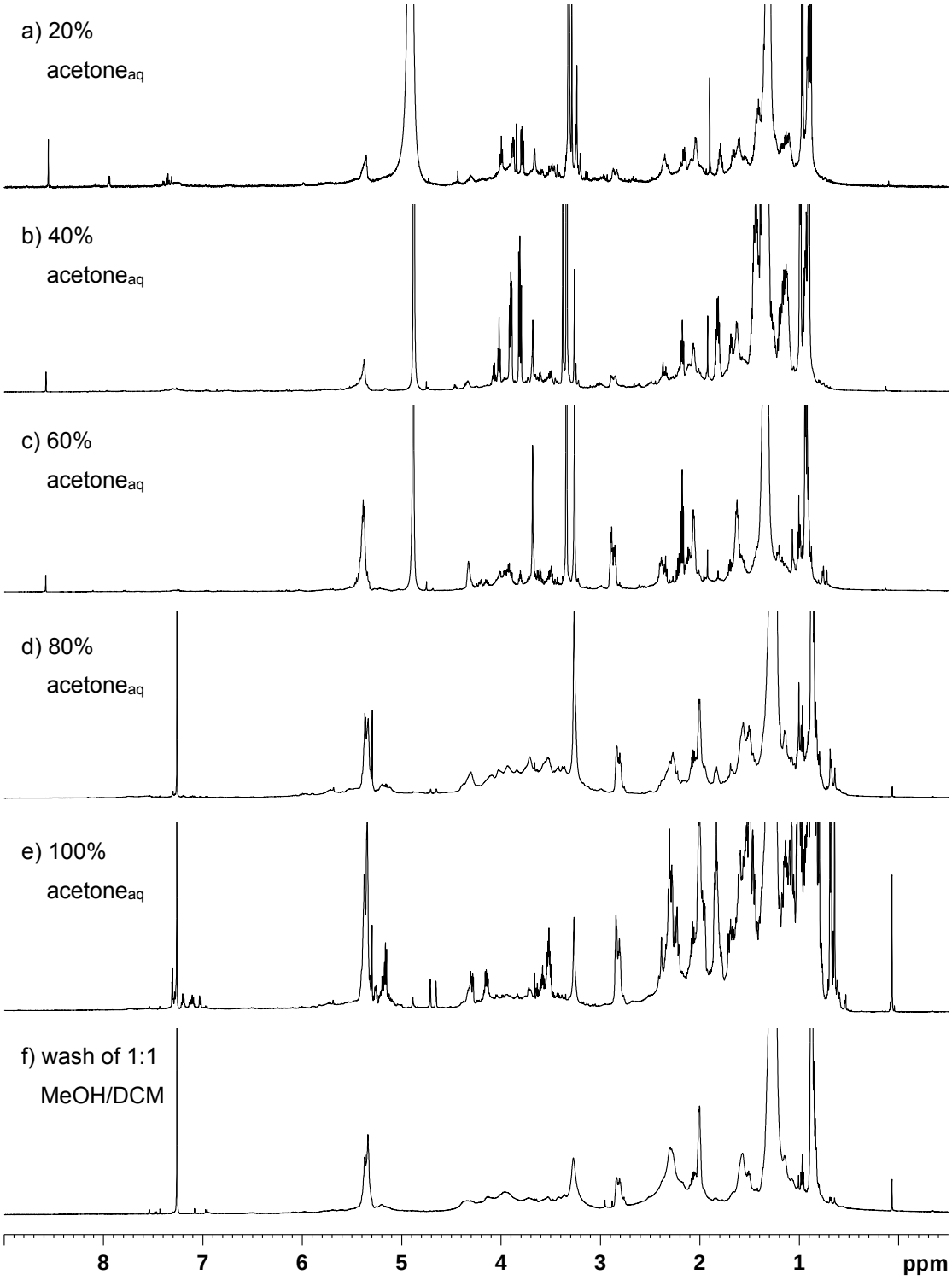

Figure 5.3: ^{1}H NMR (600 MHz) spectra of the fractions of *Atriolumn marinense* extract eluted from HP-20 resin; a) 20% acetone$_{(aq)}$(MeOD); b) 40% acetone$_{(aq)}$(MeOD); c) 60% acetone$_{(aq)}$(MeOD); d) 80% acetone$_{(aq)}$($CDCl_3$); e) 100% acetone ($CDCl_3$); f) wash of 1:1 methanol/dichloromethane ($CDCl_3$).

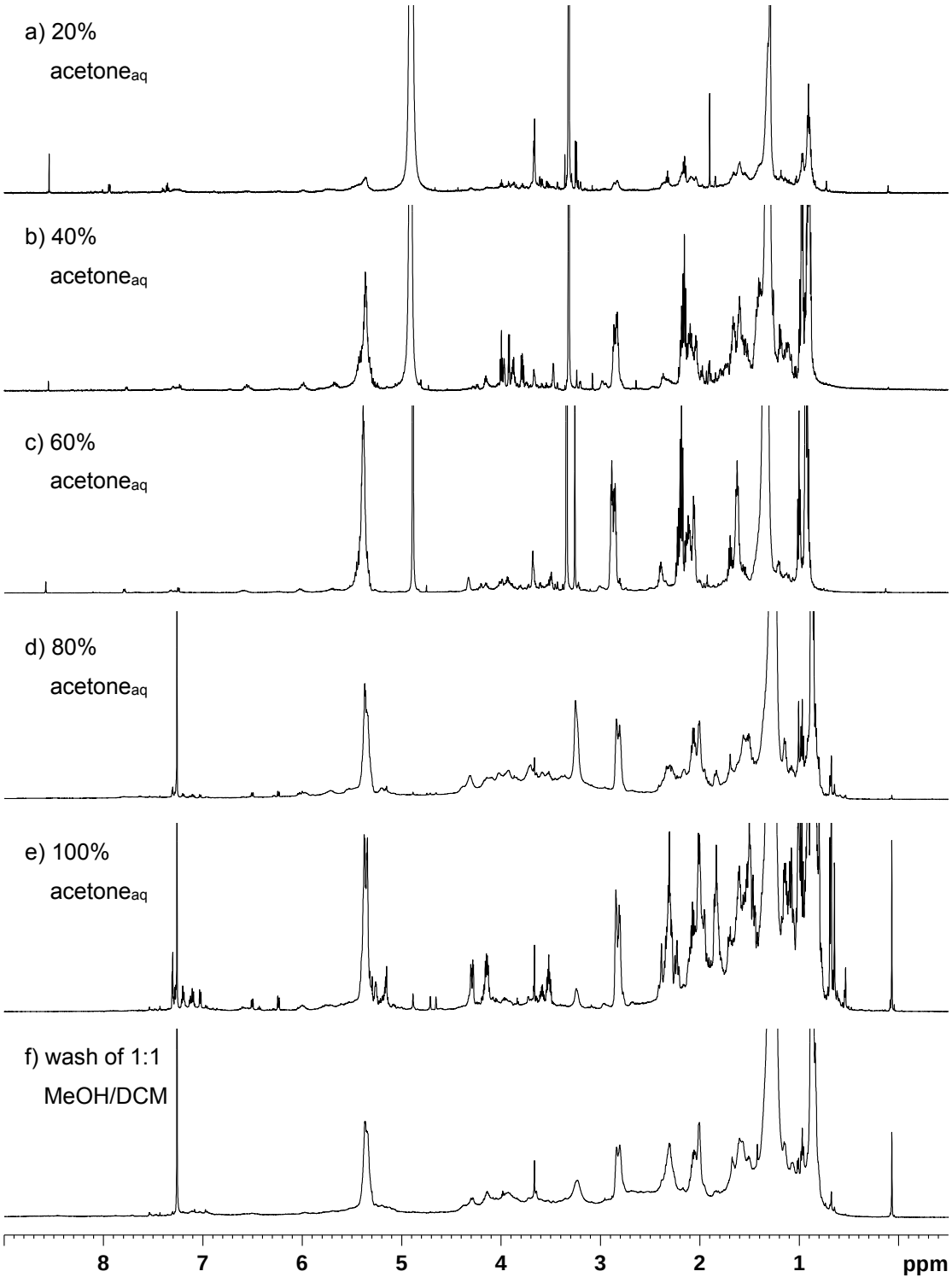

Figure 5.4: ^{1}H NMR (600 MHz) spectra of the fractions of *Clavelina* sp. extract eluted from HP-20 resin; a) 20% acetone$_{(aq)}$(MeOD); b) 40% acetone$_{(aq)}$(MeOD); c) 60% acetone$_{(aq)}$(MeOD); d) 80% acetone$_{(aq)}$($CDCl_3$); e) 100% acetone ($CDCl_3$); f) wash of 1:1 methanol/dichloromethane ($CDCl_3$).

5.2 Isolation and structure elucidation of a styrene oligomer

Interestingly, the 100% acetone fractions of both species yielded ^{1}H NMR spectra with very similar shifts in the aromatic region (δ_H 7.0 – 7.4) implying a common compound in both ascidian extracts (Figure 5.5). The 100% acetone fraction of *A. marinense* was initially purified through open column chromatography using propanediol-bonded silica (DIOL) as a stationary phase (Scheme 5.1). Based on the ^{1}H NMR spectra acquired for the fractions afforded from this chromatography, the first chromatography fraction was further purified through a series of normal phase HPLC separations as illustrated in Scheme 5.1 to yield the styrene trimer **5.1** (1.7 mg).

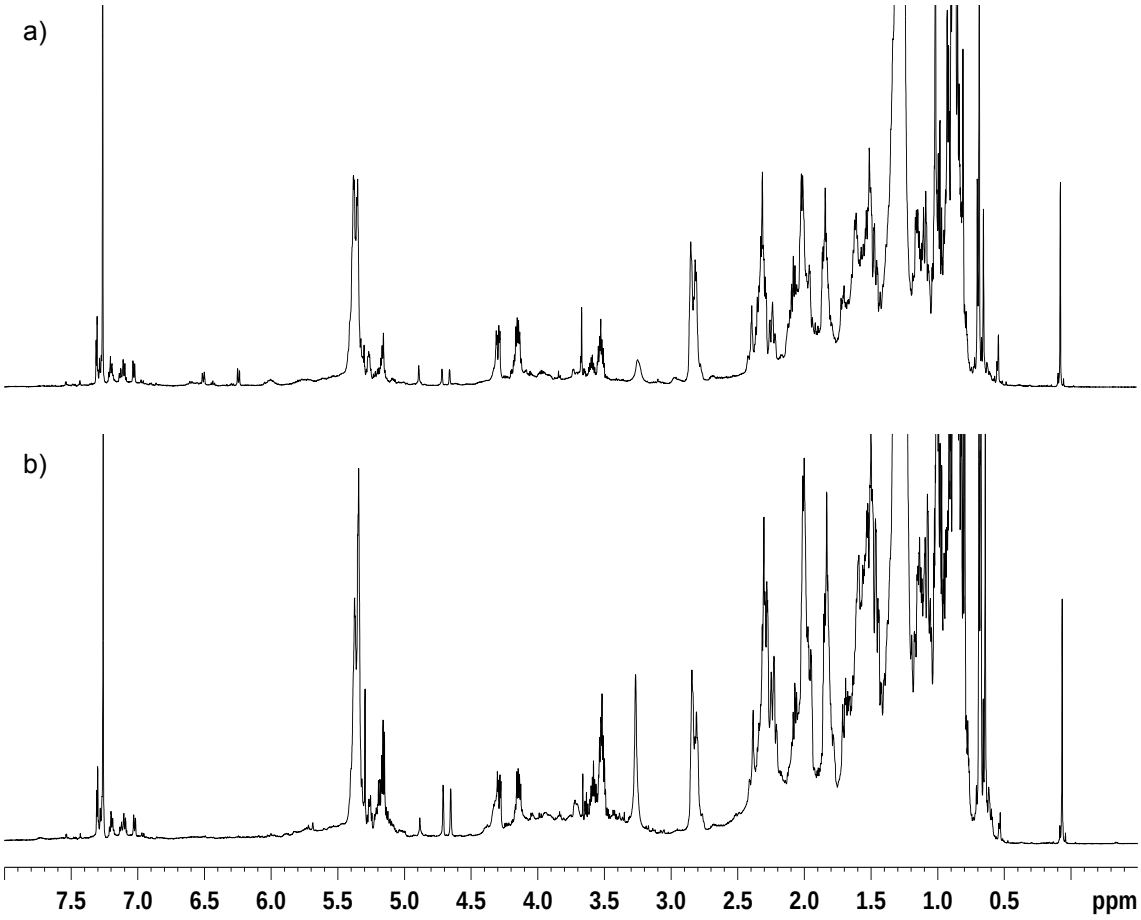

Figure 5.5: ^{1}H NMR ($CDCl_3$ 600 MHz) spectra of the 100% acetone fractions of a) *Clavelina* sp. and b) *A. marinense* eluted from the HP-20 fractionation of their crude extracts.

The ^{1}H and ^{13}C NMR spectra acquired for **5.1** isolated from *A. marinense* are illustrated in Figure 5.6. Through the analysis of the number and relative proportion of the ^{1}H and ^{13}C NMR resonances evident in these spectra a molecular formula of $C_{24}H_{24}$ was proposed for **5.1**, implying 13 double bond equivalences. Regrettably, several attempts to confirm the molecular mass of **5.1** via high resolution mass spectrometry techniques such as LC-ESI-MS

and GC-EI-MS were unsuccessful. However eventual low resolution GC-EI-MS analysis yielded a molecular ion [M^+] at *m/z* 312.1 which supported the molecular formula of $C_{24}H_{24}$ established through NMR.

The presence of two deshielded signals in the ^{13}C NMR spectrum (δ_C 114.4 and 141.1) in addition to the olefinic proton resonances [δ_H 4.89 (s) and 5.15 (s)] in the ^1H NMR spectrum of **5.1** confirmed the presence of a terminal alkene, accounting for one of the degrees of unsaturation. On further inspection of the aromatic regions of both the ^1H and ^{13}C NMR spectra, the remaining 12 double bond equivalences could be accounted for by three phenyl rings. The aromatic envelope of the ^{13}C NMR spectra of **5.1** contained three quaternary carbons (δ_C 142.4, 145.0 and 146.7) and nine aromatic methine carbons (δ_C 125.6, 126.1, 126.4, 127.3, 127.7, 128.3, 128.26, 128.291 and 128.293) with the varying intensities of these resonances implying a level of chemical equivalence brought about by symmetry. The corresponding region of the ^1H NMR spectrum was, however, complicated by the presence of highly overlapped multiplets which hampered assignment of the relevant proton and carbon chemical shifts in subsequent 2D NMR experiments. Accordingly, the Bruker simulation software, WIN-DAISY,[81] was utilised to facilitate the assignment of these aromatic resonances.

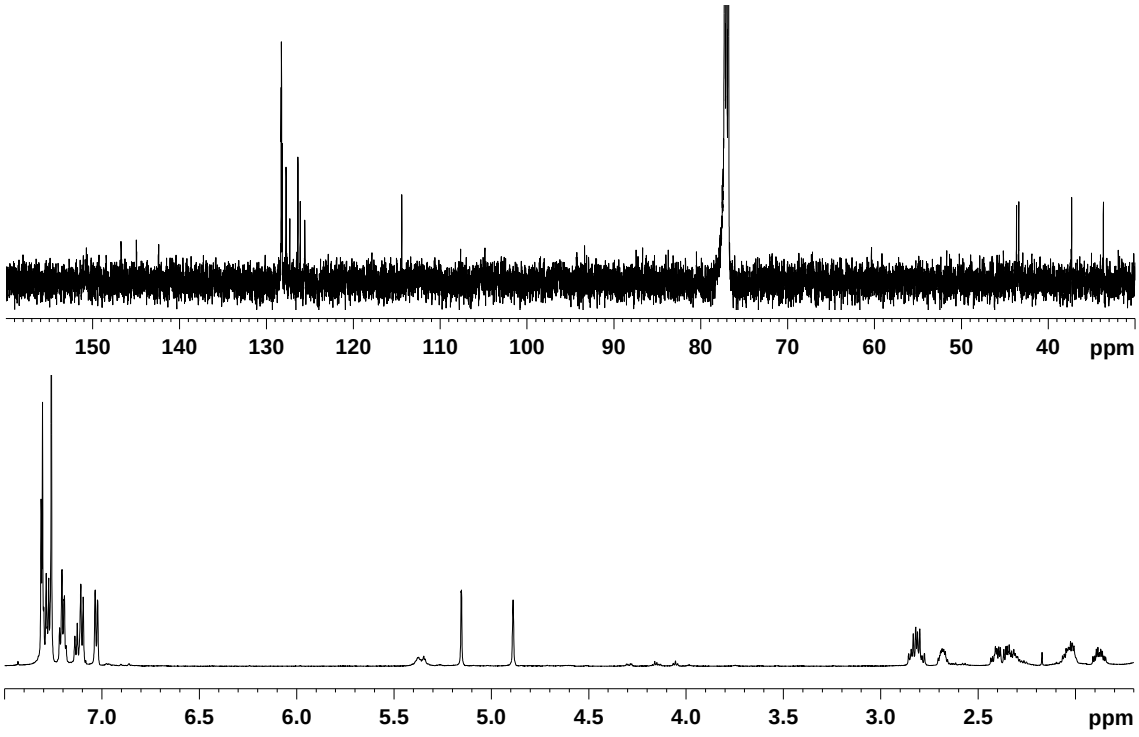

Figure 5.6: ^1H ($CDCl_3$, 600 MHz, bottom) and ^{13}C ($CDCl_3$, 150 MHz, top) NMR spectra obtained for **5.1**.

Simulations and iterations produced *via* WIN-DAISY have successfully established the coupling constants and conformations of fluorine and phosphorous containing compounds whose ^{1}H NMR spectra are complicated due to the additional splitting produced by these nuclei.[221–223] The spectrum simulation aspect of WIN-DAISY calculates energy levels using the time-independent Schroedinger equation.[81] For a fragment to be simulated, the total spin values, chemical and magnetic equivalences, in addition to fragment factorising are used to build up the Hamilton matrix.[81] Fragment factorising helps to reduce the calculation time for simulations and iterations by splitting the large spin system into smaller fragments which are not interacting with each other through coupling. The fragment factorising process leads to the running of a series of smaller, simpler simulations to produce the composite simulation of the total spin system. To assist in identifying the structural fragments which produced the complicated pattern of peaks in the aromatic region (δ_H 7.00 – 7.35) of the ^{1}H NMR spectrum, this region was processed by defining integrations, picking peaks, and determining multiplet couplings before loading the data into WIN-DAISY. Through the use of the integration and multiplet data WIN-DAISY intuitively divided the aromatic region into four fragments. The simplest of these fragments was a singlet resonating at δ_H 7.26 consistent with the $CDCl_3$ solvent peak. The other three fragments each contained five spin systems divided into three groups *i.e.* each fragment possessed a C2 symmetry resulting in chemically equivalent protons. With this information entered into WIN-DAISY a simulation was run to produce a spectrum of the complete spin system as well as subspectra corresponding to the factorised fragments.

Once this simulation was completed, WIN-DAISY was used to perform a series of iterative calculations in order to establish a more accurate set of resonant frequencies, line widths and scalar coupling constants.[81] Figure 5.7 depicts the aromatic region (6.95 – 7.40 ppm) of these iterated subspectra and the complete spin system alongside the original ^{1}H NMR spectra obtained for **5.1**. The simulated spectrum of the complete aromatic spin system, along with the $CDCl_3$ solvent is a good match to the original spectrum, and the subspectra of the individual fragments indicate the presence of three distinct aromatic systems which do not interact with each other *via* ^{1}H scalar coupling. There is a similarity in the subspectra in Figure 5.7(c) and (d) where the frequencies and scalar couplings were confirmed through the WIN-DAISY iterations to be δ_H 7.10 (2H, d, *J* = 7.6 Hz), 7.29 (2H, dd, *J* = 7.6, 7.4 Hz), and 7.20 (1H, t, *J* = 7.4 Hz) and δ_H 7.03 (2H, d, *J* = 7.6 Hz), 7.20 (2H, dd, *J* = 7.6, 7.5 Hz), and 7.13 (1H, t, *J* = 7.5 Hz) respectively which is indicative of two monosubstituted phenyl moieties. The third subspectra seen in Figure 5.7(b) appears to be made up of a doublet integrating to four protons, and a complex multiplet integrating to a single proton. This subspectra is markedly different from those relating to the two monosubsituted phenyl fragments. Curiously, the observed coupling constants measured directly from the original ^{1}H NMR spectrum were *J* = 4.1 Hz for both the doublet and the multiplet, which is unusually small for vicinal coupling in a planar aromatic system.[80,224] However, inspection of the

frequencies and scalar couplings calculated through WIN-DAISY iteration of this fragment showed very different values *viz.* δ_H 7.31 (2H, J = 8.6 Hz), 7.31 (2H, J = 8.6, 8.2 Hz) and 7.27 (1H, J = 8.2 Hz) which would once again indicate a monsubstituted phenyl moiety. An explanation for the unusual and unexpected splitting pattern observed for the third phenyl group would be the occurrence of second order virtual coupling. Second order coupling will occur when the difference in the chemical shifts of the proton nuclei ($\Delta\nu$ in Hz) are comparable in magnitude to the coupling constants between them (J in Hz). That is to say that if $\Delta\nu/J$ is smaller than five, second order coupling will begin to affect the appearance of the spectra, initially through the production of unsymetrical multiplets which appear to "lean" towards each other.[80] The simulated spectra in Figure 5.7b) and c) illustrate slight leaning as a result of second order coupling effects, however, the splitting patterns expected for monosubstituted phenyl systems are still recognisable from these spectra. As $\Delta\nu/J$ becomes smaller the effect of second order coupling will be more prominent and can result in additional resonance peaks that cannot be explained by simple first order coupling rules. Virtual coupling is when the lines produced through the effect of second order coupling suggests an apparent coupling of protons which are not actually vicinally coupled.[80,225–228] To be more specific, second order virtual coupling will usually occur in a three spin system such as ABX, where spins B and X are coupled, the J_{ax} is zero or near zero and the chemical shifts of A and B are not only very similar, but they are strongly coupled to each other, *i.e.* $J_{ab} > \Delta\nu_{ab}$. Under these conditions spins A and B will act as a single unit, and will result in apparently false coupling constants and more complex splitting in spin X.[80,225,226] Due to the dependence on a very small difference in the chemical shifts of two coupled protons, this second order coupling phenomenon is less likely to occur when the spectrum is measured with a higher frequency spectrometer as the resolution of chemical shifts (in Hz) is improved.[226] The use of more powerful magnets with higher frequencies in modern NMR based organic structure elucidation has meant that virtual coupling is not as commonly observed or reported.[229–233] Virtual coupling may also affect the ^{1}H NMR spectra of heteronuclear systems for example in organic phosphines and phosphites.[224,226,234]

In the present system, involving the third phenyl ring in **5.1**, there are not three spins, as explained above, but rather five spins and therefore the ortho, meta, para terminology will be used instead. In this phenyl system the ortho and meta proton resonances are not chemically equivalent, however they coincidently have near identical resonant frequencies, and so appear to be magnetically equivalent. Further, these ortho and meta protons are strongly coupled to each other and as a result the four protons appear to act as one unit. Virtual coupling of this 4H unit to the para proton produced the pentet (δ_H 7.27, 1H) and a doublet (δ_H 7.31, 4H) seen in Figure 5.7a) and d), even though no actual coupling occurs between the ortho and para protons. The observed coupling constant of 4.1 Hz is an average to the meta (J = 8.2 Hz) and para (J = 0 Hz) couplings.

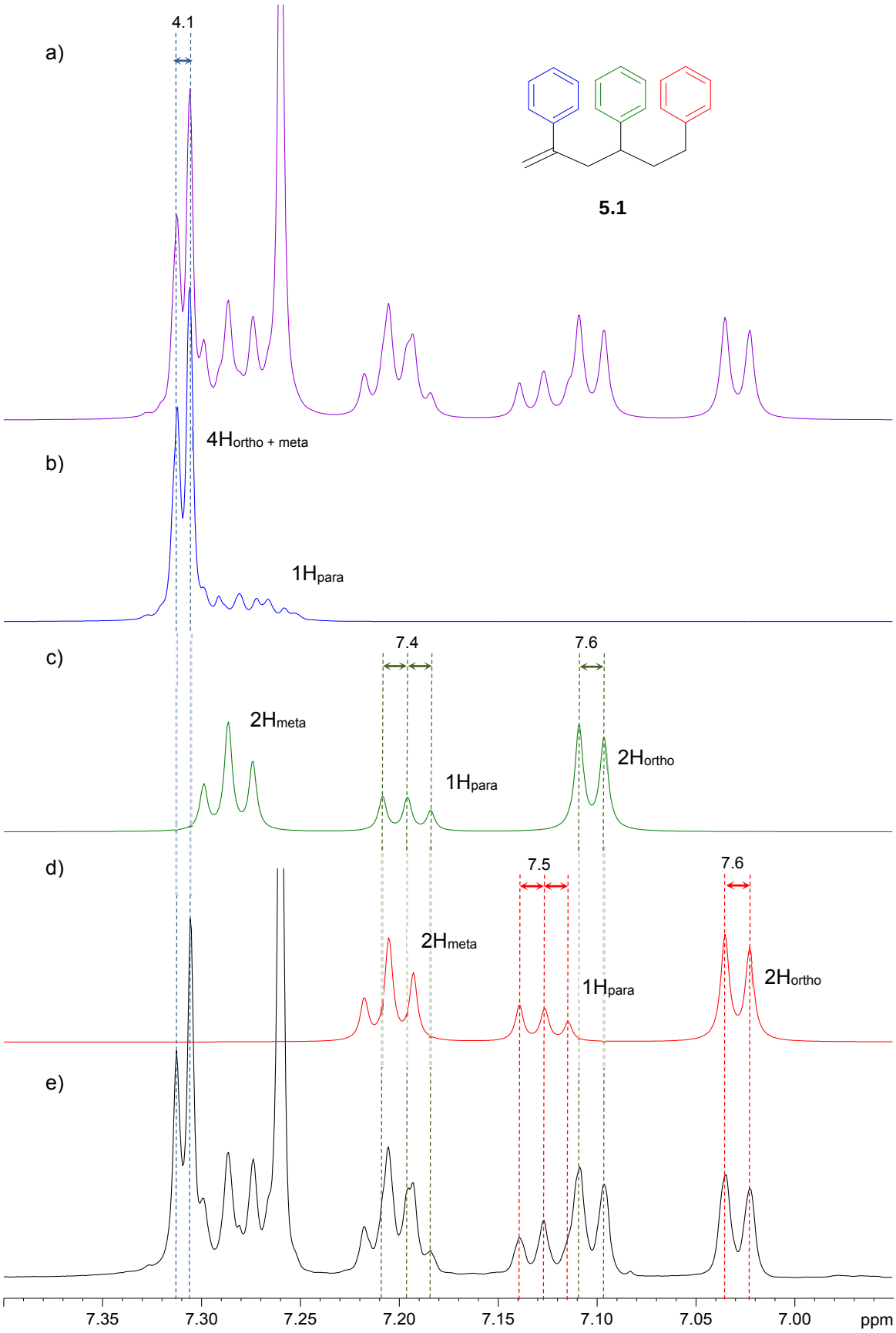

Figure 5.7: Aromatic region (δ_H 6.95-7.40) of a) WIN-DAISY simulation of the complete spin system along with b), c) and d) the simulated subspectra of the three phenyl groups and e) ^{1}H NMR (600 MHz, $CDCl_3$) of **5.1**.

Table 5.1: ^{1}H ($CDCl_3$, 600 MHz), ^{13}C ($CDCl_3$, 150 MHz) and 2D NMR data obtained for **5.1**.

Position	δ_C ppm	δ_H ppm (int., mult., *J*/Hz)	gHMBC[a]	COSY
1	114.4	5.15 (1H, s)	C-2, C-3, C-1'	H-1b
		4.89 (1H, s)	C-2, C-3	H-1a, H-3a, H-3b
2	141.1	-	-	-
3	43.4	2.84 (1H, dd, 14.2, 7.6)	C-1, C-2, C-4, C-5, C-1', C-1''	H-1b, H-3b, H-4
		2.79 (1H, dd, 14.2, 7.2)	C-1, C-2, C-4, C-5, C-1', C-1''	H-1b, H-3a, H-4
4	43.6	2.68 (1H, dtd, 9.8, 7.3, 4.6)	C-3	H-3a, H-3b, H-5a, H-5b
5	37.3	2.02 (1H, m)	C-6, C-1''	H-4, H-5b, H-6a, H-6b
		1.88 (1H, dtd, 13.6, 9.8, 5.3)	C-4, C-6, C-1'', C-1'''	H-4, H-5a, H-6a, H-6b
6	33.6	2.40 (1H, m)	C-4, C-5, C-1''', C-2'''/6'''	H-5a, H-5b, H-6b
		2.34 (1H, m)	C-4, C-5, C-1''', C-2'''/6'''	H-5a, H-5b, H-6a
1'	146.7	-	-	-
2'/6'	126.4	7.31 (2H, d, 4.1[b] 8.6[c])	C-2, C-4'	-
3'/5'	128.3	7.31(2H, d, 4.1[b] / 8.6[c], 8.2[c])	C-1'	H-4'
4'	127.3	7.27 (1H, pent., 4.1[b] / 8.2[c])	-	H-3'
1''	145.0	-	-	-
2''/6''	127.7	7.10 (2H, d, 7.6)	C-4, C-4''	H-3''
3''/5''	128.3	7.29 (2H, dd, 7.6, 7.4)	C-1'', C-3''/5''	H-2'', H-4''
4''	126.1	7.20 (1H, t, 7.4)	C-2''/6''	H-3''
1'''	142.4	-	-	-
2'''/6'''	128.3	7.03 (2H, d, 7.6)	C-6, C-4'''	H-3'''
3'''/5'''	128.2	7.20 (2H, dd, 7.6, 7.5)	C-1''' C-3'''/5'''	H-2''', H-4'''
4'''	125.6	7.13 (1H, t, 7.5)	C-2'''	H-3'''

[a] HMBC correlations are from proton(s) stated to indicated carbons

[b] Observed coupling constants

[c] Calculated coupling constants

The use of WIN-DAISY confirmed that **5.1** consisted of three monosubstituted phenyl groups which accounted for 12 of the 13 degrees of unsaturation. The ability to create simulations of the individual phenyl moieties allowed for the assignment of chemical shifts and coupling constants in this complicated region of the ^{1}H NMR spectrum and greatly facilitated the subsequent interpretation of 2D NMR spectra. Table 5.1 reports the chemical shifts and coupling constants established through WIN-DASIY simulations and iterations as well as the relevant apparent coupling constant values observed because of the effect of virtual coupling.

Correlations observed in a two-dimensional COSY NMR experiment (Table 5.1) from the methylene protons [δ_H 2.34 (m) and 2.40 (m)] to the methylene protons [δ_H 2.79 (dd, *J* = 14.2, 7.2 Hz) and 2.83 (dd, *J* = 14.2, 7.6 Hz)], as well as the long range COSY correlations between the latter methylene protons to the olefinic protons [δ_H 4.89 (s) and 5.15 (s)] indicated the presence of a contiguous six carbon chain with three substituents.

The phenyl moieties established from the WIN-DAISY simulation were then positioned along this six carbon chain based on the ^{3}J bond gHMBC correlations observed between ortho phenyl protons at δ_H 7.31, 7.10 and 7.03 and the carbon resonances at δ_C 141.1 (C_q), 43.6 (CH) and 33.6 (CH_2) respectively, placing the phenyl groups at positions 2, 4 and 6 of the carbon chain (Table 5.1 and Figure 5.8). Compound **5.1** was therefore elucidated as a styrene trimer, 2,4,6-triphenyl-1-hexene. Although this compound is a known synthetic compound, and oligomer commonly produced in the manufacturing and degradation of polystyrene plastics only the unassigned ^{13}C NMR data has been previously reported,[235] and this appears to be the first time that the ^{1}H and ^{13} NMR data of **5.1** has been fully assigned.

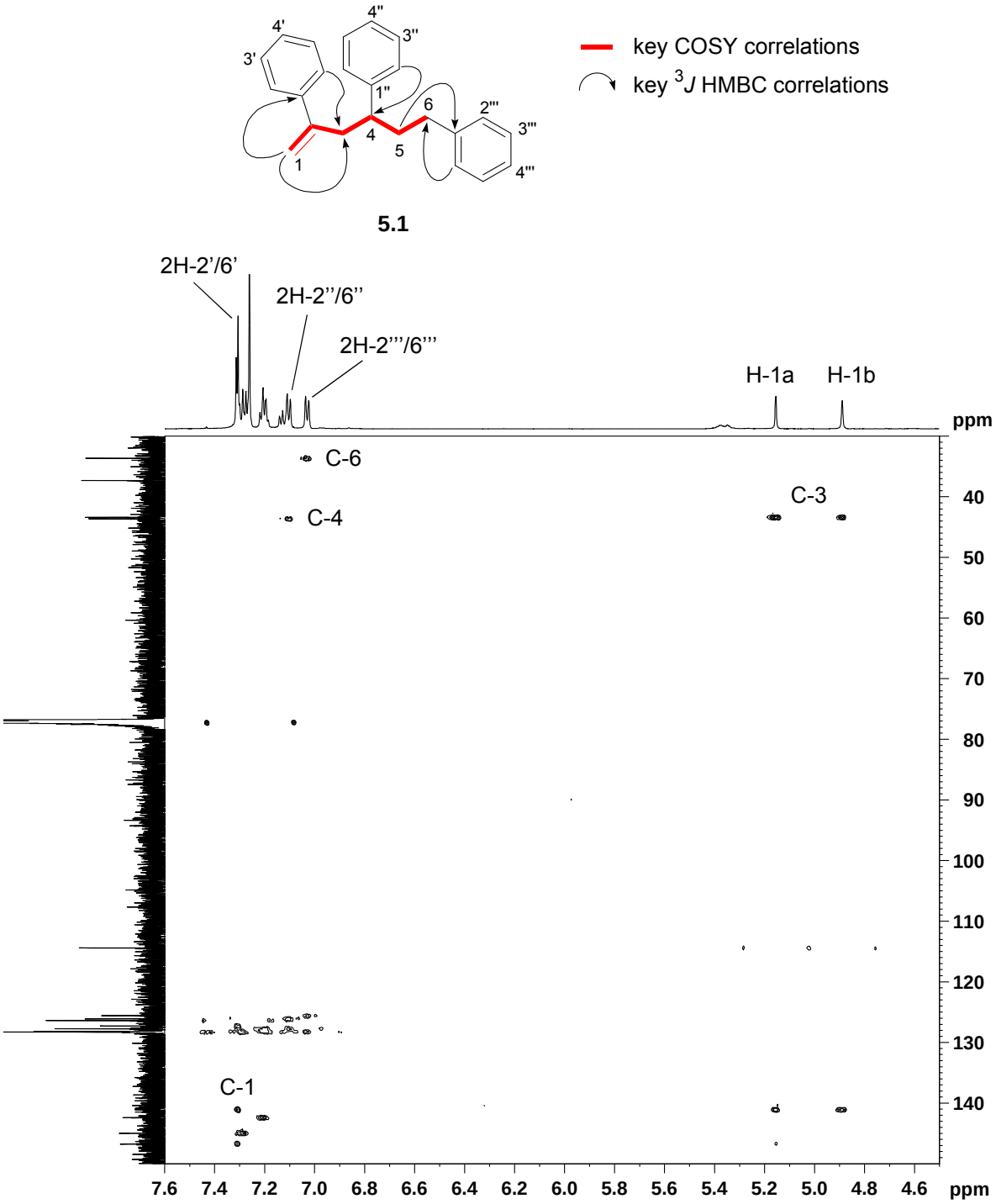

Figure 5.8: A region of the gHMBC spectrum (F1 = δ 4.5-7.6 ppm; F1 = δ 30-150 ppm) of the gHMBC spectrum ($CDCl_3$; 600 MHz) of **5.1** illustrating the three bond ^{1}H-^{13}C coupling correlations. The accompanying structure shows the key gHMBC and COSY correlations used to elucidate the structure of **5.1**.

5.3 The possible origin of 2,4,6-triphenyl-1-hexene (5.1)

The initial fractionation of the crude *A. marinense* and *Clavelina* sp. extracts utilised poly(styrene-divinylbezene) (PSDVB), a reverse-phase stationary phase also know by the trade name Diaion HP-20. The isolation of a styrene oligomer from an extract that was in contact with a styrene based adsorption resin meant that the possibility that **5.1** was an artefact of the isolation process could not be ignored. However, the use of HP-20 in the initial large scale fractionation of crude marine extracts has been standard practice in our research group for several years, and to date there have been no other cases where the styrene oligomer **5.1** was isolated during any of the chromatography procedures which utilised this resin.[236]

The numerous cross-linkages in the polymeric structure of PSDVB make it a porous support onto which organic compounds of varying polarity are able to be adsorbed. The absence of polar sites in PSDVB ensures the separation of even the most polar organic compounds without any threat of these metabolites irreversibly binding to the resin.[237,238] PSDVB can be used successfully throughout a large pH range (pH 1-13), it is stable in most organic solvents and can withstand very ionic solutions allowing for a variety of applications.[238]

The general technique employed to initially adsorb all the non-polar, semi-polar, and polar metabolites, from the crude extract onto the PSDVB resin, is known as cyclic loading and was first developed in 1996 by West and Northcote, during the fractionation of crude extracts of the New Zealand sponge *Mycale hentscheli*.[238] A typical PSDVB chromatography column is depicted in Figure 5.9. The PSDVB resin is initially primed by washing with water to remove any fine resin particles, followed by three column volumes of the polar, water miscible solvent (normally the solvent used in extraction, *i.e*. methanol or acetone). In the process of cyclic loading (Figure 5.9) an acetone or methanol solution of the crude extract is initially loaded onto the column and allowed to pass slowly through the PSDVB resin, ensuring maximum interaction and therefore adsorption of the non-polar metabolites contained in the extract onto the PSDVB beads.[238] The eluent is collected and diluted with water to approximately 50% of the original organic concentration and passed through the same column again, with metabolites of mid-polarity adhering to the PSDVB resin during this second loading.[239] This process of dilution and re-loading is continued, allowing more polar metabolites to be sequentially adsorbed until the “organic” concentration of eluent collected has been diluted with water to 12.5% of the original extract. At this stage, the eluent will often appear much paler than the crude extract loaded initially, indicating that majority of the compounds of interest have been adsorbed on the PSDVB resin beads.[239]

Figure 5.9: PSDVB column chromatography illustrating the steps involved in the cycling loading of an organic extract.

Once the PSDVB column has been loaded, it is washed with three column volumes of water to remove any inorganic salts (seawater contains *ca.* 3.5% sodium chloride). The column is then eluted with aqueous acetone or methanol, in aliquots of decreasing polarity.[239] This elution regime will result in the most polar metabolites eluted first and the least polar metabolites last. Usually, the highest proportion or biologically active metabolites are found in the mid-polar fractions and the sterols and fatty acids occur in the non-polar fractions with the organic salts, sugars and proteins emerging in the polar fractions.[238]

The process of cyclic loading of the extract is time consuming and exposes the HP-20 beads to a large volume of solvents. The two most common solvents used for cyclic loading are methanol and acetone, and so the effect of dichloromethane on the stability of the HP-20 beads was of interest to us. The initial extraction of *A. marinense* utilised both methanol, and dichloromethane, and although the dichloromethane extract was concentrated *in vacuo* before the process of cyclic loading onto the HP-20, there was still the possibility that some of

the dichloromethane remained in the extract and was loaded onto the HP-20 column. In order to investigate whether the exposure to dichloromethane could result in the degradation of the HP-20 resin to produce the styrene oligomer **5.1** two experiments were carried out.

The first experiment involved grinding a portion of HP-20 beads to form a fine powder, which was subsequently steeped in dichloromethane for 48 hours with intermittent periods of sonication in an attempt to disrupt the styrene based polymer and increase any effect which dichloromethane may have on degradation of the polystyrene. The powder was then filtered, and the filtrate dried under reduced pressure and a ^{1}H NMR spectrum acquired (Figure 5.10b). The ^{1}H NMR spectrum produced was inconclusive and contained only very weak peaks, of a similar intensity to the satellite peaks produced by the solvent ($CDCl_3$), which were not consistent with **5.1**.

The second experiment attempted to replicate the initial process of cyclic loading, without the presence of the ascidian extract. The volumes of HP-20 resin, and solvent used in this experiment were the same as those used for the *A. marinense* extract. All solvent used in extraction and fractionation of *A. marinense* were HPLC grade, thus the same level of purity of the solvents was used throughout this experiment. Since the ascidian was extracted with both methanol and dichloromethane, it is unclear how much dichloromethane may have still been present in this crude extract, after concentration, a 50 mL portion of dichloromethane was added to the methanol (500 mL) and then loaded onto the HP-20 resin. This solvent mixture was cyclic loaded onto the HP-20 column over the course of a week to ensure that the HP-20 was exposed to the methanol/acetone/dichloromethane mixture for an extended time. The HP-20 beads where then washed with 100% acetone as this was the solvent system within which the styrene oligomer **5.1** appeared. The eluent produced was concentrated *in vacuo* and analysed by ^{1}H (Figure 5.10c) and ^{13}C NMR. Although there is some noise in the aromatic regions of both the ^{1}H and ^{13}C NMR spectra, there were no distinct resonances that were consistent with corresponding resonances in the ^{1}H NMR spectrum of the 100% acetone HP-20 fraction of *A. marinense*.

The results of the two experiments indicated that exposure of HP-20 resin to dichloromethane did not produce any significant amounts of the styrene oligomer **5.1**. However, it is still unlikely that **5.1** could be considered to be present in the ascidian, and unequivocally not a product of the chromatographic medium. Fortuitously, a portion of the crude extract of *A. marinense* that had not been exposed to HP-20 resin was still available for ^{1}H NMR analysis (Figure 5.10d). However, although signals were evident in the aromatic region of the ^{1}H NMR spectrum from this extract they were not directly comparable with those observed in the ^{1}H NMR spectrum of **5.1** and the direct comparisons were deemed inconclusive.

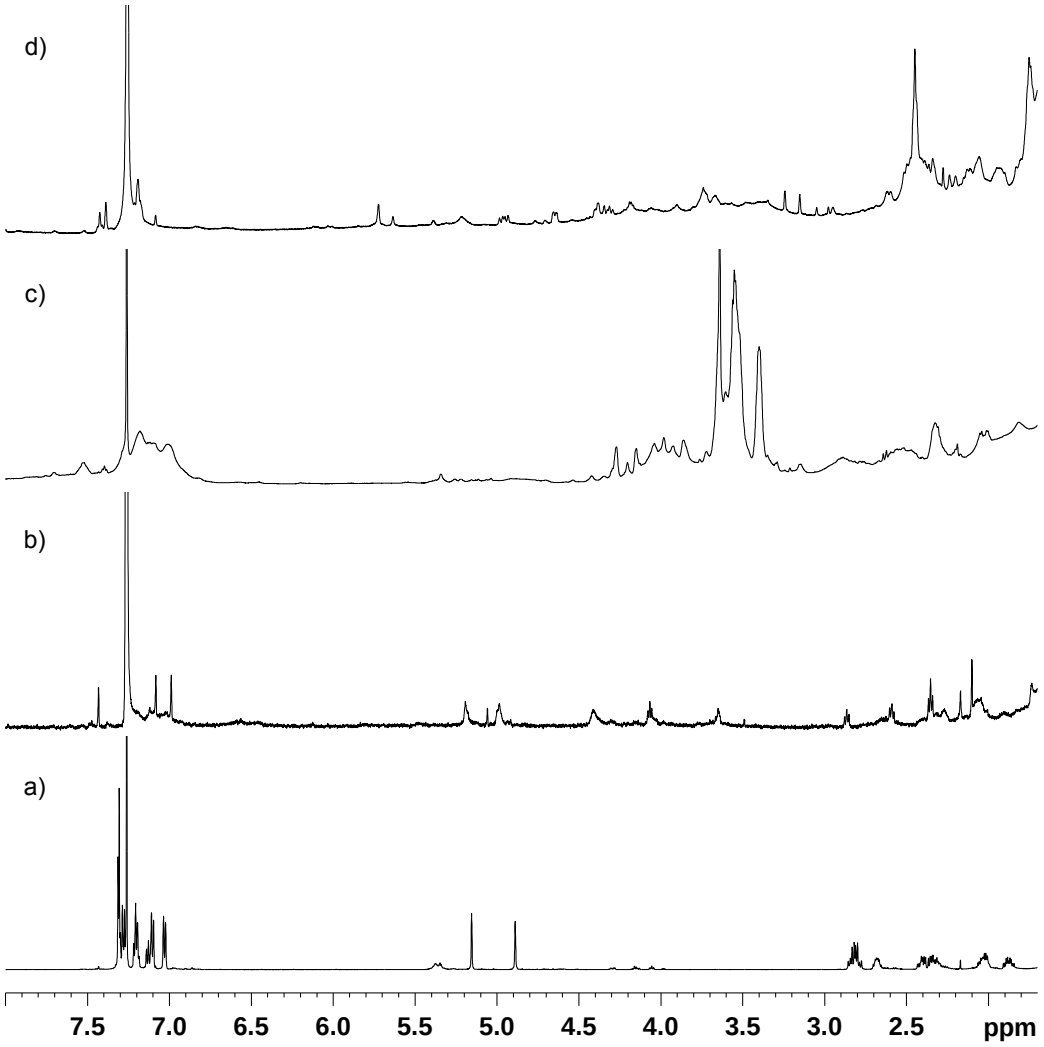

Figure 5.10: ^{1}H NMR (600 MHz) spectra of (a) compound **5.1** isolated from *A. marinense*; (b) HP-20 powder exposed to dichloromethane; (c) HP-20 exposed to the cyclic loading process without *A. marinense* extract; and (d) crude extract of *A. marinense* prior to HP-20 fractionation.

5.4 The presence of styrene oligomers in the marine environment

Polystyrene, a plastic polymer manufactured from styrene, is widely used in modern society appearing in numerous forms including building materials, packaging, containers, and disposable cutlery.[240] Along with other plastics, polystyrene is often not correctly disposed of and is known to accumulate in and pollute coastal waters. In 2012 there was an estimated 280 million tonnes of plastic goods manufactured worldwide and whilst there are promising policies in place to encourage correct disposal and recycling of plastic products, only 130 million tonnes was reported to be correctly disposed in landfills.[241,242] Within South Africa[243] and the world, there is a wealth of research dedicated to establishing the extent of coastal

and marine pollution caused by plastic waste as well as developing strategies to combat this growing threat.[243–249] Bulk plastic marine pollution has been shown to have many adverse effects to marine ecosystems where they can persist for centuries and may be ingested by, or entangle wildlife.[241,248]

The oligomers of bulk plastics such as the styrene monomer (**5.2**), dimer (**5.3**) and trimer (**5.1**) are known to have toxic effects on biological systems where they may mimic hormonal activity however the polystyrene polymer is regarded as inert and of no direct threat.[250,251] This is a somewhat naïve belief as bulk polystyrene resins has been found to contain levels of unreacted styrene oligomers which would be released slowly from the plastic materials. Possibly the most well-known example is the potentially carcinogenic effects of oligomers released from polystyrene food containers which have been found interfere with estrogenic biological pathways.[250,251] This contamination of unreacted oligomers in bulk polystyrene is a possible route for these monomer, dimers and trimers to enter the marine environment.[252]

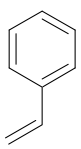

5.2

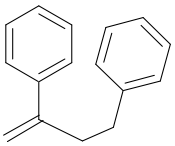

5.3

Another likely route is through the degradation of plastic waste pollution. The synthetic polymer structure of plastics ensures that they are durable materials which will degrade over long periods of time, or under fairly harsh physical conditions. However, in the marine environment these lightweight, floating plastics are exposed to high levels of sunlight, and wave action which facilitates fragmentation to produce microplastics.[248,253] Microplastics are classified as pieces of plastic debris with a diameter <1 mm, and may enter the marine environment through atmospheric and general marine degradation process, as well as a more direct route from sewage waste waters that contain microbeads, a common abrasive additive to cosmetics such as exfoliating face washes.[253,254] In recent years there has been a significant research focus on the occurrence and influence of microplastics in the marine environment, including the consideration of environmental and ecological effects due to harm caused not only by the microplastic particles, but also the potentially toxic compounds that can be adsorbed onto the particles and subsequently passively migrated through the ecosystem.[252,254,255] Microplastics have been found to contaminate shorelines,[244,256] plankton samples[248,257] and deep sea sediments[258] especially in the waters around Europe and Asia. Microplastics have also been found to be ingested by a number of animals through various feeding mechanisms, including seabirds, fish, mussels, amphipods, lugworms, barnacles, polycheates, echinoderms, and bryzoans.[244,246,248,249,253,254,259,260] The current research into microplastics appears to be mostly general in focus and is not focussed on any individual

polymer or oligomer, however in the case of the laboratory studies into the ingestion of microplastics by the mussel *Mytilus edulis* the microplastic beads used were polystyrene.[259] Since there is evidence to show that fragmented plastic debris is wide spread in the marine environment, and may be ingested by various marine biota, it is reasonable to suggest that the oligomers derived from plastic debris, like polystyrene, may persist in the marine environment as well.[252]

The presence of styrene oligomers in the marine environment has been investigated by Saido and coworkers.[261–265] These studies have assessed the presence of styrene monomer, dimer, and trimers in sea water and sand samples from numerous locations along the coastlines of the North-West Pacific Ocean[263,264] and more recently the coastlines along the North-East Pacifiic ocean including Hawaii.[265] In their studies Saido and coworkers detected **5.1**-**5.3** using selective ion monitoring gas chromatography-mass spectrometry (SIM-GC-MS).[263–265] All three oligomers were found at costal locations throughout the north Pacific, with the styrene trimer (**5.1**) commonly being detected in the highest concentrations out of the three oligomers.[263–265]

5.5 Conclusion

Although there was not enough of **5.1** available for cytotoxic evaluation against breast cancer cells it is highly unlikely that this relatively simple aromatic compound, found in only the 100% acetone fraction from the HP-20 column chromatography, was responsible for the cytotoxicity of the *A. marinense* and *Clavelina* sp. extracts. Despite the tenuous possibility that the styrene oligomer, **5.1**, isolated from *A. marinense* and *Clavelina* sp. may be a marine pollutant concentrated by the filter feeding ascidians it is more likely that this compound is an isolation artefact arising from elution of HP-20 polystyrene resin with copious volumes of solvent. However, since we cannot clearly show the presence of **5.1** in the crude extracts, or establish unequivocally that **5.1** is an artefact of isolation, the origin of this compound is still unknown.

Chapter Six:
Experimental

6.1 General Experimental Procedures

6.1.1 Analytical

NMR spectra were acquired using standard pulse sequences on Bruker Avance 400 MHz and 600 MHz Avance II spectrometers. Chemical shifts are reported in ppm and referenced to residual solvent resonances ($CDCl_3$ δ_H 7.26, δ_C 77.0, CD_3OD δ_H 3.34 δ_C 49.9, DMSO (*d*-6) δ_H 2.50 δ_C 39.5). Coupling constants are reported directly from the NMR spectra unless otherwise stated and corresponding coupling constants have not been matched. Infra-red spectra were recorded on a Perkin-Elmer Spectrum 2000 FT-IR spectrometer and Digilab FTS 3100 Excalibur HE Series with compounds as films (neat) on NaCl discs. Mass spectrometry of isolated compounds were performed on a Waters API Q-TOF Ultima instrument using electron-spray ionisation (ESI) or in the case of GC-EI-MS an Agilent 6890N GC and Agilent 5975B MS were used in electron ionisation (EI) positive mode, at the University of Stellenbosch Central Analytical Facility.

6.1.2 Chromatography involved in the isolation of ascidian metabolites

General laboratory solvents were distilled from glass before use. Analytical normal phase thin layer chromatography was performed on DC-Plastikfolien Kieselgel 60 F_{254} plates. Plates were viewed under UV light (254 nm) and developed by spraying with 10% H_2SO_4 in MeOH followed by heating. HP-20 beads used were manufactured by Diaion and supplied by Supelco. Open column chromatography was performed using Discovery® DSC-DIOL supplied by Supelco, and flash chromatography was performed using Kieselgel 60 (230-400 mesh) silica gel. Normal phase DIOL semipreparative HPLC separations were performed on a Machery-Nagel VP 250/10 Nucleosil 100-7 OH column using an Agilent 1100 Series quad pump and an Agilent 1100 diode array detector. Reversed-phase semi-preparative HPLC separations were performed on a Phenomenex Onyx Monolithic Semi-PREP C-18 column using an Agilent 1100 Series quad pump and an Agilent 1100 diode array detector, or Waters 1500-Series isocratic pump with Waters 2414 Refractive Index Detector.

6.2 Chapter Two Experimental

6.2.1 MarinLit database survey

The marine chemical literature database, MarinLit[76], was used to establish the chemistry associated with the genera of ascidians common to South Africa. Ascidian genera were entered into MarinLit using all known synonyms or previous taxonomic classifications. The resulting literature was classified as either “MNP isolation papers” when initial isolation and

elucidation of ascidian marine natural products (MNP) were reported, or "non-MNP isolation papers" when subsequent studies or reviews on the clinical, biological, ecological, synthetic, or stereochemistry or absolute configurations of ascidian metabolites were documented. The isolated natural products observed from the MarinLit genera searches were classed into two subsets, namely "nitrogenous compounds" and "non-nitrogenous compounds".

6.2.2 ^{1}H-^{15}N HMBC NMR Screening Protocol

Small representative samples (~ 2 g wet mass) of each of the 20 selected colonial ascidians were lyophilised and subsequently crushed to form a fine powder. Each of the powdered ascidian specimens were sequentially extracted with 100% MeOH followed by 100% CH_2Cl_2. Samples were concentrated *in vacuo* and subsamples of approximately 20 mg were made in DMSO (d6) for ^{1}H-^{15}N HMBC NMR experiments. Standard common nuclei gHMBC pulse program was used (Bruker Topspin hmbcgplpndqf[81]) excepting that CNST2 was changed to 90 Hz and the first and third gradient parameters were corrected to 70% and 50.1% respectively.[81] A wide sweep width of 650 ppm was set and centred at O2= 200 ppm.

6.2.3 Preparation of samples for total metal analysis and screening for organometallics and metal chelates using LC-ICP-MS/ESI-MS

All glassware and laboratory equipment used in the preparation of samples and extracts for metal analysis and LC-ICP-MS/ESI-MS screening were acid washed using 10% HNO_3 and subsequently rinsed using MilliPore® water. HPLC grade solvents were used and to prevent contamination solvents and samples were covered at all times. Where possible the transfer of samples and solvents was carried out without the use of pipettes in an attempt to minimise contamination.

For each of the 25 ascidian species three representative samples (each containing all tissues, etc.) of least 1.5 g fresh weight were taken and placed in separate acid-washed and pre-weighed falcon tubes and lyophilised. The weights of the dried triplicate samples were recorded and the falcon tubes sealed and stored at -20ºC until total metal analysis.

Extracts of each species of ascidian (~15 g wet mass) were made using HPLC grade MeOH and CH_2CH_2. Extractions were carried out in the normal way excepting that all glassware and tools used were acid washed and an iced water bath was used when sonicating the material. On concentration the extracts to dryness using a rotary evaporator an acid washed splash head adaptor was used which was further heated using a heat gun on a low setting to ensure that no water vapour within the shaft or adaptor condensed and contaminated the extract.

The crude ascidian extracts were stored at -20°C until digestion and ICP-MS analysis or LC-ICP-MS/ESI-MS screening.

The spent ascidian material remaining after the sequential extraction process was lyophilised and distributed between three separate acid-washed and pre-weighed falcon tubes and these samples were made available for total metal analysis is the need arose.

Four control samples were prepared by extracting the equivalent weight of Millipore water instead of organism and otherwise treat as if extracting an organism. Control samples were kept at -20ºC until further analysis.

6.2.4 Total Metal Concentration Analysis (ICP-MS)

Digestions of each of the dried ascidian samples (100 mg) and the organic extracts (50 mg) were carried out by adding conc. HNO_3 (1 mL, Fluka TraceSELECT® >69.5%) and leaving overnight before adding a solution of H_2O_2 (2 mL, Fluka puriss. p.a. ≥30%) and microwaving (CEM, 5 min at 50°C, 5 min at 75°C and 30 min at 95°C). After digestion each sample was made up to 25 mL with Millipore water, and stored at 4°C until ICP-MS analysis. Reference digests made were whole egg, IAEA 140, TORT-2, DOLT-4 and DORM-3. Eight calibration standards were made incorporating all the metals investigated, at varying concentrations. Since high concentrations of iron and vanadium were expected in the ascidian samples the seventh and eighth calibration standards were doped with these metals to ensure accurate measurement at high concentrations.

ICP-MS analysis of samples and standards were carried out on an Agilent 8800 triple quad ICP-MS, with micro-flow PFA nebuliser and Pt cones. Selected metals detected were Li, Be, B, Rb, Sr, Mo, Cd, Sn, Sb, Cs, Ba, Pb, U, Al, V, Cr, Mn, Fe, Co, Ni, Cu, Zn, As, and Se. The ICP-MS data for each metal were standardised to the signal for ^{73}Ge (internal standard).

6.2.5 Speciation Analysis (LC-ICP-MS/ESI-MS)

Methanolic solutions of the organic extracts of 13 ascidian species (50 mg/µL) were entered into speciation studies using an Agilent 1100 series HPLC with in-line degasser, quaternary pump, autosampler, column compartment, and single wavelength UV detector for LC-ICP-MS/ESI-MS analyses. Chromatography was carried out by injecting 100 µL of sample onto an analytical C18 Waters SunFire column with a solvent flow rate of 1 mL/min and gradient profile of 100% H_20 to 100% MeOH over 20 mins. HPLC solvents which were used for chromatography with made up with 0.1% formic acid (FA). After passing through the UV detector a passive splitter directed approximately 80-85% of the eluent flow to the ESI-MS

and 15-20% of the eluent flow to the ICP-MS. ESI-MS was performed on a Thermo Orbitrap high resolution electrospray ionisation mass spectrometer whilst ICP-MS was performed on an Agilent 8800 triple quad ICP-MS, with micro-flow PFA nebuliser and Pt cones, and 7% O_2 reaction gas. Elements detected were V (*m/z* 51), Mn (*m/z* 55) Fe (*m/z* 57), Co (*m/z* 59), Cu (*m/z* 63), Zn (*m/z* 66), As (*m/z* 75), Se (*m/z* 77), Br (*m/z* 79), Mo (*m/z* 95) and I (*m/z* 127).

6.2.6 Extraction and isolation of Distaplia skoogi metabolites

The colony of *Distaplia skoogi* Michaelsen, 1934 was collected from a depth of 25m at the White Sands Reef, Algoa Bay, South Africa (34:00.436S, 25:43.296E), on 15 July 2004 and identified by Dr. S. Parker-Nance. The voucher specimen (SAF2004-030) preserved in 5% buffered formalin is kept at the South African Institute for Aquatic Biodiversity (SAIAB), Grahamstown, South Africa. Samples of *D. skoogi* were frozen immediately after collection in the field and kept at –18 °C until extracted.

The frozen ascidian colony (309.41 g wet mass) was lyophilised and then sequentially extracted with 100% MeOH followed by 100% CH_2Cl_2. The combined organic extracts were concentrated *in vacuo* and then subjected to liquid-liquid partitioning between EtOAc and H_2O. The combined EtOAc fractions were concentrated *in vacuo* to yield 1.11 g of extract. A 350 mg aliquot of the partitioned extract was purified further with normal phase HPLC (40% EtOAc/hexane) on a semi-preparative DIOL column to afford four fractions (Scheme 2.1). Fraction 2 was subjected to normal phase DIOL HPLC (60% CH_2Cl_2/hexane) followed by further normal phase DIOL HPLC (20% CH_2Cl_2/hexane) purification to yield 3.0 mg of 3,6-dibromoindole (**2.29**) and 2.2 mg of 6-bromo-3-chloroindloe (**2.30**). Fraction 3 was further purified using a small DIOL plug (10% EtOAc/hexane), and recrystallisation from hexane to afford 2.4 mg of 6-bromo-2-oxindole **(2.28)** as colourless needles (Scheme 2.1).

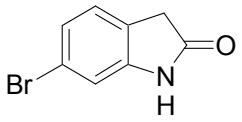

2.28

6-Bromo-2-oxindole (2.28): Colourless needles (hexane); mp 216 - 219 °C; IR (film) ν_{max} 3435, 1643, 1096 cm^{-1}; ^1H and ^{13}C NMR data see Table 2.2; ESIMS *m/z* 215 $[(M+H)^+]$ (10), 214 (100), 213 (10), 212 (97); HRESIMS *m/z* 211.9710 (calcd for $C_8H_7NO^{79}Br$ $[(M+H)^+]$, 211.9711, Δ 0.1 mmu).

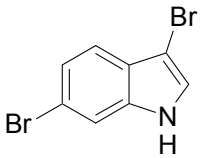

2.29

3,6-Dibromoindole (2.29): Colourless oil; IR (film) ν_{max} 3445, 1422, 1265, 1106, 895, 736 cm^{-1}; ^{1}H and ^{13}C NMR data see Table 2.3; EIMS *m/z* 276 [$(M-H)^-$] (48), 274 (100), 272 (49); HRESIMS *m/z* 271.8719 (calcd for $C_8H_4N^{79}Br_2$ [$(M-H)^-$], 271.8710, Δ 0.9 mmu).

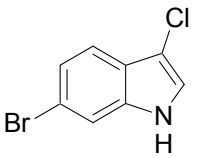

2.30

6-Bromo-3-chloroindole (2.30): Colourless oil; IR (film) ν_{max} 3445, 3055, 1265, 895, 737 cm^{-1}; ^{1}H and ^{13}C NMR data see Table 2.3; ESIMS *m/z* 232 [$(M-H)^-$] (28), 230 (100), 228 (78); HRESIMS *m/z* 227.9215 (calcd for $C_8H_4N^{79}Br\ ^{35}Cl$ [$(M-H)^-$], 227.9216, Δ 0.1 mmu).

6.2.6.1 Bioassay of 2.28 – 2.30

MDA-MB-231 breast cancer cells (ATCC HTB-26) were cultured in Dulbecco's Modified Eagle Medium (DMEM) supplemented with 5% (v/v) heat-inactivated FCS, 1 mM L-glutamine, 100 U/mL penicillin, 100 µg/mL streptomycin and 12.5 µg/mL amphotericin (PSA) at 37°C in a humidified 9% CO_2 incubator. The effect of the compounds on cell proliferation was assessed using the MTT assay (Roche) as previously described.[55,103] Cells were seeded at a density of 6000 cells per well into 96-well plates and incubated overnight, followed by treatment with a range of concentrations (0, 0.5, 5, 50, 250 and 500 µM) of the compounds or dimethyl sulphoxide (DMSO) vehicle control (0.02% v/v DMSO) for 96 hours and absorbance at 595 nm recorded using a Powerwave spectrophotometer (BioTek). The half maximal inhibitory concentration (IC_{50}) for each compound was calculated relative to the vehicle-treated control from a dose response curve (log concentration versus absorbance at 595 nm) using non-linear regression with GraphPad Prism 4 (GraphPad Inc.). Paclitaxel was included as a positive control (IC_{50} of 100 nM). All treatments were conducted in triplicate on each of the two plates.[55,103]

6.2.7 Extraction and isolation of **2.33** from Aplidium monile

The ascidian *Aplidium monile* Monniot, F., 2001 was collected by SCUBA from a depth of 12 - 15 m at Bell Buoy dive site (33° 58.998' S 25° 41.622' E), Algoa Bay, South Africa, in November 2011. The voucher specimen (TIC2011-032) preserved in 5% buffered formalin is kept at the South African Institute for Aquatic Biodiversity (SAIAB), Grahamstown, South Africa. The sample of *A. monile* was frozen immediately after collection in the field and kept at –18 °C until extracted.

The small scale MeOH/CH_2Cl_2 extraction of *A. monlie* (23.90 g) prepared for the metal analysis and LC-ICP-MS/ESI-MS screen was partitioned between CH_2Cl_2 and 70% aq. MeOH. The 676.0 mg MeOH partition was fractionated using a C-18 Sep-Pak® cartridge (Waters,10 g) and a step wise gradient to produce seven fractions (water, 10% $MeCN_{aq}$, 20% $MeCN_{aq}$, 40% $MeCN_{aq}$, 60% $MeCN_{aq}$, 80% $MeCN_{aq}$, and 100% MeCN) (Scheme 4.1 and Figure 4.6). The fourth fraction yielded 5.0 mg of **2.33**.

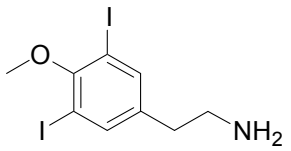

2.33

3,5-diido-4-methoxyphenethylamine (2.33): White amorphous solid; ^{1}H and ^{13}C NMR data see Table 2.4; HRESIMS *m/z* 403.9000 (calcd for $C_9H_{11}NOI_2$ [$(M+H)^+$], 403.9003 Δ 0.3 mmu).

6.3 Chapter Three Experimental

The procedure used to obtain the total metal analysis results using ICP-MS has been discussed in section 6.2.4 of this chapter. All statistical analyses were carried out using established tests within the Statistica 10 software package.

6.4 Chapter Four Experimental

The procedure used to obtain the total vanadium content of the Algoa Bay ascidians using ICP-MS has been discussed in section 6.2.4 of this chapter.

6.4.1 Isolation and elucidation of nucleosides from Aplidium monile

The ascidian *Aplidium monile* Monniot, F., 2001 was collected by SCUBA from a depth of 12 - 15 m at Bell Buoy dive site (33° 58.998' S 25° 41.622' E), Algoa Bay, South Africa, in November 2011. The voucher specimen (TIC2011-032) preserved in 5% buffered formalin is kept at the South African Institute for Aquatic Biodiversity (SAIAB), Grahamstown, South Africa. The sample of *A. monile* was frozen immediately after collection in the field and kept at –18 °C until extracted.

The larger scale extraction of *A. monile* (262.6 g wet mass) involved the sequential extraction with MeOH followed by CH_2Cl_2. Extractives of each solvent system were kept separate and concentrated to dryness under reduced pressure. Subsamples of the MeOH extract (~1 g) were fractionated using a C-18 Sep-Pak® cartridge (Waters,10 g) and a step wise gradient to produce seven fractions (water, 10% $MeCN_{aq}$, 20% $MeCN_{aq}$, 40% $MeCN_{aq}$, 60% $MeCN_{aq}$, 80% $MeCN_{aq}$, and 100% MeCN) (Scheme 4.1 and Figure 4.6). As discussed in section 6.2.7 of this chapter, the fourth fraction yielded 2,5-diiodotyrame **2.33**. The second fraction (10% $MeCN_{aq}$) was further purified using RP-HPLC with a Luna C18 column and an isocratic solvent system of 10% MeCN/H_2O (3 mL/min) to produce fractions 8-14. Fraction 12 was thymidine (**4.10**).

RP-HPLC using a C18 column and 10% MeOH/H_2O (4 mL/min) of fraction 11 produced fractions 15-22 where fractions 18 and 20 were nucleosides **4.11** and **4.13** respectively. Further RP-HPLC (C18, 5% MeOH/H_2O, 4 mL/min) of fraction 19 yielded **4.15**. RP-HPLC (C18, 10% MeOH/H_2O, 3 mL/min) of fraction 21 yielded fractions 29-31. Fraction 31 was an inseparable mixture of **4.17** and **4.40**.

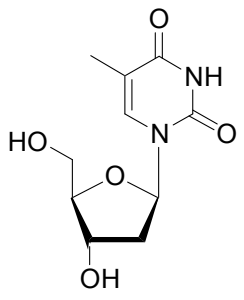

4.10

Thymidine (4.10): white amorphous solid; IR (film) ν_{max} 3464, 3403, 3237, 1692, 1640, 1619, 1474, 1421, 1266, 1092, 1054 cm^{-1}; ^1H and ^{13}C NMR data see Table 4.1; HRESIMS *m/z* 243.0988 (calcd. for $C_{10}H_{15}N_2O_5$ [$(M+H)^+$], 243.0981, Δ 0.7 mmu).

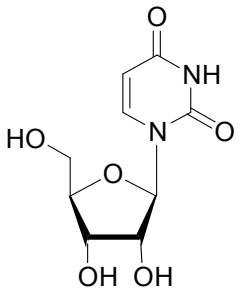

4.11

Uridine (4.11): white amorphous solid; IR (film) ν_{max} 3545, 3469, 3416, 1699, 1640, 1617, 1472, 1421, 1266, 1089, 1053 cm^{-1}; ^{1}H and ^{13}C NMR data see Table 4.1; HRESIMS *m/z* 245.0796 (calcd. for $C_9H_{13}N_2O_6$ [$(M+H)^+$], 245.0774, Δ 2.2 mmu).

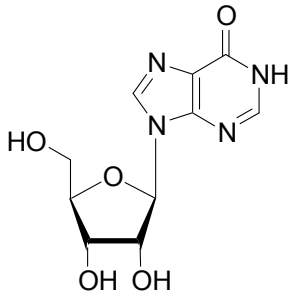

4.13

Inosine (4.13): white amorphous solid; IR (film) ν_{max} 3436, 3057, 1639, 1465, 1421, 1266, 1160, 1093, 1053 cm^{-1}; ^{1}H and ^{13}C NMR data see Table 4.1; LRESIMS *m/z* 269.8.

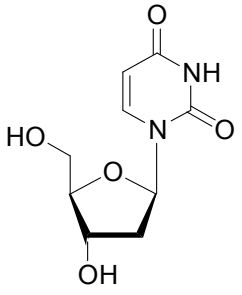

4.15

2'-deoxyuridine (4.15): white amorphous solid; IR (film) ν_{max} 3438, 3055, 1709, 1638, 1421, 1269, 1155, 1101, 1056 cm^{-1}; ^{1}H and ^{13}C NMR data see Table 4.1; HRESIMS *m/z* 229.0844 (calcd. for $C_9H_{13}N_2O_5$ [$(M+H)^+$], 229.0824, Δ 2.0 mmu).

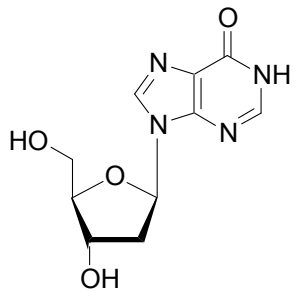

4.17

2'-deoxyinosine (4.17): white amorphous solid; IR (film) ν_{max} 3438, 1638, 1534, 1475, 1416, 1121, 1083 cm^{-1}; ^{1}H and ^{13}C NMR data see Table 4.2.

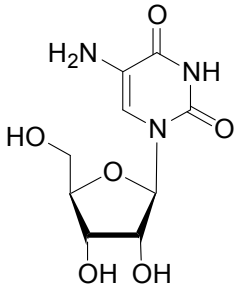

4.40

5-aminouridine (4.40): white amorphous solid; IR (film) ν_{max} 3438, 1638, 1534, 1475, 1416, 1121, 1083 cm^{-1}; ^{1}H and ^{13}C NMR data see Table 4.3.

6.4.2 Potentiometric Studies

The commercially available nucleosides **4.10**-**4.14** were purchased from Sigma-Aldrich The protonation and stability constants for the nucleosides and oxidovanadium(IV) complexes were determined by potentiometric titration of approximately 25 mL solutions. Tiamo 2.0 software was used to control all titrations which were performed using a Metrohm 794 Basic Titrino. All solutions were prepared using freshly boiled and degassed deionised milli-Q water to ensure the removal of dissolved oxygen and carbon dioxide. The ligand concentration was 1 mM and metal-to-ligand ratios of 1:1 and 1:10 were used. Titrations were performed over the pH range of 2-11 under a continuous flow of purified nitrogen using 0.1 M HCl (1 mL) and sodium hydroxide (0.1 M). The ionic strength of the titration solutions was kept constant at 0.10 M sodium chloride. Titrations were controlled using Tiamo software, and the titration rate used was 0.01 ml/min and the pausing time was 60 s. The glass electrode was calibrated for a strong acid-base reaction by the Gran-method[212] using the program GLEE[213] to determine the standard potential E^{o}. The ionic product of water (pK_w) of 13.76 at 25.0±0.1 ^{o}C in 0.10 M NaCl was used in all calculations.[214] The hydrolysis model of a oxidovanadium(IV) system

was included in the model; $[VO(OH)_3]^-$ ($\log\beta_{10-3}$ = -18.0) and $[(VO)_2(OH)_5]^-$ ($\log\beta_{20-5}$ = -22.0), $[VO(OH)]^+$ ($\log\beta_{10-1}$ = -5.94) and $[(VO)_2(OH)_2]^{2+}$ ($\log\beta_{20-2}$ = -6.95).[211] The concentration stability constants $\beta_{pqr} = [M_pL_qH_r]/[M]^p[L]^q[H]^r$ were calculated by using the computer program HYPERQUAD.[216]

Thymidine (4.10): Protonation constants established as log*K* 9.54 and 10.78. Stability constant(s) for the nucleoside-vanadyl complexation study determined as logβ 13.6 for the (1,1,0) model.

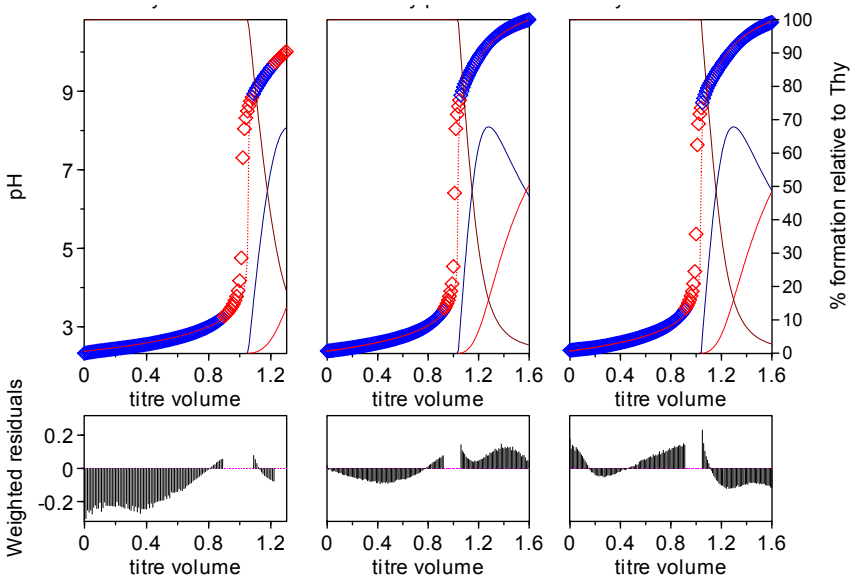

Figure 6.1: Titration and fitted curves of aqueous thymidine protonation study

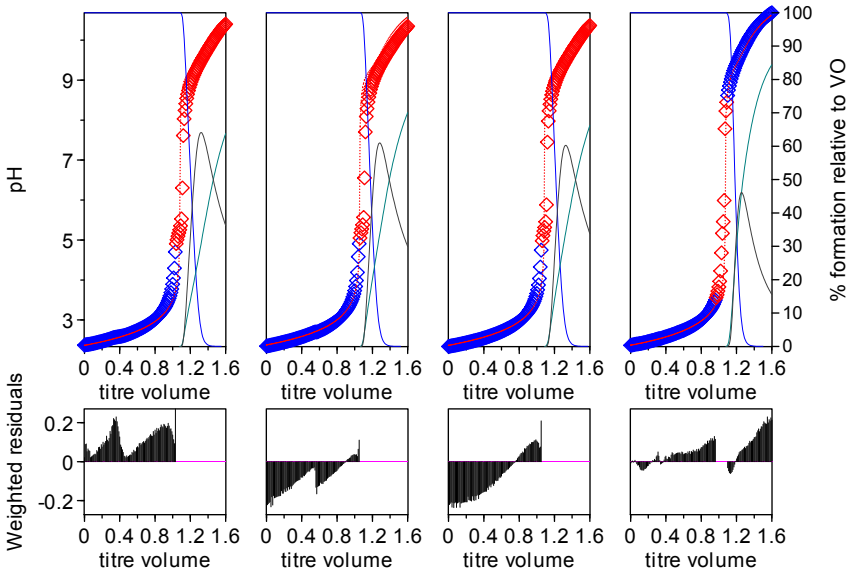

Figure 6.2: Titration and fitted curves of aqueous thymidine-vanadyl complexation study.

Uridine (4.11): Protonation constants established as log*K* 9.12 and 10.77. Stability constant(s) for the nucleoside-vanadyl complexation study determined as log*β* 10.9 for the (1,1,0) model and log*β* 13.9 for the (1,1,1) model.

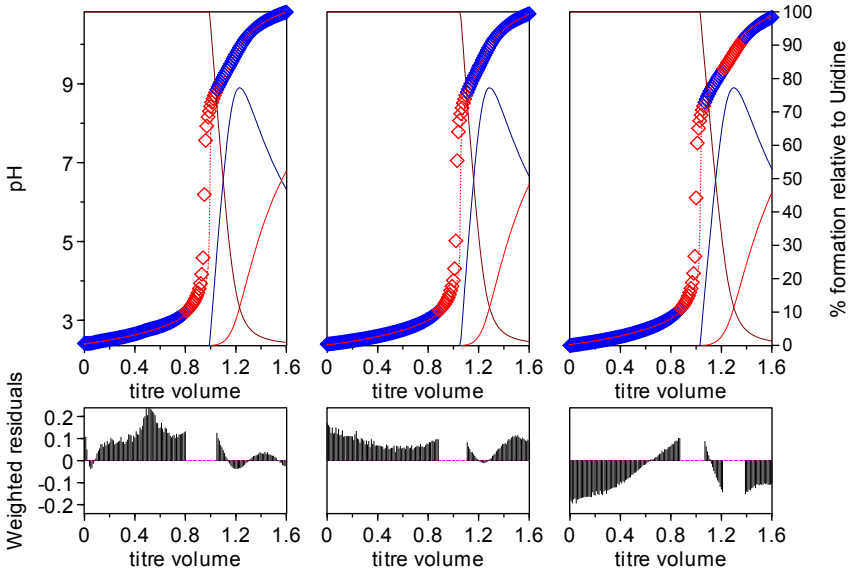

Figure 6.3: Titration and fitted curves of aqueous uridine protonation study

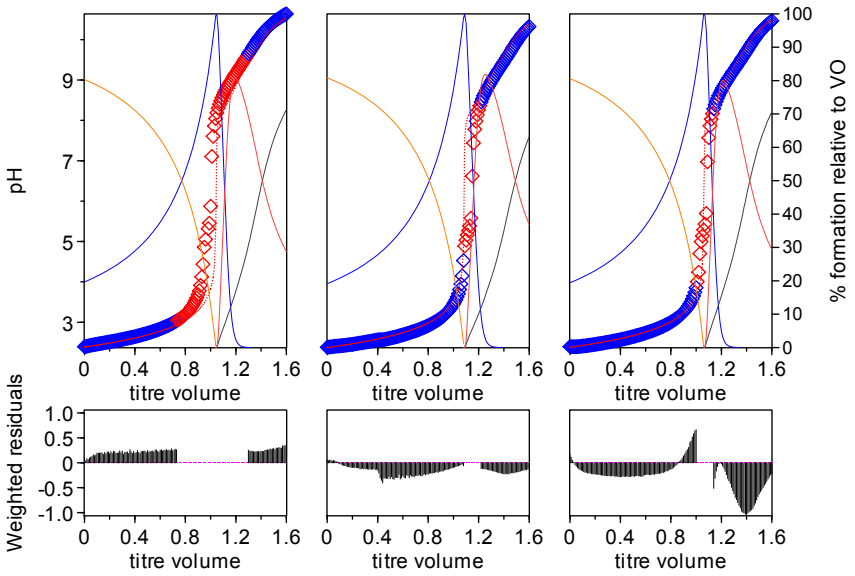

Figure 6.4: Titration and fitted curves of aqueous uridine-vanadyl complexation study.

Guanosine (4.12): Protonation constants established as log*K* 9.6, 8.87 and 2.30. Stability constant(s) for the nucleoside-vanadyl complexation study determined as log*β* 19.9 for the (1,1,0) model and log*β* 30.9 for the (1,1,1) model.

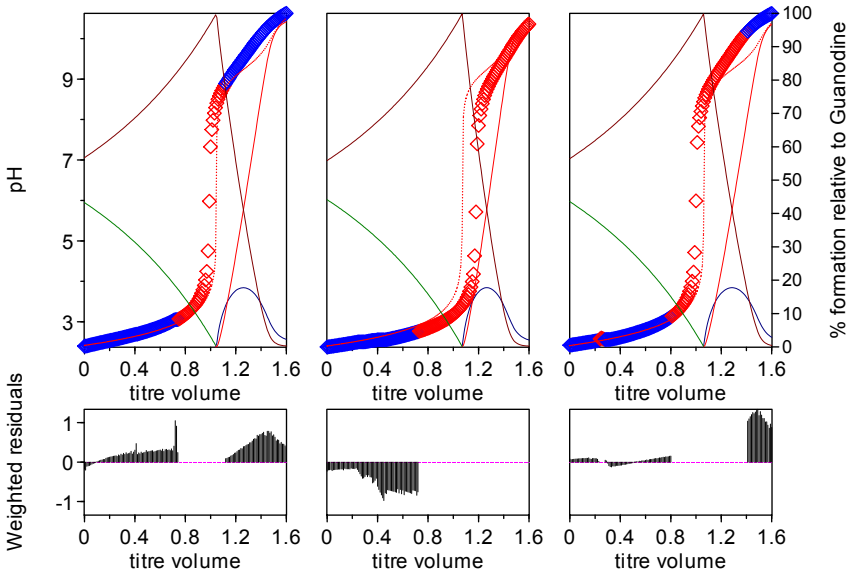

Figure 6.5: Titration and fitted curves of aqueous guanosine protonation study

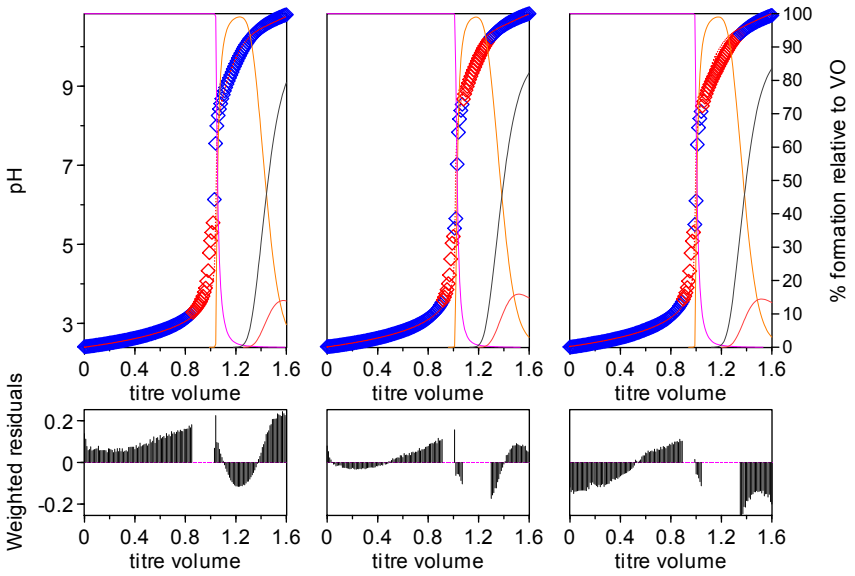

Figure 6.6: Titration and fitted curves of aqueous guanosine-vanadyl complexation study.

Inosine (4.13): Protonation constant established as log*K* 8.63. Stability constant(s) for the nucleoside-vanadyl complexation study determined as log*β* 12.2 for the (1,1,0) model and log*β* 17.8 for the (1,1,1) model.

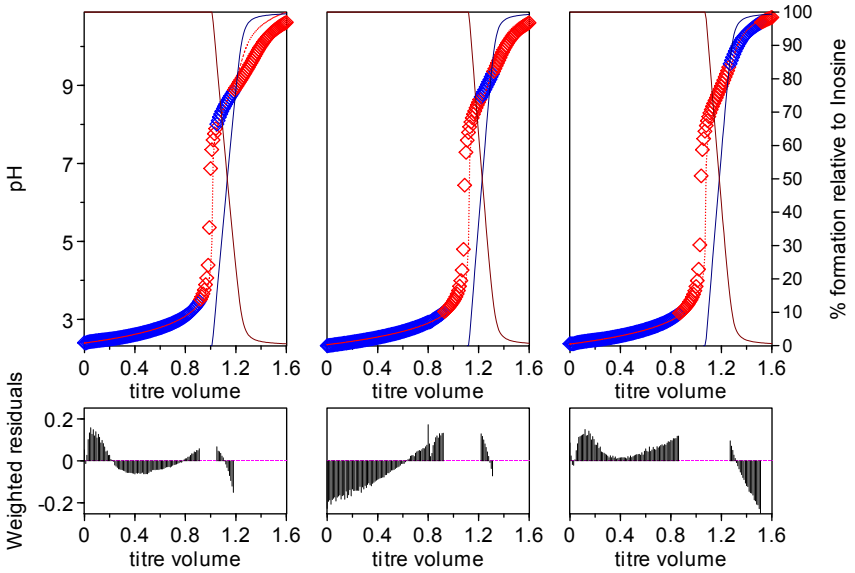

Figure 6.7: Titration and fitted curves of aqueous inosine protonation study

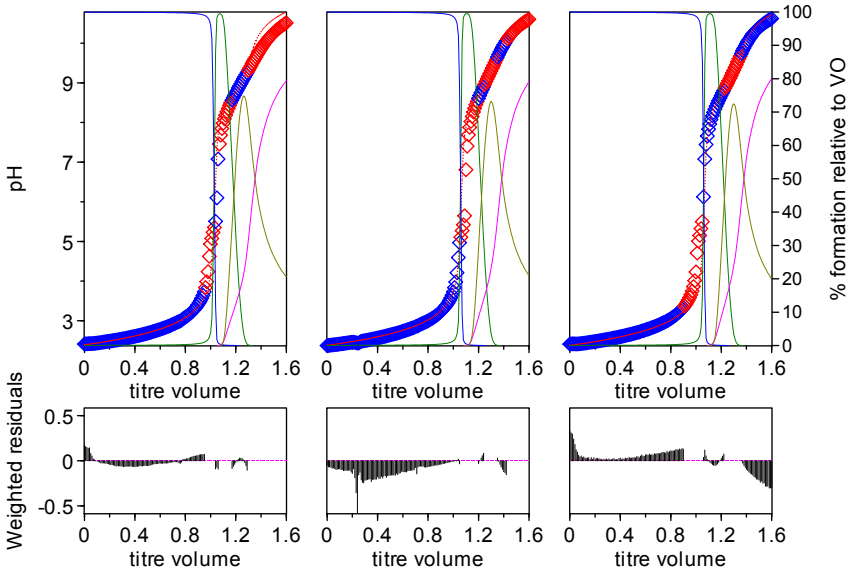

Figure 6.8: Titration and fitted curves of aqueous inosine-vanadyl complexation study.

Adenosine (4.14): Protonation constants established as log*K* 11.04 and 3.65. Stability constant(s) for the nucleoside-vanadyl complexation study determined as log*β* 10.8 for the (1,1,0) model and log*β* 16.2 for the (1,1,1) model.

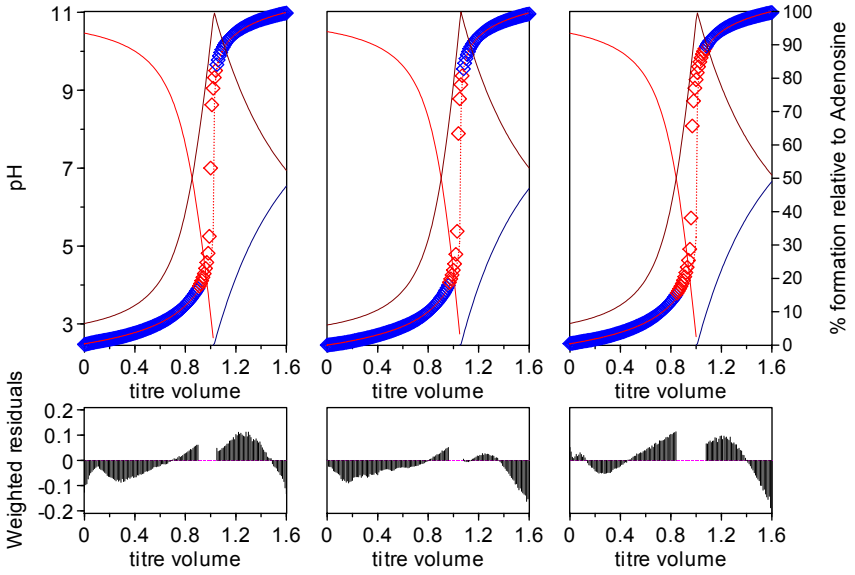

Figure 6.9: Titration and fitted curves of aqueous adenosine protonation study

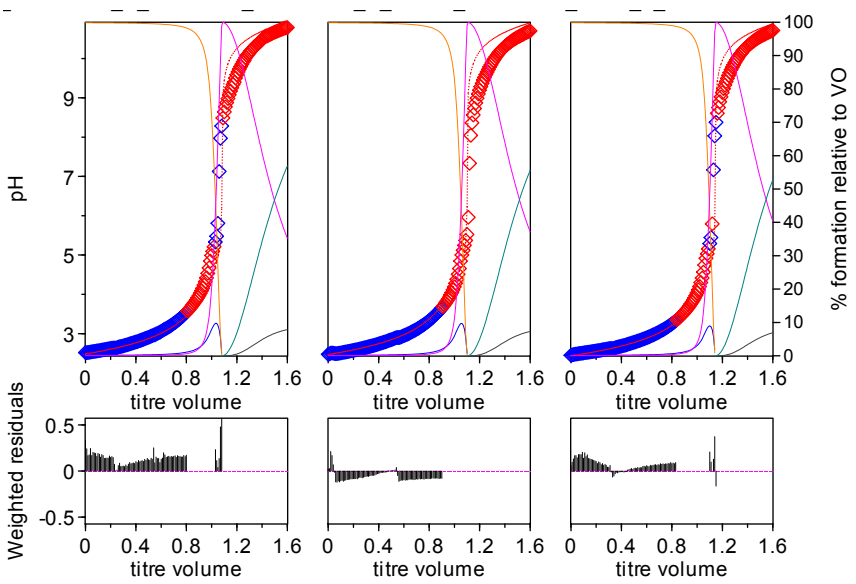

Figure 6.10: Titration and fitted curves of aqueous adenosine-vanadyl complexation study.

6.5 Chapter Five Experimental

6.5.1 Animal material

Atriolum marinense Kott, 2001 (TIC2011-025) was collected using SCUBA in November 2011 from the Algoa Bay dive site, known as Shy Shark reef (25°41'34.14"E) and stored at -20°C until lyophilisation and extraction. *Clavelina* sp. (SAF2004-029) was collected from a depth of 21 m at White Sands reef (25°42'34.38"E), Algoa Bay, South Africa and kept at -20°C until lyophilisation and extraction.

6.5.2 Bioassay

Lyophilised samples of *Atriolum marinense* (132 g wet mass to 31 g dry mass) and *Clavelina* sp. (157 g wet mass to 39 g dry mass) were each sequentially extracted with MeOH and CH_2Cl_2. The CH_2Cl_2 extractives were concentrated to dryness under reduced pressure and redissolved in their respective MeOH extracts before being cyclic loaded onto HP-20 resin. The HP-20 resin was washed with with water to remove inorganic salts and then stripped with aqueous Me_2CO mixtures of decreasing polarity (20%, 40%, 60%, 80% Me_2CO/H_2O and 100% Me_2CO) to afford five fractions per ascidian species (Figure 5.2). Fractions were concentrated *in vacuo*. HPLC grade solvents were used throughout.

Subsamples of 1 mg of each of the 5 HP-20 fractions of the two ascidian extracts were submitted into a biological assay against breast cancer cell line MDA-MB-231 (see section 6.2.6 of this chapter). The percentage viability of the cancer cells was determined after exposure to 5 µg/mL and 50 µg/mL of each fraction.

*6.5.3 Isolation of **5.1** from Atriolum marinense*

The fifth fraction (100% Me_2CO) obtained from the HP-20 fractionation of the extract of *A. marinense* was further purified by DIOL HPLC with 20% EtOAc/hexane followed by DIOL HPLC with 16.6% EtOAc/hexane and finally by DIOL HPLC with 10% DCM/hexane to yield the styrene trimer **5.1**. The Bruker software WIN-DAISY was used to establish the structure of **5.1**.

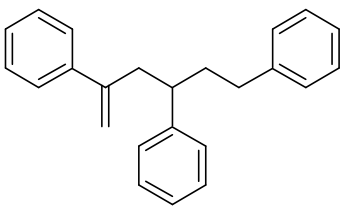

5.1

Styrene trimer (5.1): colourless oil; ^{1}H and ^{13}C NMR data see Table 5.1; EIMS *m/z* (rel. int.) 312.1 [M^+] (10), 207.0 (46), 117.0 (74), 91.0 (100).

6.5.4 Attempts to establish if 5.1 is an artefact of HP-20 fractionation

A portion 5 g of HP-20 beads were ground into a fine powder and steeped in CH_2Cl_2 for 48 hours with periods of sonication. The powder was then filtered and the filtrate dried under reduced pressure and a ^1H NMR spectrum acquired.

The second experiment replicated the initial process of cyclic loading on to HP-20 resin, without the presence of the ascidian extract. A volume of 250 mL of HP-20 resin was subjected to the process of cyclic loading using HPLC grade solvents. The 500 mL of MeOH was doped with 50 mL of CH_2Cl_2 prior to cycling loading. The solvent mixture was cyclic loaded onto the HP-20 resin over the course of a week. The HP-20 column was then striped with 100% acetone. The eluent collected was concentrated to dryness under reduced pressure and analysed using ^1H NMR.

Appendix A:
Principal component analysis (PCA) factor loading plots obtained from the total metal analysis data of 25 Algoa Bay ascidians

Appendix A1: Factor loading plots with case labels relating to taxonomic families

The factor loading plots presented in this appendix relate to the principal component analysis conducted on the metal concentration data obtained for 25 species of Algoa Bay ascidians and discussed in detail in Chapter 3. Each data point relates to an ascidian species and clustering of data plots within a particular area of the plot indicates similar factor scores between ascidian relating to the metals which predominate within them. In the case of Appendix A1 the ascidian species are labelled according to their taxonomic families in an attempt to establish any phylogenetic relationships between ascidian species and metal concentrations.

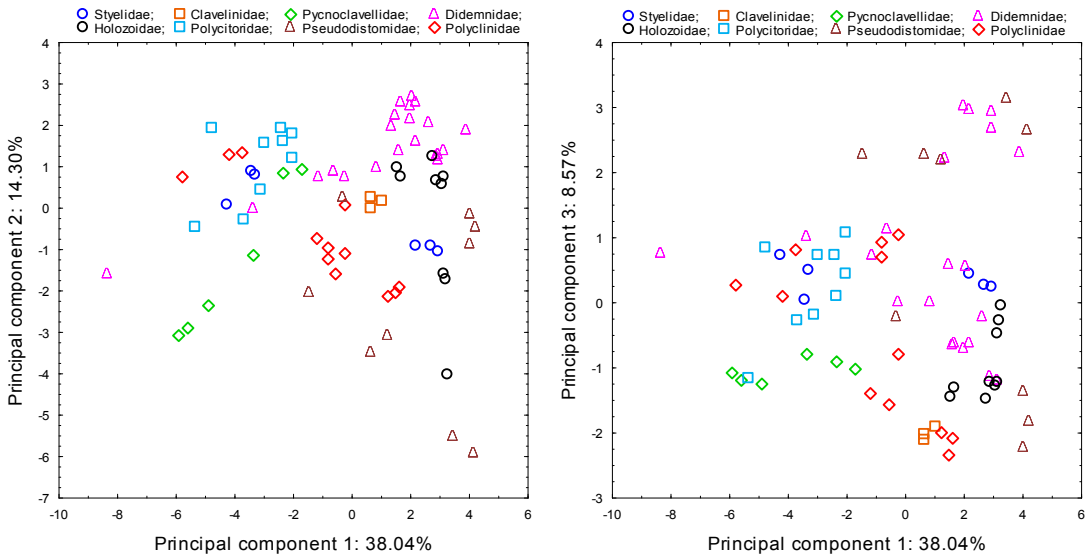

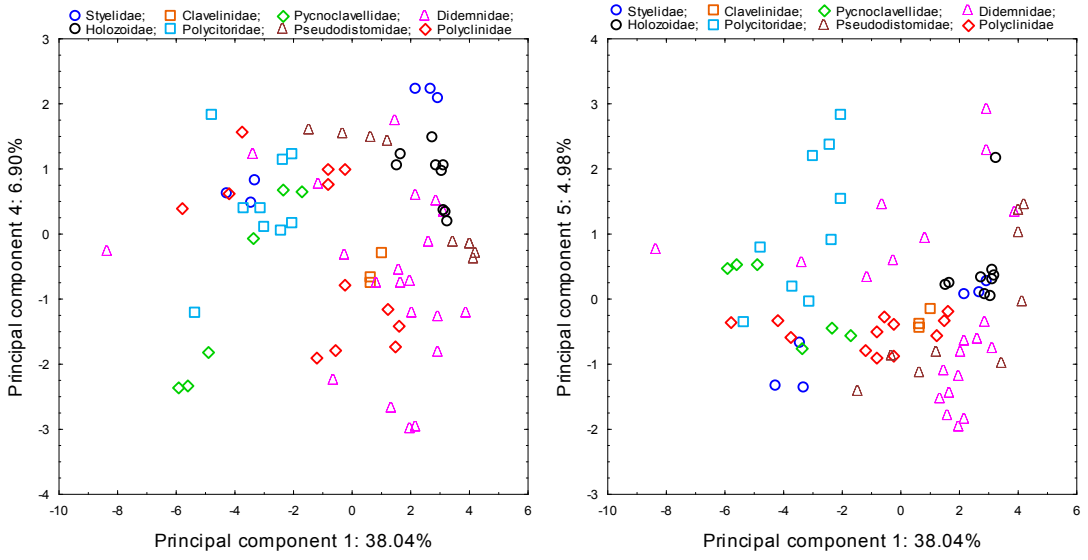

Appendix A1 continued

.

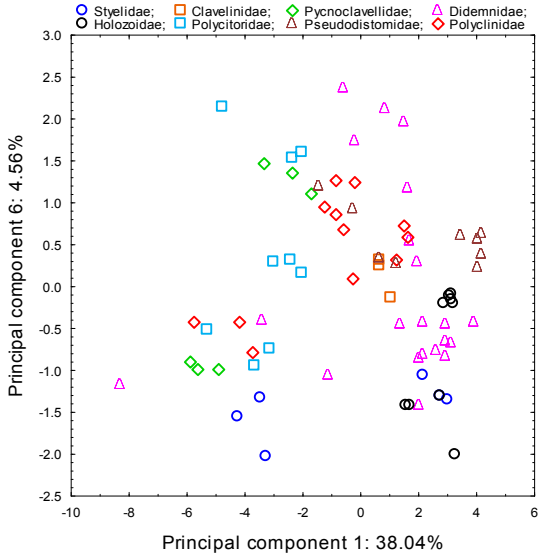

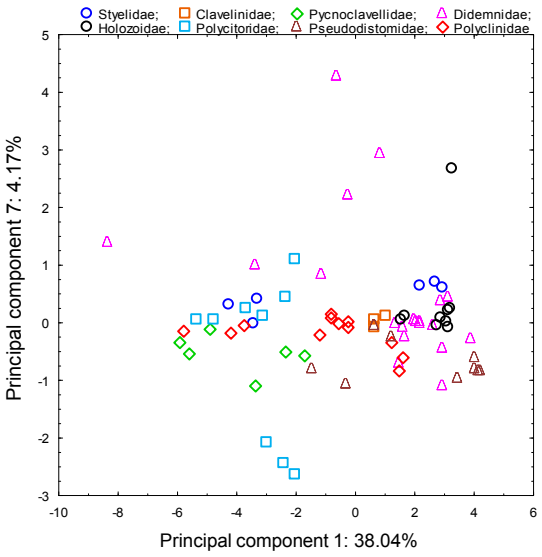

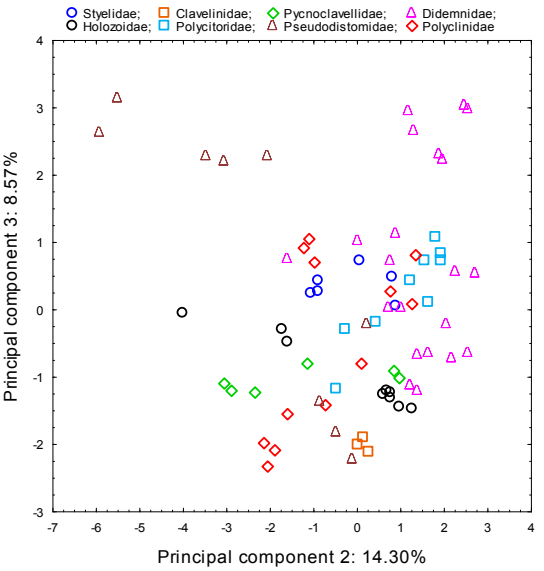

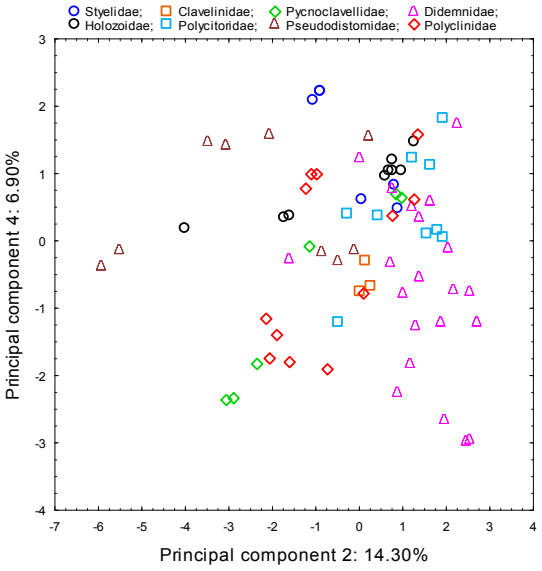

Appendix A1 continued

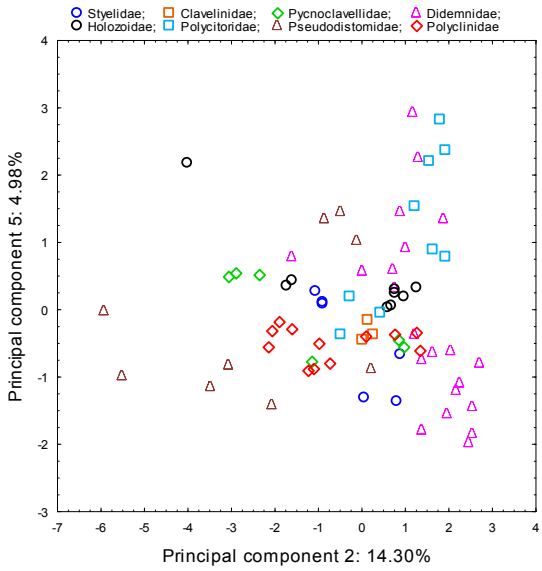

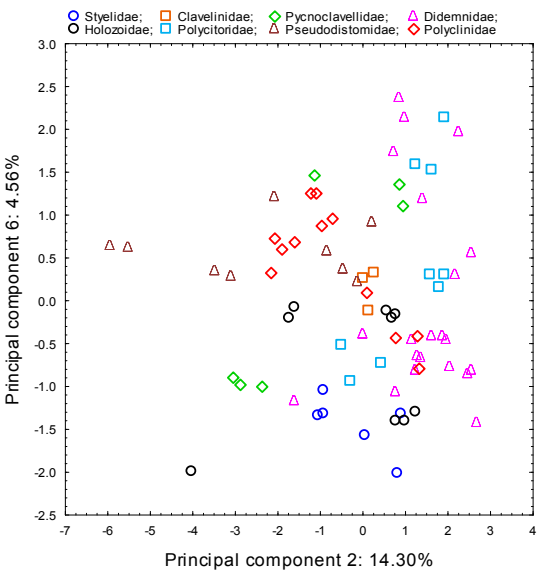

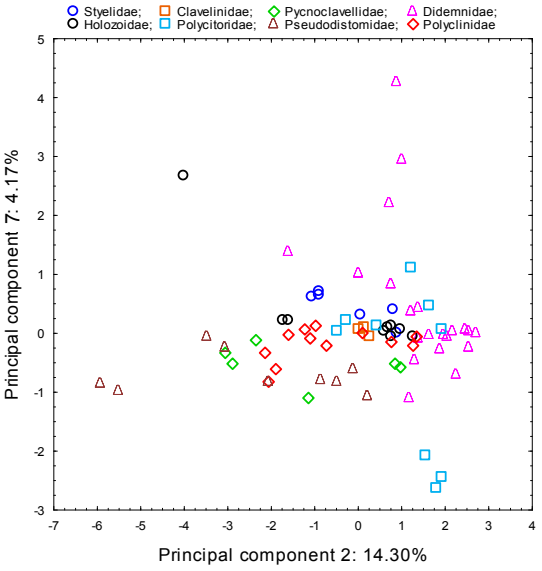

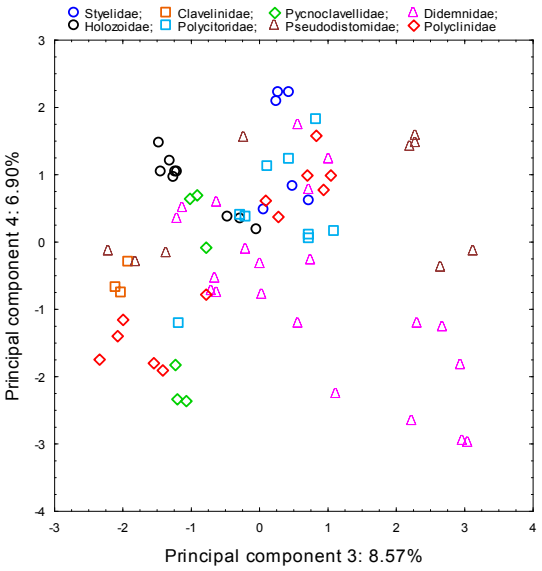

Appendix A1 continued

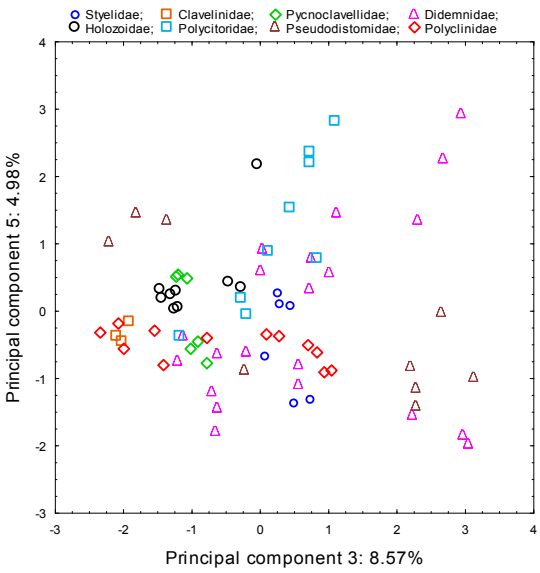

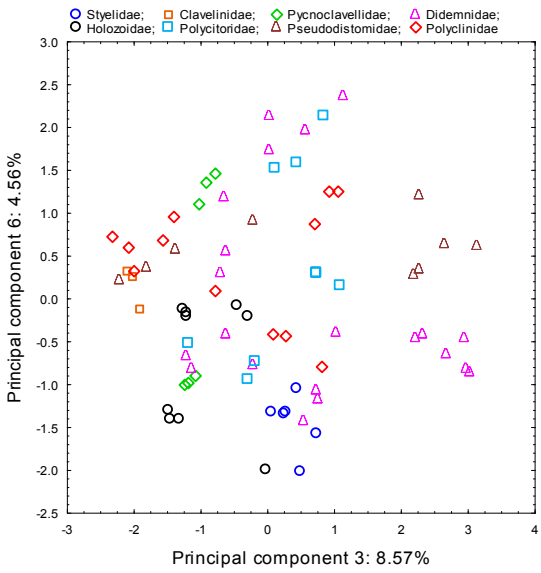

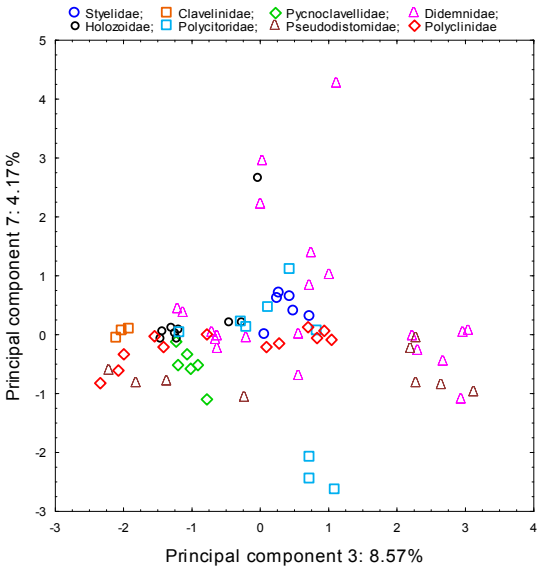

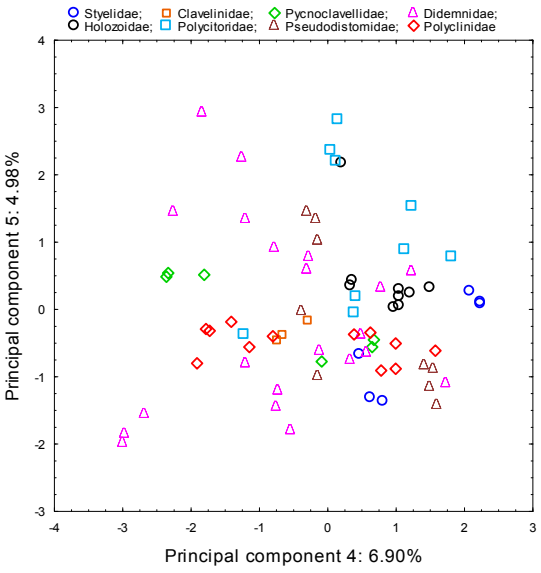

Appendix A1 continued

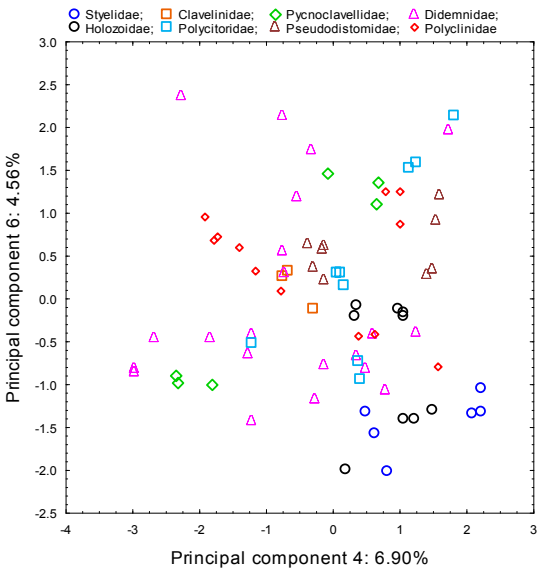

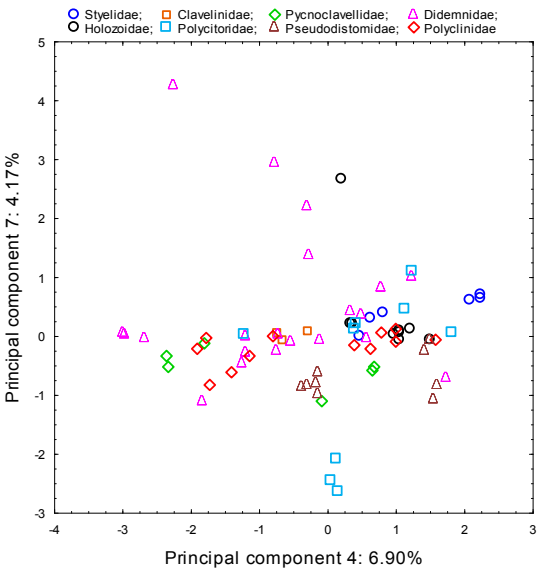

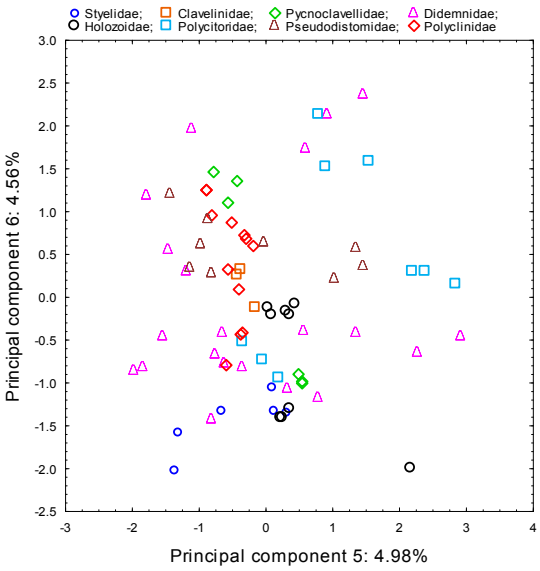

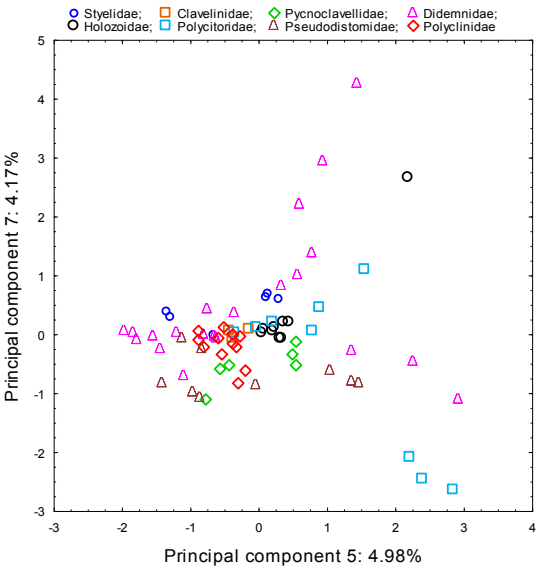

Appendix A1 continued

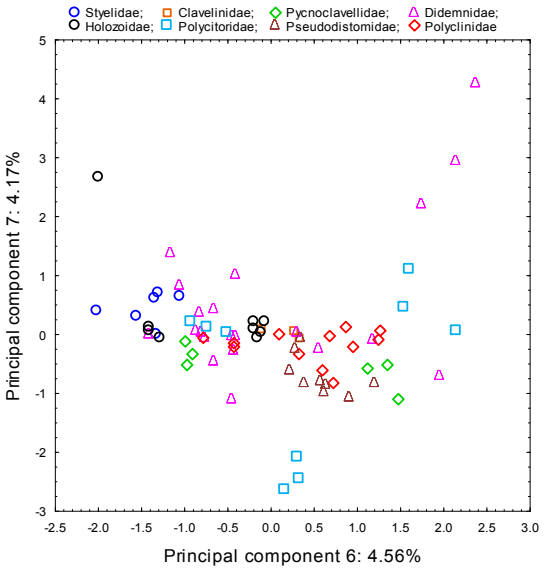

Appendix A2: Factor loading plots with case labels relating to collection site

The factor loading plots presented in this appendix relate to the principal component analysis conducted on the metal concentration data obtained for 25 species of Algoa Bay ascidians and discussed in detail in Chapter 3. Each data point relates to an ascidian species and clustering of data plots within a particular area of the plot indicates similar factor scores between ascidian relating to the metals which predominate within them. In the case of Appendix A2 the ascidian species are labelled according to their collection sites in an attempt to establish any spatial relationships between collection site and metal concentrations.

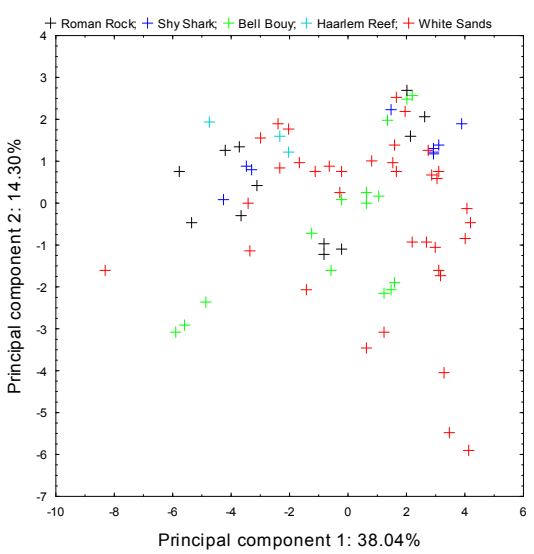

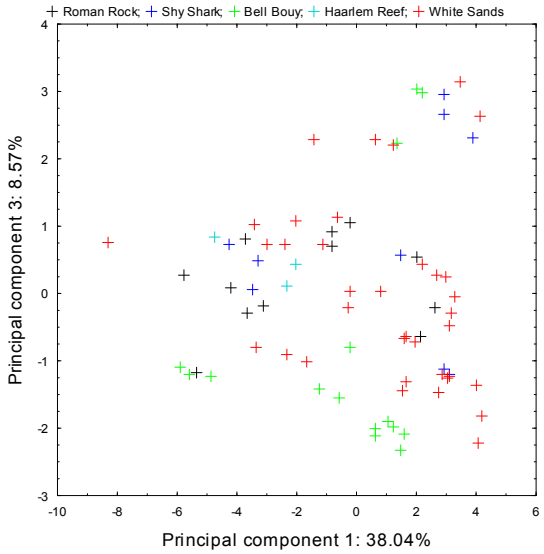

Appendix A2 continued

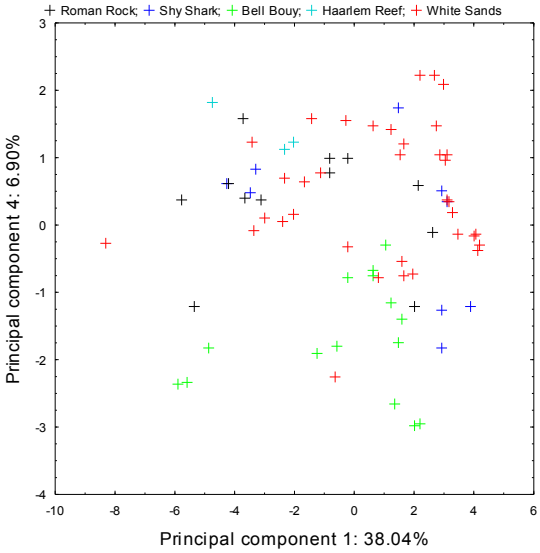

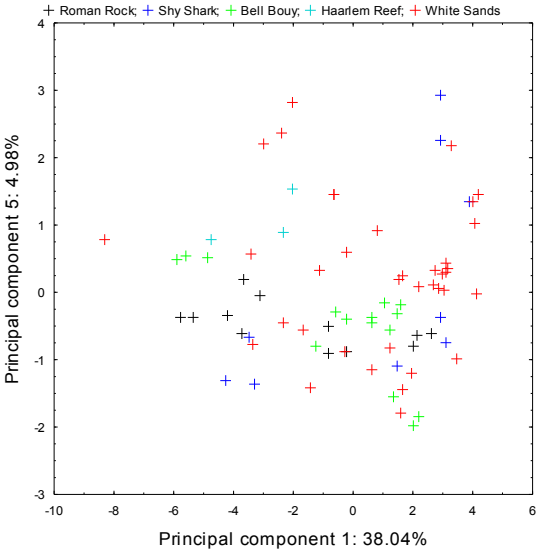

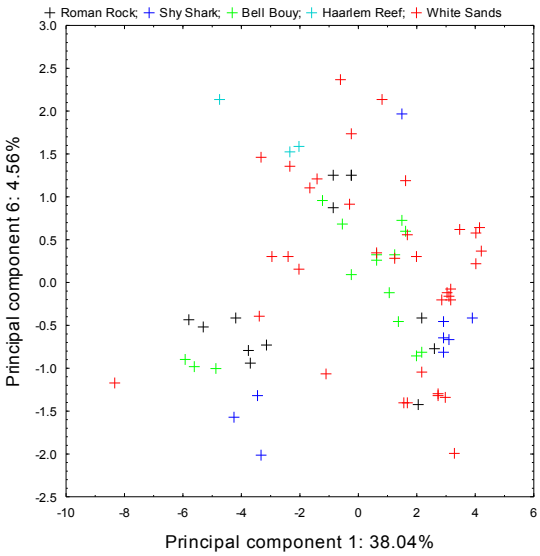

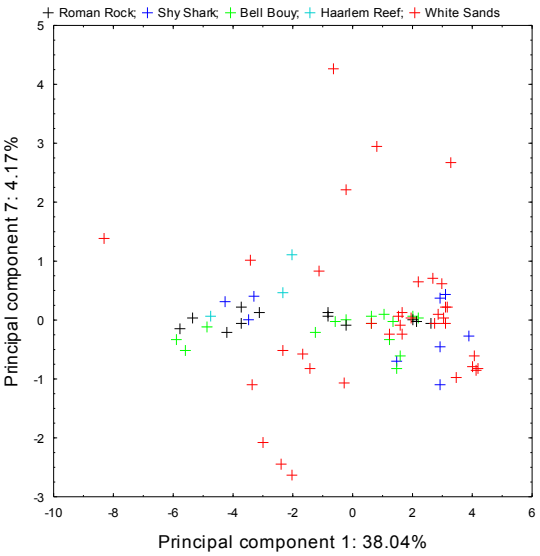

Appendix A2 continued

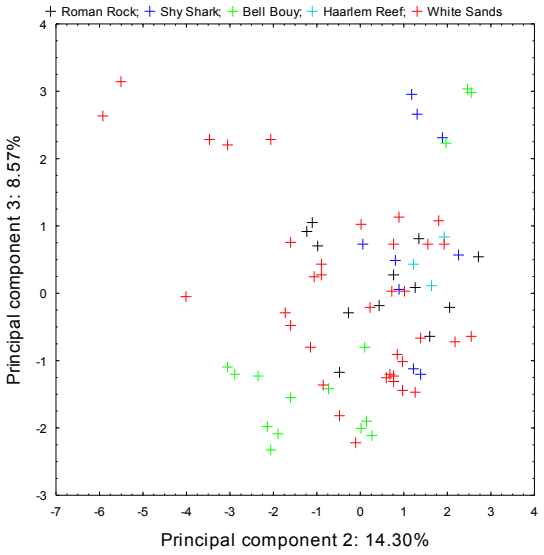

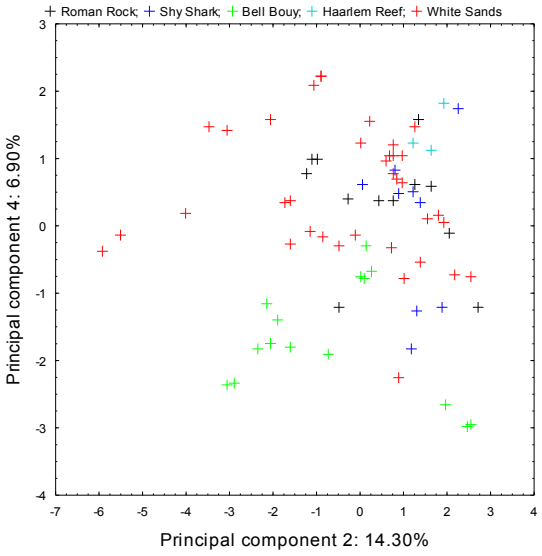

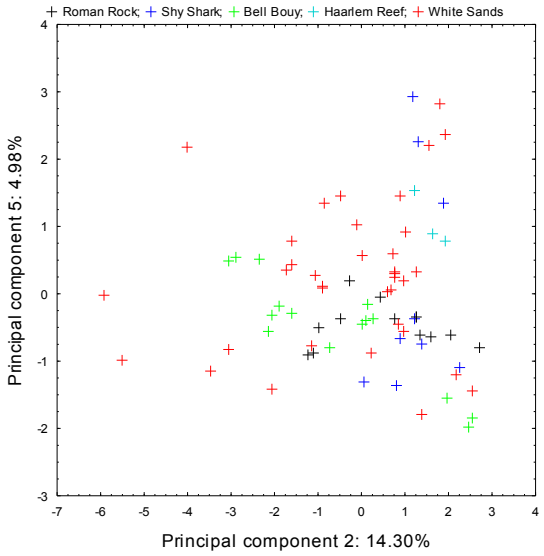

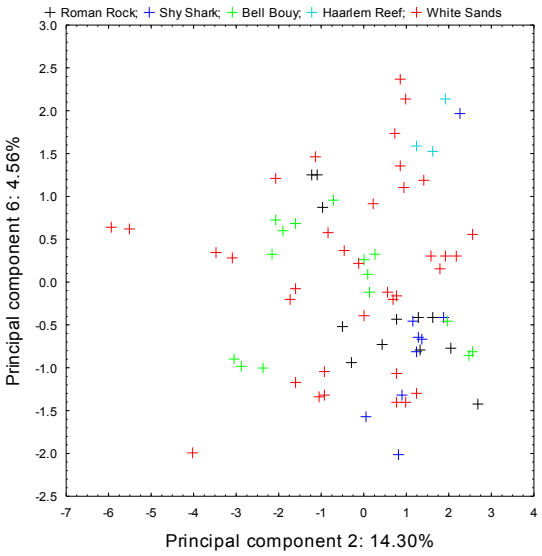

Appendix A2 contintued

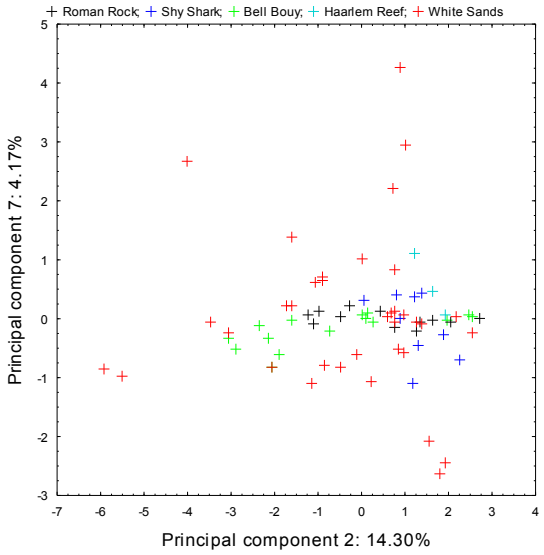

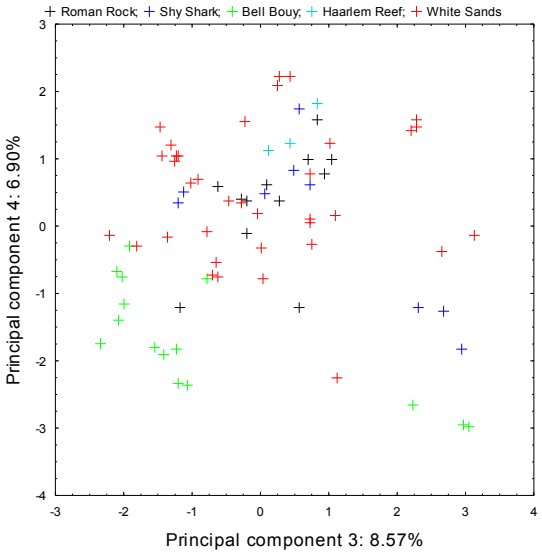

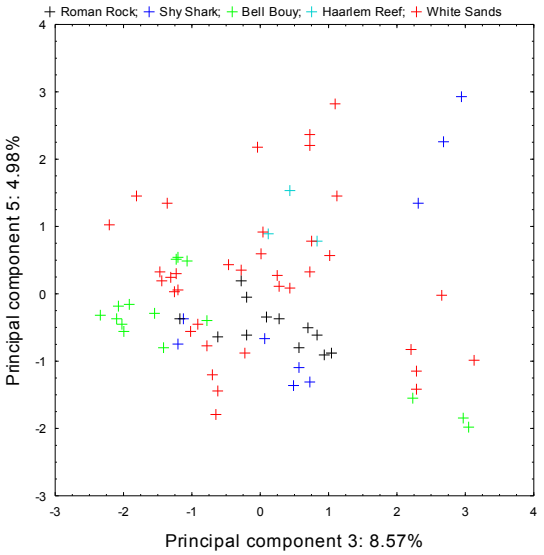

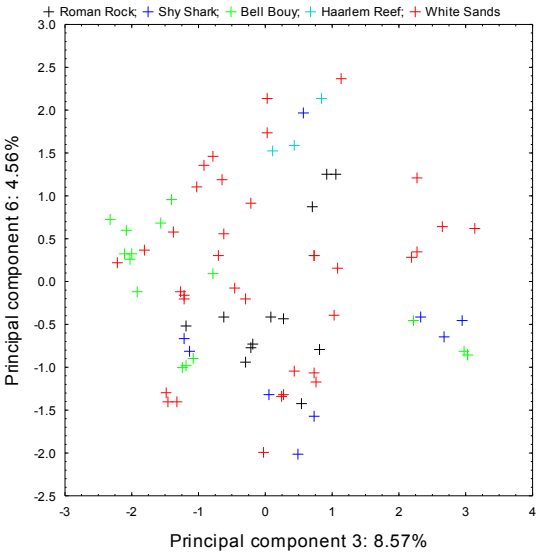

Appendix A2 continued

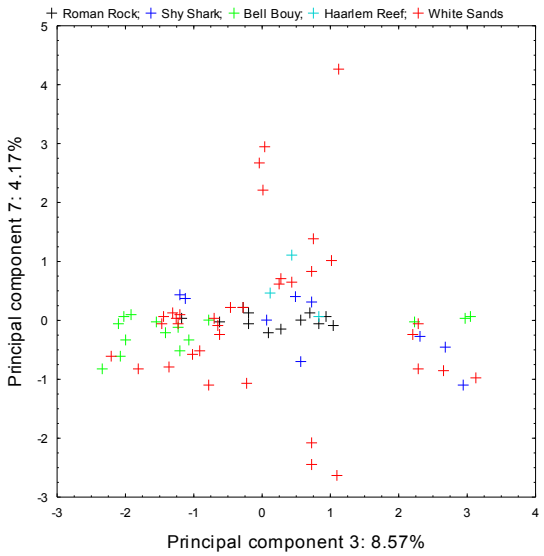

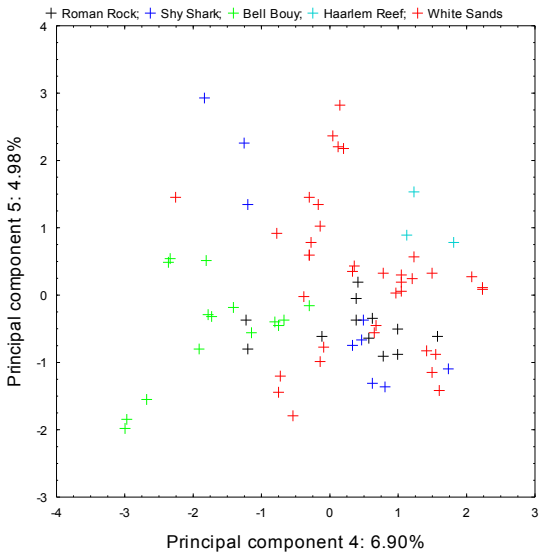

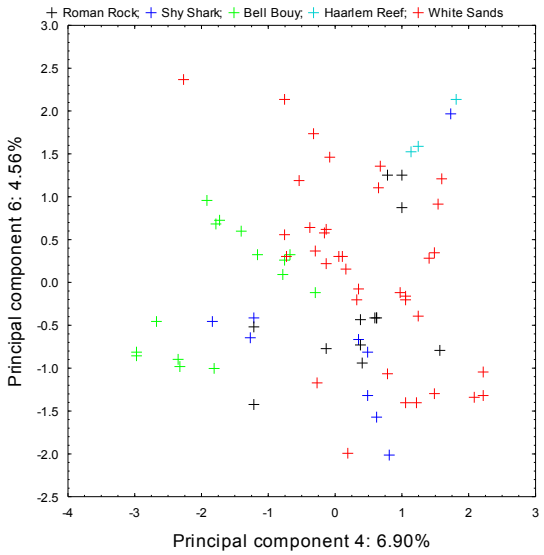

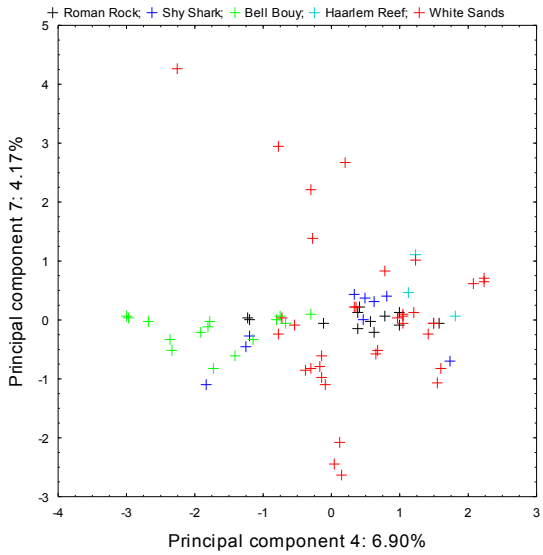

Appendix A2 continued

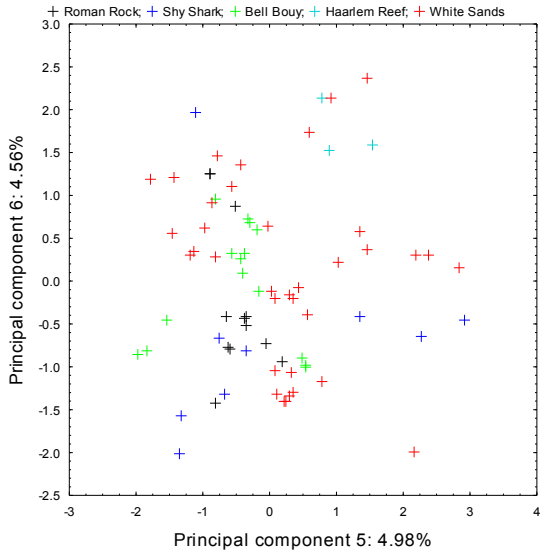

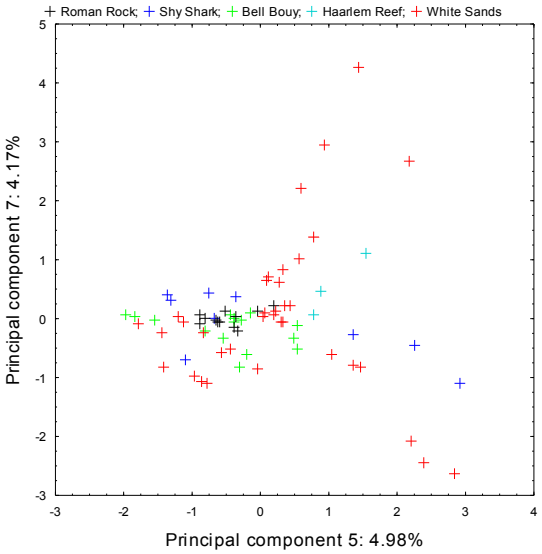

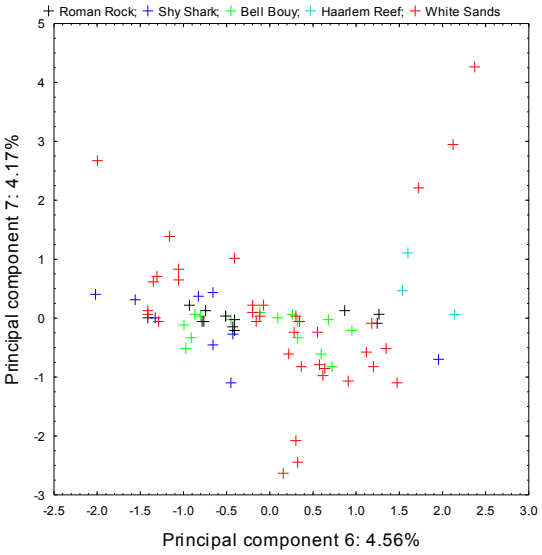

Appendix A3: Factor loading plots with case labels relating to collection year

The factor loading plots presented in this appendix relate to the principal component analysis conducted on the metal concentration data obtained for 25 species of Algoa Bay ascidians and discussed in detail in Chapter 3. Each data point relates to an ascidian species and clustering of data plots within a particular area of the plot indicates similar factor scores between ascidian relating to the metals which predominate within them. In the case of Appendix A3 the ascidian species are labelled according to their year of collection in an attempt to establish any temporal relationships between collection year and metal concentrations.

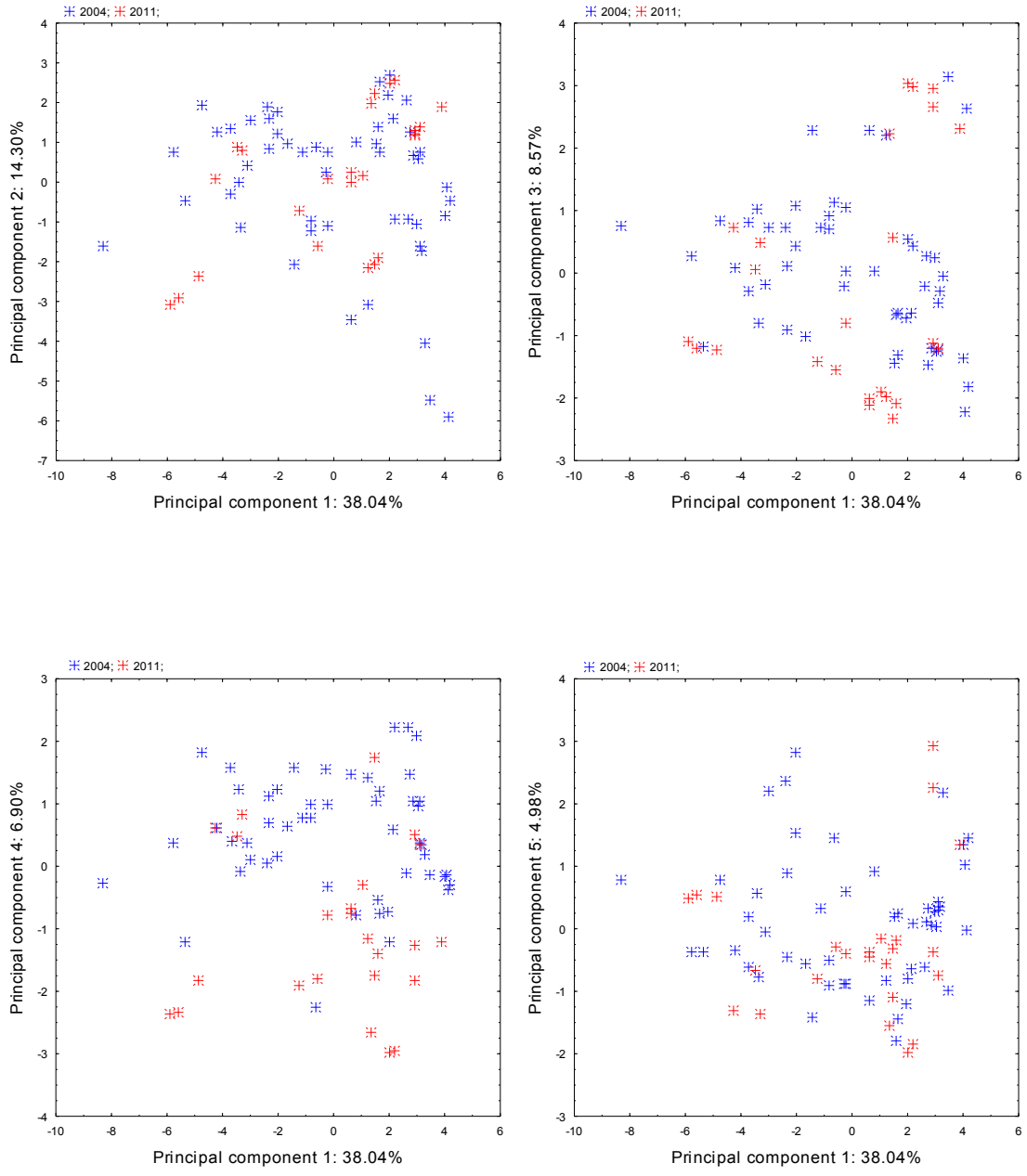

Appendix A3 continued

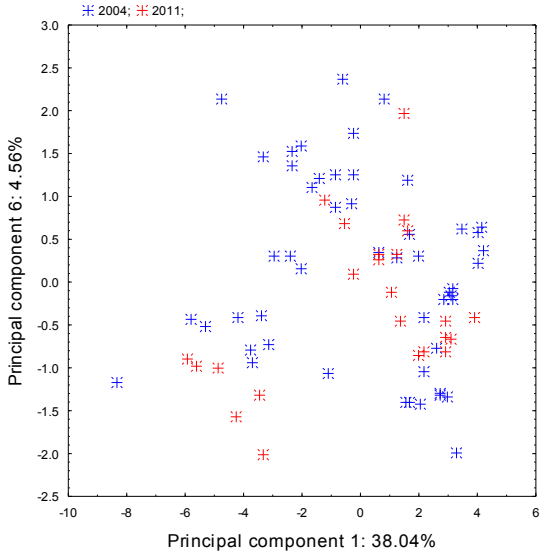

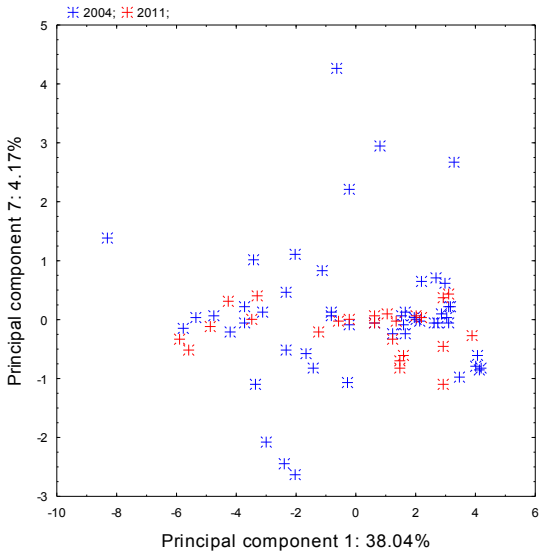

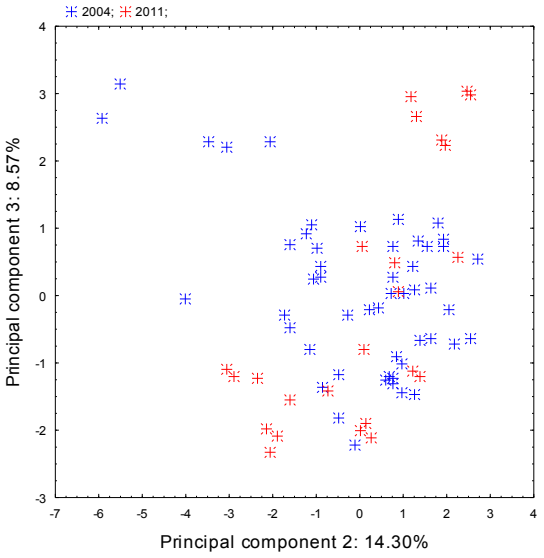

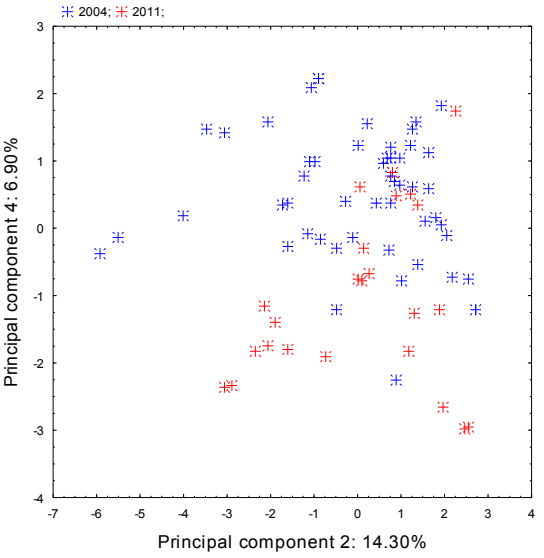

Appendix A3 continued

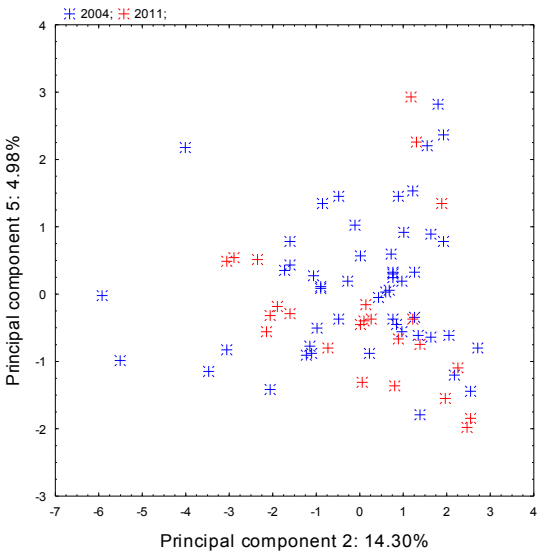

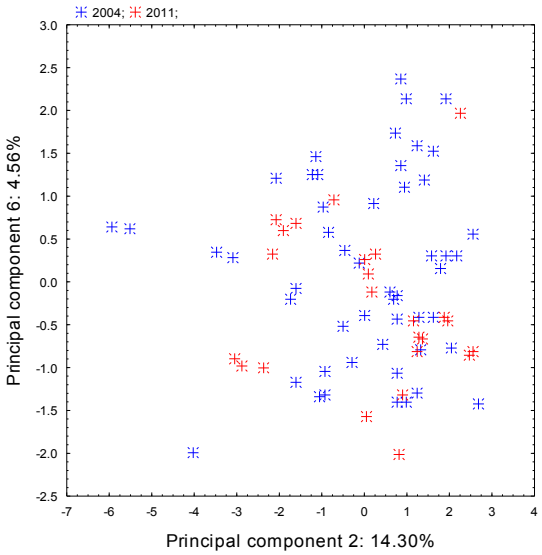

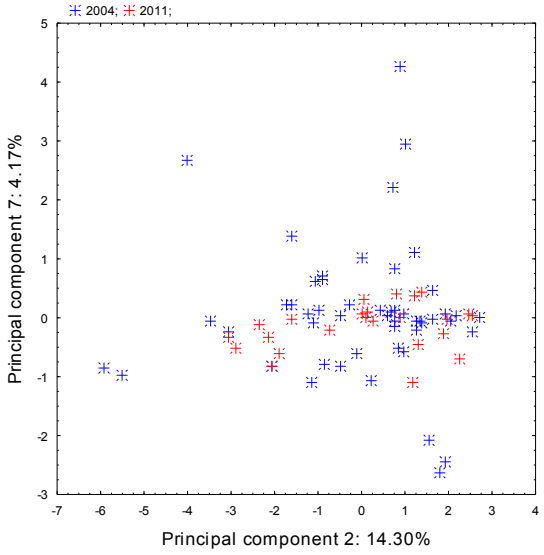

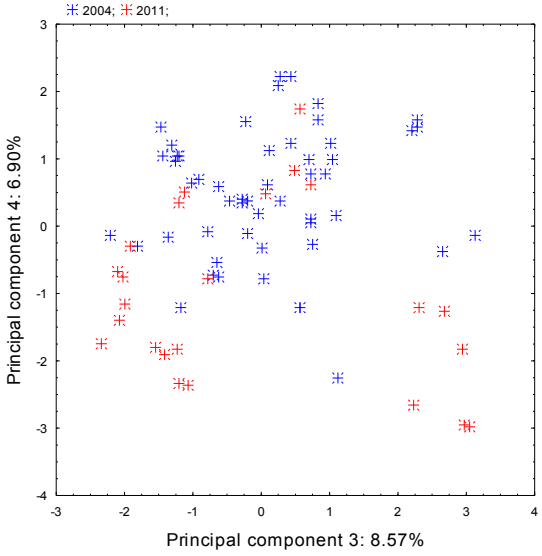

Appendix A3 continued

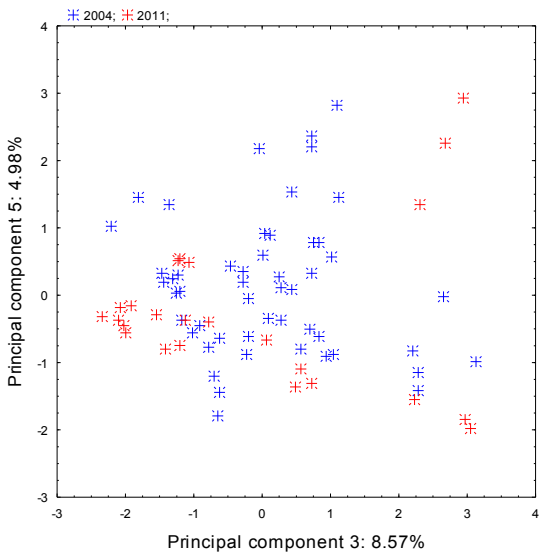

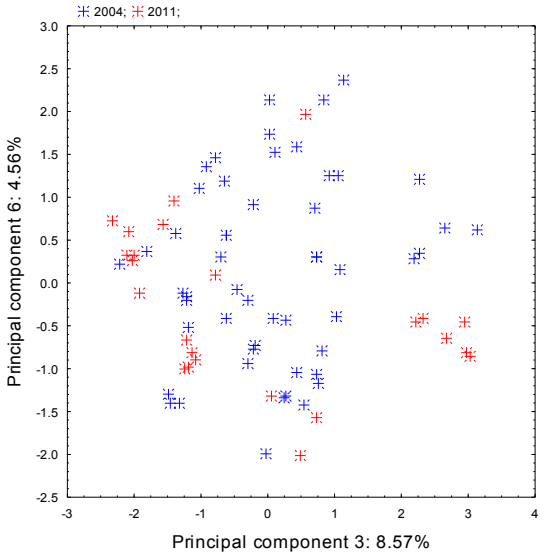

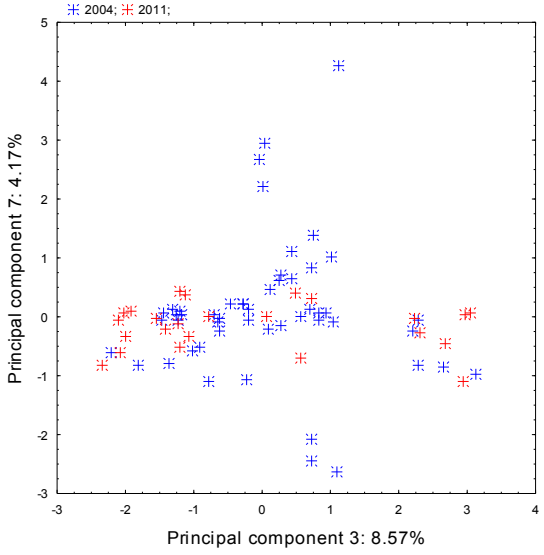

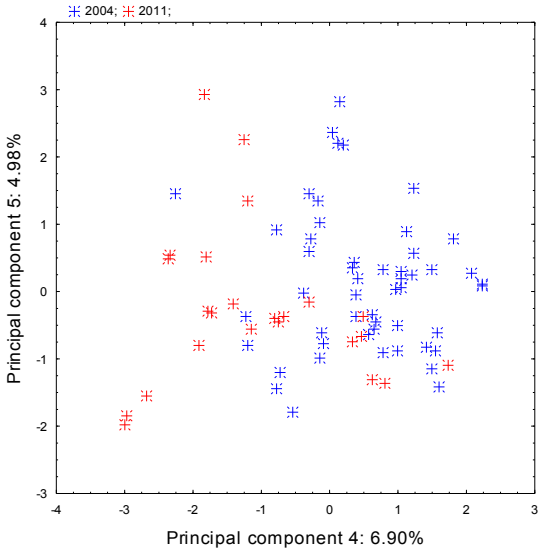

Appendix A3 continued

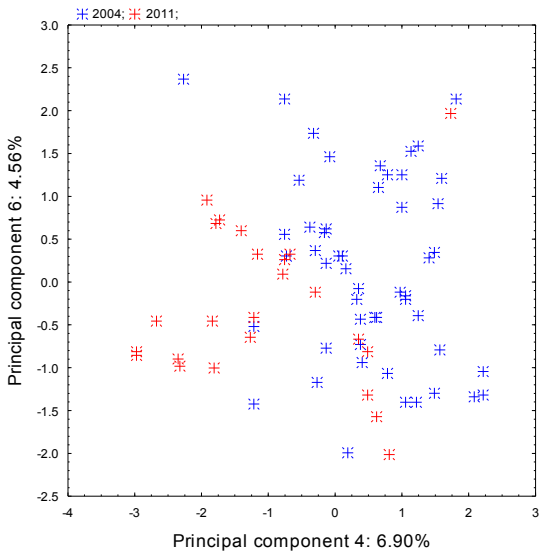

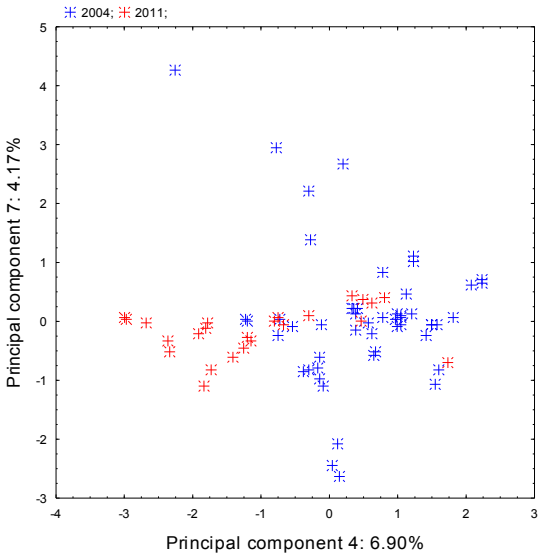

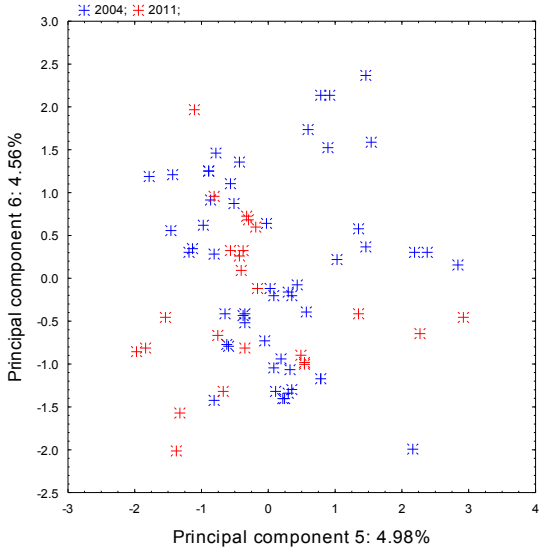

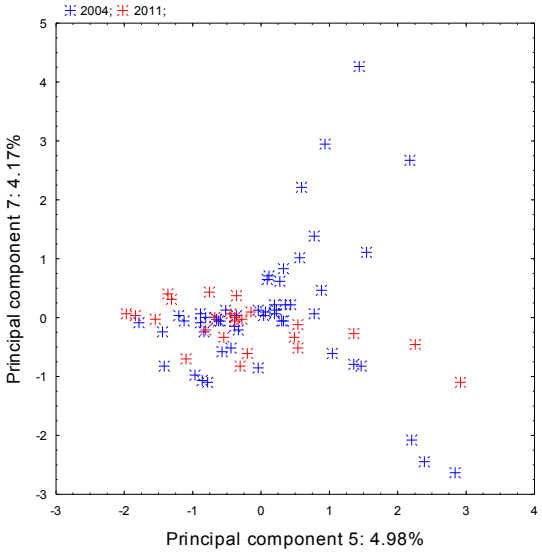

Appendix A3 continued

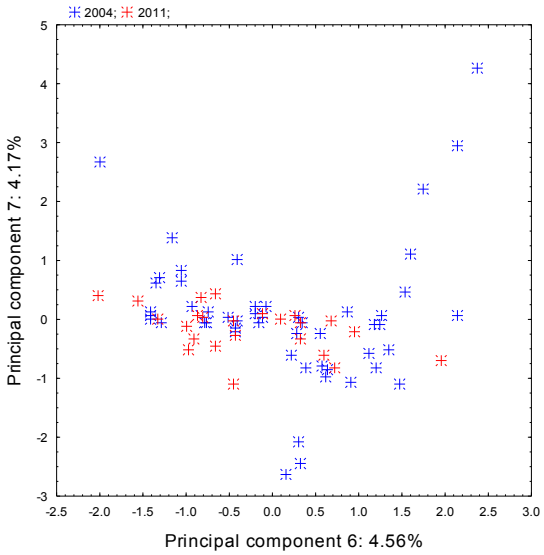

References

References and notes

(1) Andersen, R. J.; Williams, D. E. *Issues Environ. Sci. Technol.* **2000**, *13*, 55–79.

(2) Blunt, J. W.; Copp, B. R.; Keyzers, R. A.; Munro, M. H. G.; Prinsep, M. R. *Nat. Prod. Rep.* **2014**, *31*, 160–258.

(3) Hamann, M. T.; Hill, R.; Roggo, S. *Chim. Int. J. Chem.* **2007**, *61*, 313–321.

(4) Srivastava, M.; Simakov, O.; Chapman, J.; Fahey, B.; Gauthier, M. E. a; Mitros, T.; Richards, G. S.; Conaco, C.; Dacre, M.; Hellsten, U.; Larroux, C.; Putnam, N. H.; Stanke, M.; Adamska, M.; Darling, A.; Degnan, S. M.; Oakley, T. H.; Plachetzki, D. C.; Zhai, Y.; Adamski, M.; Calcino, A.; Cummins, S. F.; Goodstein, D. M.; Harris, C.; Jackson, D. J.; Leys, S. P.; Shu, S.; Woodcroft, B. J.; Vervoort, M.; Kosik, K. S.; Manning, G.; Degnan, B. M.; Rokhsar, D. S. *Nature* **2010**, *466*, 720–726.

(5) Grabowski, K.; Baringhaus, K. H.; Schneider, G. *Nat. Prod. Rep.* **2008**, *25*, 892–904.

(6) Bon, R. S.; Waldmann, H. *Acc. Chem. Res.* **2010**, *43*, 1103–1114.

(7) Li, J. W.; Vederas, J. C. *Science* **2009**, *325*, 161–166.

(8) Davies-Coleman, M. T.; Sunassee, S. N. In *Drug Discovery in Africa*; Chibale, K.; Masimbirembwe, C.; Davies-Coleman, M. T., Eds.; Spinger: Heidelberg, 2012; pp. 193–210.

(9) Gerwick, W. H.; Moore, B. S. *Chem. Biol.* **2012**, *19*, 85–98.

(10) Dias, D. a.; Urban, S.; Roessner, U. *Metabolites* **2012**, *2*, 303–336.

(11) Mayer, A. M. S.; Glaser, K. B.; Cuevas, C.; Jacobs, R. S.; Kem, W.; Little, R. D.; McIntosh, J. M.; Newman, D. J.; Potts, B. C.; Shuster, D. E. *Trends Pharmacol. Sci.* **2010**, *31*, 255–265.

(12) Querellou, J.; Børresen, T.; Boyen, C.; Dobson, A.; Höfle, M.; Ianora, A.; Jaspars, M.; Kijjoa, A.; Olafsen, J.; Rigos, G.; Wijffels, R. *Marine biotechnology. A New Vision and Strategy for Europe: Marine Board-ESF*; 2010.

(13) Proksch, P.; Edrada-Ebel, R.; Ebel, R. *Mar. Drugs* **2003**, *1*, 5–17.

(14) Liu, Y. *J. Mar. Sci. Res. Dev.* **2012**, *2*, 1–2.

(15) Sipkema, D.; Osinga, R.; Schatton, W.; Mendola, D.; Tramper, J.; Wijffels, R. H. *Biotechnol. Bioeng.* **2005**, *90*.

(16) Corey, E. J.; Gin, D. Y.; Kania, R. S. *J. Am. Chem. Soc.* **1996**, *118*, 9202–9203.

(17) Endo, A.; Yanagisawa, A.; Abe, M.; Tohma, S.; Kan, T.; Fukuyama, T. *J. Am. Chem. Soc.* **2002**, *124*, 6552–6554.

(18) Chen, J.; Chen, X.; Bois-Choussy, M.; Zhu, J. *J. Am. Chem. Soc.* **2006**, *128*, 87–89.

(19) Menchaca, R.; Martínez, V.; Rodríguez, A.; Rodríguez, N.; Flores, M.; Gallego, P.; Manzanares, I.; Cuevas, C. *J. Org. Chem.* **2003**, *68*, 8859–8866.

(20) Munro, M. H.; Blunt, J. W.; Dumdei, E. J.; Hickford, S. J.; Lill, R. E.; Li, S.; Battershill, C. N.; Duckworth, A. R. *J. Biotechnol.* **1999**, *70*, 15–25.

(21) Yeung, B. K. S. *Curr. Opin. Chem. Biol.* **2011**, *15*, 523–528.

(22) Aicher, T. D.; Buszek, K. R.; Fang, F. G.; Forsyth, C. J.; Jung, S. H.; Kishi, Y.; Matelich, M. C.; Scola, P. M.; Spero, D. M.; Yoon, S. K. *J. Am. Chem. Soc.* **1992**, *114*, 3162–3164.

(23) Molinski, T. F. *Org. Lett.* **2014**, *16*, 3849–3855.

(24) Gradishar, W. J. *Curr. Oncol. Rep.* **2011**, *13*, 11–16.

(25) Molinski, T. F.; Dalisay, D. S.; Lievens, S. L.; Saludes, J. P. *Nat. Rev. Drug Discov.* **2009**, *8*, 69–85.

(26) Katz, J.; Janik, J. E.; Younes, A. *Clin. Cancer Res.* **2011**, *17*, 6428–6436.

(27) Erwin, P. M.; López-Legentil, S.; Schuhmann, P. W. *Ecol. Econ.* **2010**, *70*, 445–451.

(28) Cooper, E. L.; Yao, D. *Drug Discov. Today* **2012**, *17*, 636–648.

(29) Menna, M.; Aiello, A. In *Handbook of Marine Natural Products*; Fattorusso, E.; Gerwick, W. H.; Taglialatela-Scafati, O., Eds.; Springer Netherlands: Dordrecht, 2012; pp. 295–385.

(30) Rinehart, K. L.; Kishore, V.; Bible, K. C.; Sakai, R.; Sullins, W.; Li, K. L. *J. Nat. Prod.* **1988**, *51*, 1–21.

(31) Zubía, E.; Ortega, M. J.; Salvá, J. *Mini. Rev. Org. Chem.* **2005**, *2*, 389–399.

(32) Edler, M. C.; Fernandez, A. M.; Lassota, P.; Ireland, C. M.; Barrows, L. R. *Biochem. Pharmacol.* **2002**, *63*, 707–715.

(33) Satoh, N.; Rokhsar, D.; Nishikawa, T. *Proc. R. Soc. London. Ser. B, Biol. Sci.* **2014**, *281*, 1–10.

(34) Monniot, C.; Francoise, M.; Pierre, L. *Coral Reef Ascidians of New Caledonia*; ORSTOM: Paris, 1991.

(35) Goodbody, I. In *Advances in Marine Biology*; Russel, F. S.; Yonge, M., Eds.; Academic Press: London and New York, 1974; pp. 1–149.

(36) Millar, R. H. *Adv. Mar. Biol.* **1971**, *9*, 1–100.

(37) Hirose, E. *Zoolog. Sci.* **2001**, *18*, 723–731.

(38) Sugumaran, M.; Robinson, W. E. *Comp. Biochem. Physiol. Part B* **2012**, *163*, 1–25.

(39) Millar, R. H. *Ann. S. Afr. Mus.* **1962**, *46*, 113–221.

(40) Parker-Nance, S. PhD Thesis: Aplousobranch ascidians (Tunicata; Ascidiacea) from southern Africa, University of Port Elizabeth, 2003.

(41) Davies-Coleman, M. T. In *Studies in Natural Products Chemistry*; Attaur-Rahman, Ed.; Amsterdam, 2005; Vol. 32, pp. 61–107.

(42) Bolton, J. J.; Davies-Coleman, M. T.; Coyne, V. E. *African J. Mar. Sci.* **2013**, *35*, 449–464.

(43) Davies-Coleman, M. T. In *Molluscs. From Chemo-ecological Study to Biotechnological Application*; Cimino, G.; Gavagnin, M., Eds.; Spinger: Berlin, Heidelberg, 2006; pp. 133–158.

(44) Fenical, W.; Jensen, P. R.; Kauffman, C.; Mayhead, S. L.; Faulkner, D. J.; Sincich, C.; Rao, M. R.; Kantorowski, E. J.; West, L. M.; Strangman, W. K.; Shimizu, Y.; Li, B.; Thammana, S.; Drainville, K.; Davies-Coleman, M. T.; Kramer, R. A.; Fairchild, C. R.; Rose, W. C.; Wild, R. C.; Vite, G. D.; Peterson, R. W. *Pharm. Biol.* **2003**, *41*, 6–14.

(45) Morris, L. A.; Jaspars, M.; Kettenes-Van Den Bosch, J. J.; Versluis, K.; Heck, A. J. R.; Kelly, S. M.; Price, N. C. *Tetrahedron* **2001**, *57*, 3185–3197.

(46) Morris, L. A.; Milne, B. F.; Jaspars, M.; Kettenes-van den Bosch, J. J.; Versluis, K.; Heck, A. J. R.; Kelly, M.; Price, N. C. *Tetrahedron* **2001**, *57*, 3199–3207.

(47) Wright, S. H.; Raab, A.; Tabudravu, J. N.; Feldmann, J.; Long, P. F.; Battershill, C. N.; Dunlap, W. C.; Milne, B. F.; Jaspars, M. *Angew. Chem. Int. Ed. Engl.* **2008**, *47*, 8090–8092.

(48) Sluiter, C. P. *Zool. Jahrb. XI Abth. f. Syst* **1898**.

(49) Monniot, C.; Monniot, F.; Griffiths, C. L.; Schleyer, M. *Ann. South African Museum* **2001**, *108*, 1–1417.

(50) Michaelsen, W. *Trans. R. Soc. S. Afr.* **1934**, *22*, 129–163.

(51) Millar, R. H. *Proc. Zool. Soc. Lond.* **1955**, *125*, 169–221.

(52) Millar, R. H. *Vidensk. Meddeles. Fra Dansk Naturhistorisk Foren.* **1964**, *127*, 159–180.

(53) Sikorska, J.; Hau, A. M.; Anklin, C.; Parker-Nance, S.; Davies-Coleman, M. T.; Ishmael, J. E.; McPhail, K. L. *J. Org. Chem.* **2012**, *77*, 6066–6075.

(54) Sikorska, J.; Parker-Nance, S.; Davies-Coleman, M. T.; Vining, O. B.; Sikora, A. E.; McPhail, K. L. *J. Nat. Prod.* **2012**, *75*, 1824–1827.

(55) Bromley, C. L.; Parker-Nance, S.; de la Mare, J.-A.; Edkins, A. L.; Beukes, D. R.; Davies-Coleman, M. T. *S. Afr. J. Chem.* **2013**, *66*, 64–68.

(56) Primo, C.; Vazquez, E. *J. Biogeogr.* **2004**, *31*, 1987–2009.

(57) Shenkar, N.; Swalla, B. J. *PLoS One* **2011**, *6*, e20657.

(58) Gibbons, M. J.; Abiahy, B. B.; Angel, M.; Assuncao, C. M. L.; Bartsch, I.; Best, P.; Biseswar, R.; Bouillon, J.; Bradford-Grieve, J. M.; Branch, W.; Burreson, E.; Cannon, L.; Casanova, J.-P.; Channing, A.; Child, C. A.; Compagno, L.; Cornelius, P. F. S.; Dadon, J. R.; David, J. H. M.; Day, J.; Della Croce, N.; Emschermann, P.; Erseus, C.; Esnal, G.; Gibson, R.; Griffiths, C. L.; Hayward, P. J.; Heard, R.; Heemstra, P.; Herbert, D.; Hessler, R.; Higgins, R.; Hiller, N.; Hirano, Y. M.; Kensley, B.; Kilburn, R.; Kornicker, L.; Lambshead, J.; Manning, R.; Marshall, D.; Mianzan, H.; Monniot, C.; Monniot, F.; Newman, W.; Nielsen, C.; Patterson, G.; Pugh, P.; Roeleveld, M.; Ross, A.; Ryan, P.; Ryland, J. S.; Samaai, T.; Schleyer, M.; Schockaert, E.; Seapy, R.; Shiel, R.; Sluys, R.; Southward, E. C.; Sulaiman, A.; Thandar, A.; van der Land, J.; van der Spoel, S.; van Soest, R.; Vetter, E.; Vinogradov, G.; Williams, G.; Wooldridge, T. *S. Afr. J. Sci.* **1999**, *95*, 8–12.

(59) Branch, G. M.; Branch, M. L. *The Living Shores of Southern Africa*; 1st ed.; C. Struik: Cape Town, 1981.

(60) Branch, G. M.; Griffiths, C. L.; Branch, M. L.; Beckly, L. E. *Two Oceans: A guide to the marine life of southern Africa*; Struik: Cape Town, 2007.

(61) Rudi, A.; Goldberg, I.; Stein, Z.; Frolow, F.; Benayahu, Y.; Schleyer, M.; Kashman, Y. *J. Org. Chem.* **1994**, *59*, 999–1003.

(62) Loya, S.; Rudi, A.; Kashman, Y.; Hizi, A. *Biochem. J.* **1999**, *344*, 85–92.

(63) Kreipl, A. T.; Reid, C.; Steglich, W. *Org. Lett.* **2002**, *4*, 3287–3288.

(64) Patil, A. D.; Freyer, A. J.; Kilmer, L.; Zuber, G.; Carte, B.; Jurewicz, Anthony, J.; Johnson, R. K. *Nat. Prod. Lett.* **1997**, *10*, 225–229.

(65) Compagnone, R. S.; Faulkner, D. J. *Tetrahedron* **1994**, *50*, 12785–12792.

(66) Davidson, B. S.; Molinski, T. F.; Barrows, L. R.; Ireland, C. M. *J. Am. Chem. Soc.* **1991**, *113*, 4709–4710.

(67) Hooper, G. J.; Davies-Coleman, M. T.; Coetzee, P. S. *Nat. Prod. Lett.* **1995**, *6*, 31–35.

(68) Rashid, M. A.; Gustafson, K. R.; Cartner, L. K.; Pannell, L. K.; Boyd, M. R. *Tetrahedron* **2001**, *57*, 5751–5755.

(69) Reddy, K. M.; Yamini, V.; Singarapu, K. K.; Ghosh, S. *Org. Lett.* **2014**, *16*, 2658–2660.

(70) Willwacher, J.; Fürstner, A. *Angew. Chem. Int. Ed. Engl.* **2014**, *53*, 4217–4221.

(71) Lei, H.; Yan, J.; Yu, J.; Liu, Y.; Wang, Z.; Xu, Z.; Ye, T. *Angew. Chem. Int. Ed. Engl.* **2014**, *53*, 6533–6537.

(72) McPhail, K. L. Personal communication, 2014.

(73) Comba, P.; Dovalil, N.; Gahan, L. R.; Hanson, G. R.; Westphal, M. *Dalt. Trans.* **2014**, *43*, 1935–1956.

(74) Freeman, D. J.; Pattenden, G.; Drake, A. F.; Siligardi, G. *J. Chem. Soc. Perkin Trans. 2* **1998**, 129–135.

(75) Wright, S. H.; Raab, A.; Feldmann, J.; Krupp, E.; Jaspars, M. In *Handbook of Marine Natural Products*; Fattorusso, E.; Gerwick, W. H.; Taglialatela-Scafati, O., Eds.; Springer Netherlands: Dordrecht, 2012; pp. 861–892.

(76) Blunt, J. W.; Munro, M. H. G. MarinLit a database of marine natural products literature, 2012.

(77) Shenkar, N.; Gittenberger, A.; Lambert, G.; Rius, M.; Moreira da Rocha, R.; Swalla, B. J.; Turon, X. Ascidiacea World Database http://www.marinespecies.org/ascidiacae (accessed Sep 2, 2014).

(78) Parker-Nance, S. Personal communications, 2014.

(79) Carroll, A. R.; Duffy, S.; Avery, V. M. *J. Org. Chem.* **2010**, *75*, 8291–8294.

(80) Crews, P.; Rodríguez, J.; Jaspars, M. *Organic Structure Analysis*; Houk, K. N.; Loundon, M. G., Eds.; 2nd ed.; Oxford University Press: New York, Oxford, 2010.

(81) Bruker Topspin Manual version 2.0.0 - DAISY, 2007.

(82) Berlinck, R. G. S.; Trindade-Silva, A. E.; Santos, M. F. C. *Nat. Prod. Rep.* **2012**, *29*, 1382–1406.

(83) Pearce, a. N.; Chia, E. W.; Berridge, M. V.; Maas, E. W.; Page, M. J.; Harper, J. L.; Webb, V. L.; Copp, B. R. *Tetrahedron* **2008**, *64*, 5748–5755.

(84) Raab, A.; Wright, S. H.; Jaspars, M.; Meharg, A. A.; Feldmann, J. *Angew. Chem. Int. Ed. Engl.* **2007**, *46*, 2594–2597.

(85) Urgast, D. S.; Adams, G. C.; Raab, A.; Feldmann, J. *J. Environ. Monit.* **2010**, *12*, 1126.

(86) Amayo, K. O.; Petursdottir, A.; Newcombe, C.; Gunnlaugsdottir, H.; Raab, A.; Krupp, E. M.; Feldmann, J. *Anal. Chem.* **2011**, *83*, 3589–3595.

(87) Raab, A.; Newcombe, C.; Pitton, D.; Ebel, R.; Feldmann, J. *Anal. Chem.* **2013**, *85*, 2817–2824.

(88) Bluemlein, K.; Raab, A.; Meharg, A. A.; Charnock, J. M.; Feldmann, J. *Anal. Bioanal. Chem.* **2008**, *390*, 1739–1751.

(89) Krupp, E. M.; Milne, B. F.; Mestrot, A.; Meharg, A. a; Feldmann, J. *Anal. Bioanal. Chem.* **2008**, *390*, 1753–1764.

(90) Morris, L. A.; Jantina, J.; Bosch, K. Van Den; Versluis, K.; Thompson, S.; Jaspars, M. *Tetrahedron* **2000**, *56*, 8345–8353.

(91) Mass spectra were processed with Xcalibur v2.0.7 copyrite Thermo Fisher Scieintific Inc.

(92) 6-Bromo-2-oxindole is commercially available from Sigma Aldrich®, CAS number [99365-40-9].

(93) López Chávez, F. J.; Chávez, P. R.; Oyama, K. *Dye. Pigment.* **2009**, *83*, 7–13.

(94) Haygood, M. G.; Schmidt, E. W.; Davidson, S. K.; Faulkner, D. J. *J. Mol. Microbiol. Biotechnol.* **1999**, *1*, 33–43.

(95) Schmidt, E. W.; Donia, M. S. *Curr. Opin. Biotechnol.* **2010**, *21*, 827–833.

(96) Schmidt, E. W.; Donia, M. S.; McIntosh, J. A.; Fricke, W. F.; Ravel, J. *J. Nat. Prod.* **2012**, *75*, 295–304.

(97) Qureshi, A.; Faulkner, D. J. *Nat. Prod. Lett.* **1999**, *13*, 59–62.

(98) Higa, T.; Scheuer, P. J. *Naturwissenschaften* **1975**, *62*, 395–396.

(99) Higa, T.; Fujiyama, T.; Scheuer, P. J. *Comp. Biochem. Physiol.* **1980**, *65B*, 525–530.

(100) Cameron, C. B.; Garey, J. R.; Swalla, B. J. *Proc. Natl. Acad. Sci. U. S. A.* **2000**, *97*, 4469–4474.

(101) Swalla, B. J.; Smith, A. B. *Philos. Trans. R. Soc. Lond. B. Biol. Sci.* **2008**, *363*, 1557–1568.

(102) Keyzers, R. A.; Gray, C. A.; Schleyer, M. H.; Whibley, C. E.; Hendricks, D. T.; Davies-Coleman, M. T. *Tetrahedron* **2006**, *62*, 2200–2206.

(103) De La Mare, J.-A.; Lawson, J. C.; Chiwakata, M. T.; Beukes, D. R.; Edkins, A. L.; Blatch, G. L. *Invest. New Drugs* **2012**, *30*, 2187–2200.

(104) Sesin, T. F.; Ireland, C. M. *Tetrahedron Lett.* **1984**, *25*, 403–404.

(105) Smith, C. J.; Venables, D. a.; Hopmann, C.; Salomon, C. E.; Jompa, J.; Tahir, A.; John Faulkner, D.; Ireland, C. M.; Faulkner, D. J.; Ireland, C. M. *J. Nat. Prod.* **1997**, *60*, 1048–1050.

(106) Ford, P. W.; Davidson, B. S. *J. Nat. Prod.* **1997**, *60*, 1051–1053.

(107) Solano, G.; Motti, C. A.; Jaspars, M. *Tetrahedron* **2009**, *65*, 7482–7486.

(108) Van Wagoner, R. M.; Jompa, J.; Tahir, A.; Ireland, C. M. *J. Nat. Prod.* **1999**, *62*, 794–797.

(109) Ciminiello, P.; Faitorusso, E.; Magno, S. *J. Nat. Prod.* **1994**, *57*, 1564–1569.

(110) Lindsay, B. S.; Battershill, C. N.; Copp, B. R. *J. Nat. Prod.* **1998**, *61*, 857–858.

(111) Schoenfeld, R. C.; Conova, S.; Rittschof, D.; Ganem, B. *Bioorganic Med. Chem.* **2002**, *12*, 823–825.

(112) Raab, A. Personal communications, 2013.

(113) Diers, J. A.; Pennaka, H. K.; Peng, J.; Bowling, J. J.; Duke, S. O.; Hamann, M. T. *J. Nat. Prod.* **2004**, *3*, 2117–2120.

(114) Galeano, E.; Martinez, A.; Thomas, O.; Robledo, S.; Munoz, D. *Quim, Nov.* **2012**, *35*, 1189–1193.

(115) Kennedy, G. R. *Gen. Comp. Endocrinol.* **1966**, *7*, 500–511.

(116) Barrington, E. J.; Thorpe, a. *Proc. R. Soc. Lond. B. Biol. Sci.* **1968**, *171*, 91–109.

(117) Gribble, G. W. *Occurrence of Halogenated Alkaloids*; Elsevier, 2012; Vol. 71.

(118) Mason, R. *Trace Metlas in Aquatic Systems*; John Wiley & Sons: Hoboken, NJ, 2013.

(119) Henze, M. *Z Physiol Chem* **1911**, *72*, 494–501.

(120) Rehder, D. *Bioinorganic Vanadium Chemistry*; John Wiley & Sons: Chichester, UK, 2008.

(121) Monniot, F. *Actual. Biochim Mar* **1978**, 185–194.

(122) Michibata, H.; Terada, T.; Anada, N.; Yamakawa, K.; Numakunai, T. *Biol. Bull.* **1986**, *171*, 672–681.

(123) Roman, D. A.; Molina, J.; Rivera, L. *Biol. Bull.* **1988**, *175*, 154–166.

(124) Lebar, M. D.; Luttenton, L.; McClintock, J. B.; Amsler, C. D.; Baker, B. J. *Polar Biol.* **2010**, *34*, 587–590.

(125) Rainbow, P. S.; Phillips, D. J. H. *Mar. Pollut. Bull.* **1993**, *26*, 593–601.

(126) Lorenzo, J. I. *Mar. Environ. Res.* **2003**, *56*, 531–553.

(127) Cebrian, E.; Uriz, M.-J.; Turon, X. *Environ. Toxicol. Chem.* **2007**, *26*, 2430–2439.

(128) Perez, T.; Longet, D.; Schembri, T.; Rebouillon, P.; Vacelet, J. *Mar. Pollut. Bull.* **2005**, *50*, 301–309.

(129) Papadopoulou, C.; Kanias, G. D. *Mar. Pollut. Bull.* **1977**, *8*, 229–231.

(130) Radhalakshmi, R.; Sivakumar, V.; Abdul Jaffar Ali, H. *Int. J. Curr. Microbiol. Appl. Sci.* **2014**, *3*, 755–764.

(131) Rainbow, P. S. *Environ. Pollltion* **2002**, *120*, 497–507.

(132) Carlisle, D. B. *Proc. R. Soc. London. Ser. B, Biol. Sci.* **1968**, *171*, 31–42.

(133) Nozaki, Y. *EOS, Am. Geophys. Union* **1997**, *78*, 221.

(134) Binning, K.; Baird, D. *Water SA* **2001**, *27*, 461–466.

(135) Watling, R. J.; Watling, H. R. *Waters SA* **1982**.

(136) Watling, R. J.; Watling, H. R. *Water SA* **1983**, *9*, 57–65.

(137) Fatoki, O. S.; Mathabatha, S. *Water SA* **2001**, *27*, 233–240.

(138) Lattin, J.; Carroll, J. D.; Green, P. E. *Analyzing Multivariate Data*; Thomson Brooks/Cole: Pacific Grove, California, 2003.

(139) Jackson, D. A. *Ecology* **1993**, *74*, 2204–2214.

(140) Cattell, R. B. *Multivar. Behav. Res.* **1966**, *1*, 247–276.

(141) Kaiser, H. F. *Educ. Psychol. Meas.* **1960**, *2*, 266–283.

(142) Yoshida, S.; Marikawa, Y.; Satoh, N. *Dev. Biol.* **1998**, *202*, 264–279.

(143) Cook, R. D. *Technometrics* **1977**, *19*, 15–18.

(144) Cook, R. D. *J. Am. Stat. Assoc.* **1979**, *74*, 169–174.

(145) Pérez-Portela, R.; Turon, X. *Invertebr. Biol.* **2008**, *127*, 108–120.

(146) Webb, D. A. *J. Exp. Biol.* **1939**, *16*, 499–523.

(147) Hawkins, C. J.; Kott, P.; Parry, D. L.; Swinehart, J. H. *Comp. Biochem. Physiol. Part B* **1983**, *76B*, 555–558.

(148) Ueki, T.; Michibata, H. *Coord. Chem. Rev.* **2011**, *255*, 2249–2257.

(149) Taylor, S. W.; Kammerer, B.; Bayer, E. *Chem. Rev.* **1997**, *97*, 333–346.

(150) Macara, I. A. N. G.; Mcleod, G. C.; Kustin, K. *Comp. Biochem. Physiol.* **1979**.

(151) Smith, M. J. *Experientia* **1989**, *45*, 452–457.

(152) Macara, I. G.; Mcleod, G. C.; Kustin, K. *Comp. Biochem. Physiol.* **1979**, *63*, 299–302.

(153) Macara, B. I. G.; Mcleod, G. C. *Biochem. J.* **1979**, *181*, 457–465.

(154) Smith, M. J.; Kim, D.; Horenstein, B.; Nakanishi, K.; Kustin, K. *Acc. Chem. Res.* **1991**, *24*, 117–124.

(155) Bruening, R. C.; Oltz, E. M.; Furukawa, J.; Nakanishi, K.; Kustin, K. *J. Am. Chem. Soc.* **1985**, *107*, 5298–5300.

(156) Oltz, E. M.; Bruening, R. C.; Smith, M. J.; Kustin, K.; Nakanishi, K. *J. Am. Chem. Soc.* **1988**, *110*, 6162–6172.

(157) Ryan, D. E.; Grant, K. B.; Nakanishi, K. *Biochemistry* **1996**, *14042*, 8640–8650.

(158) Kime-hunt, E.; Spartalian, K.; Carrano, C. J. *J. Chem. Soc., Chem. Commun.* **1988**, *44*, 1217–1218.

(159) Kime-hunt, E.; Spartalian, K.; Holmes, S.; Mohan, M.; Carrano, C. J. *J. Inorg. Biochem.* **1991**, *141*, 125–141.

(160) Parry, D. L.; Brand, S. G.; Kustin, K. *Bull. Mar. Sci.* **1992**, *50*, 302–306.

(161) Tincu, J. A.; Taylor, S. W. *J. Nat. Prod.* **2002**, 377–378.

(162) Oltz, E. M.; Pollack, S.; Delohery, T.; Smith, M. J.; Ojika, M.; Lee, S.; Kustin, K.; Nakanishi, K. *Experientia* **1989**, *45*, 186–190.

(163) Cai, M.; Sugumaran, M.; Robinson, W. E. *Comp. Biochem. Physiol. Part B* **2008**, *151*, 110–117.

(164) Fukui, K.; Ueki, T.; Ohya, H.; Michibata, H. *J. Am. Chem. Soc.* **2003**, *125*, 6352–6353.

(165) Ueki, T.; Adachi, T.; Kawano, S.; Aoshima, M.; Yamaguchi, N.; Kanamori, K.; Michibata, H. *Biochim. Biophys. Acta - Gene Struct. Expr.* **2003**, *1626*, 43–50.

(166) Kaczmarek, A. M.; Miermans, L.; Deun, R. Van. *Dalt. Trans.* **2013**, *42*, 4639–4649.

(167) Ueki, T.; Sakamoto, Y.; Yamaguchi, N.; Michibata, H. *Appl. Environ. MicroBbology* **2003**.

(168) Hamada, T.; Asanuma, M.; Ueki, T.; Hayashi, F.; Kobayashi, N.; Yokoyama, S.; Michibata, H.; Hirota, H. *J. Am. Chem. Soc.* **2005**, *127*, 4216–4222.

(169) Image from the RCSB PDB (www.rcsb.org) of PDB ID 1VF1.

(170) Yamamoto, S.; Matsuo, K.; Michibata, H.; Ueki, T. *Inorganica Chim. Acta* **2014**, *420*, 47–52.

(171) Ueki, T.; Nakagawa, T.; Michibata, H. *J. Inorg. Biochem.* **2012**, *116*, 70–76.

(172) Samino, S.; Michibata, H.; Ueki, T. *Mar. Biotechnol.* **2012**, *14*, 143–154.

(173) Swinehart, J. H.; Biggs, W. R.; Halko, D. J.; Schroeder, N. C. *Biol. Bull.* **1974**, *146*, 302–312.

(174) Levine, E. P. *Science* **1961**, *133*, 1352–1353.

(175) Frank, P.; Carlson, R. M. K.; Hodgson, K. O. *Inorg. Chem.* **1986**, *25*, 470–478.

(176) Frank, P.; Robinson, W. E.; Kustin, K.; Hodgson, K. O. *J. Inorg. Biochem.* **2001**, *86*, 635–648.

(177) Frank, P.; Carlson, R. M. K.; Carlson, E. J.; Hodgson, K. O. *Coord. Chem. Rev.* **2002**, *237*, 31–39.

(178) Ciereszko, L. S.; Ciereszko, E. M.; Harris, E. R.; Lane, C. A. *Comp. Biochem. Physiol. Part B* **1963**, *8*, 137–140.

(179) Crans, D. C.; Bunch, R. L.; Theisen, L. A. *J. Am. Chem. Soc.* **1989**, *111*, 7597–7607.

(180) Crans, D. C.; Harnung, S. E.; Larsen, E.; Shin, P. K.; Theisen, L. A.; Trabjerg, I. *Acta Chem. Scand.* **1991**, *45*, 456–462.

(181) Crans, D. C.; Smee, J. J.; Gaidamauskas, E.; Yang, L. *Chem. Rev.* **2004**, *104*, 849–902.

(182) Rehder, D. *Inorg. Chem. Commun.* **2003**, *6*, 604–617.

(183) Crans, D. C. *Pure Appl. Chem.* **2005**, *77*, 1497–1527.

(184) Huang, R.-M.; Chen, Y.-N.; Zeng, Z.; Gao, C.-H.; Su, X.; Peng, Y. *Mar. Drugs* **2014**, *12*, 5817–5838.

(185) Chiba, J.-Y.; Tanaka, K.; Ohshiro, Y.; Miyake, R.; Hiraoka, S.; Shiro, M.; Shionoya, M. *J. Org. Chem.* **2003**, *68*, 331–338.

(186) Khan, B. T.; Annapoorna, K. *Polyhedron* **1991**, *10*, 2465–2470.

(187) Golubev, O.; Lçnnberg, T.; Lçnnberg, H. *Helv. Chim. Acta* **2013**, *96*, 1658–1669.

(188) Knobloch, B.; Linert, W.; Sigel, H. *PNAS* **2005**, *102*, 7459–7464.

(189) Berger, S. L.; Birkenmeier, C. S. *Chem. Eng.* **1979**, *18*, 5143–5149.

(190) Baran, E. J. *J. Braz. Chem. Soc.* **2003**, *14*, 878–888.

(191) Crans, D. C.; Tracey, A. S. In *Vanadium Compounds*; ACS Symposium Series; American Chemical Society: Washington DC, 1998; pp. 2–29.

(192) Elvingson, K.; Crans, D. C.; Pettersson, L. *J. Am. Chem. Soc.* **1997**, *119*, 7005–7012.

(193) Elvingson, K.; Keramidas, A. D.; Crans, D. C.; Pettersson, L. *Inorg. Chem.* **1998**, *37*, 6153–6160.

(194) Rehder, D. *Coord. Chem. Rev.* **1999**, *182*, 297–322.

(195) Kehraus, S.; Gorzalka, S.; Hallmen, C.; Iqbal, J.; Müller, C. E.; Wright, A. D.; Wiese, M.; König, G. M. *J. Med. Chem.* **2004**, *47*, 2243–2255.

(196) Takeara, R.; Jimenez, P. C.; Costa-lotufo, L. V; Lopes, J. L. C.; Lopes, N. P. *J. Braz. Chem. Soc.* **2007**, *18*, 1054–1060.

(197) Dematтè, N.; Guerriero, A.; De Clauser, R.; De Stanchina, G.; Lafargue, F.; Cuomo, V.; Pietra, F. *Comp. Biochem. Physiol.* **1985**, *81B*, 479–484.

(198) Mitchell, S. S.; Pomerantz, S. C.; Concepción, G. P.; Ireland, C. M. *J. Nat. Prod.* **1996**, *59*, 1000–1001.

(199) Margiastuti, P.; Ogi, T.; Teruya, T.; Taira, J.; Suenaga, K.; Ueda, K. *Chem. Lett.* **2008**, *37*, 670–670.

(200) Schupp, P.; Poehner, T.; Edrada, R.; Ebel, R.; Berg, A.; Wray, V.; Proksch, P. *J. Nat. Prod.* **2003**, *66*, 272–275.

(201) Abou-Hussein, D. R.; Badr, J. M.; Youssef, D. T. A. *Nat. Prod. Sci.* **2007**, *13*, 229–230.

(202) Núñez-Pons, L.; Carbone, M.; Vázquez, J.; Rodríguez, J.; Nieto, R. M.; Varela, M. M.; Gavagnin, M.; Avila, C. *Mar. Drugs* **2012**, *10*, 1741–1764.

(203) Han, Q.-H. H.; Fan, C.-Q. Q.; Lu, Y.-N. N.; Wu, J.-P. P.; Liu, X.; Yin, S. *Biochem. Syst. Ecol.* **2013**, *48*, 6–8.

(204) Dematti, N.; Guerriero, A.; Lafargue, F. O.; Pietra, F.; Chimica, I. *Comp. Biochem. Physiol.* **1986**, *84*, 11–13.

(205) Kim, J.; Pordesimo, E. O.; Toth, S. I.; Schmiz, F. J. *J. Nat. Prod.* **1993**, *56*, 1813–1816.

(206) Li, J. L.; Kim, E. La; Wang, H.; Hong, J.; Shin, S.; Lee, C.-K.; Jung, J. H. *Bioorg. Med. Chem. Lett.* **2013**, *23*, 4701–4704.

(207) Doi, Y.; Ishihashi, M.; Kobayashi, J. *Tetrahedron* **1994**, *50*, 8651–8656.

(208) Jones, A. J.; Grant, D. M.; Winkley, M. W.; Robins, R. K. *J. Phys. Chem.* **1970**, *74*, 2684–2689.

(209) Gundhla, I. Z.; Walmsley, R. S.; Ugirinema, V.; Mnonopi, N. O.; Hosten, E. *J. Inorg. Biochem.* **2014**, *145*, 11–18.

(210) Walmsley, R. S.; Tshentu, Z. R.; Fernandes, M. a.; Frost, C. L. *Inorganica Chim. Acta* **2010**, *363*, 2215–2221.

(211) Henry, R. P.; Mitchell, P. C. H.; Prue, J. E. J. *J. Chem. Soc. Dalt. Trans.* **1973**, 1156–1159.

(212) Gran, G. *Analyst* **1952**, *77*, 661–671.

(213) Gans, P.; O'Sullivan, B. *Talanta* **2000**, *51*, 33–37.

(214) Martel, A. E.; Motekaitis, R. J. *Determination and use of stability constants*; VCH: New York, 1986.

(215) Alderighi, L.; Gans, P.; Ienco, A.; Peters, D.; Sabatini, A.; Vacca, A.; Maragliano, V. *Coord. Chem. Rev.* **1999**, *184*, 311–318.

(216) Gans, P.; Sabatini, A.; Vacca, A. *Talanta* **1996**, *43*, 1739–1753.

(217) Sigel, H.; Salah, S.; Coda, N. A. *J. Am. Chem. Soc.* **1994**, *116*, 2958–2971.

(218) Al-Flaijj, O.; Shehata, M. R.; Mohamed, M. M. A.; Shoukry, M. M. *Monatshefte Fur Chemie* **2001**, *132*, 349–366.

(219) Khalil, M. M.; Fazary, A. E. *Monatshefte Fur Chemie* **2004**, *135*, 1455–1474.

(220) Kott, P. *Mem. Queensl. Museum* **2001**, *47*, 1–407.

(221) Zinin, V. N.; Il'yasov, a. V.; Weber, U.; Hägele, G.; Thiele, H. *J. Fluor. Chem.* **1995**, *70*, 289–292.

(222) Hagelet, G.; Fuhler, R.; Hoffken, H. W.; Lenzen, T.; Spiske, R.; Weber, U. *Comput. Chem.* **1995**, *19*, 283–285.

(223) Bashall, A. P.; Crowder, J.; Dronia, H.; Hagele, G.; Hudson, H. R.; Lee, R. J.; Mcpartlin, M.; Matthews, R. W.; Ollig, J. *Heteroat. Chem.* **2010**, *21*, 314–325.

(224) Keeler, J. *Understanding NMR Spectroscopy*; Second Edi.; Wiley, 2010.

(225) Jennings, W. B.; O'Connell, N.; Malone, J. F.; Boyd, D. R. *Org. Biomol. Chem.* **2013**, *11*, 5278–5291.

(226) Reich, Hans, J. Structure Determination Using NMR: 5.16 Virtual Coupling http://www.chem.wisc.edu/areas/reich/chem605/.

(227) Becker, E. D. *J. Chem. Educ.* **1965**, *42*, 591–596.

(228) Silverstein, R. M.; Silberman, R. G. *J. Chem. Educ.* **1973**, *50*, 484–486.

(229) Musher, J. I.; Corey, E. J. *Tetrahedron* **1962**, *18*, 791–809.

(230) Freeburger, M. E.; Buckles, R. E.; Stille, J. K. *Tetrahedron Lett.* **1968**, *4*, 431–435.

(231) Williams, J. L.; Sgoutas, D. S. *Chem. Phys. Lipids* **1972**, *9*, 320–331.

(232) Kotowycz, G.; Lemieux, R. U. *Chem. Rev.* **1973**, *73*, 669–698.

(233) Broom, A. D.; Christensen, L. F. *J. Org. Chem.* **1974**, *39*, 2660–2662.

(234) Bancroft, G. M.; Libbey, E. T. *Can. J. Chem.* **1973**, *51*, 1482–1484.

(235) Campbell, J. D.; Allaway, J. A.; Teymour, F.; Morbidelli, M. *J. Appl. Polym. Sci.* **2004**, *94*, 890–908.

(236) Bromley, C. L.; Popplewell, W. L.; Pinchuck, S. C.; Hodgson, A. N.; Davies-Coleman, M. T. *J. Nat. Prod.* **2012**, *75*, 497–501.

(237) Van Liedekerke, B. M.; Nelis, H. J.; Lambert, W. E.; De Leenheer, A. P. *Anal. Chem.* **1989**, *61*, 728–732.

(238) Keyzers, R. A. PhD Thesis: The Isolation of Biologically Active Secondary Metabolites from New Zealand Marine Organisms, Victoria University, 2003.

(239) Van Wyk, A. PhD Thesis: Studies in Marine Diterpene Chemistry, Rhodes University, 2008.

(240) Halden, R. U. *Annu. Rev. Public Health* **2010**, *31*, 179–194.

(241) Browne, M. A. *Nature* **2013**, *494*, 170–171.

(242) *Plastics – the Facts 2013 An analysis of European latest plastics production , demand and waste data*; 2013.

(243) Ryan, P. G.; Moore, C. J.; van Franeker, J. A.; Moloney, C. L. *Philos. Trans. R. Soc. Lond. B. Biol. Sci.* **2009**, *364*, 1999–2012.

(244) Browne, M. A.; Galloway, T. S.; Thompson, R. C. *Environ. Sci. Technol.* **2010**, *44*, 3404–3409.

(245) Rees, G.; Pond, K. *Mar. Pollut. Bull.* **1995**, *30*, 103–108.

(246) Barnes, D. K. a; Galgani, F.; Thompson, R. C.; Barlaz, M. *Philos. Trans. R. Soc. Lond. B. Biol. Sci.* **2009**, *364*, 1985–1998.

(247) Schulz, M.; Neumann, D.; Fleet, D. M.; Matthies, M. *Mar. Environ. Res.* **2013**, *92*, 61–70.

(248) Thompson, R. C.; Olsen, Y.; Mitchell, R. P.; Davis, A.; Rowland, S. J.; John, A. W. G.; McGonigle, D.; Russell, A. E. *Science* **2004**, *304*, 838.

(249) Mudgal, S.; Lyons, L.; J, B.; Dias, D.; Faninger, T.; Johansson, L.; Dolley, P.; Shields, L.; Bowyer, C. *European Commission DG ENV: Plastic Waste in the Environment*; Paris, 2011.

(250) Kitamura, S.; Ohmegi, M.; Sanoh, S.; Sugihara, K.; Yoshihara, S.; Fujimoto, N.; Ohta, S. *Environ. Heal. Perspect.* **2003**.

(251) Genualdi, S.; Nyman, P.; Begley, T. *Food Addit. Contam. Part A. Chem. Anal. Control. Expo. Risk Assess.* **2014**, *31*, 723–733.

(252) Rochman, C. M. *Environ. Sci. Technol.* **2013**, *47*, 2439–2440.

(253) Browne, M. A.; Galloway, T.; Thompson, R.; Chapman, P. M. *Integr. Environ. Assess. Manag.* **2007**, *3*, 559–561.

(254) Hidalgo-Ruz, V.; Gutow, L.; Thompson, R. C.; Thiel, M. *Environ. Sci. Technol.* **2012**, *46*, 3060–3075.

(255) Rochman, C. M.; Manzano, C.; Hentschel, B. T.; Simonich, S. L. M.; Hoh, E. *Environ. Scieince Technol.* **2013**.

(256) Browne, M. A.; Crump, P.; Niven, S. J.; Teuten, E.; Tonkin, A.; Galloway, T.; Thompson, R. *Environ. Sci. Technol.* **2011**, *45*, 9175–9179.

(257) Frias, J. P. G. L.; Otero, V.; Sobral, P. *Mar. Environ. Res.* **2014**, *95*, 89–95.

(258) Van Cauwenberghe, L.; Vanreusel, A.; Mees, J.; Janssen, C. R. *Environ. Pollut.* **2013**, *182*, 495–499.

(259) Browne, M. A.; Dissanayake, A.; Galloway, T. S.; Lowe, D. M.; Thompson, R. C. *Environ. Sci. Technol.* **2008**, *42*, 5026–5031.

(260) Rochman, C. M.; Hoh, E.; Kurobe, T.; Teh, S. J. *Sci. Rep.* **2013**, *3*, 3263.

(261) Saido, K.; Taguchi, H.; Kodera, Y.; Ishihara, Y.; Ryu, I.-J.; Chung, S.-Y. *Macromol. Res.* **2003**, *11*, 87–91.

(262) Amamiya, K.; Saido, K.; Sato, H.; Ou, C.; Lejano, B. A.; Che, Q. In *International Offshore and Polar Engineering Conference*; 2010; Vol. 7, pp. 1111–1115.

(263) Saido, K.; Amamiya, K.; Sato, H.; Okabe, A.; Ogawa, N.; Kamaya, Y.; Kogure, K.; Nishimura, M.; Okukawa, K.; Kusui, T. *Bunseki Kagaku* **2012**, *61*, 629–636.

(264) Saido, K.; Koizumi, K.; Sato, H.; Ogawa, N.; Kwon, B. G.; Chung, S.-Y.; Kusui, T.; Nishimura, M.; Kodera, Y. *Sci. Total Environ.* **2014**, *473-474*, 490–495.

(265) Kwon, B. G.; Saido, K.; Koizumi, K.; Sato, H.; Ogawa, N.; Chung, S.-Y.; Kusui, T.; Kodera, Y.; Kogure, K. *Environ. Pollut.* **2014**, *188*, 45–49.